

THESIS
4
2010

This is to certify that the
dissertation entitled


STUDIES OF THE STILLE REACTION USING ^{119}TIN NMR
AND RELATED REACTIONS

presented by

NICOLE M. TORRES

has been accepted towards fulfillment
of the requirements for the

Doctoral degree in Chemistry



Major Professor's Signature

9-15-2009

Date

MSU is an Affirmative Action/Equal Opportunity Employer

LIBRARY
Michigan State
University

PLACE IN RETURN BOX to remove this checkout from your record.
TO AVOID FINES return on or before date due.
MAY BE RECALLED with earlier due date if requested.

DATE DUE	DATE DUE	DATE DUE

STUDIES ON

in

STUDIES OF THE STILLE REACTION USING ^{119}TIN NMR
AND RELATED REACTIONS

By

Nicole M. Torres

A DISSERTATION

Submitted to
Michigan State University
in partial fulfillment of the requirements
for the degree of

DOCTOR OF PHILOSOPHY

Chemistry

2010

STUDIES

The Stille

formation, primary

control and retain

the Stille reaction

sequence that is

nontransferable

dimethylstannanes

the differences exist

comprehensive study

forthcoming, we per

determine relative co

conditions. These st

not many of the re

lead in the follow

ABSTRACT

STUDIES OF THE STILLE REACTION USING ^{119}Sn NMR AND RELATED REACTIONS

By

Nicole M. Torres

The Stille reaction is a widely utilized method for carbon-carbon bond formation, primarily due to its high functional group tolerance and ability to control and retain regio- and stereochemistries. Our groups initial interest in the Stille reaction began with the development of a hydrostannation Stille sequence that is catalytic in tin. Unfortunately, limitations of the nontransferable ligands on tin required the use of more toxic trimethylstannanes vs. tributylstannanes. Conventional wisdom suggests that rate differences exist between trimethyl and tributyl stannanes, however no comprehensive studies to prove this have been reported. To address this shortcoming, we performed a series of rate studies using ^{119}Sn NMR to determine relative cross coupling rates across a variety of organohalides and conditions. These studies revealed much about the course of this reaction, with many of the results proving unexpected. These findings are discussed in detail in the following dissertation with particular attention paid to the

mechanistic aspects of the Stille coupling and the corresponding synthetic implications.

Copyright by
NICOLE M. TORRES
2010

To my parents and grandparents
for their everlasting love and support

ACKNOWLEDGEMENTS

I would like to express my deepest gratitude to my advisor, Professor Robert E. Maleczka, Jr. for his guidance, support, and enthusiasm for chemistry. Thank you for the opportunity to work in your lab and for fostering my development as a chemist. Perhaps more importantly, thank you for always believing in me.

Thank you to my guidance committee members, Professors Gregory Baker, Jetze Tepe, and James McCusker, for intriguing discussions and suggestions about kinetics! Thank you also to Professor Mitch Smith, for all of the time and support you have given me over these past five years. I would like to thank all of the Professors at MSU for being open to students coming and asking questions, your dedication, and your friendships. Given the nature of my work, I am extremely grateful to Dr. Daniel Holmes for teaching me the ins and outs of the NMR.

Many thanks to the past and current Maleczka group members, especially Jill Muchnij and Ron Rahaim who were instrumental in the early stages of my graduate career. Thank you also to Jerome Lavis for his work on germanium couplings. Thank you to other friends in the department, especially Erin Vogel and Amanda Palumbo.

I would like to thank all my family for always being there for me, especially my mom (Jinann), dad (Carlos) stepdad (Rod), and stepmom (Helen). Without your love and support, I would not have made it this far. To my sister Julia and brother Victor, thank you for lighting up my life.

Finally, I would like to thank Troy Knight. You have been there for me through every step of the way, you have had so much patience with me, and you have taught me so much. I am proud of you for everything you have accomplished and happy that I could be a part of it. I am grateful for your love and friendship, and I am excited to start our lives together!

TABLE OF CONTENTS

LIST OF TABLES	xi
LIST OF FIGURES	xiii
LIST OF SCHEMES	xx
LIST OF ABBREVIATIONS AND SYMBOLS	xxiii
Chapter 1. An Introduction to the Stille Reaction	1
1.1. Synthetic Importance of the Stille Coupling	1
1.2. The Catalytic Cycle	3
1.2.1. Ligand Substitution: Associative vs. Dissociative	4
1.2.2. Ligand Substitution: Direct vs. Solvent Assisted	6
1.3. Oxidative Addition: Pd Insertion into C-X bond	7
1.4. Transmetalation: Transfer of Tin Ligand to Palladium	9
1.4.1. Mechanism of Transmetalation	9
1.4.2. Improvements on the Transmetalation Step	12
1.5. Reductive Elimination: Carbon-Carbon Bond Formation and Pd Regeneration	14
1.6. Towards a Better Understanding of the Stille Reaction	15
Chapter 2. An Introduction to Kinetics, ^{119}Sn NMR, and Data Analysis	16
2.1. Homogeneous Catalysis Kinetics	16
2.2. Development of a Data Acquisition Method	17
2.3. Properties of ^{119}Sn NMR	20
2.4. Data Analysis Methods	25
Chapter 3. Quantifying Rate Differences for Trialkyl Stannanes	28
3.1. Initial Objective of the Study	28
3.2. Coupling Partner Choices	28
3.3. Discussion on Stannane Coupling Partners	29
3.4. Discussion on Aryl Halide Coupling Partners	30
3.5. Preparation of Vinyl Stannanes	31
3.6. Development of the Standard Kinetics Procedure	35
3.7. Monitoring the Course of the Stille Reaction with ^{119}Sn NMR	37

3.8. Control Experiments	38
3.9. Preliminary Study on Electrophile Scope Leading to Phenyl Exchange	44
3.10. Aryl Iodide Couplings	48
3.11. Aryl Bromide Couplings	54
3.12. Mechanistic Considerations of Aryl Bromide Couplings.....	56
 Chapter 4. Quantifying Rate Differences for Trialkyl Stannanes: Expanding Scope.....	67
4.1. Conditions to be Screened	67
4.2. Solvent Effects	67
4.2.1. <i>N</i> -Methyl-2-pyrrolidinone (NMP)	67
4.2.2. Benzene	70
4.3. Ligand Effects	79
4.3.1. Tri-2-furylphosphine (TFP).....	81
4.3.2. Tri- <i>tert</i> -butylphosphine P(<i>t</i> -Bu) ₃	95
4.3.3. Triphenylphosphine	97
4.4. Conclusions.....	98
 Chapter 5. Side Reactions of the Stille Reaction.....	99
5.1. Why Use an Internal Standard?	99
5.2. Me ₄ Sn As the Internal “Standard”	99
5.3. Formation of Transient Tin Species.....	102
5.4. Implications of Aryl Tin Formation.....	112
5.5. Relation of Aryl Tin Formation to Homocoupling.....	114
5.6. Insight into the Basis of R for X vs. R for R Transmetallation.....	118
 Chapter 6. Effect of Additives on the Rate of the Stille Reaction.....	123
6.1. Reassessing the Goals of Our Study	123
6.2. The 2 nd Generation Hydrostannation/Stille Sequence Catalytic in Tin ^{33,56,57}	123
6.3. Correlating Stille Kinetic Data to the Hydrostannation/Stille Sequence	126
6.4. The Fluoride Effect	127
6.4.1. Couplings of Aryl Iodides in the Presence of Aqueous KF/TBAF	129
6.5. The Water Effect on Aryl Iodide Couplings	133
6.6. Fluoride and Water Effect on Aryl Bromides	137
6.7. Insight into the Mechanism of Fluoride and Water Activation.....	139

6.8. The Copper Effect	144
6.8.1. Aryl Iodide Couplings in the Presence of CuI	146
6.8.2. Aryl Bromide Couplings in the Presence of CuI.....	153
6.9. Determining the Impact of the Order of Addition for Reactions with CuI.....	155
 Chapter 7. Heck-Like Cross Couplings of Vinyl Germanes.....	 163
7.1. Why Germanium?	163
7.2. Development of Organogermane Reactions.....	164
7.3. Synthesis of Vinyl Germanes	168
7.4. Finding the Right Coupling Conditions	170
7.5. Mechanistic Insight	176
7.6. Conclusions.....	182
 Chapter 8. Future Work	 183
 Chapter 9. Experimental Details	 188
 REFERENCES.....	 296

LIST OF TABLES

Table 2.1. Determination of the Relaxation Time in THF and NMP.....	25
Table 3.1. Synthesis of Vinyl Stannanes.....	33
Table 3.2. Methyl Protection of Hydroxyl Stannanes	33
Table 3.3. Vinyl Stannane Synthesis.....	34
Table 3.4. Standard Kinetics Sample Preparation	36
Table 3.5. Pd Concentration Dependence Data	44
Table 3.6. Determination of Cross-Coupled and Phenyl Transfer Product Distribution.....	48
Table 3.7. Aryl Iodide Couplings in THF	49
Table 3.8. Temperature Dependent Rate Constants	53
Table 3.9. Aryl Bromide Couplings in THF.....	55
Table 4.1. Aryl Iodide Couplings in NMP	68
Table 4.2. Aryl Bromide Couplings in NMP	70
Table 4.3. Aryl Halide Couplings in Benzene.....	72
Table 4.4. Ligand Effects ²⁵	81
Table 5.1. Testing Conditions for Formation of the Unknown Tin Species	105
Table 5.2. Testing Conditions for Formation of Phenyl Tin from Tin Halide	111
Table 5.3. Product Yields for Stille Reactions in THF	116
Table 5.4. Product Yields for Stille Reactions in NMP and Benzene.....	117

Table 6.1. Comparison of Results Using Me vs. Bu Trialkylstannanes	127
Table 6.2. Fluoride Effect on Me/Bu Rate Differences	133
Table 6.3. The Copper Effect: Farina & Liebskind's Results ²²	146
Table 6.4. Effect of CuI on Reaction Rate	148
Table 6.5. CuI Effect with Higher Catalyst Loading and Temperature: Farina's Results	151
Table 6.6. Timing of CuI Addition and Impact on Reaction Outcome in THF	155
Table 6.7. Qualitative Experiments to Determine the Effect of the Order of Addition for Reactions with CuI and the Effect of Air	157
Table 6.8. Order of Addition for Reactions with CuI	159
Table 6.9. CuI Effect on Me/Bu Ratio Under Farina's Conditions	161
Table 7.1. Hydrogermylations	169
Table 7.2. Screening Heck Conditions	172
Table 7.3. Comparing Stille vs. Heck Conditions	173
Table 7.4. Scope of Coupling with Various Aryl Halides at 0.05 M	175
Table 7.5. Scope of Coupling with Various Aryl Halides at 0.2 M	176
Table 7.6. Concentration Impact on Z/E Ratios	177
Table 7.7. Cross-coupling of Unhindered Vinyltributylgermanes	179
Table 7.8. Effect of Germane Geometry on Coupling	182
Table 9.1. Reagent Amounts for Pd Dependence Study	206
Table 9.2. Reagent Amounts for Aryl Bromide Dependence Study	233

LIST OF FIGURES

Figure 1.1. Selected Natural Products Prepared with a Stille Coupling as a Key Synthetic Step	2
Figure 1.2. Open Transition State ¹⁴	10
Figure 2.1. ¹ H NMR of Vinyl Protons in Starting Material and Product	19
Figure 2.2. ¹¹⁹ Sn NMR Spectrum of Distinct Vinyl Stannanes in THF	20
Figure 2.3. Spin States During an NMR Experiment	21
Figure 2.4. Pulse Sequence of a Typical ¹¹⁹ Sn NMR Kinetics Experiment. All kinetics experiments utilized inverse gated decoupling where ¹ H decoupling is only performed during the acquisition (green box) and not during the rest period (blue line). For the reaction with 40 , the recycle delay (d1) is set to 28 sec as shown.....	24
Figure 2.5. First Order Exponential Curve Fitting with OriginPro 7.5. 186 MHz ¹¹⁹ Sn NMR spectra were obtained every 5 min over the course of the reaction of 40 with PhI under a Pd ₂ dba ₃ /AsPh ₃ catalyst system. Each spectrum was integrated relative to the first to obtain the relative integration data shown in the black trace. The solid red line represents the fit to a first order exponential decay model to reveal $\tau = 58.7 \pm 0.71$ min, which is related to k_{obs} by $1/\tau$ where $k_{\text{obs}} = 0.017 \text{ min}^{-1}$	27
Figure 3.1. Substituted Vinyl Stannanes of Interest	30
Figure 3.2. Electrophiles of Interest.....	31
Figure 3.3. Course of the Stille Reaction Monitored by ¹¹⁹ Sn NMR.....	38
Figure 3.4. Verification of Zero-Order Electrophile Dependence. 186 MHz ¹¹⁹ Sn NMR relative integration data for the consumption of 40 upon coupling with either 1.2 equiv (black trace) or 2.2 equiv (red trace) of PhI under a Pd ₂ dba ₃ /AsPh ₃ catalyst system. Both sets of data were fit to	

a first order exponential decay model (not shown) to reveal $k_{\text{obs}} = 0.006 \text{ min}^{-1}$ 40

Figure 3.5. Verification of Pseudo-First-Order Stannane Dependence. 186 MHz ^{119}Sn NMR relative integration data for the consumption of either 1.0 equiv (black trace) or 0.5 equiv (red trace) of **40** upon coupling with 1.2 equiv of PhI under a $\text{Pd}_2\text{dba}_3/\text{AsPh}_3$ catalyst system. Both sets of data were fit to a first order exponential decay model (not shown) to reveal $k_{\text{obs}} = 0.006 \text{ min}^{-1}$. Instantaneous rates are approximated for illustrative purposes only, as the slope of a tangent line is equal to the instantaneous rate. The true value is determined by the following relationship: $\text{rate} = k_{\text{obs}}[\text{Sn}]$. For 1.0 equiv, $[\text{Sn}] \approx 0.19 \text{ M}$ and for 0.50 equiv, $[\text{Sn}]$ is $\approx 0.095 \text{ M}$ 41

Figure 3.6. Pd Concentration Dependence. The 186 MHz ^{119}Sn NMR relative integration data for the consumption of **39** or **40** upon coupling with PhI under different $\text{Pd}_2\text{dba}_3/\text{AsPh}_3$ catalyst loadings were obtained and the data were fit to a first order exponential decay model (not shown) to obtain k_{obs} for each catalyst loading and stannane combination (red trace: **39** R = Me, blue trace: **40** R = Bu). The $\ln(k_{\text{obs}})$ vs. $\ln([\text{Pd}])$ were then plotted to reveal a linear relationship between k_{obs} and $[\text{Pd}]$. The black solid lines represent a fit to a linear regression model and gave a slope of 1.0 and 1.2 for **39** and **40**, respectively, indicating a first order dependence on Pd concentration. 43

Figure 3.7. Plot of Temperature Dependence for Trimethyl and Tributyl Stannane Reactions. 186 MHz ^{119}Sn NMR relative integration data for the consumption of **39** (*top*) or **40** (*bottom*) upon coupling with PhI under a $\text{Pd}_2\text{dba}_3/\text{AsPh}_3$ catalyst system at 40 °C (black trace), 50 °C (red trace), and 55 °C (blue trace). All sets of data were fit to a first order exponential decay model (not shown) to reveal the rate constants outlined below in Table 3.8..... 52

Figure 3.8. Arrhenius Plot to Determine the Activation Energy, E_a . An Arrhenius Plot was prepared by plotting $\ln(k_{\text{obs}})$ vs. $1/T$, where the k_{obs} values at various temperatures were determined in Table 3.8. The black lines represent a fit to a linear regression model, with the slope = $-E_a/R$.

For **39**, $E_a = 12.4$ kcal/mol (fit A: red solid line) or 8.4 kcal/mol when only 45 and 50 °C are fit (fit B: red dashed line) and for **40**, $E_a = 6.8$ kcal/mol.....54

Figure 3.9. Determination of Electrophile Dependence. 186 MHz ^{119}Sn NMR relative integration data for the consumption of **41** or **42** upon coupling with 1.2 equiv (black), 3.5 equiv (red), 5.3 equiv (green), or 7.1 equiv (blue) of 4-bromobenzotrifluoride. The data were fit to a first order exponential decay model (not shown) to obtain k_{obs} . The solid colored lines are to guide the eye. The $\ln(k_{\text{obs}})$ vs. $\ln([\text{ArBr}])$ were then plotted (inset) to reveal a linear relationship between k_{obs} and $[\text{ArBr}]$. The red solid lines represent a fit to a linear regression model and gave a slope of 0.9, indicating first order aryl bromide concentration dependence.58

Figure 3.10. Stille coupling of **42** with 4-iodobenzotrifluoride monitored by ^{19}F NMR.61

Figure 3.11. Stille coupling of **42** with 4-bromobenzotrifluoride monitored by ^{19}F NMR.....61

Figure 3.12. ^{19}F NMR Spectra of the Oxidative Addition of 4-Iodobenzotrifluoride (Scheme 3.8) Compared with the Unknown Signals Observed During the Stille Coupling of **42** with 4-Iodobenzotrifluoride (Scheme 3.7).....64

Figure 4.1. Coupling of **39** or **40** with PhI in Benzene. 186 MHz ^{119}Sn NMR relative integration data for the consumption of **39** (black) or **40** (green) upon coupling with PhI under a $\text{Pd}_2\text{dba}_3/\text{AsPh}_3$ catalyst system in benzene. Data for **39** from $t = 0$ -20 min was fit to a linear regression plot (inset, red solid line). First order exponential fit (red solid line) did not provide an accurate fit. Data for **40** was fit to a first order exponential decay model (blue solid line).73

Figure 4.2. Stannantrane: Activation of Sn–C Bond74

Figure 4.3. Coordination of Stannanes to Palladium75

Figure 4.4. Individual Experiments. 186 MHz ^{119}Sn NMR relative integration data for the consumption of **39** (black trace) or **40** (red trace) upon coupling with 1.2 equiv of PhI under a $\text{Pd}_2\text{dba}_3/\text{AsPh}_3$ catalyst system in benzene. Both sets of data were fit to a first order exponential decay model (not shown) to reveal for **39**, $k_{\text{obs}} = 0.0044 \text{ min}^{-1}$ and for **40**, $k_{\text{obs}} = 0.022 \text{ min}^{-1}$ 78

Figure 4.5. Competition Experiment. 186 MHz ^{119}Sn NMR normalized relative integration data for the consumption of **39** (black trace) and **40** (red trace) upon coupling with 1.2 equiv of PhI under a $\text{Pd}_2\text{dba}_3/\text{AsPh}_3$ catalyst system in benzene. Both sets of data were fit to a first order exponential decay model (not shown) to reveal for **39**, $k_{\text{obs}} = 0.005 \text{ min}^{-1}$ and for **40**, $k_{\text{obs}} = 0.01 \text{ min}^{-1}$ 79

Figure 4.6. Studies of Couplings with Pd/TFP. 186 MHz ^{119}Sn NMR relative integration data for the consumption of **39** (black trace) or **40** (red trace) upon coupling with 1.2 equiv of PhI under a $\text{Pd}_2\text{dba}_3/\text{TFP}$ catalyst system. Both sets of data were fit to a first order exponential decay model (not shown) after the induction period (~100 min) to reveal for **39**, $k_{\text{obs}} = 0.033 \text{ min}^{-1}$ and for **40**, $k_{\text{obs}} = 0.024 \text{ min}^{-1}$ 82

Figure 4.7. Autocatalytic Reaction Process..... 83

Figure 4.8. Determining if a Protected Hydroxyl Affects Autocatalysis. 186 MHz ^{119}Sn NMR relative integration data for the consumption of **42** (black trace) upon coupling with 1.2 equiv of PhI under a $\text{Pd}_2\text{dba}_3/\text{TFP}$ catalyst system. The data was fit to a first order exponential decay model (not shown) after the induction period (~500 min) to reveal a $k_{\text{obs}} = 0.024 \text{ min}^{-1}$ 85

Figure 4.9. Relative Decay of $\text{Pd}(\text{P}t\text{-Bu}_3)_2$ (**74**) and $\text{Pd}(\text{P}t\text{-Bu}_3)_2(\text{H})(\text{Br})$ (**77**) During the Oxidative Addition of PhBr in 2-Butanone at 70 °C.⁴⁷ Reproduced with permission from Barrios-Landeros, F.; Carrow, B. P.; Hartwig, J. F. *J. Am. Chem. Soc.* **2008**, *130*, 5842–5843. Copyright 2008 American Chemical Society..... 86

Figure 4.10. Oxidative Addition of $\text{Pd}_2\text{dba}_3/\text{TFP}$ to PhI in THF. Selected 202 MHz ^{31}P NMR spectra during an arrayed experiment monitoring the oxidative addition of $\text{Pd}_2\text{dba}_3/\text{TFP}$ to PhI in THF. The first spectra (from front to back) was taken before the addition of PhI, the second was taken immediately following the addition of PhI, and the third was taken after the reaction proceeded for 2 h by which time a new signal appeared at -1.5 ppm..... 90

Figure 4.11. Coupling of **39** and PhBr by $\text{Pd}/\text{P}(t\text{-Bu})_3$ Monitored by GC. Consumption of **39** upon coupling with 1.2 equiv of PhBr under a $\text{Pd}_2\text{dba}_3/\text{PPh}_3$ catalyst system as monitored by GC with mesitylene as an internal standard. The concentration was determined by comparison to the appropriate calibration curve. The black trace represents the data collected by GC. The two red dots represent an extrapolation if the reaction proceeded by first order kinetics while the red solid line represents a fit of the data that would be first order to a first order exponential decay model..... 97

Figure 5.1. Course of the Stille Reaction Monitored by ^{119}Sn NMR..... 102

Figure 5.2. Spiked ^{119}Sn NMR Experiment. The lower 186 MHz ^{119}Sn NMR spectrum shows the crude reaction mixture for the coupling of **39** with 4-bromoanisole in a $\text{Pd}_2\text{dba}_3/\text{AsPh}_3$ catalyst system where by a small amount of a tin compound was formed at -31 ppm. The upper spectrum shows the crude mixture spiked with an authentic sample of 4-trimethylstannylanisole, showing a signal at -31 ppm. 109

Figure 5.3. Possible Structures for the ^{119}Sn NMR Signal at +50 ppm 111

Figure 5.4. Interplanar Angles Between Aryl Plane and Metal Coordination Plane 121

Figure 6.1. Reaction Profile of Fluoride Additive Effect. 186 MHz ^{119}Sn NMR relative integration data for the consumption of **39** or **40** without fluoride (black trace) and with fluoride (red trace) upon coupling with 1.2 equiv of PhI under a $\text{Pd}_2\text{dba}_3/\text{AsPh}_3$ catalyst system. All sets of data were fit to a first order exponential decay model (not shown) to reveal for **39** without fluoride, $k_{\text{obs}} = 0.016 \text{ min}^{-1}$ and with fluoride, $k_{\text{obs}} = 0.21$

min⁻¹ and
min⁻¹

Figure 6.2. Re
NMR relat
(bottom) u
catalyst sy
presence o
All sets of
shown). Th
Figure 6.1.
40 with wa

Figure 6.3. Deta
NMR relat
coupling w
in the prese

Figure 6.4. Reac
relative inte
1.2 equiv of
of fluoride (l
presence of v

Figure 6.5. Activa

Figure 6.6. Mecha

Figure 6.7. Energy

Figure 6.8. Overc
¹¹⁹Sn NMR r
mmol) upon c
catalyst system
presence of 5 μ
5 μ L of water (l
of water (blue t

min⁻¹ and for **40**, $k_{\text{obs}} = 0.0068 \text{ min}^{-1}$ and with fluoride, $k_{\text{obs}} = 0.048 \text{ min}^{-1}$ 131

Figure 6.2. Reaction Profile with Water as an Additive. 186 MHz ¹¹⁹Sn NMR relative integration data for the consumption of **39** (*top*) or **40** (*bottom*) upon coupling with 1.2 equiv of PhI under a Pd₂dba₃/AsPh₃ catalyst system in the absence of fluoride and water (black trace), in the presence of fluoride (red trace), or in the presence of water (blue trace). All sets of data were fit to a first order exponential decay model (not shown). The rate constants with and without fluoride were described in Figure 6.1. For the reaction of **39** with water, $k_{\text{obs}} = 0.27 \text{ min}^{-1}$ and for **40** with water, $k_{\text{obs}} = 0.036 \text{ min}^{-1}$ 134

Figure 6.3. Determination of Water Activation Dependence. 186 MHz ¹¹⁹Sn NMR relative integration data for the consumption of **39** or **40** upon coupling with 1.2 equiv of PhI under a Pd₂dba₃/AsPh₃ catalyst system in the presence of the indicated amount of water..... 136

Figure 6.4. Reaction Profile of Water as an Additive. 186 MHz ¹¹⁹Sn NMR relative integration data for the consumption of **40** upon coupling with 1.2 equiv of PhBr under a Pd₂dba₃/AsPh₃ catalyst system in the absence of fluoride (black trace), in the presence of fluoride (red trace), or in the presence of water (blue trace). 138

Figure 6.5. Activation of Stannane by Hydrogen Bonded Chelation..... 141

Figure 6.6. Mechanism of Transmetallation..... 143

Figure 6.7. Energy Diagram of a Retro-Transmetallation Mechanism²⁰ ... 144

Figure 6.8. Overcoming the Inhibitory Effects of CuI with H₂O. 186 MHz ¹¹⁹Sn NMR relative integration data for the consumption of **58** (0.1 mmol) upon coupling with 1.2 equiv of PhI under a Pd₂dba₃/AsPh₃ catalyst system in the absence of any additives (black trace), in the presence of 5 μL of water (red trace), in the presence of 8 mol% CuI and 5 μL of water (green trace), or in the presence of 8 mol% CuI and 15 μL of water (blue trace). The solid colored lines are to guide the eye..... 153

Figure 6.9. Effect of CuI Using Farina's Order. 186 MHz ^{119}Sn NMR relative integration data for the consumption of trimethylvinyltin (57 , black traces) or tributylvinyltin (58 , red traces) upon coupling with 1.2 equiv of PhI under a $\text{Pd}_2\text{dba}_3/\text{AsPh}_3$ catalyst system in the absence of any additives (solid traces) or in the presence of 8 mol% CuI (dashed traces).	162
Figure 7.1. Activation of Ge-Carbon Bond by Oxygen Chelation.....	182
Figure 8.1. Stannanes with No Coordinative Oxygen	185
Figure 8.2. Pattenden's Sequential Stille Coupling Partners	186
Figure 8.3. Proposed One-Pot Stille Coupling Partners	186
Figure 8.4. Head to Tail Controlled Couplings	187

LIST OF SCHEMES

Scheme 1.1. The Stille Reaction	2
Scheme 1.2. Mechanism of the Stille Reaction	4
Scheme 1.3. Ligand Substitution Process	5
Scheme 1.4. DFT Calculations: Associative vs. Dissociative Pathway ⁸	6
Scheme 1.5. Direct Nucleophilic Attack or Solvent Assisted Attack as Possible Pathways for Associative Ligand Substitution	7
Scheme 1.6. Nucleophilic Aromatic Substitution.....	8
Scheme 1.7. Three-Center Mechanism	8
Scheme 1.8. Stille's Inversion of α -Stereochemistry ¹⁴	10
Scheme 1.9. Falck's Retention of α -Stereochemistry ¹⁷	11
Scheme 1.10. Dual Catalytic Cycle	12
Scheme 1.11. Facile Reductive Elimination.....	15
Scheme 3.1. Palladium Catalyzed Hydrostannation.....	32
Scheme 3.2. <i>In Situ</i> Tin Hydride Generation	32
Scheme 3.3. Initial Stille Reaction of Interest for Kinetics Study	36
Scheme 3.4. Stille Coupling with 4-Bromoanisole	45
Scheme 3.5. Aryl-Phenyl Exchange Process Leading to Cross-Coupled and Phenyl Transfer Products	46
Scheme 3.6. Mechanism of Transmetallation ⁸	50
Scheme 3.7. Stille Coupling Monitored by ¹⁹ F NMR	60

Scheme 3.8. Oxidative Addition of 4-Iodobenzotrifluoride	63
Scheme 4.1. Formation and Inhibition of the Active Catalyst.....	75
Scheme 4.2. Competition Experiment to Test for Trimethyl Stannane Coordination.....	77
Scheme 4.3. Effect of Products On Autocatalysis.....	84
Scheme 4.4. Oxidative Addition Studies by Hartwig ⁴⁷	86
Scheme 4.5. Catalytic Cycle for the Regeneration of Hydrido Palladium Halide	87
Scheme 4.6. Proposed Preparation of TFP ₂ Pd(H)(I) 79	91
Scheme 4.7. Impact of P(<i>t</i> -Bu) ₃ on Bromobenzene Coupling.....	97
Scheme 5.1. Stille Reaction Utilizing Me ₄ Sn as an Internal Standard.....	100
Scheme 5.2. Kocheshkov Disproportionation for the Synthesis of Alkyl Tin Halides.....	100
Scheme 5.3. Synthesis of 2-Tributylstannylfuran.....	107
Scheme 5.4. Benzyl Stannane Formation Observed by Stille ⁵²	112
Scheme 5.5. Pathway to the Formation of Aryl Tins and Resulting Compounds.....	113
Scheme 5.6. R for X vs. R for R Illustration	119
Scheme 5.7. Possible Mechanism of R for R Transmetallation.....	121
Scheme 6.1. Hydrostannation/Stille Sequence Catalytic in Tin.....	124
Scheme 6.2. Me ₃ SnCl as the Tin Source	125
Scheme 6.3. Bu ₃ SnCl as the Tin Source	126

Scheme 6.4. Fluoride Activation of Stannates ⁵⁸	128
Scheme 6.5. Promoting the Stille Reaction with CsF.....	129
Scheme 6.6. Stille Coupling to Determine Fluoride Effect	130
Scheme 7.1. Allylations with Allyl Germane ⁶¹	165
Scheme 7.2. Cross-Couplings of Germastranes ⁶⁵	166
Scheme 7.3. Vinyl Tris(trimethylsilyl)germane Couplings by Wnuk ⁷¹⁻⁷³ ..	167
Scheme 7.4. Trichlorogermane Couplings by Kosugi ⁷⁸	167
Scheme 7.5. Germane Cross-Coupling with Inversion of Olefin Geometry ³¹	170
Scheme 7.6. Proposed Mechanism of Germanium Cross-Coupling	171
Scheme 7.7. Synthesis of Z Germanes.....	180

LIST C

1	1
2	2
3	3
4	4
5	5
6	6
7	7
8	8
9	9
10	10
11	11
12	12
13	13
14	14
15	15
16	16
17	17
18	18
19	19
20	20
21	21
22	22
23	23
24	24
25	25
26	26
27	27
28	28
29	29
30	30
31	31
32	32
33	33
34	34
35	35
36	36
37	37
38	38
39	39
40	40
41	41
42	42
43	43
44	44
45	45
46	46
47	47
48	48
49	49
50	50
51	51
52	52
53	53
54	54
55	55
56	56
57	57
58	58
59	59
60	60
61	61
62	62
63	63
64	64
65	65
66	66
67	67
68	68
69	69
70	70
71	71
72	72
73	73
74	74
75	75
76	76
77	77
78	78
79	79
80	80
81	81
82	82
83	83
84	84
85	85
86	86
87	87
88	88
89	89
90	90
91	91
92	92
93	93
94	94
95	95
96	96
97	97
98	98
99	99
100	100

LIST OF ABBREVIATIONS AND SYMBOLS

γ	gyromagnetic ratio
Δ	change
Ac	acetyl
ACN	acetonitrile
AgNO ₃	silver nitrate
aq	aqueous
B_0	magnetic field
Bu	butyl
cat	catalytic
CH ₂ Cl ₂	dichloromethane
CuTC	copper(I)-thiophene-2-carboxylate
Cy	cyclohexyl
d1	recycle delay
dba	dibenzylideneacetone
<i>E</i>	entgegen (German for opposite)
EI	electron ionization
Et	ethyl
equiv	equivalents

FID	free induction decay
GC	gas chromatography
GC/MS	gas chromatography/mass spectrometry
h	hour
HRMS	high resolution mass spectrometry
Int	internal
<i>k</i>	rate constant
M	molarity
Me	methyl
mL	milliliter
min	minute
mmol	millimole
mol	mole
m.p.	melting point
NBS	<i>N</i> -bromosuccinimide
NMP	<i>N</i> -methyl-2-pyrrolidinone
NMR	nuclear magnetic resonance
NOE	nuclear Overhauser effect
Ph	phenyl
PMHS	polymethylhydrosiloxane

RDS

n

al

SM

TBABr

TBAF

TBS

ti

TEP

TEF

TMS

Z

RDS	rate determining step
rt	room temperature
sat.	saturated
SM	starting material
TBABr	tetrabutylammonium bromide
TBAF	tetrabutylammonium fluoride
TBS	<i>t</i> -butyldimethylsilyl
Tf	triflate
TFP	tri-2-furylphosphine
THF	tetrahydrofuran
TMS	trimethylsilyl
Z	zusammen (German for together)

Chapter 1. An Intro

1.1. Synthetic Impo

Carbon-carbon

manipulations in sym

of simple organic su

products. Cross-cou

trates) under pallad

bond formation. Exa

organotin), Suzuki³

(organozinc) reaction

the high functional

reaction conditions

used in convergen

late stage natural pr

group manipulation

synthesis. Conjugate

A few examples whe

are highlighted.

Chapter 1. An Introduction to the Stille Reaction

1.1. Synthetic Importance of the Stille Coupling

Carbon-carbon bond forming reactions are among the most useful manipulations in synthetic organic chemistry; they allow for the elaboration of simple organic substrates into larger, more complex, and more valuable products. Cross-couplings of organometallics and organic halides (or triflates) under palladium catalysis are a common method for carbon-carbon bond formation. Examples of such include the Stille^{1,2} (organotin = organotin), Suzuki³ (organoboron), Hiyama (organosilane), and Negishi⁴ (organozinc) reactions. The Stille reaction (Scheme 1.1) is often used due to the high functional group tolerance of the organotin reagents and the mild reaction conditions necessary to effect coupling. Therefore, it has been useful in convergent approaches to highly functionalized compounds (i.e. late stage natural product synthesis) without the need for tedious protecting group manipulations that may severely diminish the overall yield of a synthesis. Conjugated π systems are particularly accessible by this method. A few examples where the Stille reaction has been utilized as a key synthetic step are highlighted in Figure 1.1. Additionally, the increased access to

organotin reagents⁵ and the stability to both air and moisture has allowed for the implementation of this method.

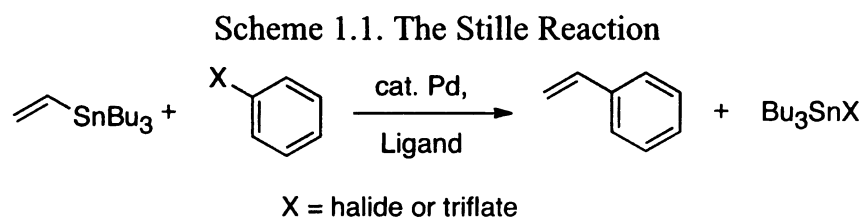
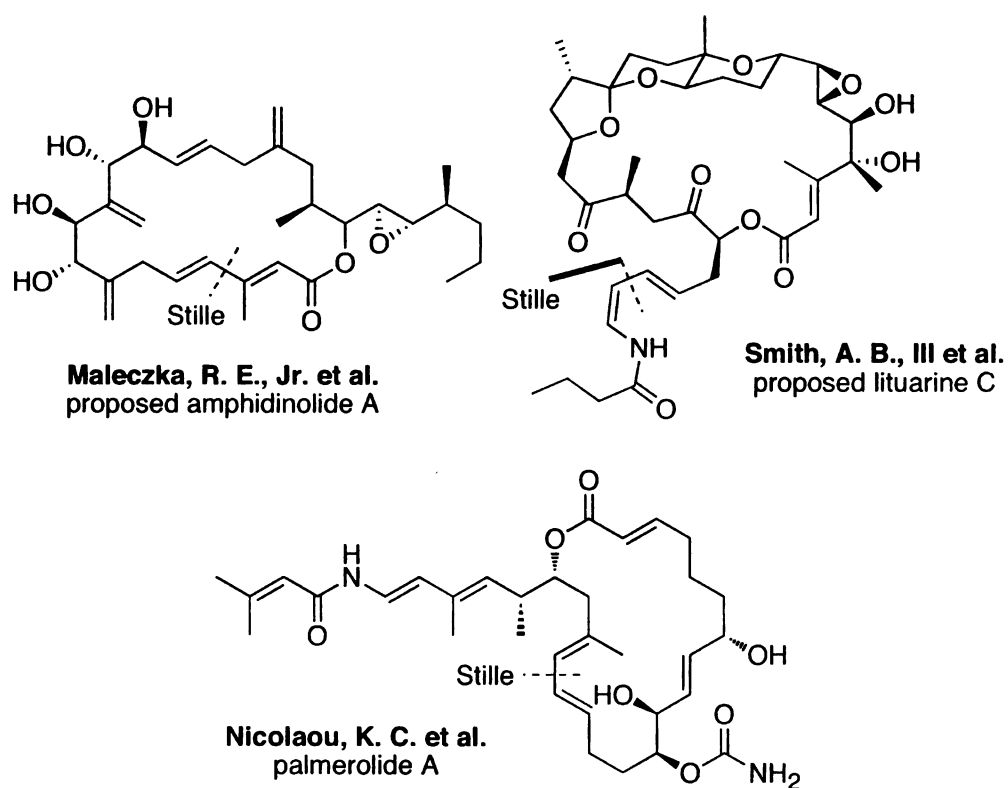


Figure 1.1. Selected Natural Products Prepared with a Stille Coupling as a Key Synthetic Step

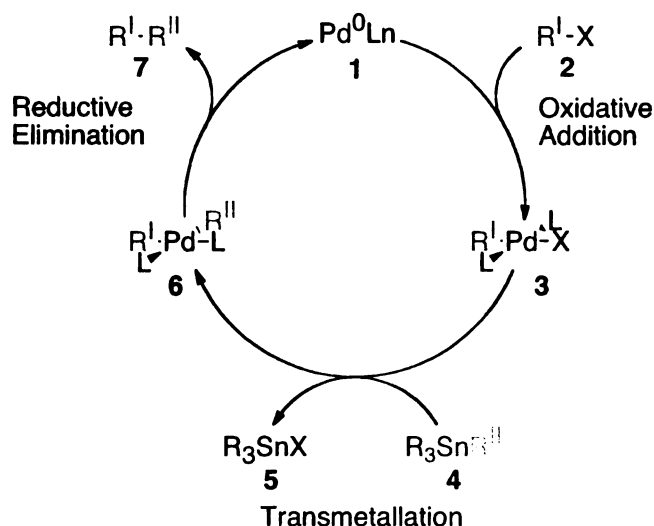


1.2. The Catalytic Cycle

Cross-coupling reactions are most often mediated by catalytic amounts of palladium through a three step catalytic cycle. The main steps of the catalytic cycle are common to all cross coupling reactions and include oxidative addition, transmetallation, and reductive elimination as shown in Scheme 1.2 specifically for the Stille reaction. Oxidative addition occurs when a Pd(0) species (1) inserts into a carbon-halide or -triflate bond to form an activated Pd(II) species (3). Transmetallation involves the transfer of an organo group from the organometallic to Pd while also producing the tin halide by-product (5). Lastly, reductive elimination of the Pd(II) species (6) affords the cross-coupled organic product (7) and regenerates the Pd(0) catalyst (1).⁶ Mechanistically however, these steps are quite complex. Ligand isomerizations, dissociations, and substitutions are necessary for the reaction to progress and should not be overlooked in order to fully understand the “mechanism” of the Stille reaction, or any other cross-coupling reaction.



Scheme 1.2. Mechanism of the Stille Reaction

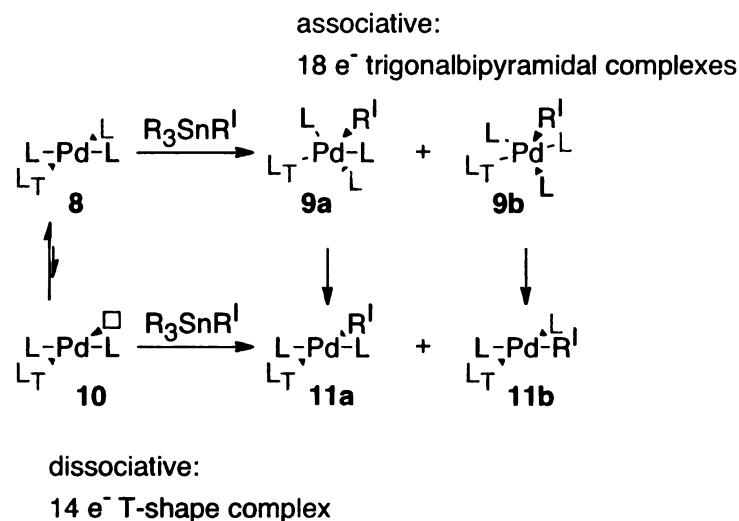


1.2.1. Ligand Substitution: Associative vs. Dissociative

The catalytic cycle is a series of ligand substitutions and isomerizations about palladium. To achieve ligand substitution, two pathways are plausible: associative or dissociative. In an associative mechanism, a nucleophile attacks the 16 e^- square planar Pd center (**8**) resulting in an 18 e^- trigonalbipyramidal complex (**9**) (Scheme 1.3).⁷ The site of substitution to afford **11** is dependent on the *trans* effect of the ligands. In the dissociative mechanism, the ligand with the highest *trans* influence determines which ligand will dissociate to afford a 14 e^- T-shape complex (**10**) in which the nucleophile may then occupy the vacant site to afford **11**.⁷ Although there are two possible pathways, dissociative

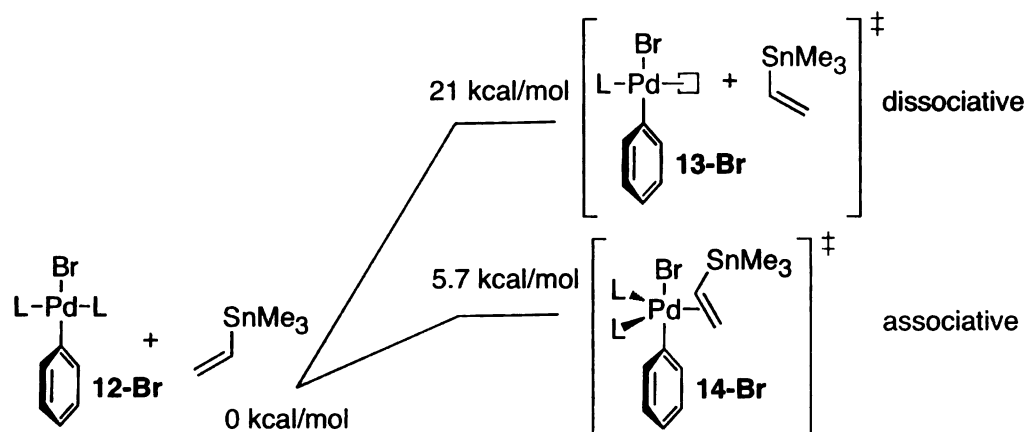
mechanisms are rare in ligand substitution processes. Typically a very electron rich metal center such as Pt is necessary to invoke a dissociative mechanism and it is realized that in most cases ligand substitutions in the Stille reaction occur by an associative mechanism.^{2,7}

Scheme 1.3. Ligand Substitution Process



Recently, Espinet conducted DFT calculations that provide further evidence for a dominant associative process.⁸ He showed that the transmetallation step has a 21 kcal/mol barrier to overcome in a dissociative process but only a 5.7 kcal/mol barrier through an associative process when $L = AsH_3$ in the gas phase (Scheme 1.4). The same trend is observed with PPh_3 as the ligand in the gas phase as well as in THF for both ligands. This clearly indicates that ligand substitutions favor an associative process.

Scheme 1.4. DFT Calculations: Associative vs. Dissociative Pathway⁸

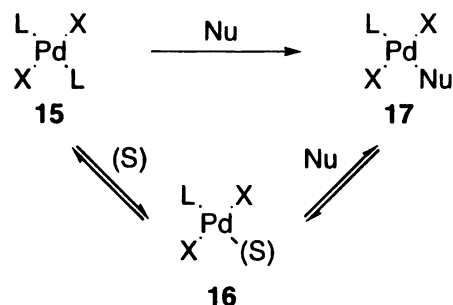


1.2.2. Ligand Substitution: Direct vs. Solvent Assisted

Although ligand substitutions are typically envisioned as a direct replacement of one ligand with an incoming nucleophile (Nu), it can also proceed through a solvent assisted pathway (Scheme 1.5). Solvent molecules are in high concentration relative to other ligands or nucleophiles. Thus, when a strongly coordinating solvent such as *N*-methyl-2-pyrrolidinone (NMP) is utilized, it is able to replace ligands through an associative mechanism, providing a more activated Pd species. This solvento complex may then undergo substitution with the nucleophile. The overall ligand substitution is achieved either directly or by solvent assisted pathways, but the solvent assisted pathways greatly facilitate ligand substitutions.² Solvent molecules can aid in ligand substitutions, as well as help to stabilize Pd

complexes throughout the catalytic cycle to avoid decomposition to unreactive Pd black.

Scheme 1.5. Direct Nucleophilic Attack or Solvent Assisted Attack as Possible Pathways for Associative Ligand Substitution



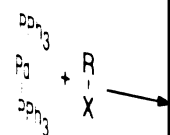
1.3. Oxidative Addition: Pd Insertion into C-X bond

Oxidative addition involves insertion of a low-valent, coordinatively unsaturated nucleophilic $\text{Pd}(0)$ species into a carbon-halide or -triflate bond. This species is accessed through solvent assisted ligand dissociation of the precatalyst, PdL_4 , to afford the solvent stabilized “active” catalytic species, $(\text{S})\text{PdL}_2$. Formation of these types of stabilized compounds have been observed and intensely studied by Jutand and Amatore.⁹

Initially however, two mechanisms for the oxidative addition to aryl halides were proposed by Stille.¹⁰ One proposal is similar to nucleophilic aromatic substitution¹¹ (Scheme 1.6) where electron withdrawing substituents on the ring have been shown to facilitate the oxidative addition

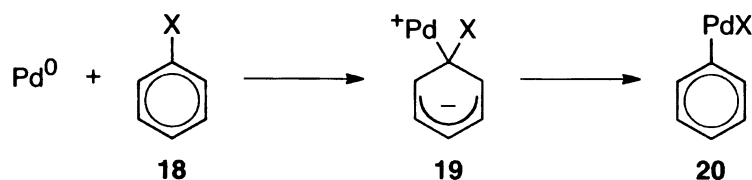
process. The second
 mechanism via a th
 cis complex (23). If
 NMR, only the *trans*
 product has an R g
 ous influence of t
 may isomerize to t
 phosphine in a *cis* r
 the rate-determining
 the mechanism.²

Schem

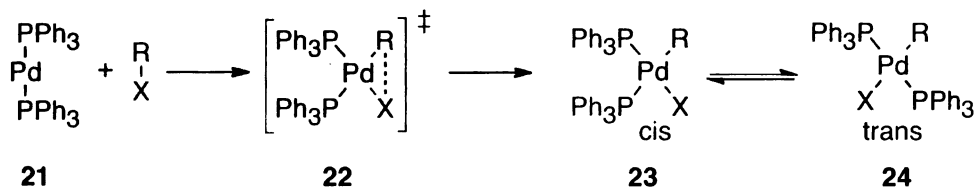


process. The second proposed mechanism proceeds through a concerted mechanism via a three-center transition state¹² (Scheme 1.7) resulting in a *cis* complex (**23**). However, upon monitoring the oxidative addition by ³¹P NMR, only the *trans* oxidative addition product (**24**) was observed. The *cis* product has an R group and phosphine ligand in a *trans* relationship. The *trans* influence of these ligands results in destabilization and the product may isomerize to the thermodynamically stable *trans* isomer (with R and phosphine in a *cis* relationship).¹³ This isomerization occurs fast relative to the rate-determining transmetallation step and is typically not considered in the mechanism.²

Scheme 1.6. Nucleophilic Aromatic Substitution



Scheme 1.7. Three-Center Mechanism



14. Transmetalation

While oxidative

cross coupling react

step is unique to

understood step of

transfer of a ligand

palladium. Initial st

by $^1\text{P NMR}$ reveals

even upon addition

found to be zero-or

These results sug

organohalide electro

elimination, and an

transmetalation is

reaction. Organotr

additive addition w

14.1. Mechanism of

In the origin

suggested to take

1.4. Transmetallation: Transfer of Tin Ligand to Palladium

While oxidative addition and reductive elimination are common to all cross coupling reactions and have been studied in depth, the transmetallation step is unique to each cross coupling reaction and is thus the least understood step of the Stille reaction. Overall, transmetallation involves transfer of a ligand coordinated to tin in exchange for a ligand coordinated to palladium. Initial studies where Stille monitored the course of the reaction by ^{31}P NMR revealed the observation of only the oxidative addition product, even upon addition of excess stannane.^{1,14} Furthermore, the reaction was found to be zero-order in electrophile (iodobenzene) by Stille and others. These results suggest that transmetallation is the slow step when organohalide electrophiles are utilized, while oxidative addition, reductive elimination, and any necessary isomerizations occur much faster. *Therefore, transmetallation is considered the rate-determining step for the Stille reaction.* Organotriflate electrophiles proved more complex¹⁵ such that oxidative addition was suggested as the rate-determining step in THF.¹⁶

1.4.1. Mechanism of Transmetallation

In the original mechanistic proposal by Stille, transmetallation was suggested to take place by an $\text{S}_{\text{E}}2$ mechanism (in which Pd is the

2

electrophile) via a

supports experimen

carbon to tin occur

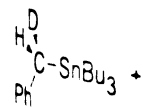
hexamethylphospho

workers observe

PdCu catalyst sys

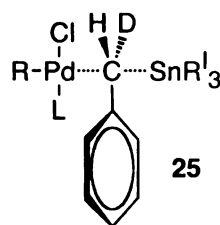
was necessary to ac

Scheme

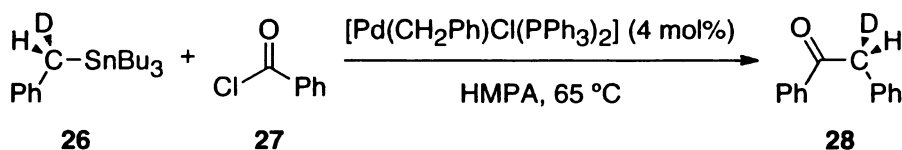


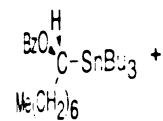
electrophile) via an open transition state (Figure 1.2).¹⁴ This proposal supports experimental evidence that inversion of configuration at the α -carbon to tin occurs when subjected to Stille cross-coupling conditions in hexamethylphosphoramide (HMPA).¹⁴ About a decade later, Falck and coworkers observed retention of configuration in toluene when utilizing a Pd/Cu catalyst system.¹⁷ Reevaluation of the transmetallation mechanism was necessary to account for retention *and* inversion of stereochemistry.

Figure 1.2. Open Transition State¹⁴



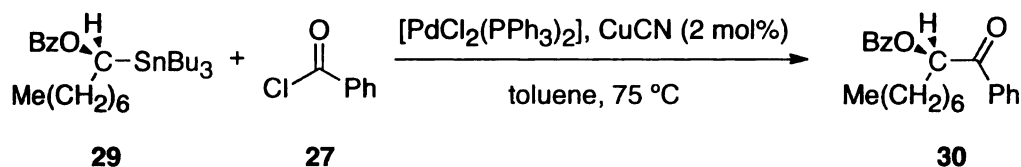
Scheme 1.8. Stille's Inversion of α -Stereochemistry¹⁴





A dual catalytic cycle is proposed for the opposing stereochemical transition state is an associative process.² The bridge resulting from the Pd complex (35) is coupled product. Even stereochemistry at the transition state proposed by Still may be formed. With product. This pathway is carbon. The dominant environment. General open mechanism is while the cyclic mechanism. Espinet has verified

Scheme 1.9. Falck's Retention of α -Stereochemistry¹⁷

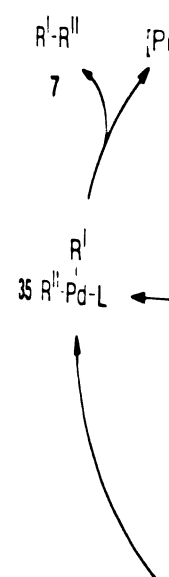


A dual catalytic cycle (Scheme 1.10) proposed by Espinet can account for the opposing stereochemical outcome where either a cyclic or open transition state is possible and where both pathways operate by an associative process.^{2,18} The cyclic transition state pathway forms a Sn–X–Pd bridge resulting from substitution for L (not X) and subsequently affords the *cis* Pd complex (35) and immediate reductive elimination to give the cross-coupled product. Evaluation of the transition state suggests retention of stereochemistry at the α -carbon. Following an open transition state similar to that proposed by Stille, both *cis* (6) and *trans* (33) transmetallation products may be formed, with the *cis* isomer directly leading to the cross-coupled product. This pathway results in inversion of stereochemistry at the α -carbon. The dominant pathway is dependent on the substrates and environment. Generally, although there are many determining factors, the open mechanism is favored for triflates and very polar solvents (i.e. HMPA), while the cyclic mechanism is favored for halides since bridging can occur. Espinet has verified the possibility for both an open^{16,19} and cyclic^{8,20}

mechanism by kinetic

by NMR. Espinet.

intermediates involv



14.2. Improvement

It has been sh

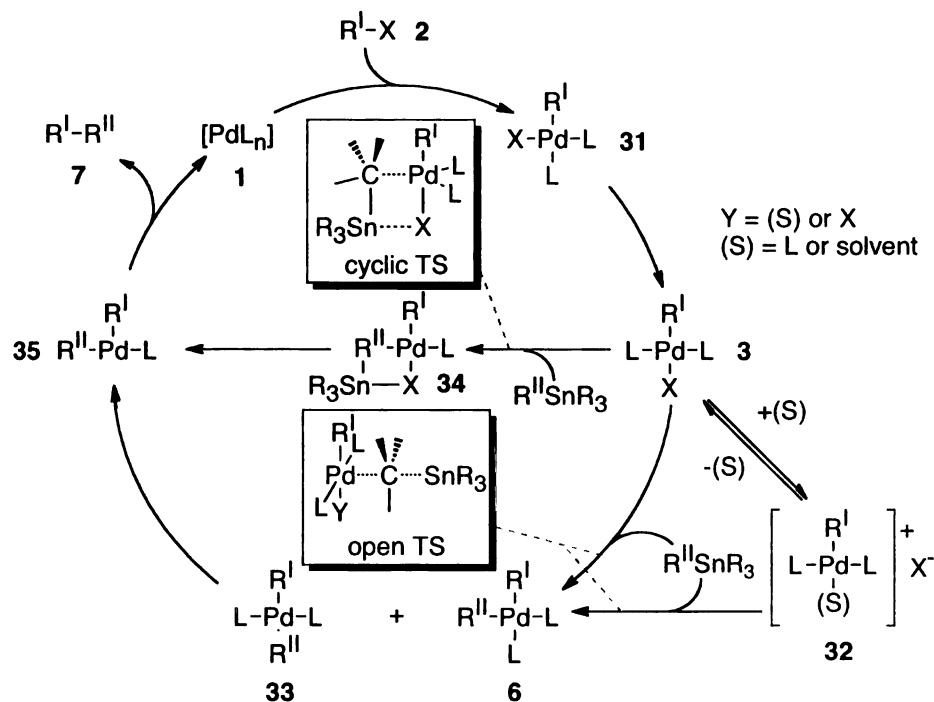
mechanism of the

partners¹⁵ and additi

ected to a review

mechanism by kinetically deducing the pathway and observing intermediates by NMR. Espinet,⁸ along with Alvarez and deLera²¹, have revised the intermediates involved in the dual catalytic cycle based on DFT calculations.

Scheme 1.10. Dual Catalytic Cycle



1.4.2. Improvements on the Transmetalation Step

It has been shown that solvent^{14,17} can greatly affect the outcome and mechanism of the reaction. Other studies have indicated that coupling partners¹⁵ and additives,^{15,19,22,23} can affect changes as well. The reader is directed to a review on the Stille reaction, published by Farina in 1997, for a

more in depth and

and additives.²⁴

A major a

rate enhancement

ligands.²⁵ Prior

$\text{Pd}(\text{PPh}_3)_4$. Howe

to store it in the

since the ligands

with stable Pd_2Cl_2

mixture to the S

catalytic behavior

performed under

demonstrate that

large rate enhan

respectively. Fur

ligand ratio of 1

further increase

down, confirmin

more in depth analysis of the scope and limitations of the coupling partners and additives.²⁴

A major advancement for the Stille reaction was Farina's report on rate enhancements using tri-2-furylphosphine (TFP) and AsPh₃ as Pd ligands.²⁵ Prior to this report, the most common Pd catalyst used was Pd(PPh₃)₄. However, this catalyst is somewhat unstable; care must be taken to store it in the freezer and use it in a glove box, or at least a glove bag since the ligands are susceptible to oxidation. Farina showed that starting with stable Pd₂dba₃, premixing it with PPh₃, then subjecting this catalyst mixture to the Stille coupling partners resulted in a reaction with identical catalytic behavior to that with Pd(PPh₃)₄. These reactions could also be performed under mild reaction temperatures of only 50 °C. He went on to demonstrate that substituting either TFP or AsPh₃ as the ligand resulted in large rate enhancements, *two to three orders of magnitude* over PPh₃, respectively. Furthermore, controlling the stoichiometry with a palladium to ligand ratio of 1:2 would favor formation of the active (S)PdL₂ species and further increase the rate of reaction. Excess ligand slowed the reactions down, confirming that ligand dissociation is a key step in the catalytic cycle.

Ligand inhibition

reaction conditions

15. Reductive EL

Regeneration

Overall, re

forming step and c

are coupled together

transmetallation m

and can immediately

act in a *cis* relation

dissociation substitu

Reductive e

preceding *cis* prod

of both β -hydride

the reductive elim

elimination is ofte

very facile reaction

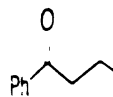
elimination suggest

Ligand inhibition factors were calculated based on these results.²⁵ These reaction conditions are now commonly used in Stille couplings.

1.5. Reductive Elimination: Carbon-Carbon Bond Formation and Pd Regeneration

Overall, reductive elimination is the actual carbon-carbon bond-forming step and occurs when two organogroups in a *cis* relationship on Pd are coupled together and eliminate a reduced Pd(0) species. In the cyclic transmetallation mechanism, transmetallation directly forms the *cis* product and can immediately undergo reductive elimination. If the organogroups are not in a *cis* relationship, they must first isomerize via solvent assisted ligand dissociation/substitutions described in Sections 1.2.1 and 1.2.2.

Reductive eliminations are thought to be fast reactions once the preceding *cis* product is formed. In fact, Stille found that a species capable of both β -hydride elimination and reductive elimination (**36**) only produces the reductive elimination product (**37**) (Scheme 1.11).¹ Since β -hydride elimination is often a problem in organometallic chemistry because it is a very facile reaction, the preference for reductive elimination over β -hydride elimination suggests that reductive elimination is faster.



37

1.6. Towards

Numerical

additives. 19.22

mechanism. C

focus on the

ligands on tin

stannane is im

the non-trans

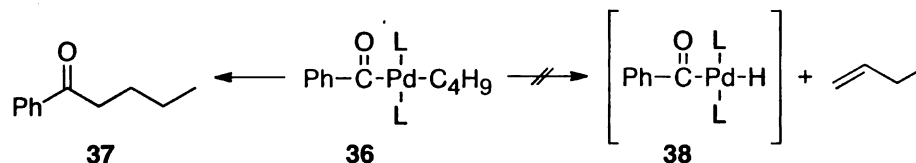
stannanes rea

beneficial to

our objective

ligands on tin

Scheme 1.11. Facile Reductive Elimination



1.6. Towards a Better Understanding of the Stille Reaction

Numerous studies have shown that solvent,^{14,17} ligands on Pd,^{25,26} additives,^{19,22} and electrophiles²⁷ can change the kinetics and/or operative mechanism. Our approach to further understanding the Stille reaction was to focus on the stannane. Specifically, we asked how the non-transferable ligands on tin (denoted R in Scheme 1.2) would affect the reaction since the stannane is involved in the rate determining transmetallation step. Typically the non-transferable ligands are either methyl or butyl, where the trimethyl stannanes react faster, but are more toxic and more expensive. It would be beneficial to further understand the differences between them and it became our objective to provide relative rates of reaction per the non-transferable ligands on tin.

Chapter 2. An

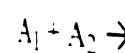
2.1. Homogene

As discus

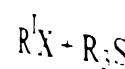
three-step proc

reductive elimi

second order rea



or more specific



Since the transi

the reaction wi

dependent on

$[R^1PdX]$ and s

$$\text{rate} = k_{\text{tran}}$$

Since Pd is cata

of R^1PdX is c

constant k_{trans}

equation then t

Chapter 2. An Introduction to Kinetics, ^{119}Sn NMR, and Data Analysis

2.1. Homogeneous Catalysis Kinetics

As discussed in Chapter 1, the Stille reaction proceeds through a three-step process including oxidative addition, transmetallation, and reductive elimination (Figure 1.1). The reaction scheme is a catalyzed second order reaction of the form



or more specifically



Since the transmetallation is said to be rate determining, the overall rate of the reaction will be defined by this step. The rate equation should then be dependent on both the concentration of the oxidative addition product ($[\text{R}^{\text{I}}\text{PdX}]$) and starting stannane ($[\text{Sn}]$)

$$\text{rate} = k_{\text{trans}}[\text{Sn}][\text{R}^{\text{I}}\text{PdX}] \quad (3)$$

Since Pd is catalytic and there is excess electrophile ($\text{R}^{\text{I}}\text{X}$), the concentration of $\text{R}^{\text{I}}\text{PdX}$ is constant relative to Sn and can be combined with the rate constant k_{trans} to obtain a new observable rate constant, k_{obs} . The rate equation then becomes independent of $\text{R}^{\text{I}}\text{X}$ and can be reevaluated as the

pseudo first order

$$\text{rate} = k_{\text{obs}}$$

(4) It should be

$$[X] < [Sn].$$

$[PdX]$ will d

to deviate from

integration of

$$\ln[Sn]_t =$$

or the exponen

$$[Sn]_t = [S$$

where the con

consumption of

2.2. Developm

We next

the ability to r

of monitoring

track with one

then used for

time point and

pseudo first order rate law

$$\text{rate} = k_{\text{obs}}[\text{Sn}]$$

(4) It should be realized that this analysis is only valid when $[\text{R}^{\text{I}}\text{X}] > [\text{Sn}]$. If $[\text{R}^{\text{I}}\text{X}] < [\text{Sn}]$, towards the end of the reaction, when $[\text{R}^{\text{I}}\text{X}]$ approaches zero, $[\text{R}^{\text{I}}\text{PdX}]$ will decrease and no longer be constant. This will cause the kinetics to deviate from first order behavior.

Integration of Eq. 4 reveals the linear equation

$$\ln[\text{Sn}]_t = \ln[\text{Sn}]_0 - k_{\text{obs}}t \quad (5)$$

or the exponential function

$$[\text{Sn}]_t = [\text{Sn}]_0 e^{-k_{\text{obs}}t} \quad (6)$$

where the consumption of stannane is exponential in time and therefore consumption of stannane may be monitored to study the kinetics.

2.2. Development of a Data Acquisition Method

We next decided upon a method to monitor the reaction. We required the ability to monitor consumption of the stannane and also have the option of monitoring product formation to ensure that consumption and formation track with one another. Gas chromatography meets these requirements and is often used for kinetic studies. Unfortunately, aliquots must be taken for each time point and are typically worked up or filtered. This is not only tedious

and allows for lar

points collected. 7

analyze the data:

treatment puts gre

highest error as t

problem, only the

simple kinetics ex

features toward the

Monitoring

associated with G

and formation of th

Also, running the

points to be collec

One disadvantage

we would be perfor

reactions be done

would be utilized

deuterated solvents

THF- d_4 costs ~\$15

more importantly,

and allows for larger amounts of error, but also limits the number of data points collected. Therefore, one must rely on linear regression analysis to analyze the data: $\ln[\text{Sn}]$ vs. time is plotted where the slope = $-k$. This treatment puts great emphasis on the later parts of the reaction that has the highest error as the signal to noise ratio approaches zero. To avoid this problem, only the first few half-lives of the reaction are typically analyzed in simple kinetics experiments but could allow one to miss key mechanistic features toward the end of the reaction.

Monitoring reaction progress by NMR can alleviate shortcomings associated with GC. With ^1H NMR, the consumption of starting material and formation of the product can be monitored simultaneously (Figure 2.1a). Also, running the reaction in the spectrometer allows for numerous data points to be collected as well as minimization of human error/interference. One disadvantage is that the use of deuterated solvents is necessary. Since we would be performing a series of studies, it was important that all of the reactions be done at precisely the same concentration. Therefore, solutions would be utilized for the preparation of each sample, making the use of deuterated solvents unreasonable from a cost standpoint: A 0.7 mL vial of THF- d_8 costs ~\$15 and over \$100 for NMP- d_9 . Furthermore and perhaps more importantly, we did not want to be confined by the availability of

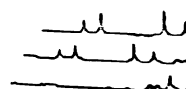
deuterated solvents

by suppressing the

However, in our case

not ideal for quantitation

Figure 2.1. ^1H NMR



a) ^1H NMR

We then compare

of ^1H NMR, but also

the atoms in the

competition experiments

distinct signal in

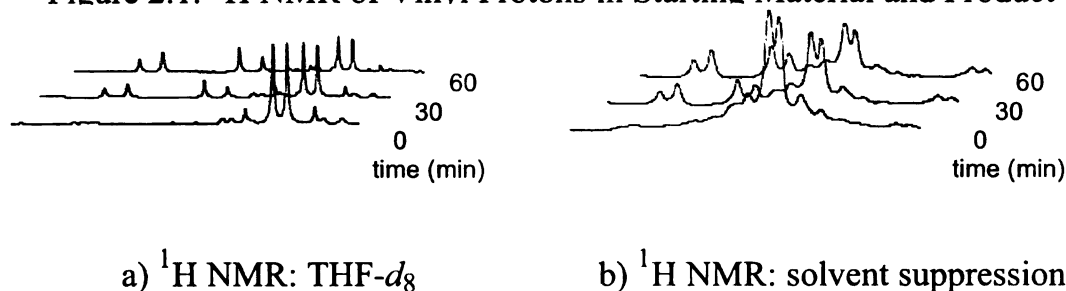
^1H NMR spectrum

that we would be

are often ignored

deuterated solvents as the study progressed. Protonated solvents may be used by suppressing the intensity of the solvent signal with presaturation. However, in our case this resulted in peak broadening and overlap, which is not ideal for quantitative analysis (Figure 2.1b).

Figure 2.1. ^1H NMR of Vinyl Protons in Starting Material and Product



We then considered ^{119}Sn NMR. This method retains the advantages of ^1H NMR, but allows for the use of protonated solvents since there are no tin atoms in the solvent. ^{119}Sn NMR would also allow for us to run competition experiments between trialkyl stannanes. Each stannane has a distinct signal in the ^{119}Sn NMR (Figure 2.2) whereas the vinyl protons in a ^1H NMR spectrum would be difficult to distinguish. It is also advantageous that we would be able to monitor the fate of the tin species as tin by-products are often ignored in the context of kinetic studies.

Figure 2.2

Me_4Sn

0

2.3. Properties

The pro

order to utilize

we had to co

properties of t

sample is plac

will align with

test will occur

as the energy

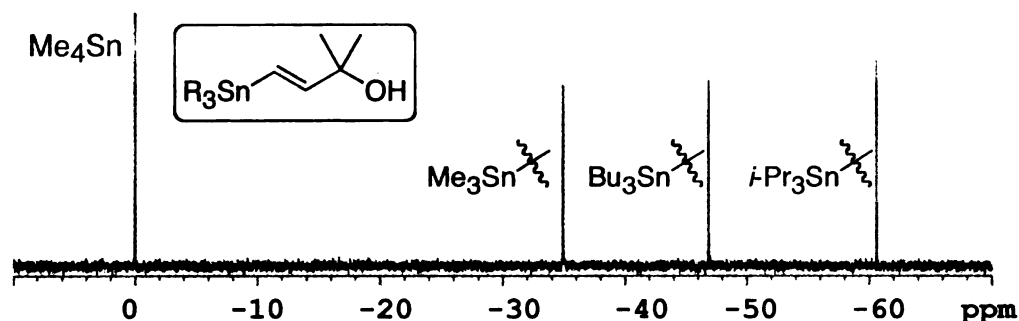
radio frequenc

uncertainty pr

environment is

emission ($\sim 1/2$ t

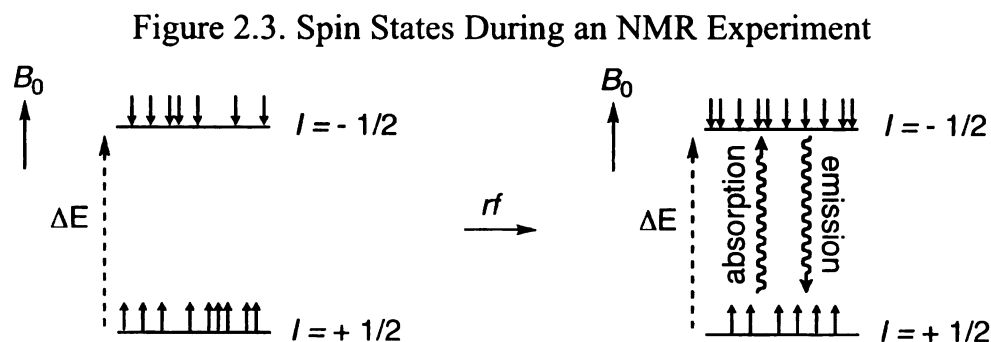
Figure 2.2. ^{119}Sn NMR Spectrum of Distinct Vinyl Stannanes in THF



2.3. Properties of ^{119}Sn NMR

The process of how NMR data is obtained often goes unconsidered. In order to utilize ^{119}Sn NMR as a true representation of the reaction course, we had to consider the underlying principles of NMR as well as the properties of the Sn nucleus. When an NMR experiment is performed, the sample is placed in a magnetic field, B_0 , where a slight majority of the spins will align with the magnetic field in the ground state of spin $+\frac{1}{2}$ while the rest will occupy $-\frac{1}{2}$. The preference for $+\frac{1}{2}$ over $-\frac{1}{2}$ occupancy is increased as the energy difference between these two states is increased. When a short radio frequency (RF) pulse with a frequency spread due to the Heisenberg uncertainty principle is applied, excitation of all the nuclei in the local environment is achieved in the form of absorption (from $+\frac{1}{2}$ to $-\frac{1}{2}$) and emission ($-\frac{1}{2}$ to $+\frac{1}{2}$) (Figure 2.3). Since the ground state of $+\frac{1}{2}$ has slightly

higher occupancy, there will be net absorption. The absorption of energy back to the ground state is displayed in the NMR spectra as a signal after Fourier transform of the FID. It is important to understand the correlation between all of these factors: Increasing B_0 , increases the energy difference between the spin states, which in turn increases the occupancy of the lower spin states allowing for greater net absorption upon irradiation and a larger observed signal.



The energy difference between the two spin states is dependent on the constant \hbar , the magnetic field, and the gyromagnetic ratio (γ) by

$$\Delta E = \gamma \hbar B_0 \quad (7)$$

Here it is necessary to discuss the importance of the gyromagnetic ratio in the context of tin NMR. There are three spin $\frac{1}{2}$ tin nuclei: ^{115}Sn , ^{117}Sn , and ^{119}Sn . We will be utilizing ^{119}Sn because it has the highest natural abundance of 8.59%. The Sn nuclei all exhibit negative gyromagnetic ratios

where that of ^{119}Sn

with respect to ΔE .

it does have implica

The nuclear C

that is doubly irradi

$$\eta = (I - I_0) / I_0$$

where η is the effec

I is the intensity w

be described as

$$\eta_{\max} = \gamma_{\text{irr}} / 2\gamma$$

If the two nuclei

enhancement of the

tion, γ is negative for

our study is to obs

want to artificially

an NOE build-up.

sequence of the N

decoupling such th

the acquisition tim

where that of ^{119}Sn is -10.0317. The fact that it is negative is not important with respect to ΔE , as this just means that $-1/2$ is the ground state. However, it does have implications regarding the data acquisition.

The nuclear Overhauser effect is a phenomenon in which one nucleus that is doubly irradiated can enhance the signal of another and is defined by

$$\eta = (I - I_0)/I_0 \quad (8)$$

where η is the effect (or enhancement), I is the intensity with irradiation, and I_0 is the intensity without double irradiation. The maximum effect, η_{max} , can be described as

$$\eta_{\text{max}} = \gamma_{\text{irr}}/2\gamma_{\text{obs}} \quad (9)$$

If the two nuclei are the same (i.e. both are protons), there is net enhancement of the signal. However, in regards to proton decoupling of the tin, γ is negative for tin and would thus decrease the signal. Since the key to our study is to observe the consumption of our starting stannane, we do not want to artificially deplete the stannane signal. Care must be taken to avoid an NOE build-up, which is actually depletion in this case. In the pulse sequence of the NMR experiment (Figure 2.4) we use inverse gated proton decoupling such that decoupling (the green box) is only performed during the acquisition time. The time preceding the acquisition is the rest time

where NOE's ma

during the rest tim

recycle delay (d1)

value is determin

the applied RF.

recovered. If sub

depletion of the s

Each nucleus ha

Therefore, the d

It was found that

where NOE's may build up if set to decouple. By avoiding decoupling during the rest time, we avoid depleting the signal. It is important to set the recycle delay (d1) to an appropriate value in the pulse sequence as well. This value is determined by the time constant (T_1) in which the spins relax after the applied RF. When $d1 = 5 \times T_1$, 99.33% of magnetization has been recovered. If substantial time is not given, this too will result in artificial depletion of the signal because relaxation relates to occupation of spin states. Each nucleus has a different relaxation time in different environments. Therefore, the d1's for the stannanes of interest were obtained (Table 2.1). It was found that relaxation time was independent of solvent.

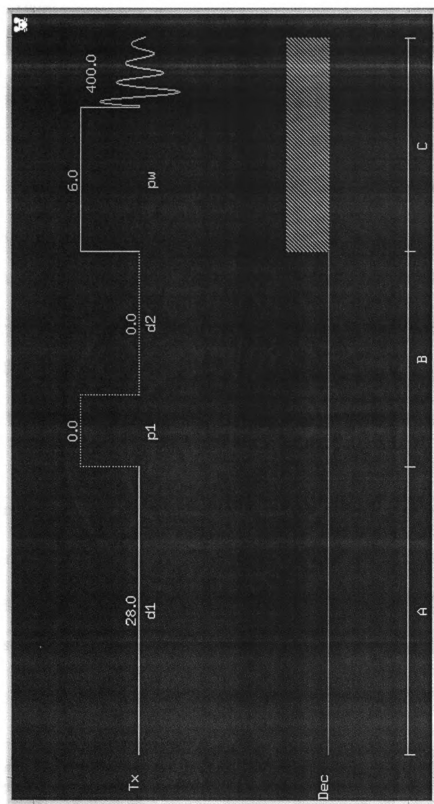


Figure 2.4. Pulse Sequence of a Typical ^{19}Sn NMR Kinetics Experiment. All kinetics experiments utilized inverse gated decoupling where ^1H decoupling is only performed during the acquisition (green box) and not during the rest period (blue line). For the reaction with 40, the recycle delay ($d1$) is set to 28 sec as shown.

Table 2.1. Detec

With the ¹¹⁹

performed such th
throughout the cou
concentration deter
integrated relative t

2.4. Data Analysis

Once data w
the macro *intall3*.[†]
be integrated over
integration values
the series was set to
fit. The integratio

[†] *intall3* is a macro wh
integrate all spectra w
first spectra.

[‡] Typically kinetics p
the stannane is m

Table 2.1. Determination of the Relaxation Time in THF and NMP

$\text{R}_3\text{Sn}-\text{CH}=\text{C}(\text{OH})\text{CH}_3$		
R	T_1 (sec)	d_1 (sec)
Me (39)	1.65	10
Bu (40)	5.80	28

With the ^{119}Sn parameters defined, arrayed experiments could be performed such that spectra are acquired at designated time intervals throughout the course of the reaction. The use of internal standards for concentration determination is unnecessary because the signals could be integrated relative to each other.

2.4. Data Analysis Methods

Once data were collected, the spectra were identically integrated using the macro *intall3*.[†] This allows for spectra in a given arrayed experiment to be integrated over precisely the same regions as well as normalizing the integration values relative to each other. For instance, the first spectrum in the series was set to 100 and the subsequent spectra are integrated relative to that. The integration values[‡] (stannane consumption) were then plotted vs.

[†] *intall3* is a macro written by Dr. Daniel Holmes of the Max T. Rogers NMR Facility to integrate all spectra within an arrayed experiment over the same region and relative to the first spectra.

[‡] Typically kinetics plots show concentration vs. time. However, ~2 min passes from the time the stannane is injected into the sample and the data collection begins. At this point,

time. The pro

2.5) to a first

the reaction in

a portion of the s
that concentrat
concentration. Is

time. The program OriginPro 7.5²⁸ was used to plot and fit the data (Figure 2.5) to a first order exponential function (Eq. 6) to obtain a rate constant for the reaction in the form of the lifetime, τ , where $k = 1/\tau$.

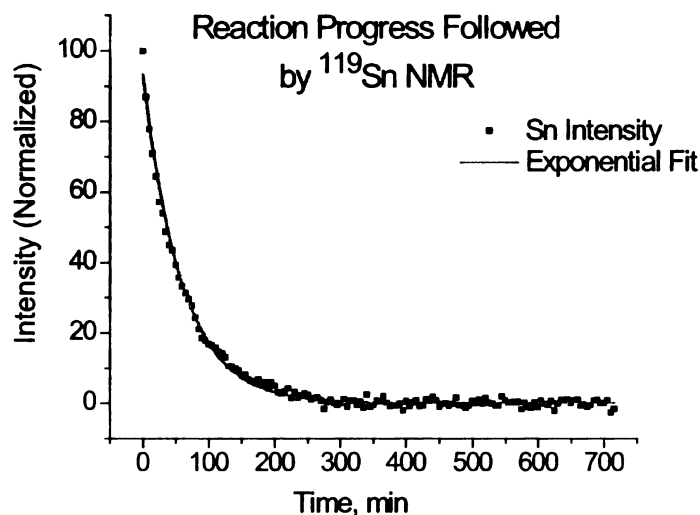
a portion of the starting material has already been consumed and we cannot be sure of the exact concentration. Therefore, the signal intensity, which is a proportional value to concentration, is used instead.

a) Gr

Intensity (Normalized)
100
80
60
40
20

Figure 2.5. First (O) and second (●) order ^{119}Sn NMR spectra of the reaction of **40** with **1**. The first order spectrum was integrated and the data shown in the table were fitted to a first order exponential decay related to k_{obs} by $1 - e^{-k_{\text{obs}}t}$.

a) Graphical representation of exponential fit



b) Numerical parameters from fit

$$\text{Equation: } y = Ae^{-x/\tau} + y_0$$

$$R^2 = 0.99502$$

$$y_0 = 0.16169 \pm 0.13013$$

$$A = 93.06808 \pm 0.68886$$

$$\tau = 58.71986 \pm 0.71412$$

Figure 2.5. First Order Exponential Curve Fitting with OriginPro 7.5. 186 MHz ^{119}Sn NMR spectra were obtained every 5 min over the course of the reaction of **40** with PhI under a $\text{Pd}_2\text{dba}_3/\text{AsPh}_3$ catalyst system. Each spectrum was integrated relative to the first to obtain the relative integration data shown in the black trace. The solid red line represents the fit to a first order exponential decay model to reveal $\tau = 58.7 \pm 0.71$ min, which is related to k_{obs} by $1/\tau$ where $k_{\text{obs}} = 0.017 \text{ min}^{-1}$.

Chapter 3. Quan

3.1. Initial Objec

Most of the
transmetallation
organohalides. Cha
of the reaction. T
solvent and Pd lig
non-transferable
knowledge that t
counterparts, no i
understand the exte
the trimethyl stanna
stannanes, it would
over the other. Thus
community with a s
trialkyl stannanes ac

3.2. Coupling Partn

The Stille reac
bonds between vari

Chapter 3. Quantifying Rate Differences for Trialkyl Stannanes

3.1. Initial Objective of the Study

Most of the kinetic studies on the Stille reaction have regarded transmetallation as the rate-determining step for reactions with organohalides. Changes to this step should lead to changes in the overall rate of the reaction. Therefore, many studies have focused on the effects of solvent and Pd ligands. In addition, the ligands employed on the stannane (non-transferable ligands) have an impact. Although it is common knowledge that trimethyl stannanes couple faster than their tributyl counterparts, no in depth systematic studies have been performed to understand the extent and generality of these differences. Given the fact that the trimethyl stannanes are far more toxic and more expensive than tributyl stannanes, it would be useful to further understand the benefits of using one over the other. Thus, our first objective was to provide the synthetic organic community with a systematic analysis of the coupling rates between these trialkyl stannanes across a range of electrophiles.

3.2. Coupling Partner Choices

The Stille reaction is useful in the formation of new carbon-carbon σ bonds between variations of sp^3 , sp^2 , and sp -hybridized carbon atoms.

However, sp^2 -

towards coupl

side-reaction i

and are preval

Since co

thought it was

ouple vinyl s

vinyl stannane

3.3. Discussion

We util

Access to st

hydrostannatio

propargylic po

opposed to t

precedented.²⁹

protection of 3

However, $\text{sp}^2\text{-sp}^2$ couplings are most common as they are highly activated towards coupling, are known to retain olefin geometry¹, and have limited side-reaction issues. The resulting conjugated π systems are easily accessed and are prevalent in natural products (highlighted briefly in Chapter 1).

Since conjugated π systems are often the target of Stille couplings, we thought it was important to utilize them in our studies. We therefore chose to couple vinyl stannanes with aryl halides due to the ease of access to the vinyl stannane partners and the commercial availability of aryl halides.

3.3. Discussion on Stannane Coupling Partners

We utilized the stannanes outlined in Figure 3.1 for our studies. Access to stannanes **39-40** and **43-44** can be realized through the hydrostannation of the corresponding alkynes. The fully substituted propargylic position allows for selective formation of the *E* isomer as opposed to the internal isomer; this regioselectivity has been well precedented.²⁹ Stannanes **41** and **42** can be accessed through methyl protection of **39** and **40**, respectively.

Alth

kinetics ma

its methyl c

the proton c

hydrogen bo

any involve

activate met

stannanes ac

thus elimina

kinetics acro

would also b

with respect t

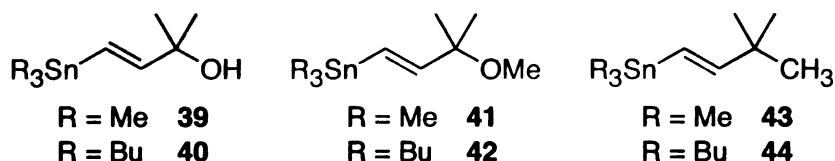
34. Discussion

To pro

electrophilic a

withdrawing, a

Figure 3.1. Substituted Vinyl Stannanes of Interest



Although the Stille reaction is tolerant of functional groups, the kinetics may still be affected by their presence. Protection of the hydroxyl as its methyl ether would allow for identification of problems associated with the proton of the hydroxyl functionality. Possible problems could arise from hydrogen bonding or the acidity of the proton. Furthermore, we could probe any involvement of the oxygen. Heteroatom chelation has been shown to activate metal-carbon bonds.^{30,31} To address whether the oxygen in the vinyl stannanes activates the tin atom, we replaced the OH and OMe with a CH₃, thus eliminating the possibility for chelation. We could then compare the kinetics across substrates to understand the involvement of the oxygen. We would also be able to test the versatility and generality of the Stille reaction with respect to the kinetics.

3.4. Discussion on Aryl Halide Coupling Partners

To provide a generalized study on Stille cross-couplings, the electrophilic aryl halide coupling partners should possess electron neutral, withdrawing, and donating substituents. We chose to have substitution at the

para position to

arenes can be pro

the steric influen

are often used f

However, they s

widely utilized o

compared with

chlorides. Theref

our study as we

would be easier t

The substrates tha

35. Preparation o

The vinyl st

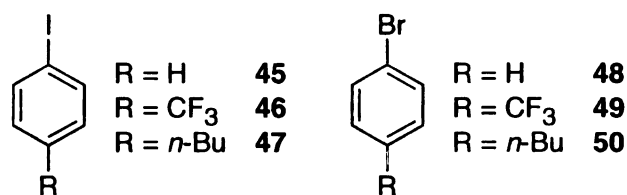
section 3.3. They c

reaction (Scheme

40yne, 29.32 Notabl

para position to avoid problems associated with sterics (*ortho* substituted arenes can be problematic) since we were mainly interested in learning about the steric influence of the tin ligands. Regarding the halide,²⁴ aryl iodides are often used for kinetic studies because they undergo facile reactions. However, they suffer from instability and high cost. Aryl bromides are widely utilized due to higher stability, higher availability, and lower cost compared with aryl iodides, and higher reactivity compared to aryl chlorides. Therefore, the corresponding aryl bromides would be included in our study as well. We also preferred to use liquid substrates since they would be easier to introduce into the reaction prior to an NMR experiment. The substrates that met these criteria are outlined in Figure 3.2.

Figure 3.2. Electrophiles of Interest



3.5. Preparation of Vinyl Stannanes

The vinyl stannane choices for our kinetic studies were discussed in section 3.3. They can be readily accessed by a Pd catalyzed hydrostannation reaction (Scheme 3.1) involving the *syn* addition of a tin hydride to an alkyne.^{29,32} Notably, this method does not produce the *Z* isomers. A

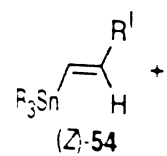
drawback to this

necessary. Meth

source of the tin

the hydrostannate

Sch



reductive

53.

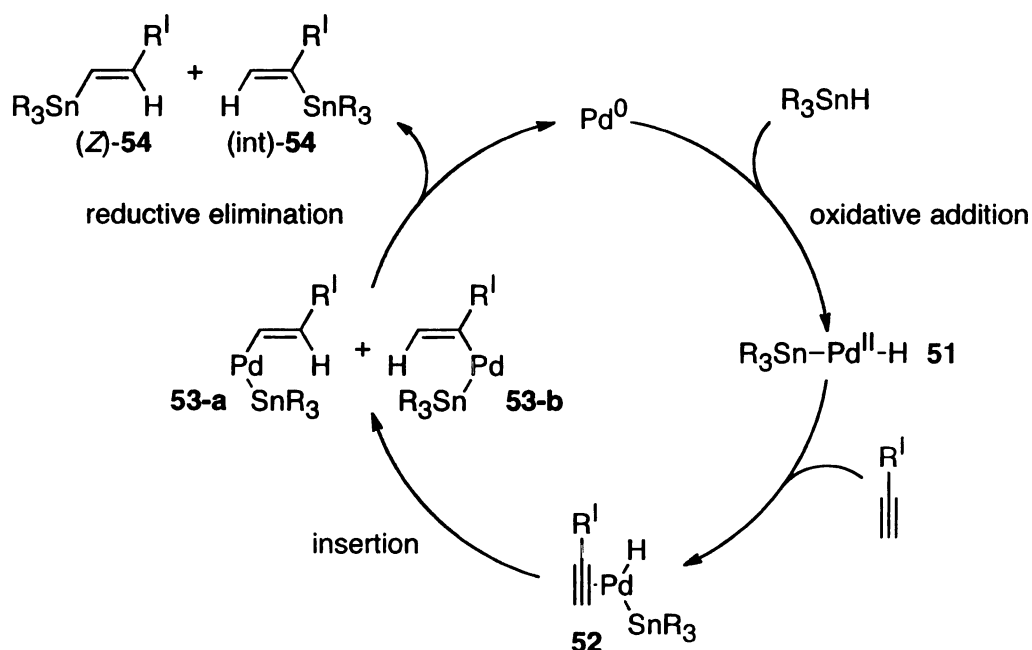
S

R

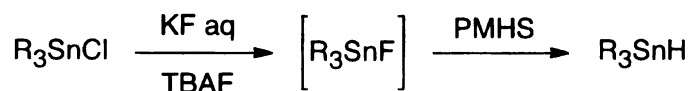
The hydro
utilized to synthe
the synthesis of

drawback to this method is that preparation of the air sensitive tin hydride is necessary. Methods developed by Maleczka et al.³³ can provide an *in situ* source of the tin hydride (Scheme 3.2), which subsequently participates in the hydrostannation reaction.

Scheme 3.1. Palladium Catalyzed Hydrostannation



Scheme 3.2. *In Situ* Tin Hydride Generation



The hydrostannation method developed by Maleczka et al.³³ was utilized to synthesize the vinyl stannanes and is outlined in Table 3.1. For the synthesis of stannane **44** (entry 6), a slight excess of the alkyne was

necessary to co

problems of the

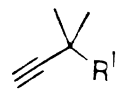
reduced pressure

stannane **43**, since

be removed in th

41 and **42** were

respectively. The

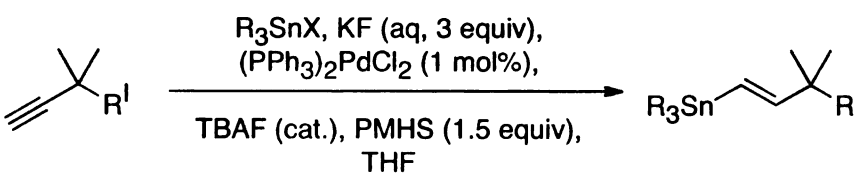


entry
1
2
3
4 ^a
5
6

^a KF was n

necessary to consume all of the Bu_3SnH as to avoid SiO_2 separation problems of the non-polar stannane. Any residual alkyne was removed under reduced pressure. Excess alkyne was not necessary for the synthesis of stannane **43**, since Me_3SnH is slightly soluble in H_2O and any excess could be removed in the extraction/wash work-up procedure. Methoxy stannanes **41** and **42** were accessed by etherification of pure stannanes **39** and **40**, respectively. These syntheses are outlined in Table 3.2.

Table 3.1. Synthesis of Vinyl Stannanes



entry	R	R ^I	X	time	temp	product: yield
1	Me	OH	Cl	1 h	rt	39 : 37%
2	Bu	OH	Cl	2.5 h	rt	40 : 80%
3	Cy	OH	Cl	7.5 h	50 °C	55 : 53%
4 ^a	<i>i</i> -Pr	OH	F	1.5 h	rt	56 : 94%
5	Me	CH ₃	Cl	1.5 h	rt	43 : 20%
6	Bu	CH ₃	Cl	1.5 h	rt	44 : 66%

^a KF was not necessary for in situ SnF generation

Table

R_3Sn
entr
1
2

In order to

prepared the uns

These substrates

much of the trim

solution in THF

method demon

vinyl stannane

Sille.³⁵ The re

Table 3.2. Methyl Protection of Hydroxyl Stannanes

$\text{R}_3\text{Sn}-\text{CH}=\text{C}(\text{Me})_2\text{OH} \xrightarrow[\text{THF, 80 } ^\circ\text{C, 4 h}]{\text{NaH, MeI,}} \text{R}_3\text{Sn}-\text{CH}=\text{C}(\text{Me})_2\text{OMe}$		
entry	R	product: yield
1	Me (39)	41 : 84%
2	Bu (40)	42 : 83%

In order to compare our results to previous studies by Farina, we prepared the unsubstituted vinyl trimethyl and tributyl stannanes as well. These substrates are quite volatile and even with purification by distillation, much of the trimethyl vinyl stannane was lost and could only be isolated as a solution in THF. Tributyl vinyl stannane was prepared by the Grignard method demonstrated by Seyferth,³⁴ where the more sensitive trimethyl vinyl stannane was prepared by the adapted procedure of Scott, Crisp, and Stille.³⁵ The reaction conditions and yields are described in Table 3.3.

Table 3.3. Vinyl Stannane Synthesis

$\text{R}_3\text{SnCl} \xrightarrow[\text{THF, 66-67 } ^\circ\text{C, 5.5 h}]{\text{CH}_2=\text{CHMgBr}} \text{CH}_2=\text{CHSnR}_3$				
entry	R	time	temp	product: yield
1	Me	5.5 h	70 °C	57 : 4%
2	Bu	20 h	70 °C	58 : 87%

3.6. Develo

With

first Stille

conditions

developed

used to ob

NMR spe

concentrat

concentrat

concentrat

concentrat

commonly

density, th

the volum

that each

ligand re

combining

prepared

green sig

Pd ligand

3.6. Development of the Standard Kinetics Procedure

With the synthesis of the vinyl stannanes completed, we chose the first Stille coupling reaction of interest as shown in Scheme 3.3. The conditions were based on the widely utilized Pd/ligand combination developed by Farina²⁵ and were discussed in Section 1.4.2. Benene-*d*₆ was used to obtain field lock since these reactions would be carried out in a NMR spectrometer. Since reaction kinetics are dependent on substrate concentration, it was essential that our reactions were carried out at the same concentration and that we knew the precise volume of each reaction. A final concentration of ~0.2 M in stannane was desired since this is a common concentration used in organic synthesis (e.g. 1 mmol reactions are commonly run in 5 mL of solvent). Each stannane of interest has a different density, thus a different volume to incorporate in the reaction. To normalize the volume incorporated across stannanes, 1 M solutions were prepared so that each reaction would utilize the same volume of solution. The Pd and ligand required time to “premix” to obtain the active catalyst before combining all reagents.²⁵ Therefore, a solution of the Pd and ligand was prepared and stirred for about 10 min until color change from purple to green signified formation of the active catalyst. A set volume of the Pd/ligand solution could then be utilized for each reaction, ensuring

consistent

followed

0.1857 M

34.

To

ethyl halide

irrelevant

consistent catalyst loadings. The electrophile would then be added neat followed by an additional amount of THF to bring the concentration to 0.1857 M in the organostannane. The standard protocol is described in Table 3.4.

Scheme 3.3. Initial Stille Reaction of Interest for Kinetics Study

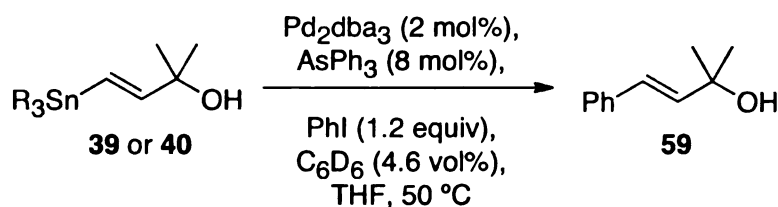


Table 3.4. Standard Kinetics Sample Preparation

reagent/solution	volume added to sample
C_6D_6	50 μL
39 or 40	200 μL ^a
Pd_2dba_3	600 μL ^b
AsPh_3	
PhI	27 μL
additional THF	200 μL
Total Stannane Concentration: 0.1857 M	

^a THF solution that is 1 M in **39** or **40**

^b THF solution that is 0.0067 M in Pd and 0.0267 M in AsPh_3

To prepare the samples, all of the reagents except the electrophile (aryl halide) were added to an NMR tube. The order of addition was irrelevant. The sample was inserted into a 500 MHz spectrometer, heated to

50 °C.[†] tur

then ejected

was reinserted

Further det

was describ

3.7. Monit

Usin

us to see t

product, an

know from

products t

observed

course of

¹¹⁹Sn NMR

are visibl

broadene

the signa

[†] The NMR
temperature

50 °C,[†] tuned to the ^{119}Sn nucleus, and properly shimmed. The sample was then ejected so that the electrophile could be added, after which the sample was reinserted, reshimmed, and an arrayed kinetics experiment was initiated. Further details are available in the experimental section. Work up of the data was described in Section 2.4.

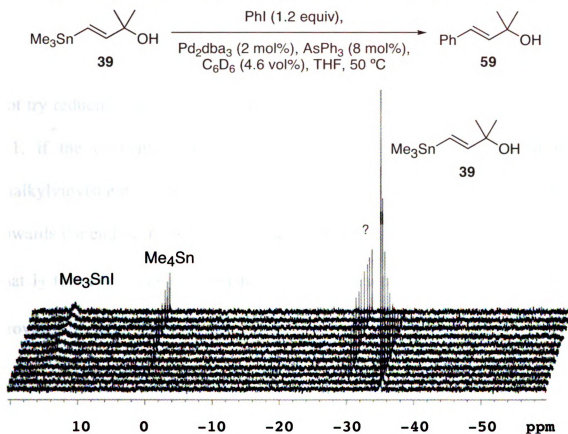
3.7. Monitoring the Course of the Stille Reaction with ^{119}Sn NMR

Using ^{119}Sn NMR to monitor the course of the Stille reaction allows us to see the consumption of the stannane, formation of the tin halide by-product, and any other tin containing species formed during the reaction. We know from experiments using ^1H NMR and by analyzing the reaction products that stannane consumption tracks with Stille coupling. We do not observed stannane decomposition. Figure 3.3 shows that monitoring the course of a Stille coupling (for the reaction in Scheme 3.3 where $\text{R} = \text{Me}$) by ^{119}Sn NMR is a viable method. The starting material and by-product peaks are visible and distinct. The tin halide signal is somewhat suppressed and broadened due to a longer relaxation time and oligomerization, which causes the signal to drift downfield upon increased concentration.³⁶ Two other

[†] The NMR temperature was calibrated using ethylene glycol every few months. Actual temperatures ranged from 50.3-50.6 °C.

unexpected tin containing species are also observed that would likely be overlooked by other monitoring methods. These species will be discussed in detail in Chapter 5.

Figure 3.3. Course of the Stille Reaction Monitored by ^{119}Sn NMR



3.8. Control Experiments

With the standard protocol for the kinetics study developed, it was essential to verify our assumptions of zero-order electrophile dependence, pseudo-first-order stannane dependence, and that Pd concentration is consistent and can be incorporated in an observable rate constant, k_{obs} . The

control experiment

varying the stoichi

Upon double

outlined in Schem

profile as seen in

electrophile when

not try reducing th

21. if the conce

trialkylvinylstanna

towards the end of

that I_2 formation w

provided the same

control experiments were performed on the reaction outlined in Scheme 3.3, varying the stoichiometries accordingly.

Upon doubling the amount of iodobenzene added to the reaction outlined in Scheme 3.3 where $R = \text{Bu}$, there was no effect on the reaction profile as seen in Figure 3.4. This verifies that the reaction is zero-order in electrophile when run under pseudo-first order stannane conditions. We did not try reducing the amount of iodobenzene. As discussed earlier in Section 2.1, if the concentration of RX is less than the concentration of the trialkylvinylstannane, we would observe deviations from first order kinetics towards the end of the reaction. We also ran a reaction in the dark to be sure that I_2 formation was not initiated by light. Reaction in the dark and light provided the same rate profiles.

Bu₃Sn

16

Figure 3.-
¹¹⁹Sn NMR
coupling
under a P
order exp

Sim

stannane.

stannane.

remain th

concentra

where R =

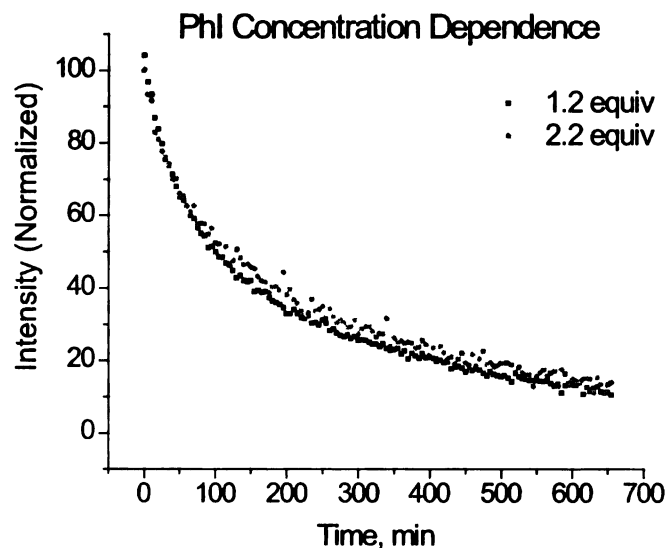
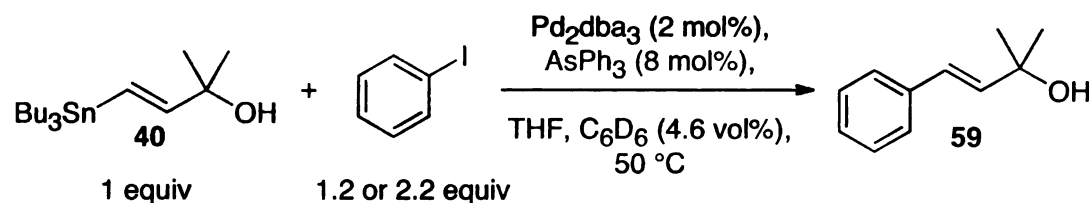


Figure 3.4. Verification of Zero-Order Electrophile Dependence. 186 MHz ^{119}Sn NMR relative integration data for the consumption of **40** upon coupling with either 1.2 equiv (black trace) or 2.2 equiv (red trace) of PhI under a $\text{Pd}_2\text{dba}_3/\text{AsPh}_3$ catalyst system. Both sets of data were fit to a first order exponential decay model (not shown) to reveal $k_{\text{obs}} = 0.006 \text{ min}^{-1}$.

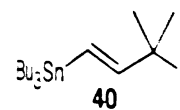
Since the reaction conditions set forth are pseudo-first-order in stannane, we would expect that by reducing the concentration of the stannane, the *rate* of the reaction would change but the *rate constant* would remain the same because $\text{rate} = k_{\text{obs}}[\text{Sn}]$. When only half of the tin concentration (0.5 equiv) was used for the reaction outlined in Scheme 3.3 where $\text{R} = \text{Bu}$, the instantaneous rate was less than when 1 equiv was used,

as expected. This

at t_0 (signifying t

rate constants w

reaction first orde



1.0 or 0.50 equiv

Intensity (Normalized)

Figure 3.5. Ver
MHz ^{119}Sn NM
equiv (black tra
equiv of PhI un
fit to a first or
 0.006 min^{-1} . In
only, as the slop
value is determ
equiv, $[\text{Sn}] \approx 0.$

as expected. This is visualized by comparing the slopes of the tangent lines at t_0 (signifying the instantaneous rate) as seen in Figure 3.5. However, the rate constants were the same for both reactions, which is indicative of a reaction first order in stannane.

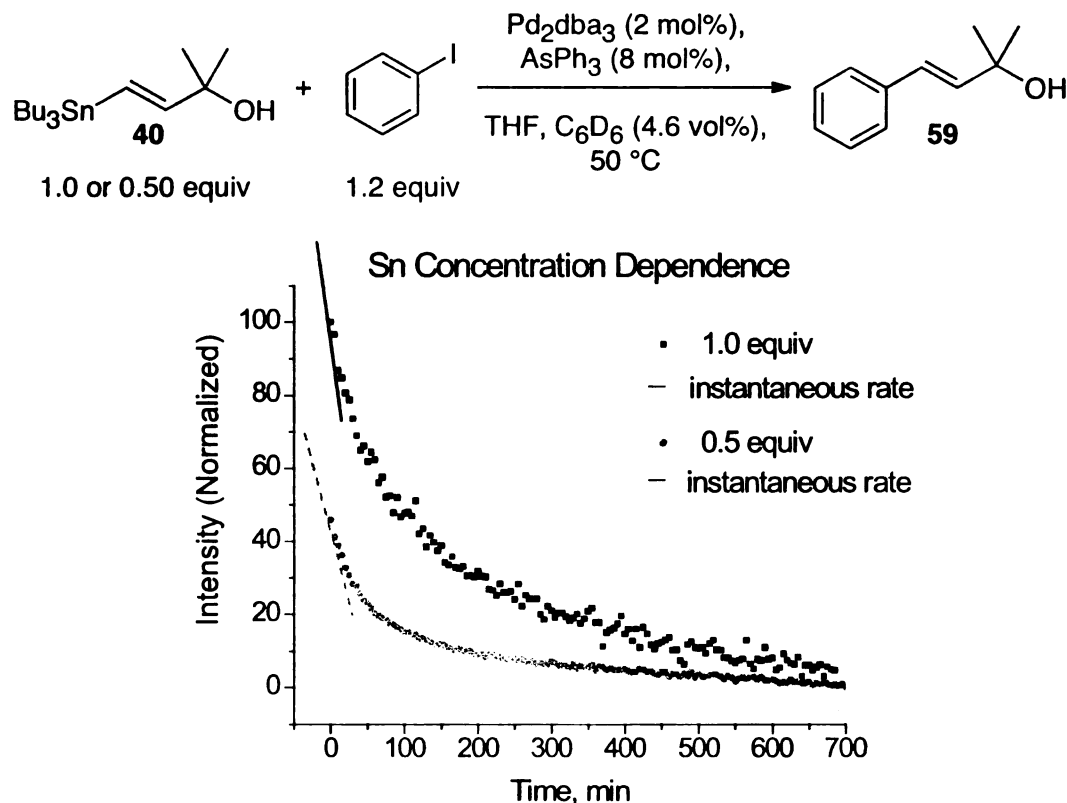


Figure 3.5. Verification of Pseudo-First-Order Stannane Dependence. 186 MHz ^{119}Sn NMR relative integration data for the consumption of either 1.0 equiv (black trace) or 0.5 equiv (red trace) of **40** upon coupling with 1.2 equiv of PhI under a $\text{Pd}_2\text{dba}_3/\text{AsPh}_3$ catalyst system. Both sets of data were fit to a first order exponential decay model (not shown) to reveal $k_{\text{obs}} = 0.006 \text{ min}^{-1}$. Instantaneous rates are approximated for illustrative purposes only, as the slope of a tangent line is equal to the instantaneous rate. The true value is determined by the following relationship: $\text{rate} = k_{\text{obs}}[\text{Sn}]$. For 1.0 equiv, $[\text{Sn}] \approx 0.19 \text{ M}$ and for 0.50 equiv, $[\text{Sn}]$ is $\approx 0.095 \text{ M}$.

To establ

Figure 3.6 for b

The data indica

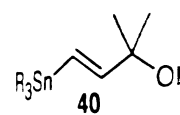
media varies lin

the reaction to t

Figure 3.6. Tab

in k_{ss} .

To establish continuity of the catalyst, we ran the reaction outlined in Figure 3.6 for both R = Me and Bu over a range of catalyst concentrations. The data indicate that the amount of active catalyst present in the reaction media varies linearly with the amount of catalyst added at the beginning of the reaction to the same extent for both the trimethyl and tributyl stannanes (Figure 3.6, Table 3.5). The Pd concentration may therefore be incorporated in k_{obs} .



1.0 equiv

log (k_{obs})

Figure 3.6. Pd
relative integrat
PhI under differe
data were fit to
 k_{obs} for each c
Me, blue trace
reveal a linear
represent a fit
for 39 and 4
concentration.

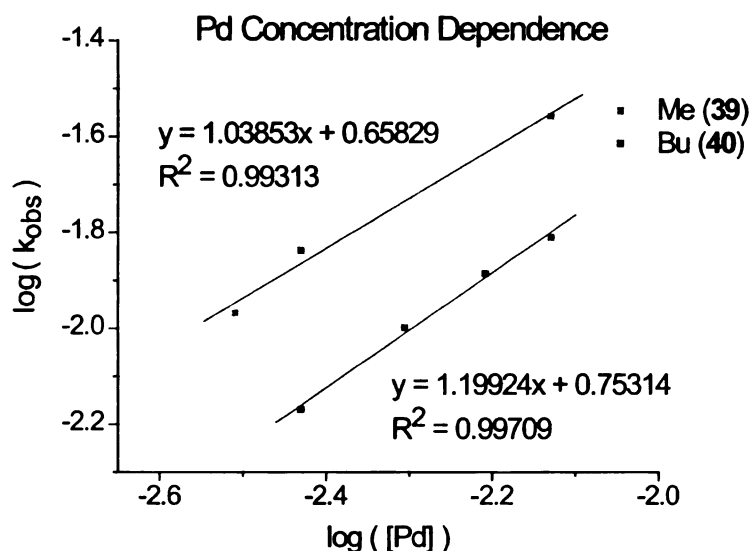
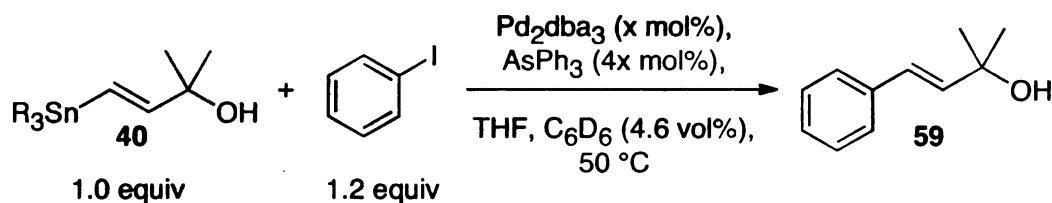


Figure 3.6. Pd Concentration Dependence. The 186 MHz ^{119}Sn NMR relative integration data for the consumption of **39** or **40** upon coupling with PhI under different $\text{Pd}_2\text{dba}_3/\text{AsPh}_3$ catalyst loadings were obtained and the data were fit to a first order exponential decay model (not shown) to obtain k_{obs} for each catalyst loading and stannane combination (red trace: **39** R = Me, blue trace: **40** R = Bu). The $\ln(k_{\text{obs}})$ vs. $\ln([\text{Pd}])$ were then plotted to reveal a linear relationship between k_{obs} and $[\text{Pd}]$. The black solid lines represent a fit to a linear regression model and gave a slope of 1.0 and 1.2 for **39** and **40**, respectively, indicating a first order dependence on Pd concentration.

R =

0.

0.

0.

3.9. Preliminary

Exchange

The

the electron

arenes were

in a benzene

revealed

work-up

coupled products

was not

products

oxidative

Table 3.5. Pd Concentration Dependence Data

[Pd], M		log [Pd]	k_{obs}	log (k_{obs})
R = Me (39)	R = Bu (40)			
0.0031		-2.51	0.01074	-1.97
0.0037		-2.43	0.0145	-1.84
	0.0037	-2.43	0.0068	-2.17
	0.050	-2.31	0.01	-2.0
	0.0062	-2.21	0.013	-1.89
0.0074		-2.13	0.02764	-1.56
	0.0074	-2.13	0.01543	-1.8

3.9. Preliminary Study on Electrophile Scope Leading to Phenyl Exchange

Thus far, all experiments have been performed using iodobenzene as the electrophilic aryl halide. To gain an understanding of how substituted arenes would affect the rate, 4-bromoanisole was utilized as the electrophile in a bench-top reaction (Scheme 3.4). Monitoring the reaction by TLC revealed that the stannane was mostly consumed after 10.5 h. After reaction work-up and purification, two products were identified: the desired cross-coupled product (**60**) and a phenyl coupled product (**59**). The phenyl product was not a result of impure 4-bromoanisole. In fact, phenyl exchange products are quite common when PPh_3 is utilized as the Pd ligand.³⁷⁻⁴¹ After oxidative addition, transfer of a phenyl from the Pd ligand, PPh_3 , in

exchange

process i

Ar to ari

addition

PhXPdL

(Scheme

transfer h

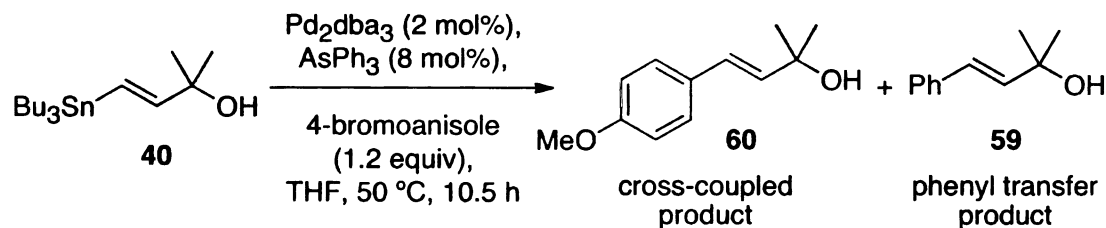
arsine der

Bu_3Sn

4

exchange for the aryl Pd ligand (from the electrophile) can occur. This process is presumed to proceed through a reductive elimination of PPh_3 and Ar to afford the phosphonium salt $(\text{Ph}_3\text{ArP}^+\text{X}^-)$ (**62**) and $\text{Pd}(0)$. Oxidative addition of a P-Ph bond of the phosphonium salt would then lead to a PhXPdL_2 species (**63**) capable of transmetallation and reductive elimination (Scheme 3.5). Less is known regarding triphenylarsine ligands although transfer has been observed and used as a method to construct various aryl arsine derivatives.⁴²

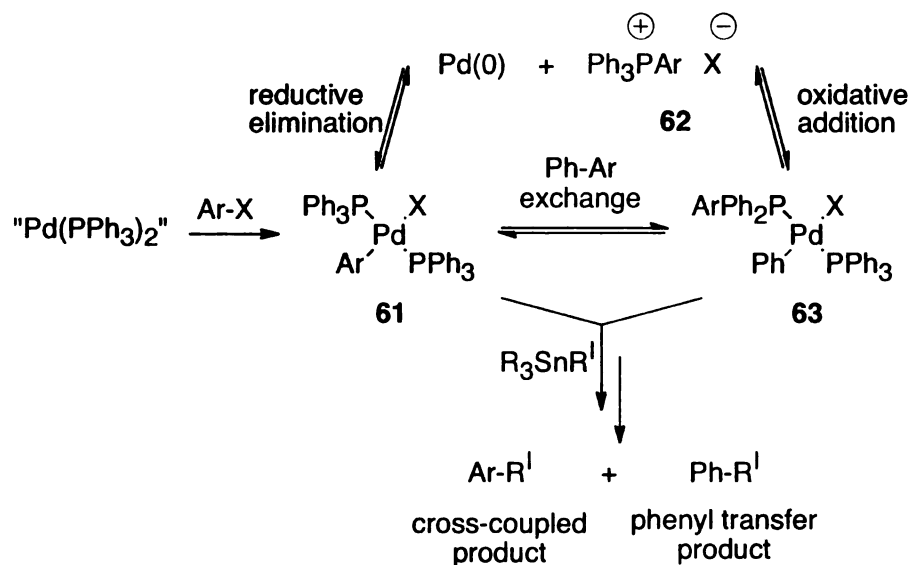
Scheme 3.4. Stille Coupling with 4-Bromoanisole





We became
complicate our
stannane, but w
Different electr
reaction. Howe
reaction. As lo
stannane react
regarding the r
products shou
the stannane e

Scheme 3.5. Aryl-Phenyl Exchange Process Leading to Cross-Coupled and Phenyl Transfer Products



We became concerned that the phenyl transfer processes would complicate our kinetic analysis. The exchange itself is independent of the stannane, but would alter the catalytic species during the experiments. Different electronically substituted ligands are known to affect rates of reaction. However, we were particularly interested in relative rates of reaction. As long as the catalytic systems for the trimethyl and tributyl stannane reactions are similar, we should obtain useful information regarding the relative rates of reaction. For this to be true, the distribution of products should be the same at any given point of the reaction regardless of the stannane employed. We therefore ran separate bench-top Stille couplings

of the trimethyl

the reaction was

Table 3.1

down for each a

For the trimethyl

product produce

and tributyl stan

that there is lit

should not impac

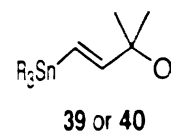
ten-transferable

we initiated our s

of the trimethyl and tributyl stannanes with 4-bromoanisole. After 3 hours the reaction was stopped to determine the distribution of the two products.

Table 3.1 shows the total yield for both products as well as a break down for each and the percentage of phenyl transfer product out of the total. For the trimethyl and tributyl reactions, the percentage of phenyl transfer product produced was 42% and 46%, respectively. Assuming the trimethyl and tributyl stannanes react through the same mechanism, these data indicate that there is little problem arising from the phenyl transfer process and should not impact our kinetic studies on the relative rates of reaction per the non-transferable ligands on tin. With the necessary control experiments run, we initiated our systematic study of cross-couplings with aryl iodides.

Table 3.6. Det



entry	R
1	Me (39)
2	Bu (40)

3.10. Aryl Iodide

Utilizing t

we monitored the

iodides. The obs

Table 3.7. Trime

corresponding tri

Me Bu ratio rela

presence of the fr

of the reaction si

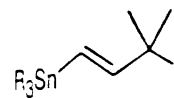
degree (e.g. comp

Table 3.6. Determination of Cross-Coupled and Phenyl Transfer Product Distribution

$ \begin{array}{c} \text{R}_3\text{Sn}-\text{CH}=\text{C}(\text{OH})\text{Me}_2 \xrightarrow[\text{THF, 50 }^\circ\text{C, 3 h}]{\text{Pd}_2\text{dba}_3 \text{ (2 mol\%), AsPh}_3 \text{ (8 mol\%), 4-bromoanisole (1.2 equiv)}} \\ \textbf{39 or 40} \end{array} $					
			$ \begin{array}{c} \text{MeO}-\text{C}_6\text{H}_4-\text{CH}=\text{C}(\text{OH})\text{Me}_2 \\ \textbf{60} \\ \text{cross-coupled product} \end{array} $	+	$ \begin{array}{c} \text{Ph}-\text{CH}=\text{C}(\text{OH})\text{Me}_2 \\ \textbf{59} \\ \text{phenyl transfer product} \end{array} $
entry	R	total product % yield	cross-coupled (60) % yield	phenyl transfer (59) % yield	phenyl transfer/total product
1	Me (39)	30	17.5	12.5	0.42
2	Bu (40)	26	14	12	0.46

3.10. Aryl Iodide Couplings

Utilizing the conditions and reagents outlined earlier in this chapter, we monitored the rate of the reaction for vinyl stannanes coupled with aryl iodides. The observable rate constants, k_{obs} , were determined as shown in Table 3.7. Trimethyl stannanes showed reactivity 1.4-2.4 times that of the corresponding tributyl stannanes. These rate differences are presented as a Me/Bu ratio relative to Bu for each R^I/electrophile combination. The presence of the free hydroxyl does not appear to alter the mechanistic course of the reaction since methyl protection does not affect the rate to a large degree (e.g. comparison of entries 3 & 4 vs. 9 & 10).



entry	Y
1	H
2	H
3	CF ₃
4	CF ₃
5	<i>n</i> -Bu
6	<i>n</i> -Bu
7	H
8	H
9	CF ₃
10	CF ₃
11	<i>n</i> -Bu
12	<i>n</i> -Bu

^aMe Bu ratios
electrophile R¹

^bDetermined by
NMR grade TM

It appears

allow for a more

addition is the ra

oxidative addition

Table 3.7. Aryl Iodide Couplings in THF

entry	Y	R	R ^I	Sn	<i>k</i> _{obs} (min ⁻¹)	relative rates of Me/Bu ^a	yield ^b
1	H	Me	OH	39	0.015	2.38/1	59: 34%
2	H	Bu	OH	40	0.006		59: 51%
3	CF ₃	Me	OH	39	0.039	2.29/1	61: 87%
4	CF ₃	Bu	OH	40	0.017		61: 79%
5	<i>n</i> -Bu	Me	OH	39	0.013	1.41/1	62: 30%
6	<i>n</i> -Bu	Bu	OH	40	0.009		62: 36%
7	H	Me	OMe	41	0.018	1.50/1	63: 60%
8	H	Bu	OMe	42	0.012		63: 65%
9	CF ₃	Me	OMe	41	0.032	2.13/1	64: 87%
10	CF ₃	Bu	OMe	42	0.015		64: 82%
11	<i>n</i> -Bu	Me	OMe	41	0.019	1.90/1	65: 45%
12	<i>n</i> -Bu	Bu	OMe	42	0.010		65: 70%

^a Me/Bu ratios are the relative rates of methyl to butyl for each electrophile/R^I combination.

^b Determined by ¹H NMR analysis of the crude reaction mixture using NMR grade TMS-O-TMS as the internal standard.

It appears that more electron withdrawing substituents, such as CF₃, allow for a more facile reaction. This may lead one to believe that oxidative addition is the rate-determining step. However, it must be realized that the oxidative addition product species must still act as an electrophile to achieve

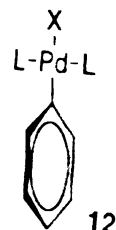
vinyl stannane

Therefore, we

transmetallation

substituents acc

the reactions



oxidative addition
product

Determinat

was carried out at

by others at 50 °C

balance between t

progress by NMR

reaction, as indicate

$$k = Ae^{-E_a/RT}$$

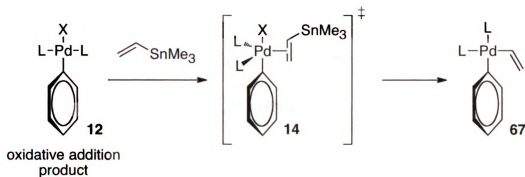
and can be linearized

$$\ln(k) = \ln(A) +$$

vinyl stannane coordination and subsequent transmetallation (Scheme 3.6).⁸

Therefore, we would see a substituent effect on the rate even when transmetallation is the rate-determining step whereby electron poor substituents accelerate the reaction and electron rich substituents slow down the reactions

Scheme 3.6. Mechanism of Transmetallation⁸



Determination of the relative rates of trimethyl and tributyl stannanes was carried out at 50 °C to correlate our data with previous kinetic studies by others at 50 °C. Furthermore, this temperature achieves a good rate balance between the fast and slow reactions in order to monitor reaction progress by NMR. However, temperature can greatly affect the rate of reaction, as indicated by the Arrhenius equation, which is defined as

$$k = A e^{-E_a/RT} \quad (7)$$

and can be linearized by

$$\ln(k) = \ln(A) + (-E_a/R)(1/T) \quad (8)$$

Since we

tributyl stannane

the trimethyl and

energy barriers.

40, 50, and 55

temperature dependence

1/T (Figure 3.8)

E_a/R . For the reaction

40. $E_a = 6.8$ kcal

are fit (fit B), the

energy of 40. With

are not significant

methyl and butyl

than different activation

trimethyl and tributyl

have relatively the

reactions are often

should be applicable

Since we are interested in the rate differences between trimethyl and tributyl stannanes, it is important that the rate differences are a reflection of the trimethyl and tributyl ligands, and not a reflection of different activation energy barriers. To this end, we repeated entries 1 and 2 from Table 3.7 at 40, 50, and 55 °C under our standard conditions (Figure 3.7). The temperature dependence data was then plotted as an Arrhenius plot, $\ln(k)$ vs. $1/T$ (Figure 3.8), where the slope of the linear regression fit is equal to $-E_a/R$. For the reaction with **39**, $E_a = 12.4$ kcal/mol and for the reaction with **40**, $E_a = 6.8$ kcal/mol. However, if only the data for **39** at for 45 and 50 °C are fit (fit B), the $E_a = 8.4$ kcal/mol and is more in line with the activation energy of **40**. Within the range of temperatures studied, the E_a differences are not significant for these lines to cross, such that rate differences between methyl and butyl appear to be a reflection of the steric differences rather than different activation energy barriers. This trend further supports that the trimethyl and tributylstannanes react through the same mechanism since they have relatively the same activation barrier. In addition, Stille coupling reactions are often performed from rt to 100 °C, therefore our rate data should be applicable to those situations as well.

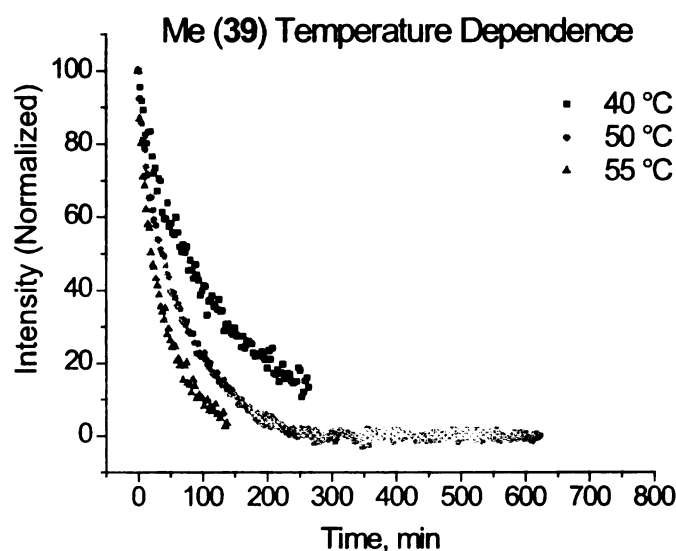
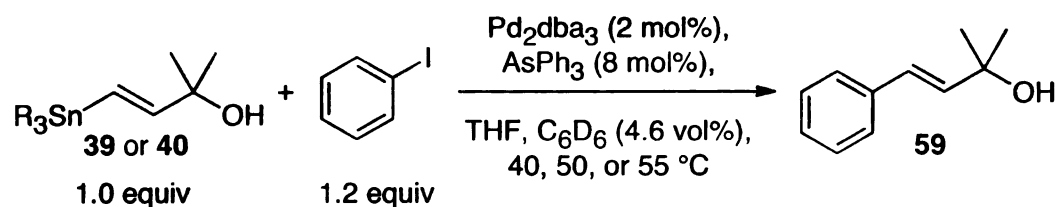


Figure 3.7. Plot of Temperature Dependence for Trimethyl and Tributyl Stannane Reactions. 186 MHz ^{119}Sn NMR relative integration data for the consumption of **39** (*top*) or **40** (*bottom*) upon coupling with PhI under a $\text{Pd}_2\text{dba}_3/\text{AsPh}_3$ catalyst system at 40 °C (black trace), 50 °C (red trace), and 55 °C (blue trace). All sets of data were fit to a first order exponential decay model (not shown) to reveal the rate constants outlined below in Table 3.8.

able

Figure 3.7 (cont'd)

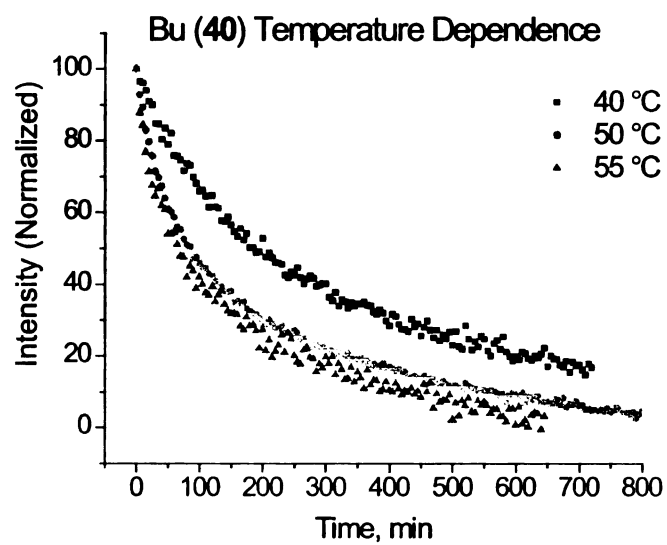


Table 3.8. Temperature Dependent Rate Constants

R	$k_{\text{obs}} \text{ min}^{-1}$		
	40 °C	50 °C	55 °C
Me (39)	0.0099	0.0150	0.0260
Bu (40)	0.0040	0.0059	0.0065
Me/Bu	2.49	2.46	4.02

Figure 3.8. Arrhenius Plot of k_{obs} vs. $1/T$. The lines represent a linear fit to the data. For 39, $E_a = 12.4$ kJ/mol. 45 and 50 °C are indicated.

3.11. Aryl Bromides

With a method we extended the study to aryl bromides. These would see the same couplings. The overall rates for trimethyl

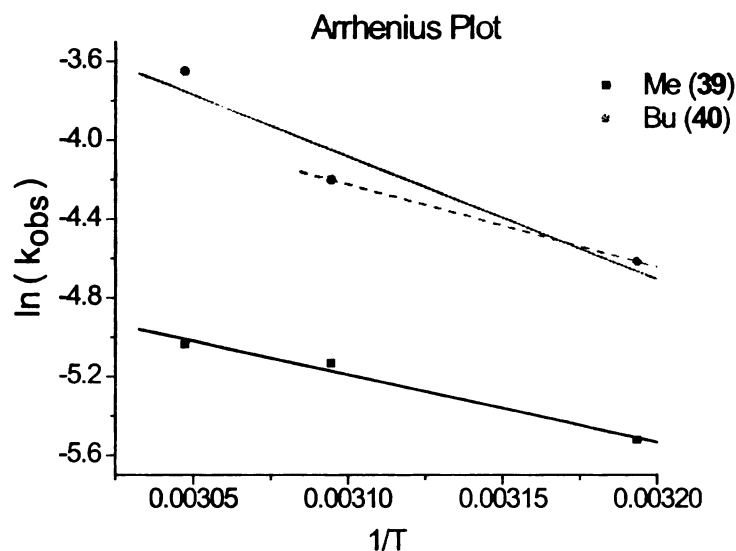


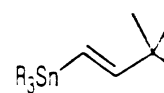
Figure 3.8. Arrhenius Plot to Determine the Activation Energy, E_a . An Arrhenius Plot was prepared by plotting $\ln(k_{\text{obs}})$ vs. $1/T$, where the k_{obs} values at various temperatures were determined in Table 3.8. The black lines represent a fit to a linear regression model, with the slope = $-E_a/R$. For 39, $E_a = 12.4$ kcal/mol (fit A: red solid line) or 8.4 kcal/mol when only 45 and 50 °C are fit (fit B: red dashed line) and for 40, $E_a = 6.8$ kcal/mol.

3.11. Aryl Bromide Couplings

With a method for studying the kinetics of the Stille reaction in hand, we extended the studies to include couplings with the corresponding aryl bromides. These results are reported in Table 3.9. We expected that we would see the same types of Me/Bu rate differences seen with aryl iodide couplings. The overall rates of the reaction were much slower than the corresponding aryl iodide couplings. Much to our surprise, the coupling rates for trimethyl and tributyl stannanes with aryl bromides were similar.

This suggests th

reevaluation of



entry	Y
1	H
2	H
3	CF_3
4	CF_3
5	<i>n</i> -Bu
6	<i>n</i> -Bu
7	H
8	H
9	CF_3
10	CF_3
11	<i>n</i> -Bu
12	<i>n</i> -Bu

^a Me Bu ratios at electrophile R^1

^b Determined by NMR grade T.M.

^c Yield of **65** and

This suggests that transmetallation is no longer the rate-determining step and reevaluation of the mechanistic course of the reaction is necessary.

Table 3.9. Aryl Bromide Couplings in THF

entry	Y	R	R ^I	Sn	<i>k</i> _{obs} (min ⁻¹)	relative rates of Me/Bu ^a	yield ^b
1	H	Me	OH	39	0.0073	1.16/1	59 : 35%
2	H	Bu	OH	40	0.0062		59 : 33%
3	CF ₃	Me	OH	39	0.0210	1.11/1	61 : 49%
4	CF ₃	Bu	OH	40	0.0230		61 : 83%
5	<i>n</i> -Bu	Me	OH	39	0.0065	0.92/1	62 : 23%
6	<i>n</i> -Bu	Bu	OH	40	0.0058		62 : 23%
7	H	Me	OMe	41	0.0051	1.09/1	63 : 45%
8	H	Bu	OMe	42	0.0047		63 : 51%
9	CF ₃	Me	OMe	41	0.0200	1.31/1	64 : 44%
10	CF ₃	Bu	OMe	42	0.0190		64 : 58%
11	<i>n</i> -Bu	Me	OMe	41	0.0046	1.05/1	65 : 33%
12	<i>n</i> -Bu	Bu	OMe	42	0.0035		65 : 37% ^c

^a Me/Bu ratios are the relative rates of methyl to butyl for each electrophile/R^I combination.

^b Determined by ¹H NMR analysis of the crude reaction mixture using NMR grade TMS-O-TMS as the internal standard.

^c Yield of **65** and the phenyl transfer product **63** combined.

3.12. Mechanistic Considerations of Aryl Bromide Couplings

We observe different rate determining steps when using either aryl iodides or bromides. Looking back to the mechanism described in Scheme 1.2, it is unlikely that isomerization or reductive elimination would be the rate-determining step since they are independent of halide. One logical explanation is that oxidative addition is the rate-determining step. Although we performed control experiments to exclude this possibility, these studies were performed on aryl iodides. Given the common consensus that transmetallation is the rate-determining step, we thought that our control experiments were sufficient. This assumption is common in kinetic studies on the Stille reaction and other cross-coupling reactions and has proven a lesson in itself; do not extend the generality of any studies beyond the examined scope.

In addition to the Me/Bu data, other observations were consistent with oxidative addition as the rate-determining step. Reactions of electron neutral and electron rich electrophiles (Table 3.9, entries 1-2, 5-8 and 11-12) did not reach completion and black precipitate was observed. We suspect that the catalyst decomposed as a result of a slow oxidative addition and is in accordance with Stille's⁴³ findings. Also, self-catalyzed Pd decomposition has been reported.⁴⁴ In contrast, couplings with an electron deficient aryl

halide (entries 5-6 and 7)

more facile oxidative

catalyst was compro

To further tes

aryl bromide conc

oxidative addition i

the rate should be

(*E*)-trimethyl (41)

(42) with 4-bromo

constant dependen

$\log(k_{obs})$ is plotted

indicating that th

were obtained by

assumption that th

still reflects the c

consumed after th

takes place. Fur

bromobenzotrifluor

halide (entries 5-6 and 11-12) went to completion. We submit that here a more facile oxidative addition allowed the reactions to proceed before the catalyst was compromised.

To further test whether the oxidative addition is rate determining, an aryl bromide concentration dependence study was performed. If the oxidative addition is the rate-determining step for aryl bromide couplings, the rate should be a function of electrophile concentration. The reaction of (*E*)-trimethyl (**41**) and (*E*)-tributyl(3-methoxy-3-methylbut-1-enyl)stannane (**42**) with 4-bromobenzotrifluoride at different concentrations reveals a rate constant dependence on electrophile concentration (Figure 3.9). When $\log(k_{\text{obs}})$ is plotted vs. $\log[\text{E}^+]$, a linear correlation is realized with a slope of 1 indicating that the reaction is first order in aryl bromide. Although our data were obtained by monitoring stannane consumption and were based on the assumption that the transmetallation is the rate-determining step, our data still reflects the overall reaction progress since the stannane can only be consumed after the rate-determining oxidative addition (for aryl bromides) takes place. Furthermore, studies monitoring the consumption of 4-bromobenzotrifluoride by ^{19}F NMR provided the same rate profile as when

the stannane wa

excess electrophil

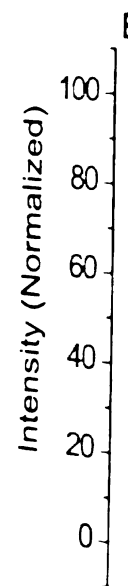
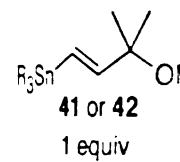


Figure 3.9. Determination of the rate of decay of the XMR relative intensity of the signal due to coupling with 1.2 equiv (blue) of 4. The curve represents an exponential decay. The blue line is used to guide the eye. The curve reveals a linear relationship between the logarithm of the intensity and time, representing a fit to the data, indicating first order kinetics.

the stannane was monitored by ^{119}Sn NMR after taking into account the excess electrophile that is utilized.

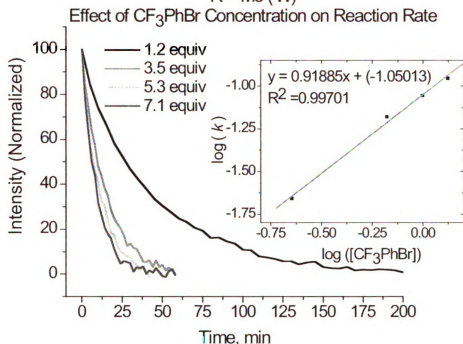
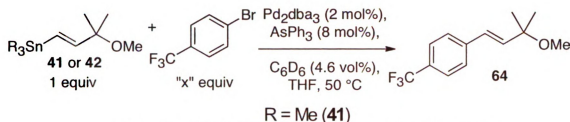
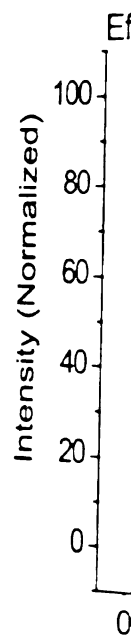
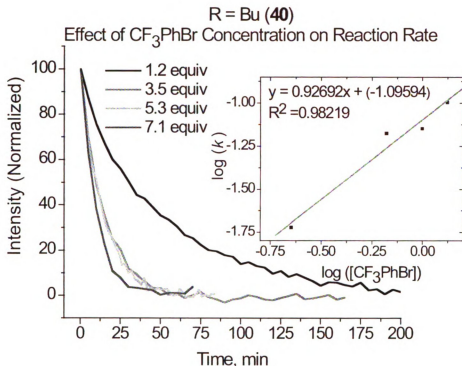


Figure 3.9. Determination of Electrophile Dependence. 186 MHz ^{119}Sn NMR relative integration data for the consumption of **41** or **42** upon coupling with 1.2 equiv (black), 3.5 equiv (red), 5.3 equiv (green), or 7.1 equiv (blue) of 4-bromobenzotrifluoride. The data were fit to a first order exponential decay model (not shown) to obtain k_{obs} . The solid colored lines are to guide the eye. The $\ln(k_{\text{obs}})$ vs. $\ln([\text{ArBr}])$ were then plotted (inset) to reveal a linear relationship between k_{obs} and $[\text{ArBr}]$. The red solid lines represent a fit to a linear regression model and gave a slope of 0.9, indicating first order aryl bromide concentration dependence.



While reacting
various stoichiometries
we deemed it important to
synthesize **39-44**. The
43 and **44** with their
profiles were obtained
spectroscopically and
was coupled with
Furthermore, in reaction
amount of electrophile

Figure 3.9 (Cont'd)



While reactions of all stannane/bromo-electrophile combinations in various stoichiometries all pointed to oxidative addition as rate determining, we deemed it important to probe the influence of the oxygen substituents in stannanes **39-44**. Therefore we reacted tert-butyl substituted vinyl stannanes **43** and **44** with 4-bromo- and 4-iodobenzotrifluoride. Similar reaction profiles were observed when the bromide was coupled with spectroscopically clean stannanes **39**, **41**, and **43** as well as when the iodide was coupled with spectroscopically clean stannanes **40**, **42**, and **44**. Furthermore, in reactions of 4-bromobenzotrifluoride and **44**, doubling the amount of electrophile accelerated the reaction. These data indicate that

there is no peculiar

oxidative addition

across a range of st

^{19}F NMR st

iodobenzotrifluoride

signals for the rea

observed with the

different resting sp

resting state whe

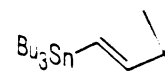
addition product 3

rate determining is

observations are

determining step o

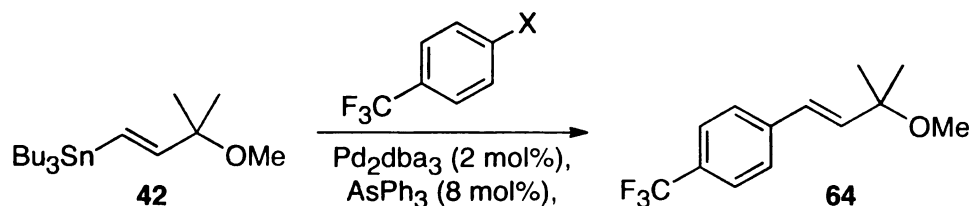
Schem

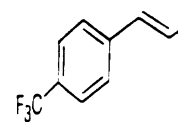


there is no peculiar effect of the oxygen in stannanes **39-42** and that oxidative addition remains rate determining for the reaction of aryl bromides across a range of stannanes.

^{19}F NMR studies were performed on reactions with 4-bromo and 4-iodobenzotrifluoride (Scheme 3.7). We observed several unknown minor signals for the reaction with the iodide (Figure 3.10), but no signals were observed with the bromide (Figure 3.11). In principle, we should see different resting species depending on the rate-determining step. That is, the resting state when transmetallation is rate determining is the oxidative addition product **31** or **3**, while the resting state when oxidative addition is rate determining is free Pd **1** and electrophile **2** (see Scheme 1.10). Thus our observations are consistent with the oxidative addition being the rate-determining step of the Stille reaction with aryl bromides.

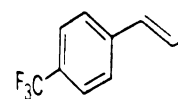
Scheme 3.7. Stille Coupling Monitored by ^{19}F NMR





-64.2

Figure 3.10. Still
by ^{19}F NMR.



-64.2

Figure 3.11. Still
by ^{19}F NMR.

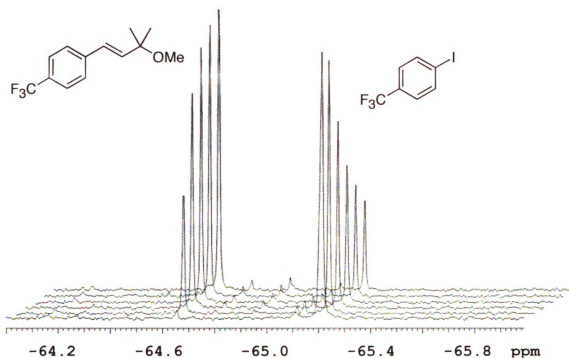


Figure 3.10. Stille coupling of **42** with 4-iodobenzotrifluoride monitored by ^{19}F NMR.

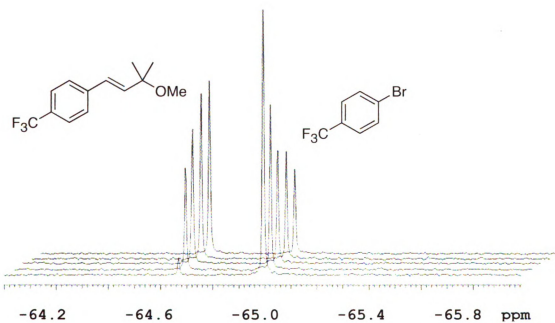


Figure 3.11. Stille coupling of **42** with 4-bromobenzotrifluoride monitored by ^{19}F NMR.

In an effort to determine whether the
aryl iodide coupling reaction was
we compared the rate of oxidative addition
product does not form. It is well
known that vinyl iodides do not
inhibit the active catalyst. However,
stannane-coordination to the catalyst
we have no firm evidence for this
during the experiment. The mechanism
these reactions is not clear. It is
consisting of the oxidative addition of
olefin. When the catalyst is added to
purple solution to give a brownish-purple
drastic color change. However, the
solution. However, the color change
brownish-purple color is not
coordinating to the catalyst
coordinated to Pd.

In an effort to determine whether the unknown signals present in the aryl iodide coupling (Figure 3.10) are oxidative addition products **31** or **3**, we compared the spectra from our kinetic Stille study with an independent oxidative addition study (Scheme 3.8) (Figure 3.12). The oxidative addition product does not correspond with the unknown signals. However, it is known that vinyl tin species are able to coordinate to Pd and as a result inhibit the active catalyst.⁹ We hypothesize that the unknown products are a stannane-coordinated variation on the oxidative addition product. Although we have no firm proof that this type of species is present, a few observations during the experimentation led us to this hypothesis. The catalyst system for these reactions is Pd₂dba₃ and AsPh₃. The Pd₂dba₃ is a dark purple powder consisting of the dibenzylideneacetone ligands coordinating to Pd via the olefin. When these reagents are mixed together in THF for ~10 min, the purple solution turns green as the olefin ligands are displaced by AsPh₃. No drastic color change occurs when the electrophile is added to this green solution. However, when the vinyl tin is then added, the color changes to a brownish-purple color. If color change to purple were indicative of an olefin coordinating to Pd, then it would follow that the vinyl stannane is coordinated to Pd in Stille reaction conditions. As a result, we would not see

the oxidative addition

species. If these sp

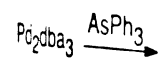
them in the ^{119}Sn N

natural abundance.

they were not ob

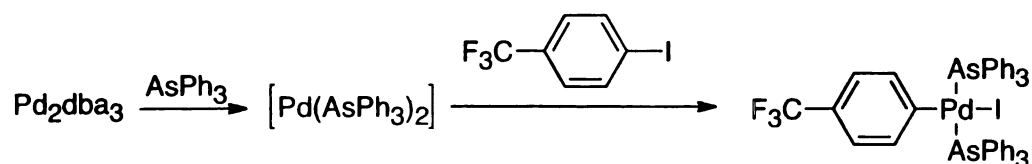
kinetics experiment

Scheme 3.



the oxidative addition product in the Stille reaction, but instead other minor species. If these species do in fact contain tin, we would expect to observe them in the ^{119}Sn NMR spectra. However, due to the low concentration, low natural abundance, and the low signal to noise in the ^{119}Sn NMR spectrum, they were not observed. It should be noted that occasionally during a kinetics experiment, a minor signal around +10 ppm is observed.

Scheme 3.8. Oxidative Addition of 4-Iodobenzotrifluoride



Oxidative
Addition
Product

-64.2 -64.1

Figure 3.12. ^{19}F NMR spectrum of the product of the reaction of iodobenzotrifluoride with the catalyst observed during the reaction (Scheme 3.7)

In conclusion, the results of the study of the oxidative addition of iodobenzotrifluoride to the catalyst show that the oxidative addition is the rate-determining step in the catalytic cycle. To the best of our knowledge, this is the first observation of the oxidative addition of Stille catalysts. Although a computational study of the oxidative addition of iodobenzotrifluoride to the catalysts shows that the oxidative addition is the rate-determining step in the catalytic cycle, the results of the study of the oxidative addition of iodobenzotrifluoride to the catalysts are in good agreement with the results of the study of the oxidative addition of iodobenzotrifluoride to the catalysts.

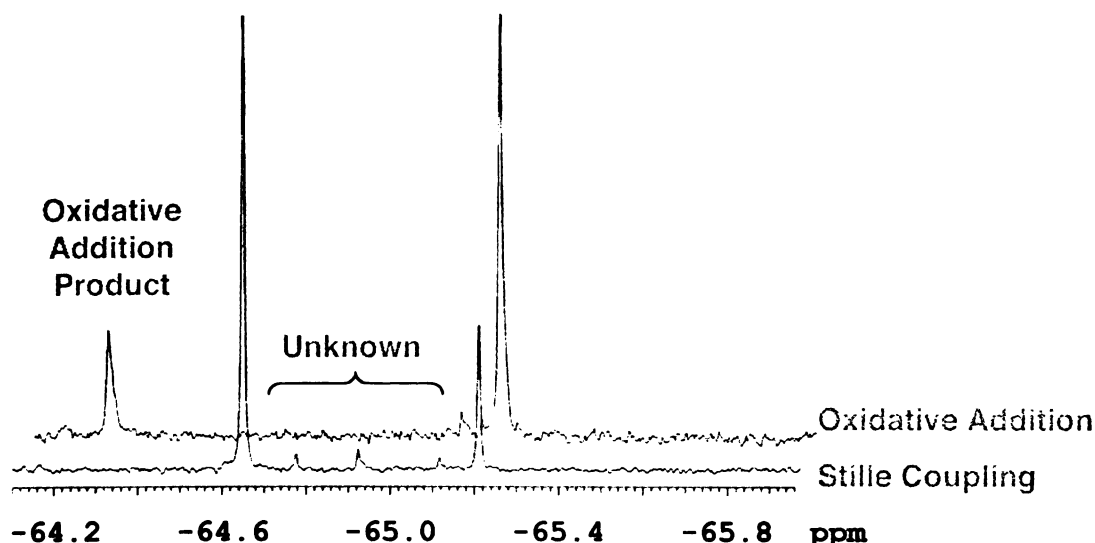


Figure 3.12. ^{19}F NMR Spectra of the Oxidative Addition of 4-Iodobenzotrifluoride (Scheme 3.8) Compared with the Unknown Signals Observed During the Stille Coupling of **42** with 4-Iodobenzotrifluoride (Scheme 3.7)

In conclusion, our studies suggest that considering the transmetallation as the rate-determining step for Stille reactions may be too broad a generalization and the halide choice is quite important regarding the kinetic course. We have provided evidence suggesting that the oxidative addition is the rate-determining step in the Stille reaction with aryl bromides. To the best of our knowledge, no reports have identified the oxidative addition of Stille couplings with aryl bromides as the rate-determining step, although a computational study by Alvarez and de Lera has indicated that the oxidative addition step might become rate determining for certain substrates and/or reaction conditions.²¹ Also, Amatore and Jutand have

indicated that the
probably the rate-de
mention that studie
cycle.⁴⁵

Our discover
understanding of th
logical choices can
well as in the opti
which an aryl brom
reaction is not reac
trimethyl stannane
would lead to no si
rate-limiting step.
supposed rate-dete
are typically expe
reaction. However
these optimization
it is apparent tha
and it would be c

indicated that the oxidative addition of low reactive aryl bromides is probably the rate-determining step in cross-coupling reactions, but go on to mention that studies have only focused on isolated steps of the catalytic cycle.⁴⁵

Our discovery is significant in that it enhances our kinetic understanding of the Stille reaction. With this data, more informed and logical choices can be made regarding electrophile and stannane partners as well as in the optimization of reaction conditions. Imagine a scenario in which an aryl bromide is to be coupled with a tributyl stannane and the reaction is not reaching expectations. Changing to the faster but more toxic trimethyl stannane, activated stannatranes, or less elaborated stannanes would lead to no significant improvement. Since the oxidative addition is the rate-limiting step, standard optimization techniques would focus on the supposed rate-determining transmetallation step, as only changes to that step are typically expected to increase the rate and overall efficiency of the reaction. However, with oxidative addition as the rate-determining step, these optimization efforts would have no beneficial impact. From our results it is apparent that optimization should focus on the oxidative addition step and it would be of no benefit to employ trimethyl stannanes. Therefore, the

less toxic and less

aryl bromide coupli

less toxic and less expensive tributyl stannanes would be sufficient for the aryl bromide coupling.

Chapter 4. Qu

Expanding Sc

4.1. Condition

Having e

Stille condition

Choices of solv

documented to

continued studie

4.2. Solvent Eff

Solvent ca

molecules assist

catalytic cycle (s

accelerate these

rate. For instanc

solvent that leads

coordinative abil

4.2.1. N-Methyl

As expect

vinyl stannanes

Chapter 4. Quantifying Rate Differences for Trialkyl Stannanes: Expanding Scope

4.1. Conditions to be Screened

Having established a foundation for our kinetic studies under common Stille conditions, we sought to determine the generality of the Stille reaction. Choices of solvent,^{14,17} Pd ligands,^{25,26} and additives^{19,22} have all been documented to affect reaction outcomes and thus became the focus of our continued studies.

4.2. Solvent Effects

Solvent can have a significant effect on the rate of reaction. Solvent molecules assist in ligand dissociations that are necessary throughout the catalytic cycle (see Sections 1.2.1–1.2.2). Highly coordinative solvents can accelerate these ligand dissociations resulting in a faster overall reaction rate. For instance, *N*-methyl-2-pyrrolidinone (NMP) is a common Stille solvent that leads to faster reaction rates relative to THF due to its higher coordinative ability and was thus our first solvent of interest.

4.2.1. *N*-Methyl-2-pyrrolidinone (NMP)

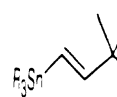
As expected, we observed faster rates (10-30 fold) upon coupling vinyl stannanes with aryl iodides in NMP (Table 4.1), than those performed

in THF (Table

than the corre-

anged from 1

of transmetall-



entry Y

1 H

2 H

3 C

4 C

5

6

^a Me Bu

electrop

^b Determ

NMR s

In t

determinin

solvent may

determining. h

in THF (Table 3.7). We also observed that trimethyl stannanes reacted faster than the corresponding tributyl stannanes 2.3-4.3 fold. Rate differences only ranged from 1.4-2.4 in THF. These results agree with previous assessments of transmetallation as the rate-determining step for aryl iodide couplings.

Table 4.1. Aryl Iodide Couplings in NMP

entry	Y	R	k_{obs} (min^{-1})	relative rates of Me/Bu ^a	yield ^b
1	H	Me (39)	0.48	4.3/1	59 : 81%
2	H	Bu (40)	0.11		59 : 74%
3	CF ₃	Me (39)	0.42	2.3/1	61 : 82%
4	CF ₃	Bu (40)	0.18		61 : 79%
5	<i>n</i> -Bu	Me (39)	0.31	3.1/1	62 : 69%
6	<i>n</i> -Bu	Bu (40)	0.10		62 : 50%

^a Me/Bu ratios are the relative rates of methyl to butyl for each electrophile.

^b Determined by ¹H NMR analysis of the crude reaction mixture using NMR grade TMS-O-TMS as the internal standard.

In the previous chapter we identified oxidative addition as the rate-determining step for aryl bromide couplings. Utilizing a more coordinating solvent may facilitate oxidative addition so that it is no longer rate determining. However, the same trends observed in THF are exhibited in

NMP: little t

when couple

bromide coup

(entries 5-6).

slow oxidative

also observed

that appeared t

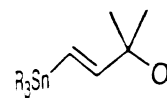
is not yet unc

addition allows

The tributyl s

oxidative additi

NMP; little to no rate difference between trimethyl and tributyl stannanes when coupled with aryl bromides (Table 4.2). The overall rates of aryl bromide couplings in NMP are faster than in THF. For electron rich arenes (entries 5-6), the reactions did not reach completion presumably because slow oxidative addition led to catalyst decomposition. This behavior was also observed in THF. More surprising were trimethyl stannane reactions that appeared to die out faster than tributyl stannane reactions. This behavior is not yet understood. One explanation could be that a slow oxidative addition allows trimethyl stannane to coordinate Pd, rendering it unreactive. The tributyl stannane coordinates less efficiently, so even though the oxidative addition is slow, the Pd remains free to react.



entry	Y
1	H
2	H
3	CH
4	CH
5	<i>n</i> -E
6	<i>n</i> -E

^a Me Bu ratios are
electrophile.

^b Determined by
NMR grade TM

4.2.2. Benzene

We perform

(entries 7-8) co

oxidative addition

most facile ary

reaction time lin

proceed much

[†] Less activated el
monitor by NMR

Table 4.2. Aryl Bromide Couplings in NMP

entry	Y	R	k_{obs} (min^{-1})	relative rates of Me/Bu ^a	yield ^b
1	H	Me (39)	0.0054	0.71/1	59 : 74%
2	H	Bu (40)	0.0076		59 : 76%
3	CF ₃	Me (39)	0.0800	0.91/1	61 : 79%
4	CF ₃	Bu (40)	0.0876		61 : 88%
5	<i>n</i> -Bu	Me (39)	0.0049	1.02/1	62 : 50%
6	<i>n</i> -Bu	Bu (40)	0.0048		62 : 61%

^a Me/Bu ratios are the relative rates of methyl to butyl for each electrophile.

^b Determined by ¹H NMR analysis of the crude reaction mixture using NMR grade TMS-O-TMS as the internal standard.

4.2.2. Benzene

We performed aryl iodide (Table 4.3, entries 1-6) and bromide (entries 7-8) couplings in a non-coordinating solvent, benzene. Since oxidative addition is the rate-determining step for aryl bromides, only the most facile aryl bromide, 4-bromobenzotrifluoride, was studied due to reaction time limitations[†] for NMR experiments. We expected reactions to proceed much slower in benzene than in THF or NMP. In fact, we did

[†] Less activated electrophiles require days of reaction time and are thus not reasonable to monitor by NMR.

1

observe this trend as seen in Table 4.3. More intriguing however, are the overall relative rate differences between trimethyl and tributyl stannanes; *tributyl stannanes seem to react faster than trimethyl stannanes!* It should be noted that, the trimethyl stannane coupled with iodobenzene (entry 1) only reached ~75% conversion and does not precisely fit a first order exponential function while the tributyl stannane reaction (entry 2) went to completion and fit a first order exponential. Therefore, the k_{obs} was determined by fitting linear portions of a $\ln[\text{Sn}]/[\text{Sn}]_0$ vs time plot for the first 20 min (Figure 4.1, inset) and it is realized that the overall reaction is less efficient using **39**. The rate data are reported in Table 4.3. It is expected that the catalyst began to decompose after this time. The rate differences between the trimethyl and tributyl stannanes upon coupling with 4-*n*-butyliodobenzene (entries 5-6) are not representative of the reaction because these reactions only proceeded to ~20% conversion. The rate constants obtained from this data do not accurately depict the reaction process and are thus not reported. However, looking solely at the reaction profile (not shown) indicated that the tributyl stannane reacted faster.

R₃Sn

entry

1

2

3

4

5^d6^d

7

8

^a Me
elec^b Dete
work^c k_{obs}
squa^d Reac
the r^e Reac

Table 4.3. Aryl Halide Couplings in Benzene

$\text{R}_3\text{Sn}-\text{CH}_2-\text{CH}(\text{OH}-\text{C}(\text{Me})_3)-\text{CH}_2-\text{X} + \text{Y}-\text{C}_6\text{H}_4-\text{X} \xrightarrow[\text{benzene, C}_6\text{D}_6 (4.6 \text{ vol\%}), 50^\circ\text{C}]{\text{Pd}_2\text{dba}_3 (2 \text{ mol\%}), \text{AsPh}_3 (8 \text{ mol\%})} \text{Y}-\text{C}_6\text{H}_4-\text{CH}_2-\text{CH}(\text{OH}-\text{C}(\text{Me})_3)-\text{CH}_2-\text{X}$

entry	X	Y	R	k_{obs} (min^{-1})	relative rates of Me/Bu ^a	yield ^b
1	I	H	Me (39)	0.013 ^c	0.63/1	59 : 27%
2	I	H	Bu (40)	0.046		59 : 53%
3	I	CF ₃	Me (39)	0.005	0.56/1	61 : 83%
4	I	CF ₃	Bu (40)	0.009		61 : 91%
5 ^d	I	<i>n</i> -Bu	Me (39)	—	—	62 : 18% ^e
6 ^d	I	<i>n</i> -Bu	Bu (40)	0.009	—	62 : 45% ^e
7	Br	CF ₃	Me (39)	0.0104	0.81/1	61 : 74%
8	Br	CF ₃	Bu (40)	0.0128		61 : 76%

^a Me/Bu ratios are the relative rates of methyl to butyl for each electrophile.

^b Determined by ¹H NMR analysis of the crude reaction mixture after work-up using NMR grade TMS-O-TMS as the internal standard.

^c k_{obs} reported from $t = 0 - 20$ min and was determined by linear least squares method.

^d Reaction only reached 20% conversion so no accurate rate information on the reaction progress could be obtained after 10 h in the NMR.

^e Reaction was run for 16 h on the bench-top

2

1

Figure
NMR
(green)
benzen
inset,
provide
decay

W
tributyl

would

stannan

carbon

stannatr

A coord

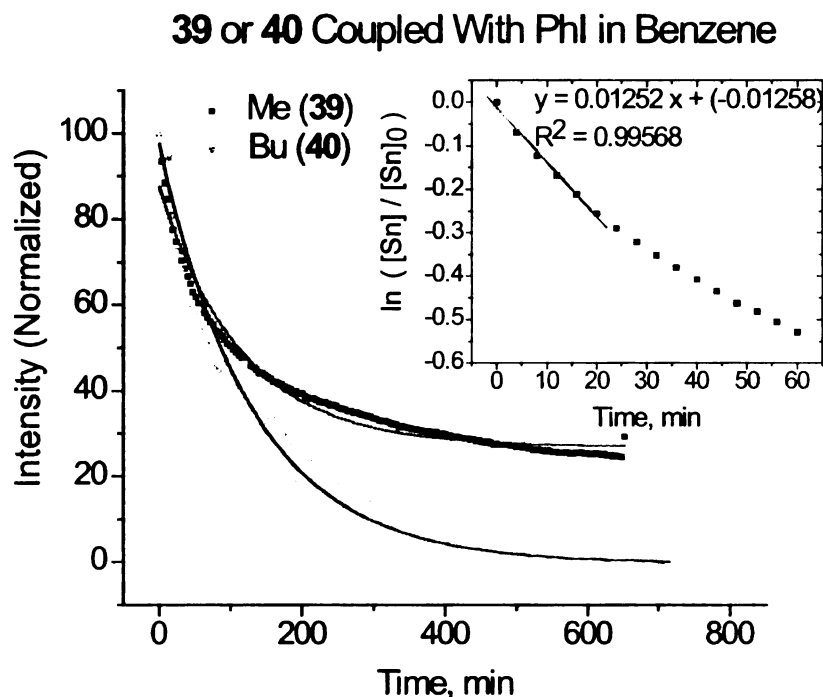


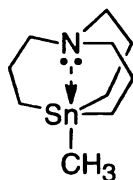
Figure 4.1. Coupling of **39** or **40** with PhI in Benzene. 186 MHz ^{119}Sn NMR relative integration data for the consumption of **39** (black) or **40** (green) upon coupling with PhI under a $\text{Pd}_2\text{dba}_3/\text{AsPh}_3$ catalyst system in benzene. Data for **39** from $t = 0$ -20 min was fit to a linear regression plot (inset, red solid line). First order exponential fit (red solid line) did not provide an accurate fit. Data for **40** was fit to a first order exponential decay model (blue solid line).

We became curious about the apparent enhanced reactivity of the tributyl stannanes vs. the trimethyl stannanes. It seems improbable benzene would activate the tributyl stannane to react faster than the trimethyl stannane. Activation occurs through coordination to tin to make the α -carbon more nucleophilic. For example, the nitrogen lone pair of a stannatrane³⁰ activates and enhances the Sn–C bond reactivity (Figure 4.2).

A coordinating solvent can also assist in ligand dissociations about Pd and

thus facilitate the reaction. We see this “activation” upon switching to benzene, a non-coordinating solvent that should not have this effect on tin. Moreover, activation of a tributyl stannane over a trimethyl stannane is unlikely simply due to the steric differences about the Sn center. Therefore, the differences may be related to catalyst activity and/or a type of deactivation of the trimethyl stannane as opposed to activation of the tributyl stannane.

Figure 4.2. Stannantrane: Activation of Sn–C Bond



We looked to kinetic studies of oxidative addition by Amatore and Jutand with respect to the active catalyst to further understand our case (Scheme 4.1).⁹ When cross-coupling reactions are performed, the Pd precursor and ligands are typically premixed to form the active catalyst. Amatore and Jutand have shown that the bis ligated catalyst, stabilized as the solvento complex, is the active species for oxidative addition. They have also shown that this species can be rendered unreactive upon competitive coordination of a vinyl stannane, but the solvento complex is typically favored for coordinating solvents (e.g. THF and NMP).



su

co

ca

To

di

ca

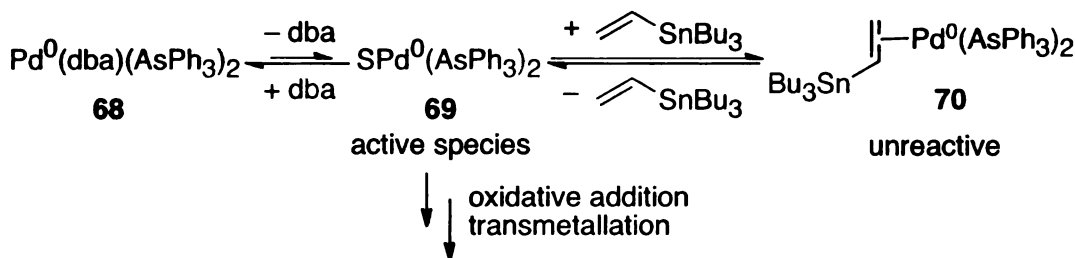
sa

re

sin

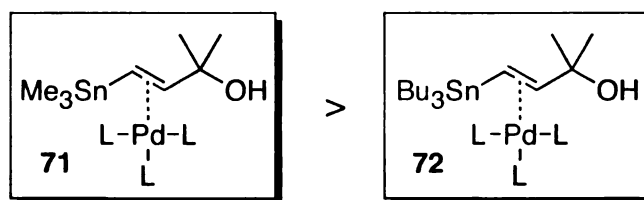
re

Scheme 4.1. Formation and Inhibition of the Active Catalyst



We believe that a non-coordinating benzene system does not allow for sufficient stabilization of the active catalyst by solvent, and instead there is competitive coordination of a vinyl stannane to Pd. Coordination inhibits the catalyst, which results in a lower concentration of active catalyst in solution. The steric differences between a trimethyl and tributyl stannane provide for different degrees of coordination such that more of the trimethyl stannane can coordinate compared with the tributyl stannane (Figure 4.3). The tributyl stannane reactions then have more free active catalyst than the trimethyl reactions, which then allows for the overall reaction to proceed more rapidly since $k_{\text{obs}} = k_{\text{trans}}[\text{PdArXL}_2]$.

Figure 4.3. Coordination of Stannanes to Palladium



To test whether the active catalyst concentration is different in the two reactions, competitive reactions should be run in the same reaction vessel

2

and con

trimethy

change

opposed

be supp

catalyst

than wh

T

slight e

catalytic

approx

stannan

it can

transme

Given

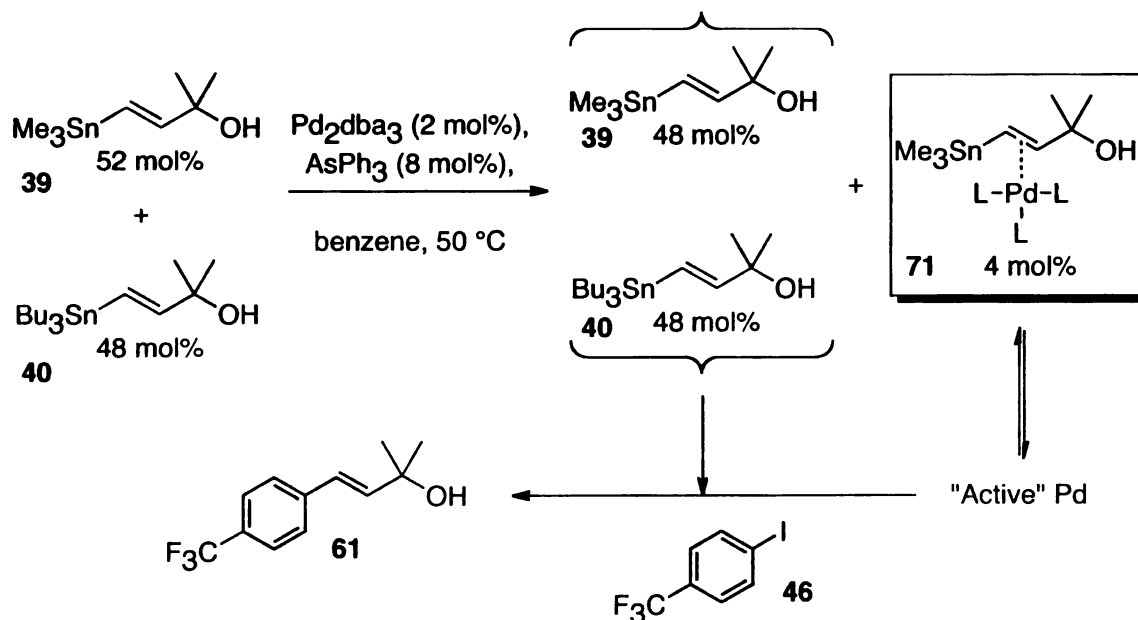
stannan

than tri

and compare the results to runs with only one of the stannanes. If the trimethyl stannane is coordinated to a higher degree, there should be no change in the trimethyl reactivity for the reaction run in competition as opposed to the independent run. However, the tributyl stannane rate should be suppressed because in competition, it would be in a lower concentration catalyst environment brought on by trimethyl stannane – Pd coordination than when run independently.

The competition experiment (Scheme 4.2) was performed with a slight excess of trimethyl stannane (**39**) to allow for coordination to the catalytic Pd to afford the unreactive species. This would result in an approximate equal distribution between free trimethyl (**39**) and tributyl (**40**) stannanes. Once the unreactive Pd species equilibrates to the active species, it can undergo an oxidative addition followed by a competitive transmetallation with either the trimethyl (**39**) or tributyl stannane (**40**). Given that trimethyl stannanes are suggested to react faster than tributyl stannanes,²⁴ we would expect trimethyl stannane (**39**) to be consumed faster than tributyl stannane (**40**) when in competition with each other.

Scheme 4.2. Competition Experiment to Test for Trimethyl Stannane Coordination



When run individually, as described in Table 4.3, entries 5-6, tributyl stannane **40** reacted faster than trimethyl stannane **39**. The reaction profile is shown in Figure 4.4. When the competition experiment described in Scheme 4.2 was performed, the rate profile for the trimethyl stannane **39** was not affected but the tributyl stannane **40** rate was suppressed (Figure 4.5). Furthermore, both 1:2 and 2:1 ratios of trimethyl to tributyl stannanes afforded the same trend. The data suggests a diminished concentration of active catalyst brought on by the presence and coordination of trimethylvinyl stannanes, e.g. **71**.

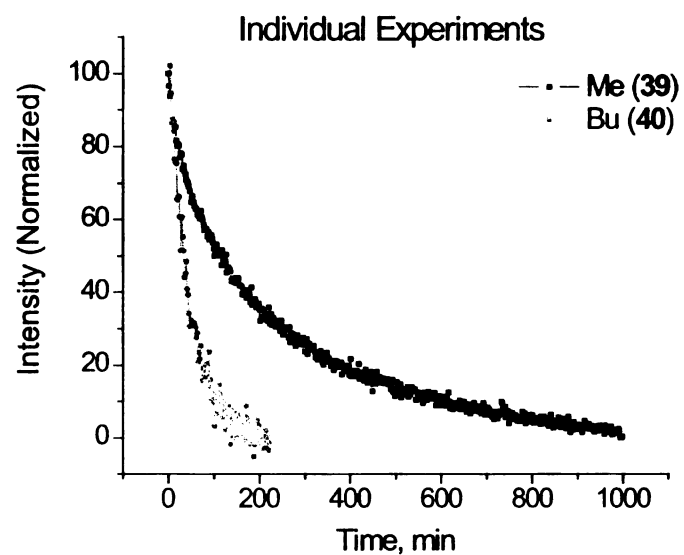


Figure 4.4. Individual Experiments. 186 MHz ^{119}Sn NMR relative integration data for the consumption of **39** (black trace) or **40** (red trace) upon coupling with 1.2 equiv of PhI under a $\text{Pd}_2\text{dba}_3/\text{AsPh}_3$ catalyst system in benzene. Both sets of data were fit to a first order exponential decay model (not shown) to reveal for **39**, $k_{\text{obs}} = 0.0044 \text{ min}^{-1}$ and for **40**, $k_{\text{obs}} = 0.022 \text{ min}^{-1}$.

Figure
relativ
trace)
system
decay
= 0.01

Not on

change

been p

reactio

43. Li

kinetic

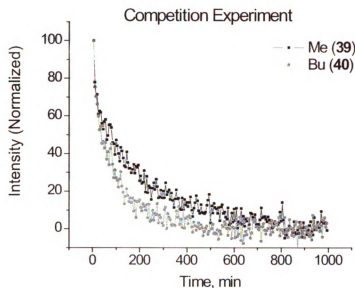


Figure 4.5. Competition Experiment. 186 MHz ^{119}Sn NMR normalized relative integration data for the consumption of **39** (black trace) and **40** (red trace) upon coupling with 1.2 equiv of PhI under a $\text{Pd}_2\text{dba}_3/\text{AsPh}_3$ catalyst system in benzene. Both sets of data were fit to a first order exponential decay model (not shown) to reveal for **39**, $k_{\text{obs}} = 0.005 \text{ min}^{-1}$ and for **40**, $k_{\text{obs}} = 0.01 \text{ min}^{-1}$.

We have seen that solvent can have a major impact on the reaction. Not only can solvent increase the rate of reaction as with NMP, but can also change the mechanistic details as seen with benzene. This scenario has not been previously reported and could be quite important when considering reaction optimization.

4.3. Ligand Effects

The electronic and steric nature of the Pd ligands can also affect the kinetics of the Stille reaction. Since ligand dissociations are necessary

throughout the catalytic cycle, a strongly coordinating ligand (strong σ donor) would be unfavorable. On the other hand, the solvent and/or ligand needs to be coordinative enough to stabilize Pd in the active (S)PdL₂ form to avoid thermal decomposition to Pd black. Moreover, the oxidative addition requires an electron rich Pd species (Pd = nucleophile, aryl halide = electrophile), while the transmetallation requires an electron poor Pd species (stannane = nucleophile, Pd = electrophile). The ligands need to achieve a good balance between these requirements has been explored and discussed by Farina.²⁵ After screening ligands for the coupling of vinyltributyl stannane and iodobenzene, he reported that AsPh₃ and tri-2-furylphosphine (TFP) were efficient ligands from a rate and yield perspective because they most likely achieve the desired ligand bonding characteristics (Table 4.4). It is unclear exactly how this balance is achieved, but may be correlated to metal-ligand bond enthalpy. Later, Fu proposed that strong σ donors may actually be good ligands, provided they are sterically bulky enough to easily dissociate such as with P(*t*-Bu)₃⁴⁶ and have given access to aryl chloride couplings that were previously resistant to oxidative addition. We sought to explore these ligand effects on the rate differences between trimethyl and tributyl stannane couplings.

431.

expect

stann.

AsPh

iodob

This

reacts

by-pr

the d

Table 4.4. Ligand Effects²⁵

$\text{Bu}_3\text{Sn}-\text{CH}=\text{CH}_2 \xrightarrow[\text{THF, 50 } ^\circ\text{C}]{\text{PhI, Pd}_2\text{dba}_3, \text{Ligand,}} \text{Ph}-\text{CH}=\text{CH}_2$			
entry	ligand	relative rate	% yield
1	PPh ₃	1	15.2
2	TFP	105	> 95
3	AsPh ₃	1100	> 95

4.3.1. Tri-2-furylphosphine (TFP)

Upon changing the palladium ligands from AsPh₃ to TFP, we expected that similar rate differences between the trimethyl and tributyl stannanes would ensue, albeit with overall slower rates as compared with AsPh₃. Much to our surprise, reacting the tributyl stannane with iodobenzene resulted in an apparent induction period as seen in Figure 4.6. This curve is indicative of an autocatalyzed reaction where starting material reacts through one pathway to produce a product (either the main product, by-product, or any side products) that is able to catalyze a faster pathway to the desired product, as outlined in Figure 4.7.

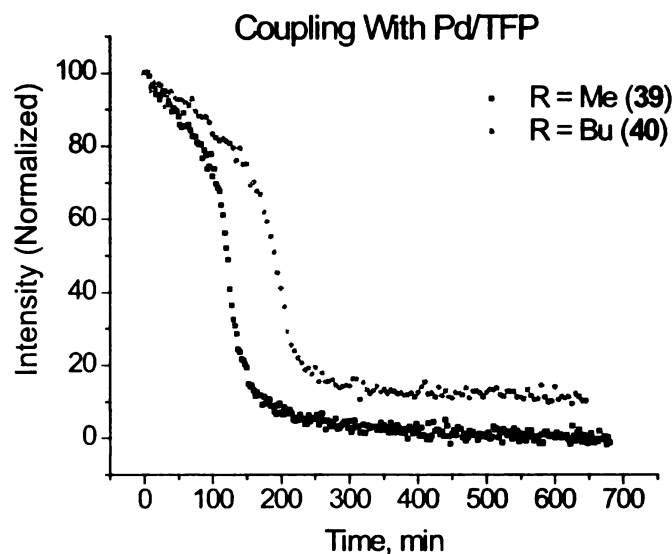
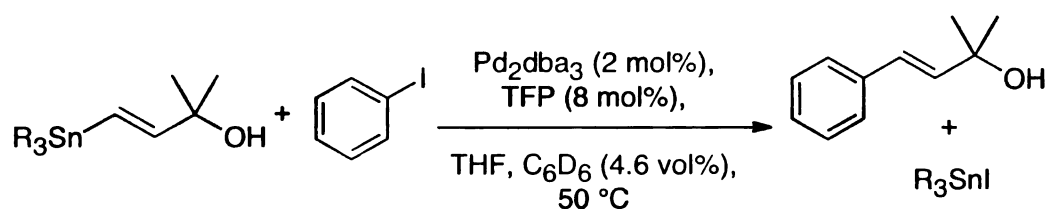


Figure 4.6. Studies of Couplings with Pd/TFP. 186 MHz ^{119}Sn NMR relative integration data for the consumption of **39** (black trace) or **40** (red trace) upon coupling with 1.2 equiv of PhI under a Pd_2dba_3 /TFP catalyst system. Both sets of data were fit to a first order exponential decay model (not shown) after the induction period (~ 100 min) to reveal for **39**, $k_{\text{obs}} = 0.033 \text{ min}^{-1}$ and for **40**, $k_{\text{obs}} = 0.024 \text{ min}^{-1}$.

reacti

discu

featur

under

cond

auto

rates

prod

at ~2

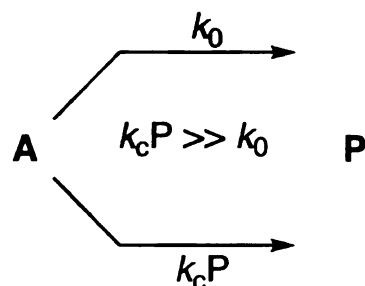
mate

solut

expe

auto

Figure 4.7. Autocatalytic Reaction Process



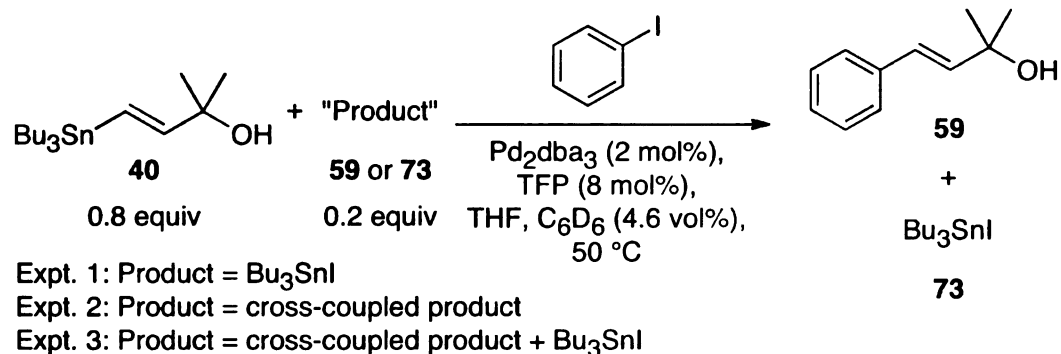
One important aspect of our kinetic studies is that for first order reactions, the initial concentration does not need to be known as was discussed in Section 2.1. For reactions exhibiting an induction period, this feature is no longer valid. Therefore, our first objective was to qualitatively understand the basis of the autocatalysis, such as finding what species or conditions cause the autocatalysis. We would then be able to implement the autocatalytic species to achieve first order behavior and quantify the relative rates of reaction.

The two main products in Stille reactions are the cross-coupled product and the tin halide by-product. Since the onset of autocatalysis occurs at ~20% conversion, we expect to have ~80% of the organostannane starting material and ~20% each of the cross-coupled and tin halide by-product in solution. To test whether either product autocatalyzes the reaction, experiments were set up to mimic the conditions at the point of autocatalysis, ~100 min (Scheme 4.3). Analysis of the reaction profile

1

revealed that the induction period was still present and to approximately the same extent when either or both of the products were incorporated.

Scheme 4.3. Effect of Products On Autocatalysis



We next asked if the free hydroxyl is involved in initiating the autocatalysis. Reactions with methoxy vinylstannane **42** also exhibit an induction period, although over a much longer period of time (Figure 4.8). The extent of free hydroxyl involvement is not yet understood but it seems to allow for faster formation of the autocatalytic species and likely involves oxygen chelation.

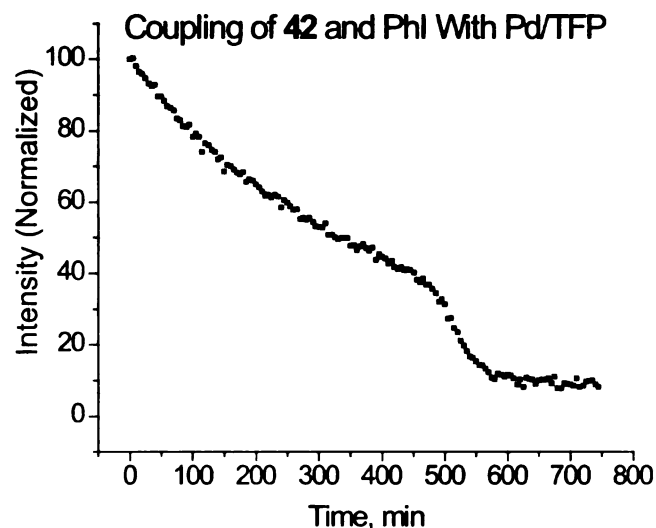
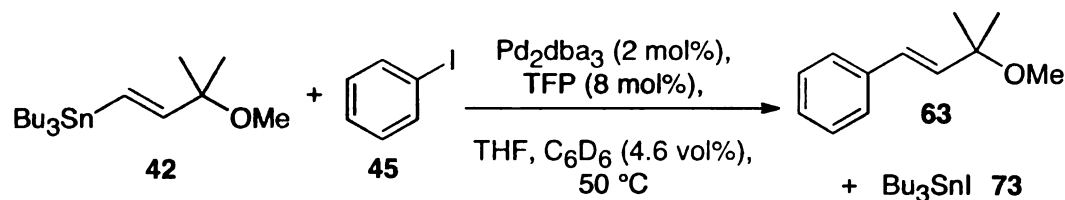


Figure 4.8. Determining if a Protected Hydroxyl Affects Autocatalysis. 186 MHz ^{119}Sn NMR relative integration data for the consumption of **42** (black trace) upon coupling with 1.2 equiv of PhI under a Pd_2dba_3 /TFP catalyst system. The data was fit to a first order exponential decay model (not shown) after the induction period (~ 500 min) to reveal a $k_{\text{obs}} = 0.024 \text{ min}^{-1}$.

4.3.1.1. Insight into the Source and Mechanism of Autocatalysis

To the best of our knowledge, autocatalysis in the context of Pd-catalyzed reactions was not reported in the literature until recently. In 2008, the Hartwig group described the autocatalytic oxidative addition kinetics of aryl bromides with a $\text{Pd}/t\text{-Bu}_3\text{P}$ system.⁴⁷

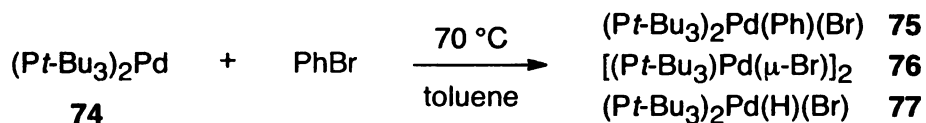
Upon oxidative addition of $(t\text{-Bu}_3)_2\text{Pd}$ to PhBr, the oxidative addition product **75** was formed. This species can undergo thermal

1

6
J
A
E
M
S
J
F
D
F
F
A

decomposition to afford the bridged halo palladium species **76** and upon further heating, decomposes to the hydridopalladium bromide **77** (Scheme 4.4).

Scheme 4.4. Oxidative Addition Studies by Hartwig⁴⁷



The oxidative addition was then performed with compounds **75-77** and revealed that **77** sufficiently catalyzed the reaction such that the oxidative addition to PhBr followed first order kinetics (Figure 4.9). Once **77** is formed and undergoes reaction with PhBr, a new catalytic cycle is formed for the regeneration of **77** as seen in Scheme 4.5.

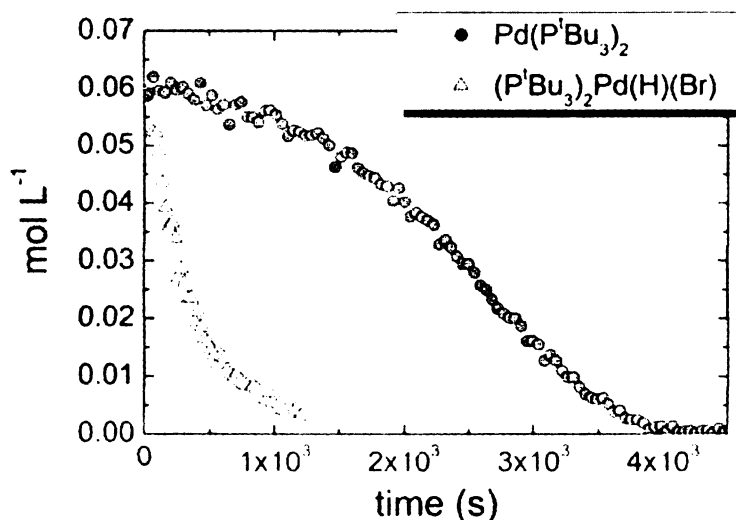
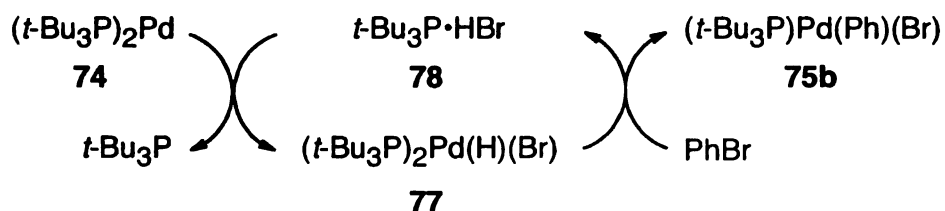


Figure 4.9. Relative Decay of $\text{Pd}(\text{P}^t\text{-Bu}_3)_2$ (**74**) and $\text{Pd}(\text{P}^t\text{-Bu}_3)_2(\text{H})(\text{Br})$ (**77**) During the Oxidative Addition of PhBr in 2-Butanone at 70 °C.⁴⁷ Reproduced with permission from Barrios-Landeros, F.; Carrow, B. P.; Hartwig, J. F. *J. Am. Chem. Soc.* **2008**, *130*, 5842–5843. Copyright 2008 American Chemical Society

2

1

Scheme 4.5. Catalytic Cycle for the Regeneration of Hydrido Palladium Halide



Our efforts to identify the species responsible for autocatalysis had focused on the reaction products but we had not considered any transient Pd species. To this end, we wanted to see if a similar hydrido palladium halide species was responsible for our autocatalysis. There are several considerations however. In the previous chapter we discussed how oxidative addition is the rate-determining step for aryl bromide couplings while transmetallation is the rate-determining step for aryl iodide couplings. We also observed autocatalysis in aryl iodide couplings with TFP as the Pd ligand. If transmetallation is rate determining for Pd/TFP systems, then we should not see this type of behavior since the species undergoing the transmetallation (the oxidative addition product analogous to **75**) would be the same regardless of the initial Pd source. This indicates that with TFP as the palladium ligand, oxidative addition may be rate determining until a sufficient concentration of a more active Pd species is formed to allow for facile reaction. We hypothesize that the initial Pd species is not reaction enough to promote a fast oxidative addition, but after slow formation of a

new Pd species, the reaction proceeds. Subsequently, transmetallation becomes rate determining such that the reaction is first order in stannane. This is observed qualitatively by comparing reaction profiles of the trimethyl vs. tributyl stannane in Figure 4.6, where the rates of the induction period between the trimethyl and tributyl stannanes are equivalent, after which there is clearly a difference in the reaction profile.

To determine whether an autocatalytic species is at play, we chose to change the order of addition in our kinetic studies. Since Hartwig reported that the oxidative addition alone afforded three different products, including the autocatalytic species **77**, we imagined that allowing the oxidative addition to proceed first, the hydrido palladium species might be formed *in situ*. Upon addition of the stannane, we would be able to see if there was an effect on the induction period due to the presence of the preformed autocatalytic species. Initially, we took a ^{31}P NMR of the $\text{Pd}_2\text{dba}_3/\text{TFP}$ mixture as seen in Figure 4.10. We expected to see a signal around -35 ppm for different Pd/dba/TFP complexes and/or a signal around -80 ppm for free TFP, both as seen by Farina and others.²⁵ However, we saw only a significant peak at -11 ppm likely corresponding to TFP oxide. We allowed the catalyst mixture and iodobenzene to react for 2 hours in the NMR at 50 °C while monitoring the ^{31}P nucleus. A reaction time of 2 hours was chosen

because the induction period lasts about 100 min with (*E*)-2-methyl-4-(trimethylstannyl)but-3-en-2-ol (**39**) as well as with the tributyl variant (**40**). By this time, a new small signal appeared in the ^{31}P NMR around -1.5 ppm. To determine whether this was the species responsible for autocatalysis, we injected (*E*)-tributyl(3-methoxy-3-methylbut-1-enyl)stannane (**42**), which had previously exhibited an induction period of ~500 min under our standard procedure (Figure 4.8), into the reaction mixture. We expected to see immediate consumption of the stannane while monitoring by ^{119}Sn NMR if we had in fact formed the autocatalytic species. Instead we saw kinetics identical to Figure 4.8 while monitoring for the first 1.5 h. In order to establish if a hydrido palladium species is responsible for the signal at -1.5 ppm and/or the autocatalysis, it should be independently synthesized, fully characterized, and tested for autocatalysis.

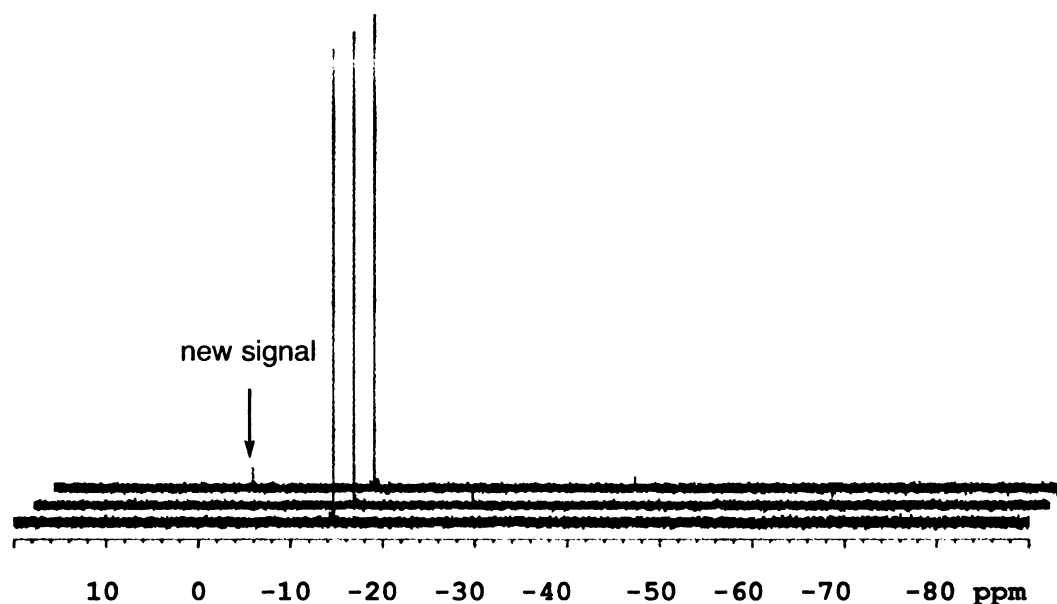


Figure 4.10. Oxidative Addition of $\text{Pd}_2\text{dba}_3/\text{TFP}$ to PhI in THF. Selected 202 MHz ^{31}P NMR spectra during an arrayed experiment monitoring the oxidative addition of $\text{Pd}_2\text{dba}_3/\text{TFP}$ to PhI in THF. The first spectra (from front to back) was taken before the addition of PhI , the second was taken immediately following the addition of PhI , and the third was taken after the reaction proceeded for 2 h by which time a new signal appeared at -1.5 ppm.

4.3.1.2. Attempts to Synthesize the Autocatalytic Species

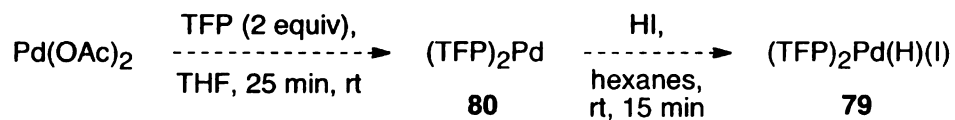
We sought to independently synthesized the hydrido palladium halide $(\text{TFP})_2\text{Pd}(\text{H})(\text{I})$ (**79**) to test its influence on the induction period. Preparation of this exact species has not been reported in the literature, although similar species have been described.^{47,48} For example, $\text{PdHCl}(\text{P-}t\text{-Bu}_3)_2$ is stable stable once isolated but may decompose if left in solution.⁴⁸ Our attempt to

2

1

make and isolate **79** started with the preparation of bis ligated palladium $\text{Pd}(\text{TFP})_2$ (**80**) via treatment of $\text{Pd}(\text{OAc})_2$ with TFP in THF (Scheme 4.6). This medium brown compound was insoluble in common NMR solvents and thus not characterized. Oxidative addition to HI was then performed on compound **80**, and again the product (**79**) was insoluble and not characterized by NMR. An IR spectra (KBr) of **79** was taken to determine whether a Pd-H bond was formed but the spectra was inconclusive. Although we could not confirm the structure of **79**, we performed a kinetic experiment with the presumed compound as the Pd catalyst. Unfortunately, we did not observe any reaction and could therefore not confirm, or deny the involvement of **79** as the autocatalytic species in Stille reactions with $\text{Pd}_2\text{dba}_3/\text{TFP}$ catalyst systems. The known HPdBrL_2 should be tested in our kinetics reaction to see if autocatalysis is affected.

Scheme 4.6. Proposed Preparation of $\text{TFP}_2\text{Pd}(\text{H})(\text{I})$ **79**



4.3.1.3. Pd/TFP System for Couplings of Unsubstituted Vinyl Stannanes

One of the most surprising aspects of the autocatalysis was that it had not been observed before with this catalyst system. In fact, Farina had



reported first order kinetics with TFP as the Pd ligand. However, his studies were performed on tributylvinylstannane coupled with iodobenzene. In order to extend our studies of relative rates to complement Farina's studies on ligand effects, we chose to study the couplings of both the unsubstituted trimethyl and tributylvinylstannanes.

Neither stannane afforded autocatalytic behavior when coupled with iodobenzene; first order behavior as reported by Farina was observed. This suggests that either 1) the autocatalytic species may be more easily formed and does not require oxygen chelation or 2) that the hydroxyl actually inhibits the reaction and/or formation of the autocatalytic species. It became clear that the reaction kinetics of Pd/TFP systems are also affected by stannane substitution and further experimentation could provide insight into the mechanism.

4.3.1.4. Insight into the Induction Period for a Pd/TFP System

We see a difference in the induction period between the free hydroxyl substituted stannanes (**39** and **40**) and the methoxy substituted stannane (**42**). Given the similar rates during the induction period between **39** and **40** (Figure 4.6), the oxidative addition may be the rate-determining step at the beginning of the reaction. We therefore chose to couple both **39** and **40** with the more activated 4-iodobenzotrifluoride. Both reactions followed first



order kinetics, where the trimethyl stannane (**39**) reacted faster than the tributyl (**40**). We next coupled unsubstituted trimethyl and tributylvinylstannanes (**57** and **58**, respectively) with iodobenzene. These reactions proceeded without an induction period as well. This provides evidence that the oxidative addition of PhI in the presence of oxygen substituted stannanes may be problematic since changing to a more activated electrophile eliminated the induction period and unsubstituted vinylstannanes coupled with PhI also did not exhibit an induction period. If the oxidative addition of PhI were simply the rate-determining step, then the reaction with **39** and **40** coupled with PhI would exhibit 1st order behavior.

It appears that the oxygen plays a role in inhibiting the reaction, and to different extents for OH's and OMe's. If we are seeing an induction period with oxygen bearing vinyl stannanes, the oxygen may somehow inhibit the oxidative addition thus making it the rate-determining step in the beginning of the reaction. Differences between the hydroxyl and methoxy vinylstannanes may stem from the ability of the hydroxyl to hydrogen bond to the TFP acting as a ligand scavenger or assisting in ligand dissociation whereas the methoxy does not have that hydrogen bonding capability and therefore has a longer induction period.

4.3.1.5. Comparison of TFP and AsPh₃ Systems

Further analysis of the reaction profile of trimethyl and tributylvinylstannanes coupled with iodobenzene in a Pd/TFP system indicated that they reacted at essentially the same rate, suggesting that the oxidative addition is the rate-determining step. However, this seems unlikely due to the fact that we have shown that the oxidative addition of iodobenzene is quite facile since the reaction course is completed before an arrayed kinetics experiment can be initiated. We believe that the coinciding rates were in fact a coincidence of competitive vinyl stannane coordination as was seen for couplings in benzene (Section 4.2.2). An analogous competition experiment was performed and the trimethylvinylstannane did react faster than the tributylvinylstannane indicating that the transmetallation is actually the rate-determining step but competitive vinyl stannane coordination to Pd can inhibit the reaction. In conclusion, it is of no benefit to employ trimethylvinylstannane over tributylvinylstannane from a kinetic standpoint. Also, trimethylvinylstannane is very volatile and tedious to prepare.

What struck our interest as well was the comparison of reaction rates between AsPh₃ and TFP as the Pd ligands. Farina reported that AsPh₃ reactions provided rates 10 times that of TFP, while we found the opposite

trend for most instances. For reactions of trimethyl and tributylvinylstannane coupled with iodobenzene run individually or in competition, the Pd/TFP system provided faster rates than the Pd/AsPh₃ system. When comparing the reaction profile after autocatalysis for both trimethyl and tributyl stannanes coupled with iodobenzene, again the Pd/TFP system was faster than the Pd/AsPh₃ system. Only for the coupling of the activated electrophiles 4-iodobenzotrifluoride with the hydroxyl stannanes was the reaction faster with Pd/AsPh₃ vs. Pd/TFP. (Note: methoxy and *t*-Bu stannanes were not studied under the TFP system) This provides further evidence that the oxidative addition is problematic for Pd/TFP systems.

4.3.2. Tri-*tert*-butylphosphine P(*t*-Bu)₃

We then became curious whether the autocatalysis and apparent limitations on the oxidative addition with Pd/TFP arise with only this particular ligand, or if another phosphine ligand would produce similar results. Bulky phosphine ligands have proved effective for oxidative addition of otherwise “inert” aryl chlorides.²⁶ The bulk of the phosphine alkyl groups coupled with the strong coordination of a phosphine allows for a balance in the overall coordinative ability of P(*t*-Bu)₃. This species is rather prone to oxidation and is therefore more complicated to use and has

2

1

C
e
M
V
C
L
P
L
J
M
a
V
a
F

not been the focus of our kinetic studies. However, we thought it prudent to see what impact it has on aryl bromide couplings since we proposed the oxidative addition as the rate-determining step.

The reaction of (*E*)-2-methyl-4-(trimethylstannyl)but-3-en-2-ol (**39**) with bromobenzene catalyzed by $\text{Pd}(\text{P}(t\text{-Bu})_3)_2$ was set up in a bench-top reaction and monitored by GC throughout the day (Scheme 4.7). However, after ~7 hours only 25% of the starting stannane had been consumed (Figure 4.11). The reaction was left overnight and by the time 21 hours had elapsed, 100% of the stannane had been consumed. First order extrapolation of the data (shown as a solid line in Figure 4.11) suggests that the reaction would not reach completion for several days if ever. It appears that an autocatalyzed system must be operating with $\text{P}(t\text{-Bu})_3$ as the Pd ligand as well in order to have full conversion after 21 hours. Although we have not analyzed a wide variety of phosphine ligands, there may be an induction period trend for phosphines involved as seen with TFP.

Scheme 4.7. Impact of P(*t*-Bu)₃ on Bromobenzene Coupling

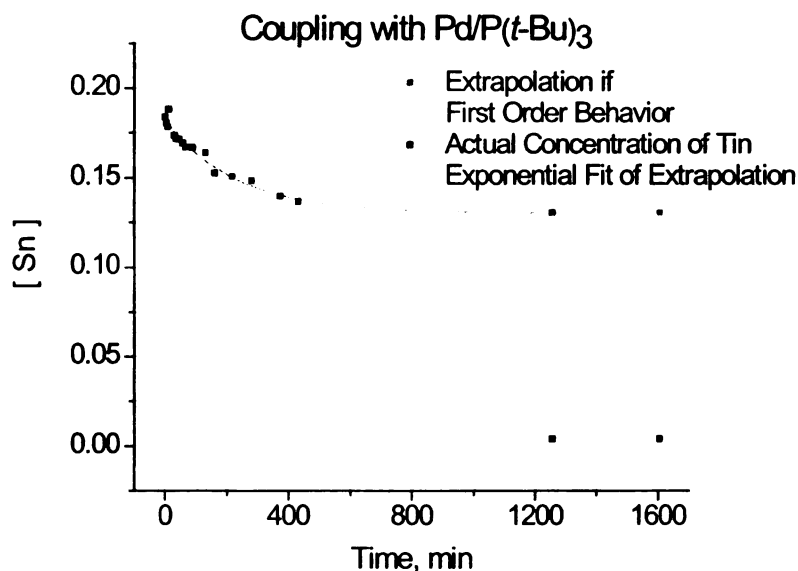
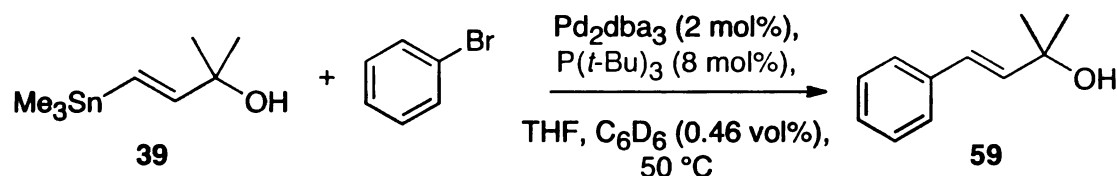


Figure 4.11. Coupling of **39** and PhBr by Pd/P(*t*-Bu)₃ Monitored by GC. Consumption of **39** upon coupling with 1.2 equiv of PhBr under a Pd₂dba₃/PPh₃ catalyst system as monitored by GC with mesitylene as an internal standard. The concentration was determined by comparison to the appropriate calibration curve. The black trace represents the data collected by GC. The two red dots represent an extrapolation if the reaction proceeded by first order kinetics while the red solid line represents a fit of the data that would be first order to a first order exponential decay model.

4.3.3. Triphenylphosphine

In an early study designed to determine whether Pd/PPh₃ is a reasonable catalyst/ligand combination to study by NMR, we ran a reaction on the bench-top and monitored the reaction progress with GC. Under a

$\text{Pd}_2\text{dba}_3/\text{PPh}_3$ catalyst system, (*E*)-2-methyl-4-(tributylstannyl)but-3-en-2-ol (**40**) and 4-iodobenzotrifluoride afforded only traces of product after 20 h. Allowing the reaction to proceed for 4 days resulted in complete consumption of the starting stannane and a large amount of cross-coupled product. No internal standard was utilized and therefore a final yield was not obtained. However, from this information it appears that again simple first order kinetics are not operable here either. Full consumption after 4 days when only traces of product were identified after 20 h, suggests that autocatalysis is at play in this phosphine system as well.

4.4. Conclusions

Although many groups have explored both solvent and ligand effects, we complemented such studies to include rate differences between trimethyl and tributyl stannanes across various solvent and ligand systems. We have provided further examples on the complexity of the Stille reaction whereby solvent can greatly affect not only the rate, but also the mechanistic pathways. Even ligands can dramatically change the mechanism. For instance, TFP has exhibited autocatalytic behavior for substituted vinyl stannane couplings and we have shown preliminary data suggesting that this may be a trend over other phosphine systems.

Chapter 5. Side Reactions of the Stille Reaction

5.1. Why Use an Internal Standard?

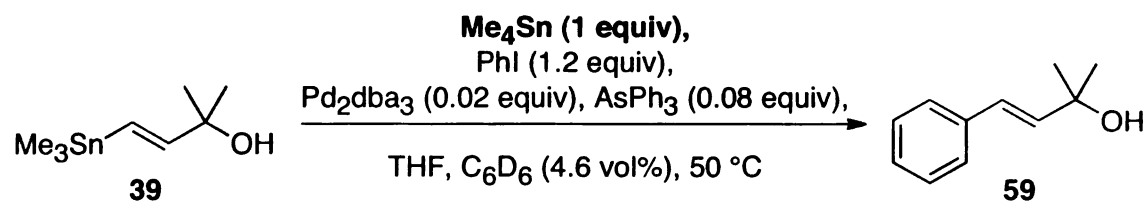
Running a reaction in an NMR spectrometer provides a pseudo internal standard since each spectrum in an arrayed experiment can be integrated relative to the first. Furthermore, as discussed in Chapter 2, we do not need to know the actual starting concentration to determine the rate constant for first order kinetics. These two characteristics in theory made it unnecessary for us to use an internal standard. However, so as to leave no doubt, we used Me₄Sn as an internal standard at the commencement of our ¹¹⁹Sn NMR kinetic studies. With that very first reaction we learned that the Stille reaction is truly complex.

5.2. Me₄Sn As the Internal “Standard”

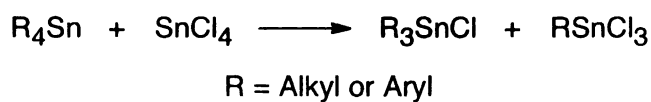
We chose to use Me₄Sn as an internal standard because 1) it is the NMR reference standard for ¹¹⁹Sn NMR and 2) alkyl ligands transfer slower than vinyl ligands and should not interfere with or complicate the reaction. However, for the coupling described in Scheme 5.1, we found that the internal *standard* peak *increased* throughout the reaction! To be sure that the increasing signal was not an artifact, we removed Me₄Sn from the mix. We

then observed the *formation* of Me_4Sn ! When we utilized the corresponding tributyl stannane, we did not observe Bu_4Sn formation. It appears that a disproportionation (ligand exchange) process occurs with the trimethyl stannanes, but perhaps the butyl ligands are too bulky and do not disproportionate as easily under the reaction conditions. Typically a Kocheshkov disproportionation³⁶ is used to prepare alkyltinhalides from tetraalkyl and tetrahalo stannanes (Scheme 5.2), but the reverse reaction, which forms tetramethyltin, has been observed by Nechaev.⁴⁹

Scheme 5.1. Stille Reaction Utilizing Me_4Sn as an Internal Standard



Scheme 5.2. Kocheshkov Disproportionation for the Synthesis of Alkyl Tin Halides



If this process proceeds from the trialkylvinylstannane, then upon disproportionation we would expect to see divinyl tins upon Me_4Sn

formation. We do not observe divinyl tin species[†] in the ^{119}Sn NMR of our kinetic experiments and therefore believe the disproportionation process proceeds from the tin halide by-product. If Me_4Sn is formed from the tin halide, then it is formed after the transmetallation step and should not interfere with the Stille coupling process. Furthermore, since Me ligands transfer slower than vinyl ligands, Me_4Sn should not enter back into the Stille cycle. It is important to note, that adding Me_4Sn intentionally does not change the rate of reaction. Therefore, we are reasonably sure that Me_4Sn is not detrimental to the reaction, although we cannot run a control experiment in absence of Me_4Sn since it is formed *in situ*.

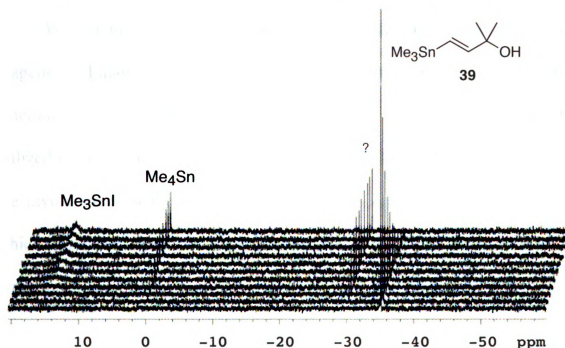
With respect to tin recycling in our catalytic tin case (to be discussed in Ch. 6), formation of Me_4Sn is a termination step in the tin catalytic cycle because of slow alkyl transfer. To advance the use of trimethylstannanes in the catalytic Stille, we first need to understand why Me_4Sn is forming, and then find a way to suppress it. As we are interested in using the less toxic tributylstannanes instead of the trimethylstannanes for this sequence, the fact that we do not see Bu_4Sn formation is in our favor.

[†] We do observe other tin species as will be discussed in the next section, but we do not observe tin species related to Me_4Sn formation.

5.3. Formation of Transient Tin Species

We have also observed the formation of a transient tin species in the ^{119}Sn NMR denoted “?” in Figure 5.1. These species are typically ~5 ppm downfield of the starting vinyl stannane signal, and are present for all substituted stannane, electrophile, and Pd/L combinations. The formation occurs faster than consumption, and both rates appear to be increased when more activated (electronwithdrawing substituted) aryl halides are used.

Figure 5.1. Course of the Stille Reaction Monitored by ^{119}Sn NMR



Our initial attempts at isolating the unknown material were unsuccessful. Given the close proximity to the starting material, we initially thought the species was a structurally related divinyl species,

$\text{Me}_2\text{Sn}(\text{CH}=\text{CHC}(\text{CH}_3)_2\text{OH})_2$, that could be correlated to the Me_4Sn formation discussed above. This was quickly dismissed since we do not see Bu_4Sn formation, but we do see corresponding unknown signals for tributylvinylstannanes. Furthermore, the ^{119}Sn spectra of independently synthesized divinyl tin did not match the unknown signal (see Ch. 9 experimental for **40b**). We considered that the starting material could isomerize to the internal or *Z* vinyl tin, but again these spectra did not match the independently synthesized stannanes.

We thought we could gain insight into the identity by determining the reagent combination that affords the unknown. To this end, we examined the reaction mixtures outlined in Table 5.1. Entry 1 mimics the conditions utilized in the Stille couplings without the electrophile, while entry 2 probes the involvement of the tin halide by-product disproportionation, neither of which produced the unknown species. We then tested the effect of a different ligand, TFP, to no prevail, and subsequently added Bu_3SnI to test the effect of the tin halide in the presence of palladium as shown in entry 3. Still, the unknown species was not formed. Treatment of **39** with I_2 , which has been known to form *in situ*, converted the vinyl tin to only the tin halide and presumably the vinyl iodide through tin-halogen exchange.

Finally, we questioned the impact of a Pd^{II} species. Subjecting vinyl stannane **39** to $\text{Pd}(\text{OAc})_2$ only resulted in Me_4Sn formation, which was surprising but uninformative with regards to formation of the unknown species. Treatment of **39** with $\text{Pd}(\text{OAc})_2$ does appear to shed some light into formation of Me_4Sn as we never considered Pd(II) mediated Me_3Sn formation. Typically when Pd(II) species are utilized in cross-coupling reactions, the active Pd(0) species is accessed by a homocoupling with the organometallic reagent.²⁴ We would therefore expect formation of a diene and tin dimer, but not Me_4Sn . Clearly a different process occurs and may be promoted by Pd(II) species.

1

10

11

12

13

14

15

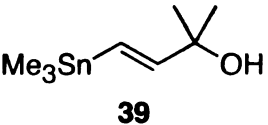
16

17

18

19

Table 5.1. Testing Conditions for Formation of the Unknown Tin Species

<div style="display: flex; align-items: center; justify-content: center;"> <div style="text-align: center; margin-right: 10px;">  <p>39</p> </div> <div style="text-align: center; margin-right: 10px;"> <p>Conditions</p> <p>THF, C₆D₆ (4.6 vol%), 50 °C</p> </div> <div style="text-align: center;"> <p>→ Unknown Tin Species</p> </div> </div>		
entry	conditions	formation of unknown?
1	Pd ₂ dba ₃ (0.02 equiv), AsPh ₃ (0.08 equiv), 4 h	No
2	Me ₃ SnI (1 equiv), overnight	No
3	Pd ₂ dba ₃ (0.02 equiv), TFP (0.08 equiv), 6 h	No
	then Bu ₃ SnI added and stirred overnight	No
4	I ₂	No, only Me ₃ SnI ^a
5	Pd(OAc) ₂	No, but Me ₄ Sn formed

^a Determined by ¹¹⁹Sn NMR. Presumably the vinyl iodide is formed as well.

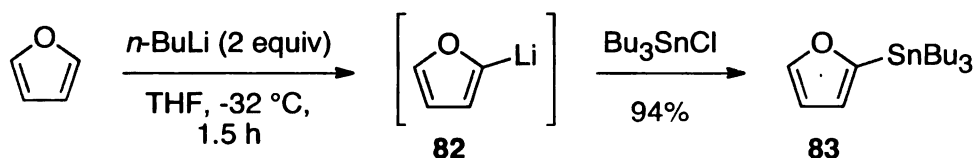
Our efforts were then turned to isolation of the unknown species for identification purposes. Kinetic profiles of previous reactions for these substrates and conditions indicated the highest amount of unknown was present in the reaction media at 200 min. To this end, tributylvinyl stannane **40** was coupled with iodobenzene by Pd₂dba₃/AsPh₃ in THF in a bench-top reaction. The reaction was cold quenched at 200 min by submerging the reaction vessel in an ice bath, then concentrated and analyzed by ¹¹⁹Sn NMR to be sure the unknown species was present. Since we originally thought the tin species was a derivative of the starting material based on the chemical shift, we were looking for a relatively polar compound during

column chromatography. This time however, we painstakingly ran a column buffered with 1% triethylamine to avoid any proteodestannylation,^{29,50,51} with an eluting solvent of 9:1 hexanes/ethyl acetate. Typically the product is separated using 8:2 hexanes/ethyl acetate. We were pleased to find that after nearly 125 fractions were collected, trace amounts of the unknown product was found in fractions 10-12 as determined by the ^{119}Sn NMR spectra. After ^1H and ^{13}C NMR and GC/MS analysis, we determined that the unknown tin species was tributylphenyltin (**81**)! This species is non-polar and original isolation attempts were focused on polar tins, which is perhaps why it was not found right away. However, it is an sp^2 tributyl stannane, which explains the close proximity of the ^{119}Sn NMR signal to the starting vinyl stannane signal.

Knowing the identity of the species allowed us to re-evaluate how it is formed. PPh_3 and AsPh_3 are both known to exchange a phenyl for aryl group in cross-coupling reactions, where the phenyl is incorporated in the cross-coupled product and not the organometallic reactant. Similarly, furyl transfer can ensue when using tri-2-furylphosphine as the ligand. For Stille conditions in $\text{Pd}_2\text{dba}_3/\text{TFP}$, we still observe a transient tin species ~ 5 ppm downfield of the starting stannane signal. For this ligand however, we would

expect the furyl stannane with a distinct chemical shifts to be formed instead of the phenylstannane. Although we were skeptical that furyl transfer was occurring, the ^{119}Sn NMR of 2-tributylstannylfuran (**83**) had not been reported, so we independently synthesized **83** via lithiation and metal-metal exchange as shown in Scheme 5.3. Comparison of the authentic 2-tributylstannylfuran ^{119}Sn NMR signal at -64 ppm does not correlate with the transient signal at -40 ppm, therefore suggesting that a ligand exchange process is not responsible for aryl tin formation.

Scheme 5.3. Synthesis of 2-Tributylstannylfuran



We next considered the phenyl arising from the electrophile. However, we see similar signals regardless of the electrophile employed. The differences between aryl groups substituted at the *para* position with H, $n\text{-Bu}$, CF_3 , and OMe may not effect a large difference in the ^{119}Sn NMR spectra since the variations are far removed from the tin atom. We therefore ran another Stille coupling (trimethylstannane **39** coupled with 4-bromoanisole by $\text{Pd}_2\text{dba}_3/\text{AsPh}_3$ in THF) to see if the electrophile aryl group is transferred to form 4-trimethylstannylanisole (**84**). To our delight, after

cold quenching the reaction at 110 min and simple work up, the crude material provided a signal around -31 ppm in the ^{119}Sn NMR (Figure 5.2). The sample was then spiked with an independently synthesized aliquot of **84** and the signals matched. To be sure the two species were in fact identical and did not simply coalesce, if for instance the transient species was actually tributylphenyltin, we next spiked the sample with an authentic sample of Bu_3SnPh . There were clearly two distinct stannane signals, although very close to each other. The ^{119}Sn NMR chemical shift range is large (+2000 to -1000 ppm) and very minute chemical shift differences are sometimes hard to distinguish even when an internal reference is utilized. Literature values often differ by ± 1 ppm depending on solvent, temperature, crude vs. clean spectra, etc.³⁶

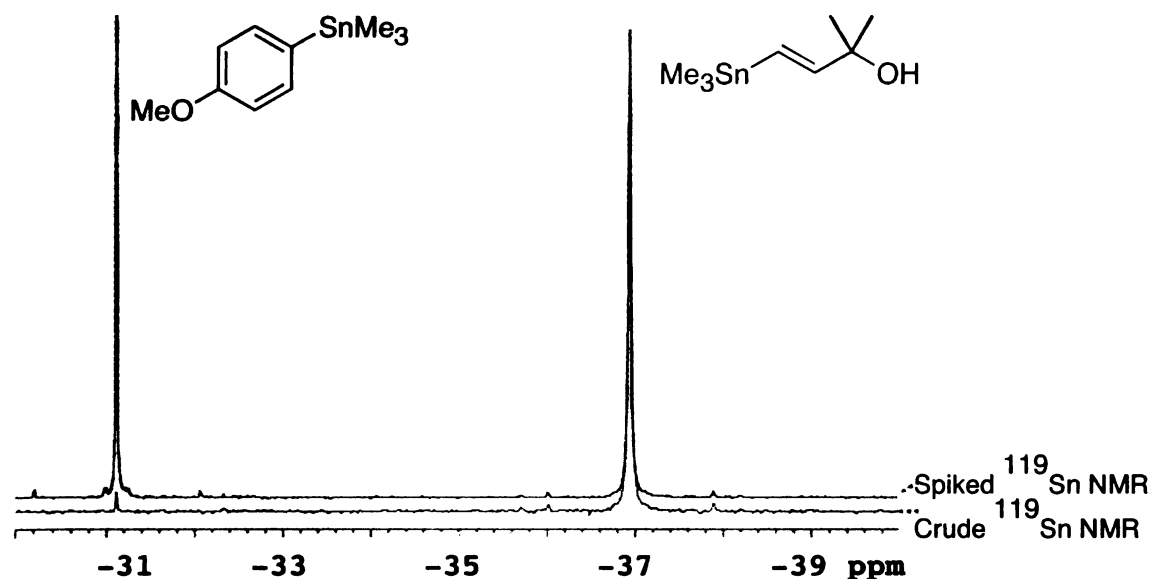


Figure 5.2. Spiked ^{119}Sn NMR Experiment. The lower 186 MHz ^{119}Sn NMR spectrum shows the crude reaction mixture for the coupling of **39** with 4-bromoanisole in a $\text{Pd}_2\text{dba}_3/\text{AsPh}_3$ catalyst system where by a small amount of a tin compound was formed at -31 ppm. The upper spectrum shows the crude mixture spiked with an authentic sample of 4-trimethylstannylanisole, showing a signal at -31 ppm.

Confirming that the signal is an aryl tin derived from the electrophile answered one question while opening to door to new ones, particularly, how and why is this happening? In our earlier attempts at initiating formation, we looked to the vinyl stannane as the tin source since we believed the unknown transient species to be a derivative and did not consider the electrophile to be involved. We now know that instead aryl tins are formed where the electrophile is the aryl source. Thus, aryl tin formation requires the presence of both a stannane and electrophile.

An early control reaction mixing a vinyl stannane and electrophile without Pd resulted in no reaction. Mixing a vinyl stannane and electrophile

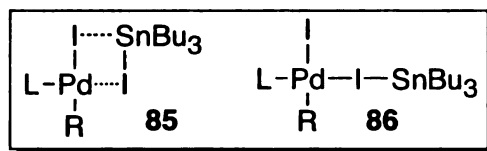
with Pd/L represents a typical Stille reaction and would not clue us into the mechanistic details. Instead, we considered that the tin halide by-product could serve as the tin source instead of the starting vinyl stannane. Therefore, we could subject the tin halide to different conditions to see if aryl tins form. This would also indicate the transfer occurs after the Stille coupling. These results are outlined in Table 5.2. When Bu₃SnI was mixed with iodobenzene at 50 °C, the phenyl stannane signal was not formed in the ¹¹⁹Sn NMR spectrum (entry 1). Even when Pd was included in the mix to facilitate any ligand exchange reactions, phenyl stannane was not formed (entry 2). However, a new signal at +50 ppm was observed. We did not identify the compound, but perhaps the Bu₃SnI can act as a ligand (Figure 5.3) for the oxidative addition product, PdL₂PhI, thus affording a new ¹¹⁹Sn signal. This hypothesis is based on Espinets identification of Bu₃SnI as a Pd ligand during the transmetallation mechanism.^{8,20} However, we would expect a hypercoordinated stannane signal to appear downfield³⁶ of the Bu₃SnI signal at ~+70 ppm. From these data it is clear that tin halide by-product is not the source of tin for aryl tin formation.

Table 5.2. Testing Conditions for Formation of Phenyl Tin from Tin Halide

$\text{Bu}_3\text{SnI} \xrightarrow[\text{THF, C}_6\text{D}_6 \text{ (4.6 vol\%), 50 }^\circ\text{C}]{\text{Conditions}} \text{Bu}_3\text{SnPh}$ <div style="display: flex; justify-content: space-around; width: 100%;"> 73 81 </div>		
entry	conditions	formation of 81 ? ^a
1	PhI (1 equiv), 1.5 h	No
2	PhI (1 equiv), Pd ₂ dba ₃ (0.02 equiv), AsPh ₃ (0.08 equiv), 45 min	No, unidentified signal appeared at +50 ppm

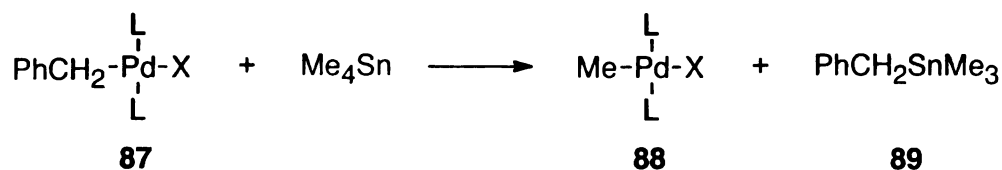
^a Determined by ¹¹⁹Sn NMR. Presumably the vinyl iodide is formed as well.

Figure 5.3. Possible Structures for the ¹¹⁹Sn NMR Signal at +50 ppm



Upon reviewing the literature, we found that in 1979 Stille reported formation of a benzylstannane **89** instead of the expected cross-coupled product **88** under stoichiometric Pd (Scheme 5.4).⁵² This represents the first R for R transmetallation vs. typical R for X transmetallation. Although there are differences in our system, for instance we are operating in a catalytic Pd environment and utilizing aryl (instead of benzyl) species, it is likely that our aryl tins are formed through an identical pathway, whereby aryl tins are formed during the transmetallation step. Our early attempts at forming the aryl tins under various conditions were unsuccessful as all of the Stille reagents (stannane, electrophile, and Pd) are necessary to produce aryl tins.

Scheme 5.4. Benzyl Stannane Formation Observed by Stille⁵²



5.4. Implications of Aryl Tin Formation

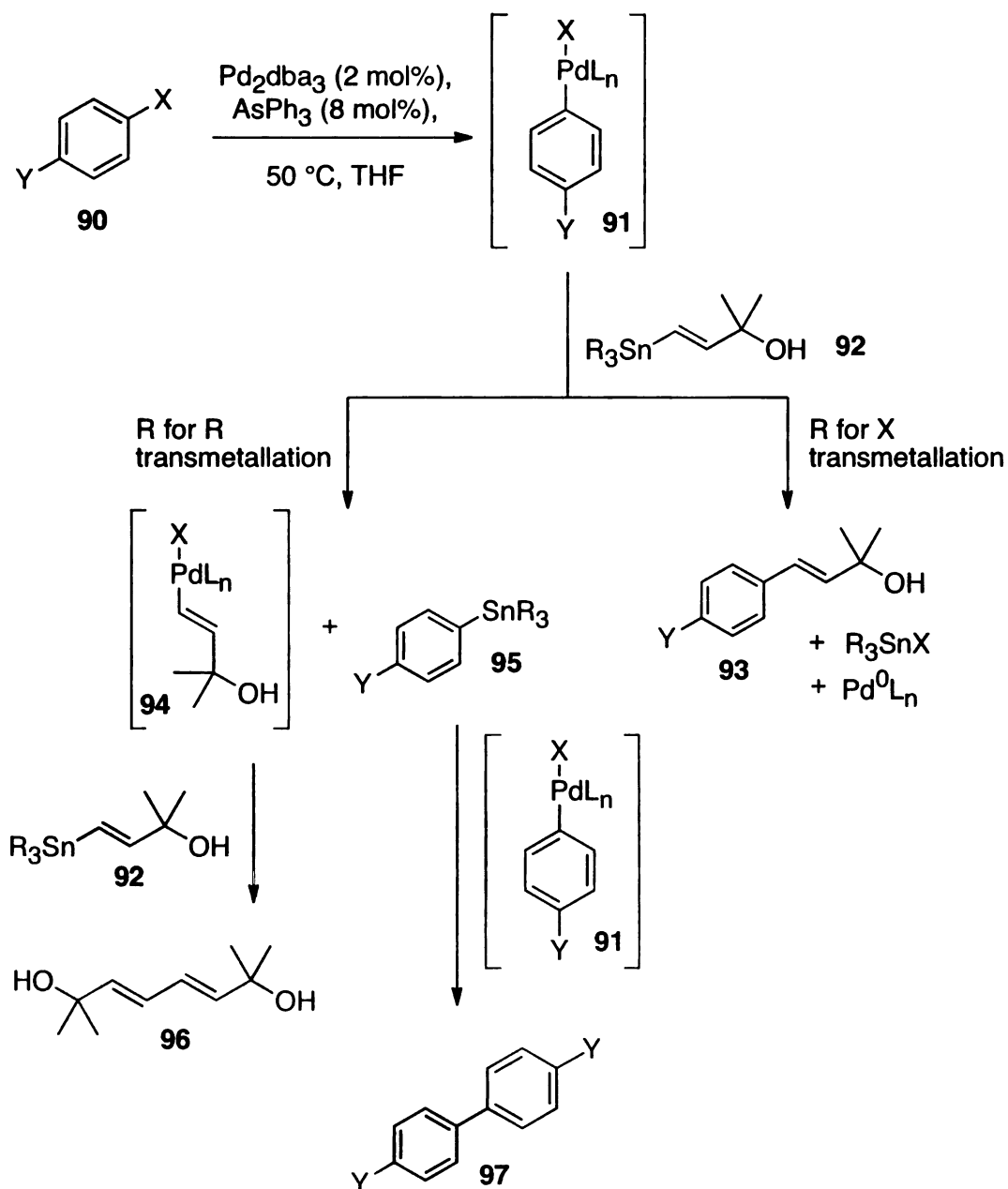
The transient aryl tin species are consumed in the Stille coupling, and therefore have a direct impact on the reaction products. Scheme 5.5 outlines the possible pathway to form aryl tins during the Stille reaction and the implications of its formation. After the oxidative addition to form **91**, transmetallation may take place by either the normal R for X transmetallation leading to **93**, or an R for R transmetallation leading to the vinyl Pd species **94** and aryl tin **95**. The vinyl Pd species **94** may then undergo a transmetallation with another vinyl stannane **92** molecule to produce the homocoupled diene **96**. Furthermore, the aryl tin **95** may couple with the more prominent aryl Pd species **91** to render the homocoupled biaryl **97**. Typically, homocoupled products are attributed to oxygen, radicals, disproportionations, or halogen-metal exchanges. Elsevier and coworkers ran several experiments in the absence of oxygen and with radical inhibitors, but none of the conditions reduced the amount of homocoupled products formed and go on to suggest that aryl tin formation is yet another pathway to afford homocoupled product formation.⁵³ Although Elsevier

2

1

suggested this idea, it appears we are the first ones to actually observe the formation of transient aryl tins in a catalytic Stille and correlate them with homocoupled products.

Scheme 5.5. Pathway to the Formation of Aryl Tins and Resulting Compounds



5.5. Relation of Aryl Tin Formation to Homocoupling

As discussed in the previous section, aryl tin formation can lead to homocoupled products derived from both the stannane and electrophile. We have identified and or isolated the diene products in our reaction media, but were unable to isolate the biaryls due to their volatility but we have observed their formation via GC/MS analysis. To gain a better idea of the product distribution for each substrate combination over various conditions, we ran all of the experiments from our kinetic studies on the bench-top and determined the yields by ^1H NMR using either TMS-O-TMS or mesitylene as an internal standard. The cross-coupled products, phenyl-transfer products, and homocoupled diene yields are presented in the following tables (Table 5.3 and Table 5.4). It should be noted that the yields presented for the homocoupled diene are based on the percentage of stannane consumed, e.g. 2 equivalents of stannane provide 1 equivalent of diene.

Looking at the homocoupled product (**102**) since it is at least in part related to aryl tin formation, there are several trends across all solvents used. Take for instance reactions run in THF, shown in Table 5.3. When tributyl stannanes and aryl bromides are cross-coupled, there is a slightly higher homocoupled diene yield than when aryl iodides are utilized with the exception of Br vs. I for the tributyl stannane in entry 4b. The differences in

diene yield between aryl bromide and aryl iodide couplings with trimethyl stannanes are more prevalent (e.g. entry 6c). Furthermore, the trimethyl stannanes give higher amounts of diene compared with tributyl stannanes in both aryl iodide and bromide cases with the exception of Me vs. Bu for iodides in entry 5c. Substitution on the aryl ring revealed that with increased electrophilicity (more electron withdrawing character), the amount of homocoupled diene is lowered. Comparing OH (**92**, entries 1-3) and OMe (**98**, entries 4-6) substituted vinyl stannanes, stannanes **98** provide higher amounts of homocoupled diene while maintaining the aforementioned trends. This is interesting in and of itself, since the rate profile of stannane consumption for stannanes **92-Me** and **98-Me** as well as **92-Bu** and **98-Bu** are identical (discussed in Ch 3), but lead to different product distributions.

Table 5.3. Product Yields for Stille Reactions in THF

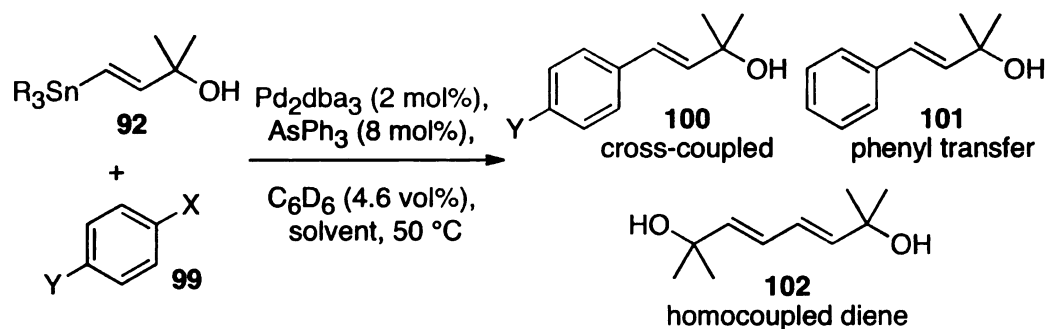
<div><div><div><div><div>$R_3\text{Sn}-\text{CH}=\text{CH}-\text{C}(\text{Me})_2\text{R}^I$</div><div>$R^I = \text{OH} \text{ (92)}$ $\text{OMe} \text{ (98)}$</div></div><div><div>$+ \text{Y}-\text{C}_6\text{H}_4-\text{X}$</div><div>99</div></div></div><div><div>$\xrightarrow[\text{THF, 50 } ^\circ\text{C}]{\text{Pd}_2\text{dba}_3 \text{ (2 mol\%)}, \text{AsPh}_3 \text{ (8 mol\%)}, \text{C}_6\text{D}_6 \text{ (4.6 vol\%)}}$</div></div><div><div><div><div><div>$\text{Y}-\text{C}_6\text{H}_4-\text{CH}=\text{CH}-\text{C}(\text{Me})_2\text{R}^I$</div><div>100</div><div>cross-coupled</div></div><div><div>$\text{C}_6\text{H}_5-\text{CH}=\text{CH}-\text{C}(\text{Me})_2\text{R}^I$</div><div>101</div><div>phenyl transfer</div></div><div><div>$\text{R}^I-\text{C}(\text{Me})_2-\text{CH}=\text{CH}-\text{CH}=\text{CH}-\text{C}(\text{Me})_2\text{R}^I$</div><div>102</div><div>homocoupled diene</div></div></div></div></div></div></div>								
entry	stannane	Y	product	% yield		% yield		
				R = Me		R = Bu		
				X:	I	Br	I	Br
1a	92	H	100		34	35	51	33
b			102		14	42	21	23
2a	92	CF ₃	100		87	49	79	83
b			101		3	11	1	9
c			102		11	36	9	9
3a	92	<i>n</i> -Bu	100		30	23	36	23
b			101		4	11	2	10
c			102		29	39	23	24
4a	98	H	100		60	45	65	51
b			102		34	55	29	28
5a	98	CF ₃	100		87	44	82	58
b			101		1	10	3	1
c			102		12	46	12	29
6a	98	<i>n</i> -Bu	100		45	33	70	37 ^a
b			101		2	11	8	
c			102		42	56	22	

^a Yield of both **100** and **101** as they overlapped in the ¹H NMR spectrum.

2

1

Table 5.4. Product Yields for Stille Reactions in NMP and Benzene



solvent = NMP								
entry	stannane	Y	product	% yield		% yield		
				R = Me		R = Bu		
				X:	I	Br	I	Br
1a	92	H	100		81	74	84	76
b			102		11	35	13	12
2a	92	CF ₃	100		82	79	76 ^a	88
b			101		<1	3		6
c			102		4	18		4
3a	92	<i>n</i> -Bu	100		69	50	57	61
b			101		<1	10	11	12
c			102		11	33	24	21

^a Yield of **100** and **101** as the signals overlapped in the 1H NMR spectrum.

4a	92
b	
5a	92
b	
c	
6a	92
b	
c	

5.6. Insight into

It is unclear

X transmetallation

difference in the

bromides. The

proceed through

R for R (see

structural confor

have considered

$(PPh_3)_2PdRX$

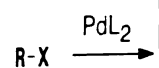
explanation.

Table 5.4 (cont'd)

solvent = benzene							
4a	92	H	100	27	n.d.	53	n.d.
b			102	37	n.d.	28	n.d.
5a	92	CF ₃	100	83	18	91	30
b			101	<1	7	2	6
c			102	16	40	7	29
6a	92	<i>n</i> -Bu	100	18	n.d.	45	n.d.
b			101	<1	n.d.	2	n.d.
c			102	44	n.d.	23	n.d.

5.6. Insight into the Basis of R for X vs. R for R Transmetallation

It is unclear why a stannane undergoes R for R vs. the common R for X transmetallation (Scheme 5.6) based on our data alone. We have seen a difference in the yield of homocoupled products between aryl iodides and bromides. The mechanism of R for X transmetallation has been shown to proceed through a Sn-X-Pd halo-bridge.^{8,20} Therefore it seems probable that R for R (see Scheme 5.7) transmetallation is a reflection of different structural conformation and coordination interactions during this step. We have considered the x-ray diffraction data by Antipin and Grushin on (PPh₃)₂PdRX square planar systems⁵⁴ and developed a preliminary explanation.



In their 19

(PPh₃)₂PdRX sy

oxidative additi

and Pd-Br influ

transmetallation.

transmetallation.

for R transmetal

arene and Sn is p

the phenyl ring

dependent on the

aryl ring has an

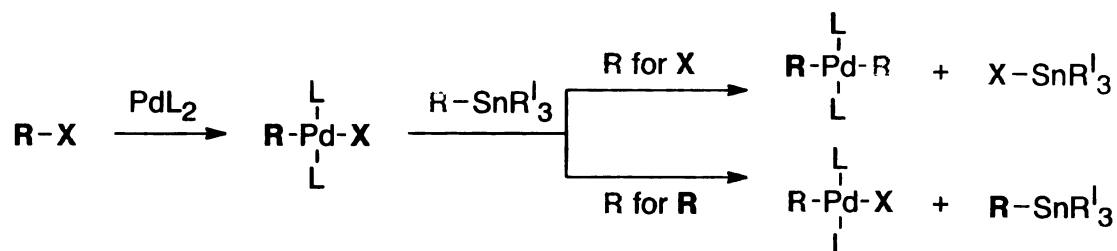
Br and I, the a

perpendicular a

the ring system

thus leading to

Scheme 5.6. R for X vs. R for R Illustration



In their 1998 paper,⁵⁴ Antipin and Grushin measured bond lengths for (PPh₃)₂PdRX systems (where X = F, Cl, Br, and I), which are akin to the oxidative addition products we are studying. The bond lengths of the Pd-I and Pd-Br influence Sn-X-Pd bridge formation leading to the R for X transmetallation. A better-matched bond length may favor R for X transmetallation, while a less matched one may turn favor to R for R. An R for R transmetallation may be favored if a coordination bridge between the arene and Sn is possible. Antipin and Grushin⁵⁴ report that the orientation of the phenyl ring with respect to the metal coordination plane is highly dependent on the nature of the halide (Figure 5.4). When X = F and Cl, the aryl ring has an interplanar angle of 71.5 and 75.4°, respectively. When X = Br and I, the aryl ring plane and metal coordination plane become more perpendicular at 86.0 and 84.8°, respectively. Changing the orientation of the ring system may expose the electron rich arene to coordinate with Sn thus leading to an associative R for R transmetallation as shown in Scheme

5.7. Furthermore

where I makes

Consequently tra

Since the

This could allo

electrophilicity o

for the less trad

bromides may ha

thus leading to

stannanes provid

halides, aryl su

However, we c

hindered trime

point. We be

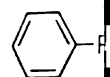
conformation

transmetallatio

5.7. Furthermore, the electrophilicity of Pd changes depending on the halide, where I makes Pd more positive (electrophilic) than the Pd in L_2PdRBr . Consequently transmetallation will be slower for bromides vs. iodides.

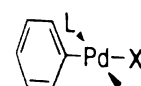
Since the aryl ring is more perpendicular for bromides vs. iodides.⁵⁴ This could allow for more arene coordination with Sn. The lower electrophilicity of the PdBr lends to a slower reaction and allows more time for the less traditional coordination to ensue. It is then reasonable that the bromides may have a higher propensity to undergo R for R transmetallation thus leading to higher amounts of homocoupled product. Trimethyl stannanes provide larger amounts of homocoupled products across solvents, halides, aryl substitution of the electrophiles, and stannane substitution. However, we cannot make a clear correlation between the less sterically hindered trimethyl stannanes and higher amounts of homocoupling at this point. We believe that a balance between coordination and structural conformation may give rise to preference between R for X and R for R transmetallation.

Figure 5.4. Inter



71.5

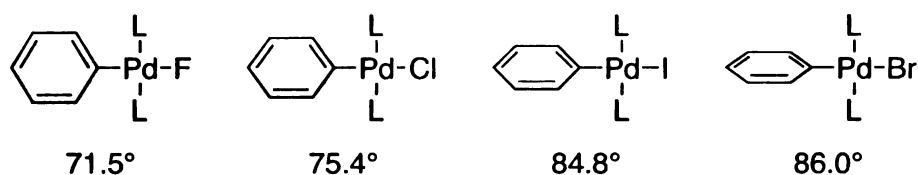
Scheme



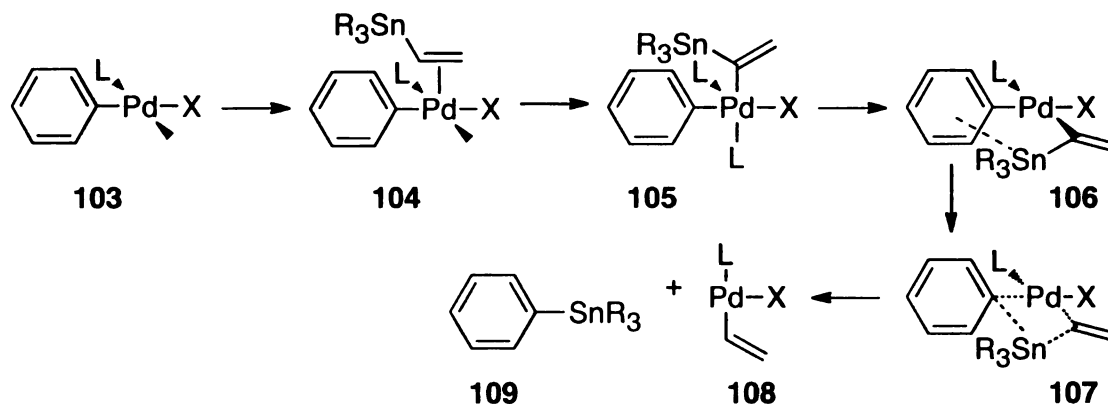
103

There is a
with respect to
cases, dark reac
note a color c
couplings whil
Therefore, it is
exchange to aff
react faster th
oxidative additi

Figure 5.4. Interplanar Angles Between Aryl Plane and Metal Coordination Plane



Scheme 5.7. Possible Mechanism of R for R Transmetallation



There is another explanation for the higher amounts of homocoupling with respect to the aryl bromide couplings. As has been noted in several cases, dark reaction media indicates the presence of molecular halides. We note a color change to an opaque dark/black color for aryl bromide couplings while the iodide reactions turn transparent reddish brown. Therefore, it is reasonable that if Br_2 is formed, it can undergo halogen-tin exchange to afford the vinyl bromide species. Then, since vinyl bromides react faster than aryl bromides,⁵⁵ the vinyl bromides could undergo oxidative addition and transmetallate with the vinyl stannane to produce the

homocoupled p

homocoupling of

exchange more e

We have

stannanes are fo

product must ar

are a transient

throughout the r

homocoupled sta

is reached in a g

products can be a

Unfortuna

on the basis of R

that the highest

iodides in NMP

aryl bromides a

obtain lesser an

and cheaper sta

homocoupled product. We can correlate this phenomenon to higher homocoupling of trimethyl stannanes because they should undergo halide-tin exchange more easily based on sterics.

We have proposed two pathways for homocoupling. Since the aryl stannanes are formed, we do know that some amount of homocoupled product must arise from the R for R pathway. However, since the aryl tins are a transient species, we do not know the total amount of formation throughout the reaction and thus cannot quantitatively correlate it with the homocoupled stannane. We do know that a threshold of ~10% aryl stannane is reached in a given experiment; therefore at least 10% of the homocoupled products can be attributed to the R for R pathway via aryl stannanes.

Unfortunately, at this juncture we are unable to draw any conclusions on the basis of R for R vs. R for X transmetallation. Our data does suggest that the highest desired product yielding reactions are those that employ aryl iodides in NMP with either trimethyl or tributyl stannanes. However, when aryl bromides are called for, one should implement the tributyl stannanes to obtain lesser amounts of side products with the benefit of using a less toxic and cheaper stannane.

Chapter 6. Effect

6.1. Reassessing

The goal is to understand how the non-transformation would provide reassessment to chemists in their work. To relate this information to the project in our group, we must consider. Thus, the remaining generation hydro-

6.2. The 2nd Ge

Tin^{33,56,57}

The toxicity of these compounds in their use. To address the hydrostannation of these compounds into the fact that these events and that these compounds produced in Still

Chapter 6. Effect of Additives on the Rate of the Stille Reaction

6.1. Reassessing the Goals of Our Study

The goal in the beginning of this project was to further understand how the non-transferable ligands on tin affect the rate of reaction. The study would provide relative rates of reaction that would aid synthetic organic chemists in their substrate and conditions choices. We would then be able to relate this information to further understand the limitations of an ongoing project in our group: a hydrostannation/Stille sequence that is catalytic in tin. Thus, the remaining kinetic studies highlight our progress toward a 3rd generation hydrostannation/Stille sequence.

6.2. The 2nd Generation Hydrostannation/Stille Sequence Catalytic in Tin^{33,56,57}

The toxicity inherent to organotin substrates is a major drawback of their use. To address this problem, the Maleczka group developed a one-pot hydrostannation/Stille sequence catalytic in tin.^{33,56,57} This method plays into the fact that both a hydrostannation and Stille coupling are Pd catalyzed events and that a stoichiometric amount of trialkyltin halide by-product is produced in Stille couplings. Central to the development of this catalytic

sequence, was t

hydride.

Scheme 6

Starting from a

fluoride, which

trialkyltin hydride

afford a vinyl c

coupling with an

trialkyltin hydride

reduction of the h

Scheme 6

Hydrostann

H—

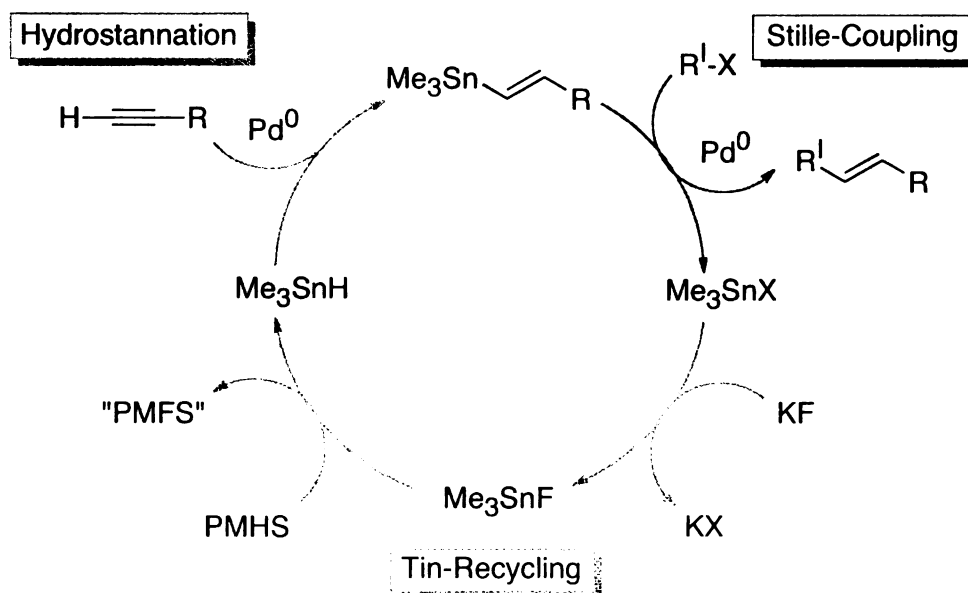
"PMF

This proto
the reaction setup

sequence, was the ability to convert the trialkyltin halide to a trialkyltin hydride.

Scheme 6.1 outlines the tin catalyzed hydrostannation/Stille cycle. Starting from a trialkyltin halide, treatment with KF affords a trialkyltin fluoride, which is then reduced to a trialkyltin hydride with PMHS. The trialkyltin hydride then participates in a Pd-catalyzed hydrostannation to afford a vinyl organostannane that subsequently undergoes Stille cross-coupling with an organohalide. Recycling of the trialkyltin halide back to trialkyltin hydride completes the catalytic cycle. Also noteworthy, no reduction of the halides were observed under these conditions.

Scheme 6.1. Hydrostannation/Stille Sequence Catalytic in Tin



This protocol minimizes the handling of the organostannanes, since the reaction setup and purification are carried out once instead of three times

for the syntheses

reaction. Further

Often times, tin

tin from the begin

The Male

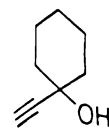
variety of substr

90% yield over

toxic Bu_3SnCl a

longer reaction

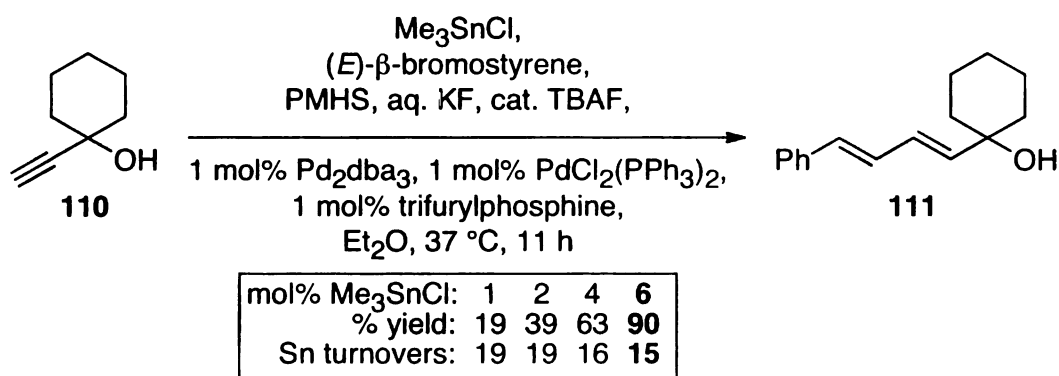
optimization was



for the synthesis of the trialkyltin hydride, hydrostannation, and Stille reaction. Furthermore, it allows one to use substoichiometric amounts of tin. Often times, tin residues are problematic to remove. Using lesser amounts of tin from the beginning allows for fewer tin residues in the end.

The Maleczka group has showcased the utility of this protocol for a variety of substrates. For example, using only 6 mol% of Me_3SnCl affords 90% yield over 15 tin-turnovers (Scheme 6.2). However, use of the less toxic Bu_3SnCl at 6 mol% met with diminished yields, lower tin-turnovers, longer reaction times, and more forcing conditions (Scheme 6.3). Further optimization was unsuccessful.

Scheme 6.2. Me_3SnCl as the Tin Source



Results

respectable results

alkyne hydrostannation

in less than 30

cycle is the Still

decided to further

stannanes in the

hydrostannation

6.3. Correlating

Sequence

Looking

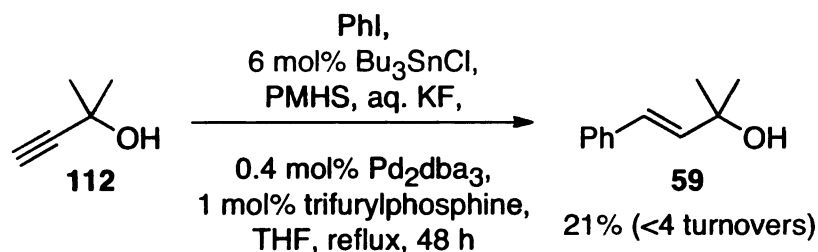
appears there is

respect to reaction

In our kinetic analysis

enhancement at

Scheme 6.3. Bu₃SnCl as the Tin Source



Results indicate that trimethylstannanes are required to obtain respectable results and that tributylstannanes prove problematic. Since alkyne hydrostannation with *in situ* generated tributyltinhydride can occur in less than 30 minutes, it seems logical that the rate-limiting step of this cycle is the Stille coupling. It was at this impasse that the Maleczka group decided to further understand the differences between trimethyl and tributyl stannanes in the Stille reaction before further attempts to optimize the hydrostannation/Stille sequence.

6.3. Correlating Stille Kinetic Data to the Hydrostannation/Stille Sequence

Looking at the data from the hydrostannation/Stille sequence, it appears there is a 4-fold benefit to using trimethyl vs. tributyl stannanes with respect to reaction time, turnover numbers, and yields as shown in Table 6.1. In our kinetic analysis of the Stille reaction, we observed a 2.4 fold rate enhancement at best for Me/Bu in THF (see Table 3.7). This indicates that

the Stille react

complex due to

tin recycling.

Table 6.1. C

M

6.4. The Fluoride

Fluoride

shown that after

resulting monox

hypervalent st

Hypervalent tin

tins. It is unli

pathway since

the Stille reaction in the hydrostannation/Stille sequence may be more complex due to the additional reagents utilized such as fluoride or PMHS for tin recycling.

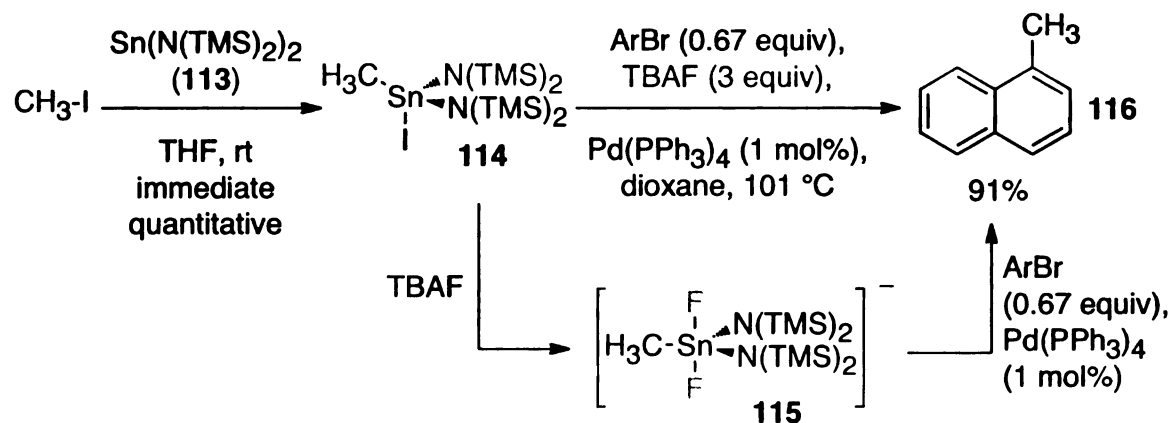
Table 6.1. Comparison of Results Using Me vs. Bu Trialkylstannanes

R	reaction time	turnover numbers	yields
Me	11 h	15	90%
Bu	48 h	<4	21%
Me/Bu	4.4/1	3.8/1	4.3/1

6.4. The Fluoride Effect

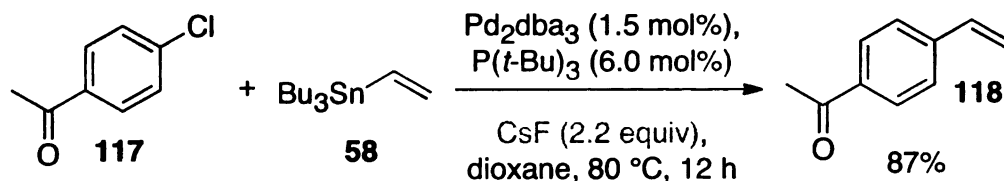
Fluoride is a well-known additive in Stille couplings. Fouquet has shown that after oxidative addition of a stannylene and alkyl halide, the resulting monoalkyl tin can be treated with TBAF to afford the activated hypervalent stannate that undergoes an efficient Stille coupling.⁵⁸ Hypervalent tin species are typically formed from heteroatom substituted tins. It is unlikely that our system is proceeding through a hypervalent pathway since we employ trialkyltins.

Scheme 6.4. Fluoride Activation of Stannates⁵⁸



However, Fu reported the cross-coupling of aryl chlorides with tributylvinyl stannane with the use of *t*-Bu₃P and CsF.²⁶ They claim that the CsF activates the stannane, although they show no evidence. Given our recent understanding of aryl bromide couplings, it seems likely that the oxidative addition of aryl chlorides would be the rate-determining step. If this is true, then activation of the stannane would not affect the rate of reaction. It could however enhance the catalytic Pd species, which would in turn affect the reaction rate. Nonetheless, we thought it would be beneficial to study the effect of aq. KF/TBAF on the rate of the Stille reaction. We envisioned that if stannane activation was possible, perhaps the more prominent rate differences between trimethyl and tributyl stannanes is a reflection of the steric ease of activation. That is, trimethyl stannanes are less sterically hindered about tin, and thus easier to activate.

Scheme 6.5. Promoting the Stille Reaction with CsF



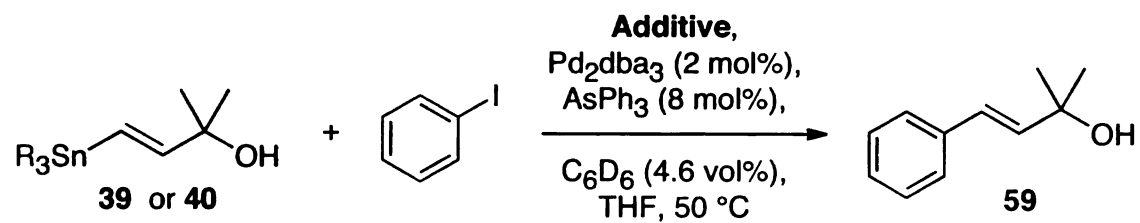
6.4.1. Couplings of Aryl Iodides in the Presence of Aqueous KF/TBAF

Our first objective was to see whether we were effecting hypercoordination of tin. We therefore treated a trimethylvinyl stannane with 3 equiv of KF (aq., 3 M) and cat. TBAF (1 drop of a 1 M THF solution) in THF (0.1857 M in tin). Hypercoordinate tin species typically appear further downfield in ^{119}Sn NMR spectra. Incrementally scanning from 400 to -200 ppm revealed only a signal at -36 ppm belonging to the starting stannane. Although we did not see evidence for a hypercoordinate tin species, we could not rule it out.

We then tested the effect of fluoride on the kinetics of the Stille coupling between trialkylvinylstannanes and iodobenzene (Scheme 6.6). The fluoride additive consisted of 3 equiv of KF (aq., 3 M) and cat. TBAF (1 drop of a 1 M THF solution). Although the reaction is biphasic, the organic phase was run at the same concentration as previous kinetic studies (see Ch. 3) and thus can be correlated to the reactions without additive. As seen in

Figure 6.1, the reaction rate was dramatically increased when both trimethyl and tributyl stannanes were utilized.

Scheme 6.6. Stille Coupling to Determine Fluoride Effect



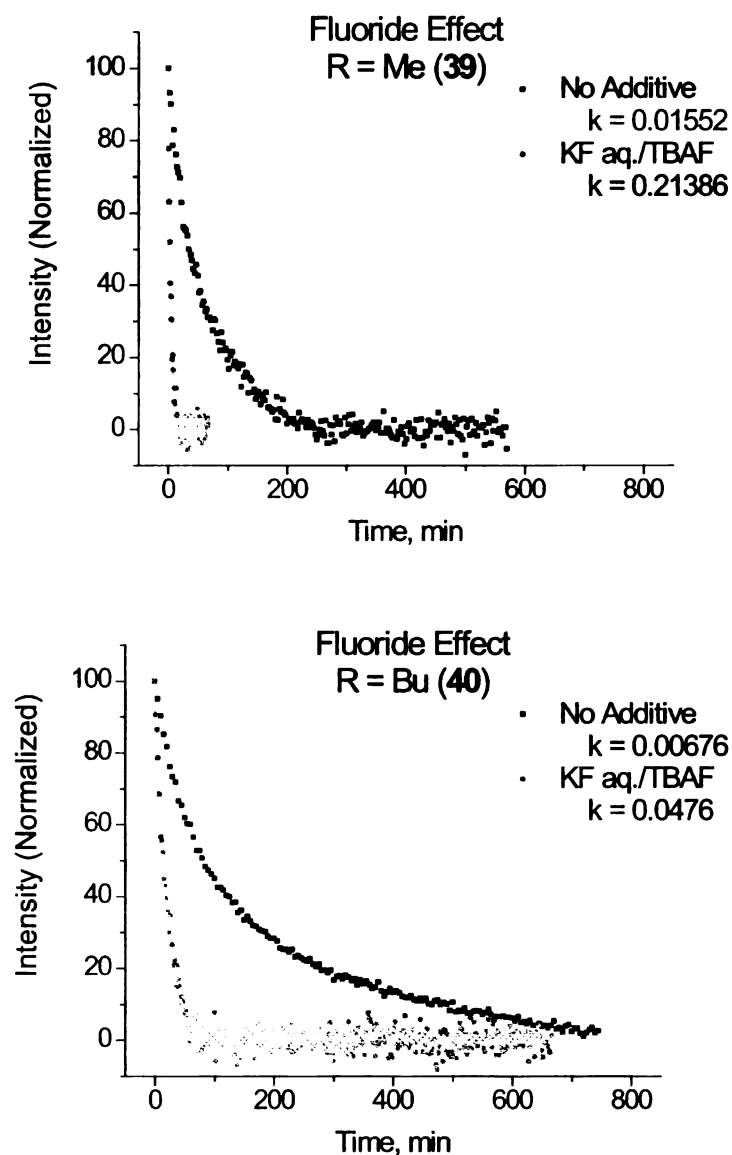


Figure 6.1. Reaction Profile of Fluoride Additive Effect. 186 MHz ^{119}Sn NMR relative integration data for the consumption of **39** or **40** without fluoride (black trace) and with fluoride (red trace) upon coupling with 1.2 equiv of PhI under a $\text{Pd}_2\text{dba}_3/\text{AsPh}_3$ catalyst system. All sets of data were fit to a first order exponential decay model (not shown) to reveal for **39** without fluoride, $k_{\text{obs}} = 0.016 \text{ min}^{-1}$ and with fluoride, $k_{\text{obs}} = 0.21 \text{ min}^{-1}$ and for **40**, $k_{\text{obs}} = 0.0068 \text{ min}^{-1}$ and with fluoride, $k_{\text{obs}} = 0.048 \text{ min}^{-1}$.

Interestingly, reactions of trimethyl and tributyl stannanes were activated to different extents. Table 6.2 outlines the effect fluoride plays on the rates of reaction. The k_{obs} (additive)/ k_{obs} (none) shows that with fluoride, the trimethyl stannane reaction was activated ~14 times that without fluoride and the tributylstannane reaction was only activated 7 fold. These different amounts of activation affect the rate differences between trimethyl and tributyl stannanes, such that the Me/Bu ratio without fluoride is only 2.3, and with fluoride, 4.5! The rate difference with fluoride is more in line with what we were observing in the hydrostannation/Stille case. Therefore, we initially concluded that the fluoride is an important factor in the hydrostannation/Stille sequence and to further understand this situation, a systematic Stille study should be conducted in the presence of fluoride. We also initially believed that we were invoking some type of stannane activation, since we observed that trimethyl stannanes were activated to a greater extent than tributyl stannanes, and this could be correlated to steric influence about tin.

Table 6.2. Fluoride Effect on Me/Bu Rate Differences

R	k_{obs} (min ⁻¹) no additive	k_{obs} (min ⁻¹) KF aq./TBAF	relative ratio additive/none
Me	0.0155	0.2139	13.8/1
Bu	0.0068	0.0476	7.0/1
Me/Bu	2.28/1	4.49/1	

Before we carried out a systematic Stille study with fluoride, we thought it prudent to take a step back and run the obvious control experiment. Since we were utilizing aqueous KF, and there are often minute amounts of water in TBAF, we wanted to determine the effect of water on the Stille reaction. Many people go to great pains to avoid the incorporation of water in the Stille reaction. For instance, they may dry solvents, flame dry glassware, and run reactions under an inert atmosphere. However, Farina has indicated in his vast overview of the Stille reaction, that moisture has been reported to be helpful sometimes, although no references were provided.²⁴ Therefore, we wanted to determine if and how water affects the reaction so that we could more clearly understand the effect of fluoride.

6.5. The Water Effect on Aryl Iodide Couplings

To determine the effect of water on the rate of the Stille reaction, the same additive experiment was performed as outlined in Table 6.2 with water as the additive. The same volume of water was added as with the aq. KF

experiment to keep the concentration of the biphasic systems consistent. Therefore, 200 μL (55.4 equiv) of deionized water was added to a 0.2 mmol reaction. The result was quite surprising; Water activated the coupling of both the trimethyl and tributyl stannanes to essentially the same level as KF/TBAF! Utilizing both HPLC grade and Milli-Q water provided the same results suggesting water is in fact activating the reaction, not trace ions.

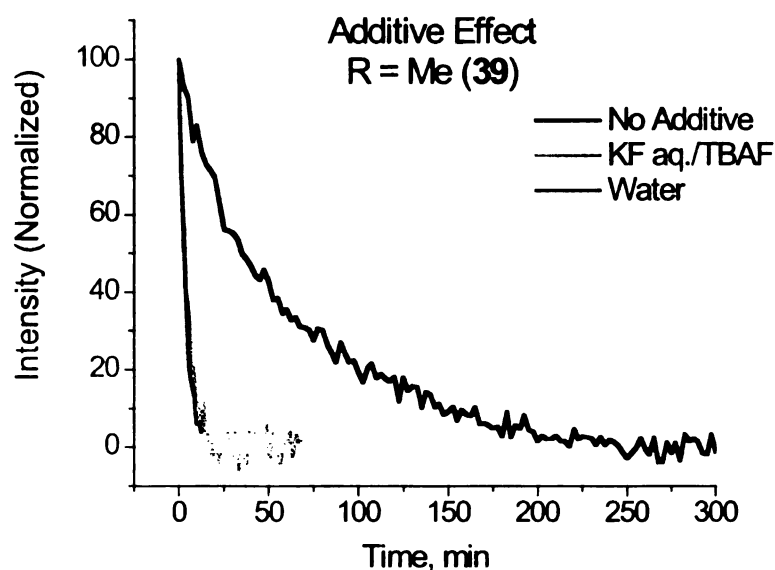
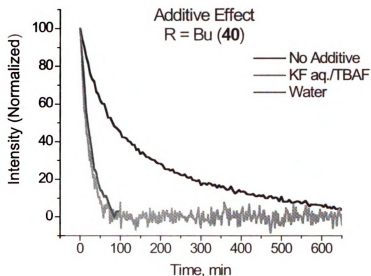


Figure 6.2. Reaction Profile with Water as an Additive. 186 MHz ^{119}Sn NMR relative integration data for the consumption of **39** (*top*) or **40** (*bottom*) upon coupling with 1.2 equiv of PhI under a $\text{Pd}_2\text{dba}_3/\text{AsPh}_3$ catalyst system in the absence of fluoride and water (black trace), in the presence of fluoride (red trace), or in the presence of water (blue trace). All sets of data were fit to a first order exponential decay model (not shown). The rate constants with and without fluoride were described in Figure 6.1. For the reaction of **39** with water, $k_{\text{obs}} = 0.27 \text{ min}^{-1}$ and for **40** with water, $k_{\text{obs}} = 0.036 \text{ min}^{-1}$.

Figure 6.2 (cont'd)



Since we had used a large excess of water (55.4 equiv), we were curious as to how much water was necessary for activation. To this end, we ran a water dependence study for both the trimethyl and tributyl stannane reactions (Figure 6.3) and found that as little as 1.4 equiv of water activated the reaction. It is likely that lower and higher amounts of water will activate the reaction as well, but our studies were limited by the fact we were running the reactions on small scale in an NMR tube. It should be noted that the water dependence test for the tributyl stannane was performed at $\sim 47^\circ\text{C}$ due to problems associated with the NMR temperature controller. The overall reactions were slower than when run at 50°C , but still had a similar correlation of rate enhancement to equivalents of water.

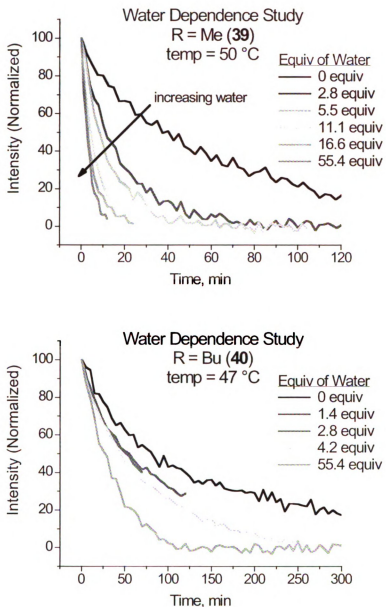


Figure 6.3. Determination of Water Activation Dependence. 186 MHz ^{119}Sn NMR relative integration data for the consumption of **39** or **40** upon coupling with 1.2 equiv of PhI under a $\text{Pd}_2\text{dba}_3/\text{AsPh}_3$ catalyst system in the presence of the indicated amount of water.

From these data it is clear that water activates the reaction and should be considered as a cheap and green additive to Stille reactions.

Unfortunately at this point, we could not pinpoint the mechanism of activation, although it seems reasonable that the activation is involved in the rate-determining transmetallation step. Further studies were needed to fully understand the details of this activation.

6.6. Fluoride and Water Effect on Aryl Bromides

We have suggested the oxidative addition is the rate-determining step for aryl bromide couplings. If water activates the transmetallation, then we would not expect water to have an influence on the reaction rate for aryl bromide couplings where the oxidative addition is rate determining. Therefore, we asked whether fluoride and/or water would activate the coupling of aryl bromides (Figure 6.4). When a trimethylvinylstannane was coupled with bromobenzene in the presence of water, after ~ 100 min the reaction was slightly faster than without water. Upon the addition of aq. KF/TBAF however, the rate was slightly increased for around the first 100 min, after which the reaction rate was dramatically increased. We have seen this type of autocatalytic behavior before when TFP was used as a Pd ligand and in Hatwig's oxidative addition studies of aryl bromides. This leads us to believe that we are forming a new Pd species *in situ*. When a tributylvinylstannane was coupled with bromobenzene, the addition of water had no effect on the rate of reaction at the beginning of the reaction, and

data was not collected after the first 165 min. Upon coupling in the presence of fluoride, modest rate acceleration was observed.

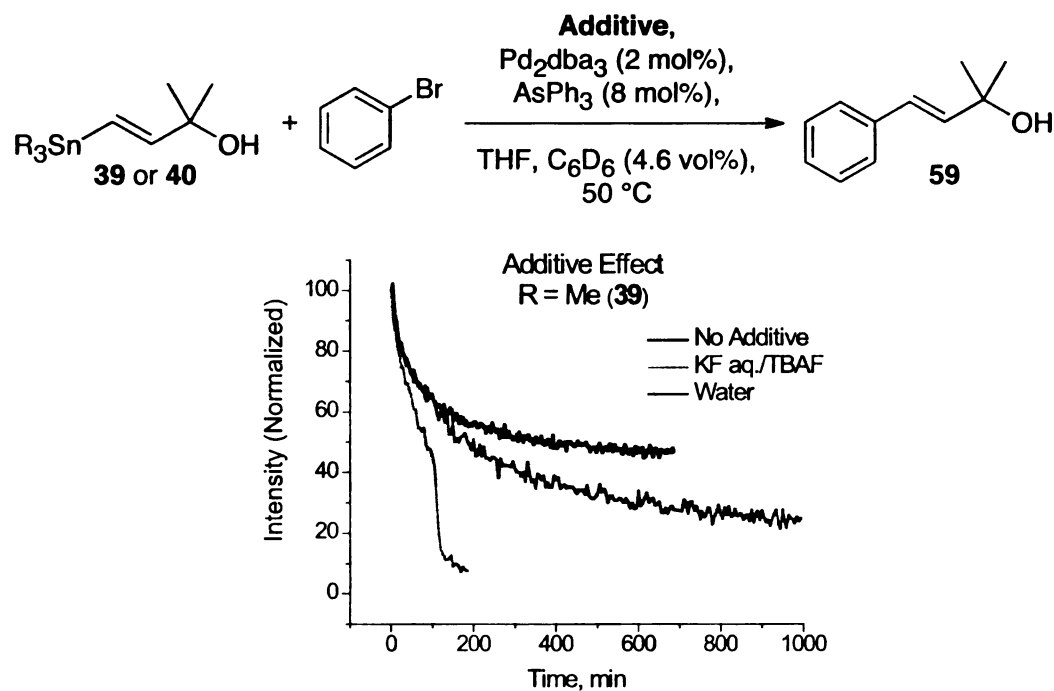
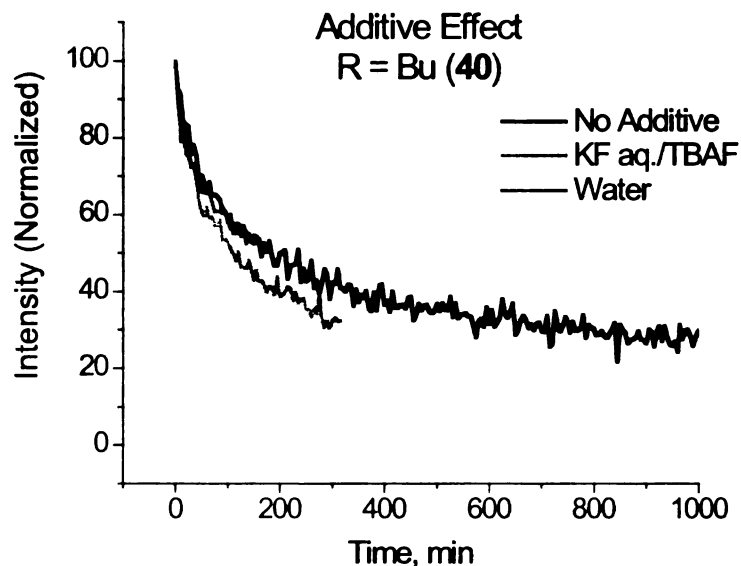


Figure 6.4. Reaction Profile of Water as an Additive. 186 MHz ¹¹⁹Sn NMR relative integration data for the consumption of **40** upon coupling with 1.2 equiv of PhBr under a Pd₂dba₃/AsPh₃ catalyst system in the absence of fluoride (black trace), in the presence of fluoride (red trace), or in the presence of water (blue trace).

Figure 6.4 (cont'd)



6.7. Insight into the Mechanism of Fluoride and Water Activation

From this preliminary data we were able to develop a hypothesis on the mechanism of activation. Since aryl iodides were activated by water and aryl bromides were not, water appears to activate the transmetallation step, which is rate determining for aryl iodides. Water can activate the transmetallation for the aryl bromide coupling, but since the oxidative addition is rate determining, there will be no observable effect. It is likely that water activates the stannane, since any activation of the catalytic Pd species should show an effect for aryl bromide couplings as well. Furthermore, the greater acceleration for trimethyl stannanes vs. tributyl stannanes correlates well with steric influences. With respect to aq. fluoride,

the aryl iodide was accelerated, but it could be due to the water. A closer look at the data reveals that at least for the tributyl coupling (Figure 6.2, bottom), that the aq. fluoride accelerates the reaction slightly more than with just water. The aryl bromide coupling with fluoride does show an effect, indicating that the activation is involved in the oxidative addition. Furthermore, the effect is autocatalytic with trimethyl stannane **39** and leads us to believe that a new catalytic Pd species is formed. We believe this new Pd species may be related to the L_2PdHX species as described in Sections 4.3.1.1 and 4.3.1.2. We do not fully understand why trimethyl stannanes appear to induce autocatalytic behavior with fluoride while the tributyl stannane exhibits first order behavior.

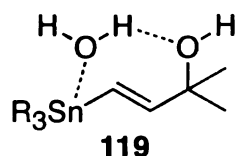
If the water in fact activates the stannane, an explanation for the mechanism remains elusive. It is unlikely that water simply activates the tetraorganostannane via hypercoordination for two reasons:

1. A heteroatom-substituted stannane is needed to achieve hypercoordination
2. The ^{119}Sn NMR spectra did not indicate the presence of hypercoordinated tin

However, we thought that with the assistance of the free hydroxyl, we might be able to effect a type of pseudo-internal chelation via hydrogen-bonded

water as shown in Figure 6.5. If this were true, we would expect that either shutting down the ability of the free hydroxyl to chelate, such as with a silyl protecting group, or by taking it away altogether, that water would not be able to activate the reaction.

Figure 6.5. Activation of Stannane by Hydrogen Bonded Chelation



To determine whether the free hydroxyl was crucial for activation, we tested if a reaction with unsubstituted tributylvinylstannane **58** was accelerated upon the addition of water. The addition of 55.4 equiv of water accelerated the reaction suggesting that the OH is not involved in water activation.

Another thought on the mechanism of activation relates to the fact that heteroatom substituted stannanes can be hypercoordinated. The mechanism of transmetallation involves the transfer of a ligand from tin to Pd. Recently it has been shown both experimentally and computationally that **124** is an intermediate in the transmetallation where X-SnR₃ serves as a Pd ligand through the halogen (Figure 6.6).^{8,20} Completion of the transmetallation step relies on this ligand to dissociate. Although we have not come across any discussions pertaining to the rate-determining step of the transmetallation,

2

1

we consider that if the ligand dissociation is the rate-determining step, then perhaps the water can facilitate dissociation and the overall rate of reaction.

Water may coordinate to tin because it is heteroatom substituted, thus affording a hypercoordinate tin ligand, which may more easily dissociate, likely via an associative pathway. One could also imagine direct attack on the Pd to kick off the 4-coordinate XSnR_3 ligand in an $\text{S}_{\text{N}}2$ -fashion. However, if water attacked Pd, it should also affect the kinetics of aryl bromide couplings in the oxidative addition. We have no hard evidence that ligand dissociation is the rate-determining step, although Espinet has indicated that the highest energy barrier obtained experimentally was for this step (Figure 6.7).²⁰

Figure 6.6. Mechanism of Transmetallation

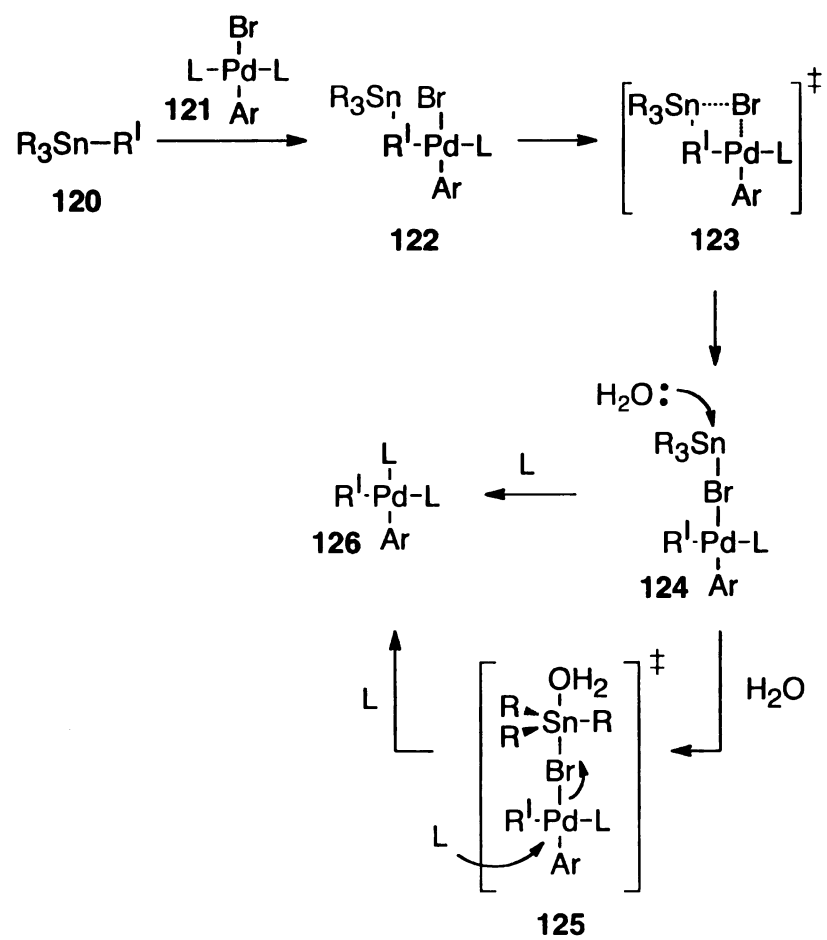
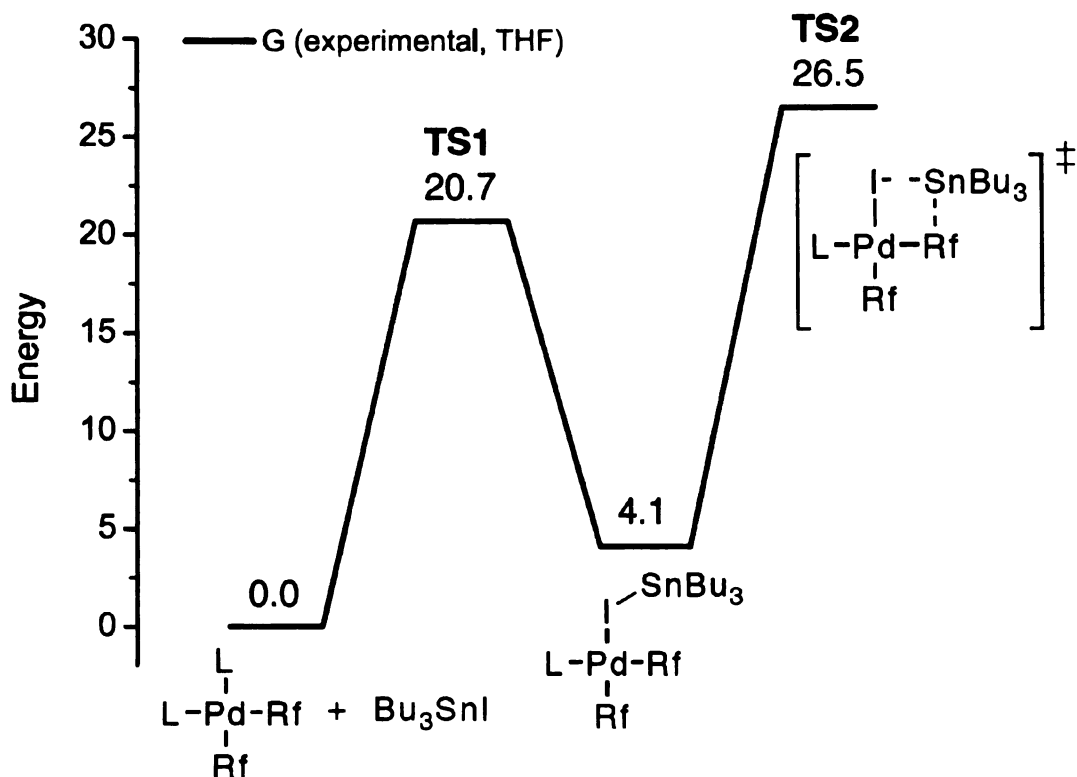


Figure 6.7. Energy Diagram of a Retro-Transmetallation Mechanism²⁰



6.8. The Copper Effect

CuI has emerged as an efficient promoter of the Stille reaction, although the mechanism is not fully understood. From the work of Farina and Liebeskind,²² it appears that two different mechanisms are possible; CuI can act as a ligand scavenger or a transmetallating agent. The reaction conditions, namely ligand and solvent coordination strength, heavily dictate which mechanism dominates. Utilizing various Pd/L/Cu loadings, they were able to reveal how the Cu was playing into the mechanism. When a mild coordinating solvent (dioxane or THF) was used in conjunction with a

strongly coordinating PPh_3 ligand, the addition of catalytic CuI acts as a ligand scavenger. When a strongly coordinating solvent (NMP or DMF) was utilized with a dissociating soft AsPh_3 ligand, instead a tin to copper transmetallation takes place. Depending on which conditions are utilized, different degrees of activation may be accomplished with the addition of catalytic copper and their results are presented in Table 6.3. We therefore became interested how the “Copper Effect” affects the relative rates of reaction for trimethyl and tributyl vinyl stannanes.

Table 6.3. The Copper Effect: Farina & Liebskind's Results²²

$\text{Bu}_3\text{Sn}-\text{CH}=\text{CH}_2 \xrightarrow[\text{Solvent, 50 } ^\circ\text{C}]{\text{Electrophile (1 equiv), Pd}_2\text{dba}_3 \text{ (5 mol\%), Ligand, CuI}} \text{Ar}-\text{CH}=\text{CH}_2$						
entry	electrophile	ligand	solvent	Pd:L:Cu molar ratio	k_{obs} (min ⁻¹)	% yield ^a
1	iodobenzene	PPh ₃	dioxane	1:4:0	2.66×10^{-5}	85
2	iodobenzene	PPh ₃	dioxane	1:4:4	523×10^{-5}	45
3	iodobenzene	PPh ₃	dioxane	1:2:0	170×10^{-5}	91
4	iodobenzene	PPh ₃	dioxane	1:2:2	547×10^{-5}	56
5	4-iodoanisole	AsPh ₃	NMP	1:4:0	5.9×10^{-3}	51
6	4-iodoanisole	AsPh ₃	NMP	1:4:4	16.6×10^{-3}	61
7	4-iodoanisole	AsPh ₃	NMP	1:4:8	21.0×10^{-3}	52
8	4-iodoanisole	AsPh ₃	NMP	1:4:16	25.2×10^{-3}	51
9 ^b	iodobenzene	AsPh ₃	DMF	1:2:0	35% ^c	56 ^d
10 ^b	iodobenzene	AsPh ₃	DMF	1:2:1	47% ^c	76 ^d

^a% Yield determined by HPLC

^bReaction run at 50 °C

^c% Conversion after 5 min determined by GLC vs. internal standard

^d% Yield determined by GLC

6.8.1. Aryl Iodide Couplings in the Presence of CuI

A series of reactions were performed to determine the rate differences of trimethyl and tributyl stannanes in the presence of CuI. For both ligand/solvent systems, the presence of CuI did not largely accelerate the reaction as was expected. In fact, the addition of CuI suppressed the rate of

reaction and was more pronounced for AsPh_3/NMP systems. This outcome is clearly in contrast to what was expected, and several aspects of the reaction were tailored to find the source of the discrepancy. For instance, the CuI utilized in Table 6.4 was freshly purified by the method of Kauffman⁵⁹ then ground to a fine powder and dried under vacuum with light heating, $\sim 30^\circ\text{C}$. Although we were confident that the CuI was pure and dry, we also purchased 99.999% pure CuI stored under argon from Strem. Utilizing this batch of CuI produced the same negative effect. Finally, we thought that the problem was a result of the stannane we were using.

Table 6.4. Effect of CuI on Reaction Rate

entry	R	Y	CuI (mol%)	ligand	solvent	k_{obs} (min ⁻¹) ^a	effect of CuI addition
1 ^b	Me	CF ₃	0	PPh ₃	THF	0.029	slightly slower
2 ^b	Me	CF ₃	8	PPh ₃	THF	0.027	
3 ^b	Bu	CF ₃	0	PPh ₃	THF	n.d.	n.d.
4 ^b	Bu	CF ₃	8	PPh ₃	THF	0.022	
5	Me	H	0	AsPh ₃	NMP	0.49	slower
6	Me	H	8	AsPh ₃	NMP	0.29	
7	Bu	H	0	AsPh ₃	NMP	0.15	slower
8	Bu	H	8	AsPh ₃	NMP	0.058	

^a Rate constants were determined by linear regression analysis.

^b Reaction profiles without CuI do not show exponential behavior.

The copper effect is regarded as relatively general; therefore we did not strictly repeat those experiments performed by Farina and Liebeskind with regards to the stannane coupling partners. Since we have noticed differences in the trends between substituted and unsubstituted vinyl stannanes, we thought it was necessary to study tributylvinylstannane **58**, which was utilized in Farina and Liebeskind's study, along with trimethylvinylstannane **57** for the context of our study. Unfortunately, the

same inhibitory trend upon the addition of CuI was observed for both stannanes in a Pd₂dba/AsPh₃ system in NMP. Lastly, we thought there might be a problem with running these reactions in the NMR. When CuI is added to the NMR tube containing all reagents except the electrophile, the CuI sinks to the bottom of the tube. We were afraid that since the CuI was insoluble in the reaction media, we were having a mass transfer problem as the CuI sits on the bottom of the reaction vessel. We were also worried that monitoring the reaction with ¹¹⁹Sn NMR was somehow giving us false data, such as any paramagnetic Cu(II) species broadening our signals. We therefore set up two reactions in parallel with and without CuI. They were run on the bench-top with magnetic stirring to alleviate any mass transfer problems. We cold quenched the reactions after 1 h 5 min at 0 °C and took a ¹H NMR of the crude reaction mixtures. The ratio of starting material to product for the reaction without CuI was ~1:1. For the reaction with CuI, there was more starting material than product, indicating that CuI inhibited the reaction. These results are in line with our observations for reactions run in the NMR. All of our results suggest that CuI does *not* accelerate the reaction. A brief review of the literature showed several instances in which

copper was utilized in Stille couplings. However, we did not come across any additional comparisons with and without Cu.

At this point we have seen the same inhibitory trend using different batches and sources of CuI as well as with different stannanes and electrophiles. We then considered that the CuI used by Farina and Liebskind may not have been pure. They report purifying the CuI by the method of Kauffman⁵⁹ as did we. This involves dissolving CuI in a saturated aq. salt solution, then precipitating the CuI out by the addition of water. Seeing as we have seen a dramatic acceleration by the addition of water, we were curious whether adventitious water in the CuI from the purification was responsible for their acceleration. We therefore developed a series of reactions with CuI to determine the amount of water necessary to 1) overcome the inhibitory effect of CuI and 2) determine the amount of water necessary to reach the activation levels reported.

For this experiment, it was essential that we replicated the literature conditions as closely as possible. We chose Farina's conditions outlined in Table 6.5 where double the typical catalyst loading is used (8% vs. 4% Pd) and higher temperature (60 °C). However, for us to monitor the reaction by ¹¹⁹Sn NMR, we brought the temperature down to 25 °C, which was still too fast, and finally down to 15 °C, which was fast but observable. We feared

that lower temperatures might cause solubility problems since the reactions are run at a much higher concentration of Pd/As.

Table 6.5. CuI Effect with Higher Catalyst Loading and Temperature:
Farina's Results

$\text{Bu}_3\text{Sn}-\text{CH}=\text{CH}_2 \text{ (58)} + \text{C}_6\text{H}_5\text{I} \xrightarrow[\text{NMP, 60 } ^\circ\text{C}]{\text{Pd}_2\text{dba}_3 \text{ (0.04 equiv), AsPh}_3 \text{ (0.16 equiv), CuI}} \text{C}_6\text{H}_5\text{CH}=\text{CH}_2$			
entry	amount of CuI	% conversion after 5 min	final % Yield
1	None	35	56
2	8 %	47	76

Farina and Liebskind's results revealed that the addition of CuI increased the rate such that at 5 min, 47% of the stannane was consumed vs. only 35% with no CuI (Table 6.5 entries 1 vs. 2). Although we observe rate suppression upon CuI addition, we could mimic a similar acceleration by instead using 5 μL (2.8 equiv) of water as seen in Figure 6.8, Expts. 1 vs. 2. We then wanted to see if and how much water can compensate for the rate inhibition of CuI. We found that on a 0.1 mmol scale reaction with CuI present, adding 5 μL (0.2775 mmol) of water produced a rate profile similar to that without CuI, thereby overcoming the inhibition (expts. 1 vs. 3). It was necessary to add 15 μL (0.8236 mmol) of water in the presence of CuI to obtain similar levels of activation we saw with only 5 μL of water or Farina saw with CuI (expts. 2 vs. 4). It is unlikely that 15 μL of water is

adventitious considering we are only using 0.0015 g of CuI, which results in a water to CuI molar ratio of 104:1. There could be lesser amounts of water present in the CuI if it was not dried properly after the purification, although not as much as is necessary to achieve acceleration. We also weighed out 0.0015 g of CuI and added 15 μ L of water to see if CuI would absorb the water. The CuI dispersed on the surface of the water, which was expected since CuI is not soluble in water. At this point we cannot conclude whether the acceleration seen by Farina is real, or an artifact of residual water in the CuI.

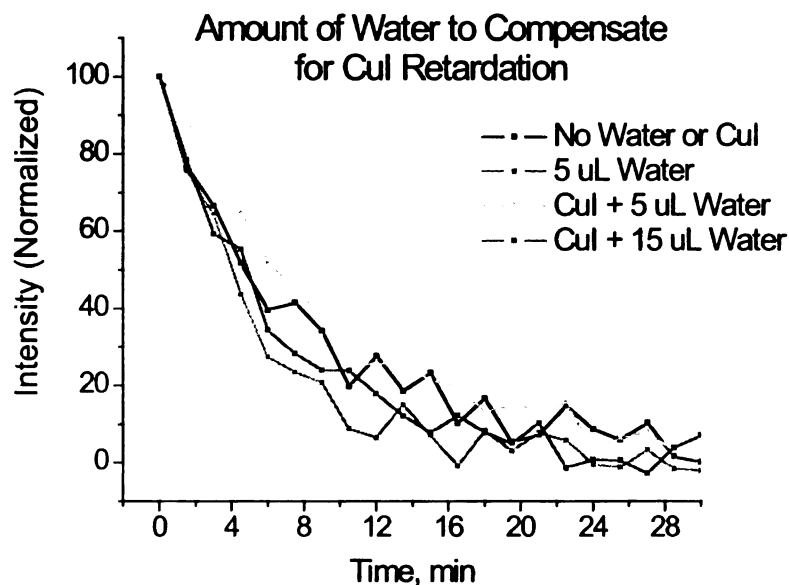
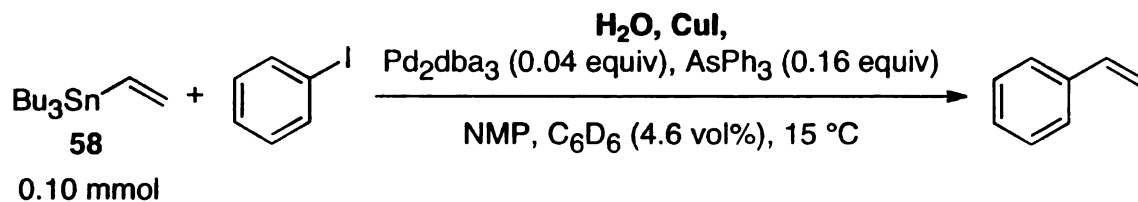


Figure 6.8. Overcoming the Inhibitory Effects of CuI with H_2O . 186 MHz ^{119}Sn NMR relative integration data for the consumption of **58** (0.1 mmol) upon coupling with 1.2 equiv of PhI under a $\text{Pd}_2\text{dba}_3/\text{AsPh}_3$ catalyst system in the absence of any additives (black trace), in the presence of 5 μL of water (red trace), in the presence of 8 mol% CuI and 5 μL of water (green trace), or in the presence of 8 mol% CuI and 15 μL of water (blue trace). The solid colored lines are to guide the eye.

6.8.2. Aryl Bromide Couplings in the Presence of CuI

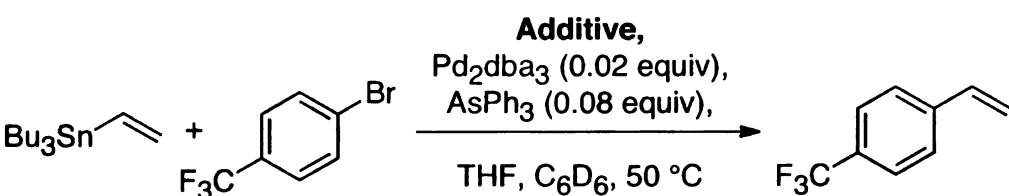
We next chose to determine the effect of CuI on aryl bromide couplings. Since the oxidative addition is rate determining, we expected that the rate would be unchanged for the AsPh_3/NMP system since CuI activation is proposed to affect the transmetallation step (*vide supra*).

However, we should see an effect for the PPh_3/THF system since CuI acts as a ligand scavenger and would thus increase the rate of oxidative addition. What we found however was that CuI shut down the reaction for both systems. We then asked how the addition of CuI would impact a reaction that was already proceeding.

Two sets of experiments were performed on the bench-top (Table 6.6). For set **A**, reaction 1 was the control in which vinyl tin and aryl bromide were allowed to react as normal for 1 h. For reaction 2, the same reaction was performed except CuI was added after 10 min and allowed to react for an additional 50 min (1 h total). After 1 h, both reactions were cold quenched, concentrated, and NMR samples were prepared. The NMR samples were also kept cold to prevent the reaction from proceeding. A ^1H NMR of each crude reaction mixture was taken and the starting material/product ratios determined (Table 6.6). From the ratios, it appears that the addition of CuI has a negative effect on the reaction even when the reaction is already proceeding. We then ran set **B**, which is identical to set **A** except the CuI was added after 25 min instead of 10 min, allowing the reaction to proceed further. The ^1H NMR of the crude reactions showed that CuI did not inhibit the reaction and may have even accelerated it to a small

degree, although this may be within experimental error. It appears that CuI does not shut down a reaction that is already proceeding after a long enough wait period. These results indicate that the order of addition is important when CuI is used. This is an important fact that was not indicated in the original report.

Table 6.6. Timing of CuI Addition and Impact on Reaction Outcome in THF

<div style="text-align: center;">  </div>				
	set A		set B	
	reaction 1	reaction 2	reaction 1	reaction 2
Initiation Period	1 h	10 min	55 min	25 min
Additive	-	CuI (0.08 equiv)	-	CuI (0.08 equiv)
Additional Time	-	50 min	-	30 min
Total Reaction Time	1 h	1 h	55 min	55 min
NMR Ratios (SM/Prod)	81/19	87/13	80/20	79/21

6.9. Determining the Impact of the Order of Addition for Reactions with CuI

Our data suggests that the order of addition is an important factor for the rate of reaction. Farina's order of addition depends on the exact reaction

conditions, and are either: solvent, electrophile, ligand, Pd, CuI, and then after 10 min at rt, equilibrated to temperature and then the stannane is added; or electrophile, CuI, solvent, Pd/L stock solution, equilibrated to temperature, and then stannane addition. Both of their systems are run under nitrogen. The differences between the two systems are when and how the Pd is introduced, either before or after the CuI, and either as separate Pd and ligand additions or as a Pd/L premixed solution. We run our reactions in air and first premix the Pd, ligand, and solvent, then to an NMR tube we add solvent, stannane, Pd/L solution, CuI, equilibrate to temperature, then add the electrophile. In both Farina and our own conditions, the CuI is present before both coupling partners are present, thus before the coupling takes place. However, they add the stannane last and run the reactions under nitrogen, while we add the electrophile last and run the reactions in air.

Several experiments were performed to test whether we could effect rate acceleration by implementing the order of addition reported by Farina compared with our order, and whether nitrogen is crucial for the acceleration. These experiments are outlined in Table 6.7. Entry 1 without CuI shows that after 5 min, the amount of starting material and product are approximately the same as determined by ^1H NMR. When CuI was used however, lower amounts of product were formed after 5 min, indicating that

the addition of CuI suppresses the reaction under our order of addition (Entry 2). For Farina's order, the presence of CuI increased the amount of product indicating that CuI accelerates the reaction (Entries 3 vs. 4). A nitrogen atmosphere was not necessary, as the reaction in air provided acceleration as well (Entry 5).

Table 6.7. Qualitative Experiments to Determine the Effect of the Order of Addition for Reactions with CuI and the Effect of Air

$\text{Bu}_3\text{Sn}-\text{CH}=\text{CH}_2 + \text{C}_6\text{H}_5\text{I} \xrightarrow[\text{NMP, rt, 5 min}]{\text{CuI (0 mol\% or 8 mol\%)}, \text{Pd}_2\text{dba}_3 (2 \text{ mol\%}), \text{AsPh}_3 (8 \text{ mol\%})} \text{C}_6\text{H}_5\text{CH}=\text{CH}_2$

entry	order of addition ^a	atmosphere	CuI (mol%)	SM vs. Prod ^b	effect of CuI
1	Conditions A	Air	0	SM \approx Prod	Suppresses
2	Conditions A	Air	8	SM > Prod	
3	Conditions B	N ₂	0	SM > Prod	Accelerates
4	Conditions B	N ₂	8	SM < Prod	
5	Conditions B	Air	8	SM < Prod	

^a Conditions A (Ours): Solvent, stannane, Pd/L solution, CuI, and electrophile. Conditions B (Farina's): electrophile, CuI, solvent, Pd/L solution, and stannane.

^b Amount of starting material vs. product as determined by ¹H NMR after 5 min.

From the results presented in Table 6.7, it is clear that the order of addition is important. During sample preparation for entries 3-5 under Farina's conditions, the reaction media turned yellow with a small amount of powder remaining at the bottom of the reaction vessel after the addition of

electrophile, then CuI, and then solvent. For our conditions, the CuI sank to the bottom of the reaction vessel and did not appear to dissolve. As a control experiment, we combined CuI with NMP and saw the same color change from clear to yellow. This suggests that we need to allow the CuI to solubilize before adding the remaining reagents. Therefore, we changed when the CuI was added, while still retaining the order of other reagents. The reason being, that it is easier to add the stannane to the reaction before the electrophile, so that the NMR can be tuned to ^{119}Sn , and then the electrophile added to initiate the reaction. Therefore, we ran parallel reactions to determine if allowing the CuI to disperse is enough to invoke rate acceleration. We ran one control of Farina's order (Conditions B) and one of our new order (Conditions C), which are indicated below. After steps 3b and 2c, the reaction turned yellow as expected. However, for Conditions C, after the stannane was added (step 3c.), the reaction turned a darker green color after sitting for the amount of time it took to add the Pd/L solution to the Conditions B experiment, around 3 min. After both experiments were set up and run for 5 min, an analysis identical to that in Table 6.7 was performed. For Farina's order, there was more product formed than remaining starting material where as for our conditions, there was more unreacted starting material left than product. This indicates that despite

allowing the CuI to dissolve, the reaction was still suppressed. At first glance, one would think that if for the AsPh₃/NMP conditions Cu and Sn undergo a transmetallation, then having the stannane present with CuI before the coupling starts would allow more time for the initial Cu-Sn transmetallation and certainly not suppress the reaction. However, given the color change to darker green after the stannane sat in the CuI solution, perhaps a transmetallation occurred and the new possibly unstable Cu species had nothing to react with (e.g. electrophile) and therefore decomposed to a Cu(II) species as indicated by the color change. Therefore, the crucial events for CuI to accelerate the Stille reaction are that CuI is allowed to dissolve and that the stannane is added last. These criteria are met with Farina's order and thus any continuing experiments should utilize these conditions.

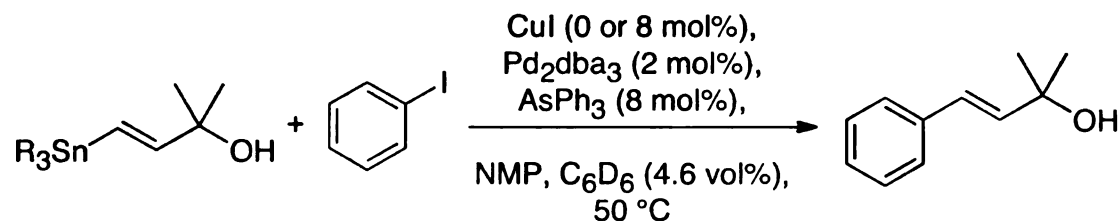
Table 6.8. Order of Addition for Reactions with CuI

Farina's Order (Conditions B)	Our New Order (Conditions C)
1a. Electrophile	1c. CuI
2b. CuI	2c. Solvent
3b. Solvent	3c. Stannane
4b. Pd/L from stock solution	4c. Pd/L from stock solution
5b. Stannane	5c. Electrophile

Having determined that we should use Farina's order of addition (Conditions B), we carried out the coupling of a substituted trimethyl and tributyl vinyl stannane with iodobenzene to determine the effect of CuI on the Me/Bu ratio. The reaction and results are shown in Table 6.9. In entries 1 vs. 2 without CuI present, the Me/Bu ratio is 4.36/1. However, the addition of CuI reduces the rate difference of Me/Bu to only 2.5/1 (entries 3 vs. 4). This is due to the fact that although CuI accelerated the reaction of the tributyl stannane to 1.45 times faster with CuI than without, while it suppresses the reaction with trimethyl stannane (see column CuI/No CuI). Since Farina did not utilize trimethyl stannanes in his study nor provide the specific details regarding the timing for the order of addition, it is difficult to understand these results at this juncture. We therefore went on to determine the effect of CuI on the Me/Bu rate differences for the coupling of unsubstituted vinylstannanes **57** and **58** with iodobenzene under Farina's conditions (Figure 6.9). While the reaction with tributylvinylstannane **58** was slightly accelerated by the addition of CuI, the reaction with trimethylvinylstannane **57** was not accelerated, nor was the rate suppressed. Perhaps in this instance the oxidative addition is the rate-determining step since the transmetallation with the sterically unhindered vinylstannane is very facile. It is clear that the stannane substitution is again a large factor in

the rate and mechanism of the Stille reaction. However, more experiments are necessary to truly understand the effect of CuI.

Table 6.9. CuI Effect on Me/Bu Ratio Under Farina's Conditions



entry	R	CuI (mol%)	k_{obs} (min ⁻¹) ^a	Me/Bu	CuI/ No CuI
1 ^a	Me	0	0.48	4.36/1	Me: 0.83/1
2 ^a	Bu	0	0.11		(entry 1/entry 3)
3	Me	8	0.40	2.5/1	Bu: 1.45/1
4	Bu	8	0.16		(entry 2/entry 4)

^a Results from Table 4.1

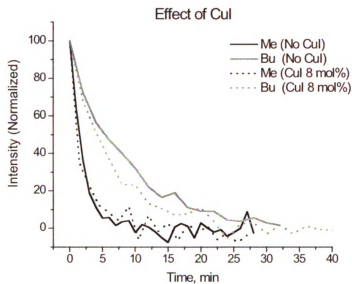
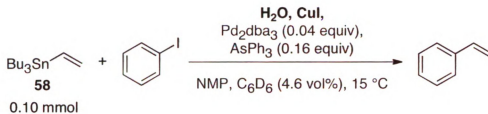


Figure 6.9. Effect of CuI Using Farina's Order. 186 MHz ^{119}Sn NMR relative integration data for the consumption of trimethylvinyltin (**57**, black traces) or tributylvinyltin (**58**, red traces) upon coupling with 1.2 equiv of PhI under a $\text{Pd}_2\text{dba}_3/\text{AsPh}_3$ catalyst system in the absence of any additives (solid traces) or in the presence of 8 mol% CuI (dashed traces).

2

1

Chapter 7. Heck-Like Cross Couplings of Vinyl Germanes

7.1. Why Germanium?

Thus far our work has been focused on understanding the reactivity differences between trimethyl and tributyl vinyl stannanes. Our reasons for embarking on this study were two fold. First of all, we would provide the synthetic organic community with relative rate data in order to logically choose substrates and conditions (trialkyl stannanes, electrophiles, solvents, additives, etc). Secondly, we could use this information to better understand the problems associated with our hydrostannation/Stille cascade in order to provide a next generation approach. Both of these purposes tie into the fact that it would be beneficial to use less toxic tributyl stannanes as opposed to the trimethyl variants. Another approach would be to eliminate the use of tin altogether while still retaining the versatility that is inherent to the Stille reaction.

Hiyama⁶⁰ (organosilane) cross-couplings are also widely utilized alternatives to Stille couplings since they are less toxic, have a decent substrate scope, and are easy to handle. The electronic structure of the silicon is similar to that of tin because they are in the same group in the periodic table. Mechanistically however, the silicon is less reactive and must be activated with fluoride for the reaction to proceed. Working our way up

the group 14 metals from tin, we come across germanium before silicon. We can infer that organogermanes may have enhanced reactivity compared with silicon and may not require activation. Furthermore, organogermanes are far less toxic than the corresponding organostannanes. For example:

Bu_3GeCl : $\text{LD}_{50} = 1970 \text{ mg/kg}$ (intraperitoneal injection in rat)

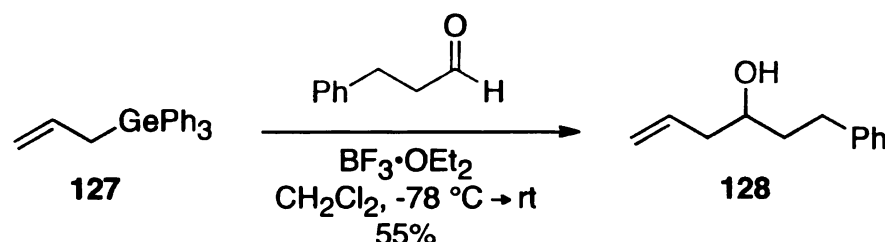
Bu_3SnCl : $\text{LD}_{50} = 117 \text{ mg/kg}$ (oral in mouse)

7.2. Development of Organogermane Reactions

Several reports have appeared in the literature exploring organogermane reactions. A report by Sano in 1986 highlights the similarity in reactivity of organogermanes with organostannanes and organosilanes.⁶¹

Allylic and allenyl germanes were prepared by desulfurizative germylation analogous to their stannylation protocol⁶² and were subsequently exploited in allylation reactions of aldehydes (Scheme 1.1). This allylation reaction indicates that Ge instills negative character on the α carbon, similar to Si and Sn organometallic nucleophiles.

Scheme 7.1. Allylations with Allyl Germane⁶¹

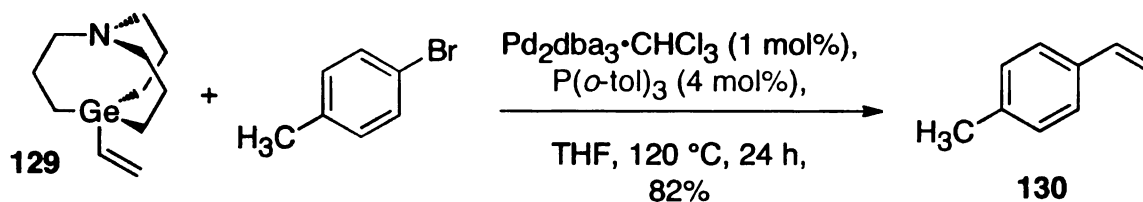


Organogermanes can also act as electrophiles. Oshima illustrated the iodo- and bromodegermylation of *Z*-vinyl germanes in 1984.⁶³ In 1990, Ikenaga and Kikukawa extended the types of organogermane transformations to include a Pd-catalyzed aryldegermylation with an arylpalladium tetrafluoroborate.⁶⁴ The reaction proceeded through an addition-elimination pathway much like aryldesilylation.

Kosugi considered a more traditional cross-coupling approach in 1996 where organogermatranes were coupled with aryl bromides under Pd catalysis.⁶⁵ Most couplings of the corresponding tributylgermanes did not provide cross-coupled products where 59-95% yields were achieved with organogermatranes.[†] This indicates that activation via the nitrogen lone pair provides a more nucleophilic species and may react along the lines of stannatranes in Stille couplings.³⁰

[†] Vinyltributyl germane coupled in 60% yield with bromotoluene. The transferable group on germatrane was vinyl, allyl, or ethynyl. When it is alkyl, the yield is <10%.

Scheme 7.2. Cross-Couplings of Germatranes⁶⁵

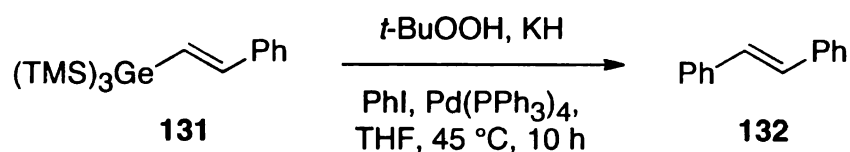


Further advances were reported in 2002 by Oshima, where aryltri(2-furyl)germanes were shown to react with aryl halides under palladium catalysis to provide access to unsymmetrical biaryls.^{66,67} Unfortunately, large amounts of TBAF (5 equiv) are necessary to achieve coupling. A mechanistic study revealed that refluxing aryltri(2-furyl)germane with TBAF for 5 h resulted in the loss of the 2-furyl ligands, most likely because fluoride has been shown to cleave Si-heteroaryl bonds⁶⁸ and can cleave Ge-heteroaryl bonds as well. This would produce a hypervalent organogermanium compound, such as $[\text{ArGe}(\text{OH})_3\text{F}]^-$, which could be responsible for the transmetallation. Tetraphenyl germanes did not couple under the same conditions, further suggesting that the Ge-heteroaryl bond is essential for these transformations. Also in 2002, Faller began reporting on the expanded scope and utility of germatrane couplings.^{69,70}

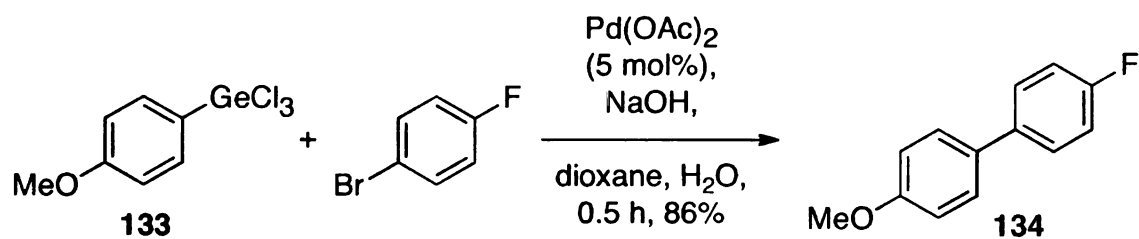
Vinyl tris(trimethylsilyl)germanes have also found their place as efficient coupling partners upon basic-oxidative treatment described by

Wnuk (Scheme 7.3).⁷¹⁻⁷³ Kosugi has continued to develop germanium coupling chemistry demonstrating that aryl trichlorogermanes, or the hydrolyzed sesquioxide variant,⁷⁴ can partake in biaryl couplings in aqueous media (Scheme 7.4). More recently Spivey has shown progress towards polymer or fluorous tagged germane couplings which are activated by photooxidation thus allowing for implementation in library syntheses.⁷⁵ Continuing efforts to expand germane synthesis^{76,77} and utility clearly indicate the viability of germanium cross-coupling chemistry.

Scheme 7.3. Vinyl Tris(trimethylsilyl)germane Couplings by Wnuk⁷¹⁻⁷³



Scheme 7.4. Trichlorogermane Couplings by Kosugi⁷⁸



Prompted by these recent reports, our group decided to explore germanium cross-couplings of tributylvinylgermanes. We imagined that information gained from our Stille kinetic studies may correlate to these

germanium cross-couplings and would give us a unique perspective on how to approach any problems.

The work presented in this chapter is a continuation of a former group member's project, Jérôme M. Lavis. The results obtained by him have been indicated and referenced to his Ph.D. Dissertation.³¹

7.3. Synthesis of Vinyl Germanes

The synthesis of vinyl germanes can be achieved through hydrogermylation of an alkyne (Table 7.1). When terminal alkynes are used, only the *E* and internal vinyl germanes are produced. The level of selectivity depends on the substitution at the propargylic position; greater substitution leads to larger *E* selectivity. Entries 4 through 8 proved difficult to separate. Careful column chromatography allowed for the separation of isomers in entry 7: 98% pure internal isomer and >99% pure *E*.

Table 7.1. Hydrogermylations

$\text{R-C}\equiv\text{C-H} \xrightarrow[\text{THF, rt, 8 h}]{\text{Pd(PPh}_3)_4 \text{ (3 mol \%), Bu}_4\text{GeH (1.2 equiv)}} \text{Bu}_3\text{Ge-CH=CH-R (E)} + \text{Bu}_3\text{Ge-C(=CH}_2\text{)-R (int)}$

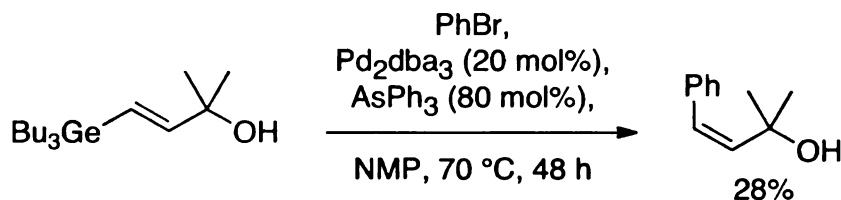
entry	alkyne	product	% yield ^a	E/int ^b
1		135a	96	100% E
2		135b	89	100% E
3 ^c		135c	73	100% E
4 ^c		135d	64	4.0/1
5 ^c		135e	75	3.8/1
6 ^c		135f	78	3.6/1
7		135g	81	1.7/1 ^d
8 ^c		135h	62	1.3/1
9		135i	91	100% E

^a Isolated material^b Determined by ¹H NMR analysis of the isolated product.^c Results from Jérôme Lavis' dissertation³¹^d Determined by ¹H NMR analysis of the crude reaction mixture; reaction time: 14.5 h

7.4. Finding the Right Coupling Conditions

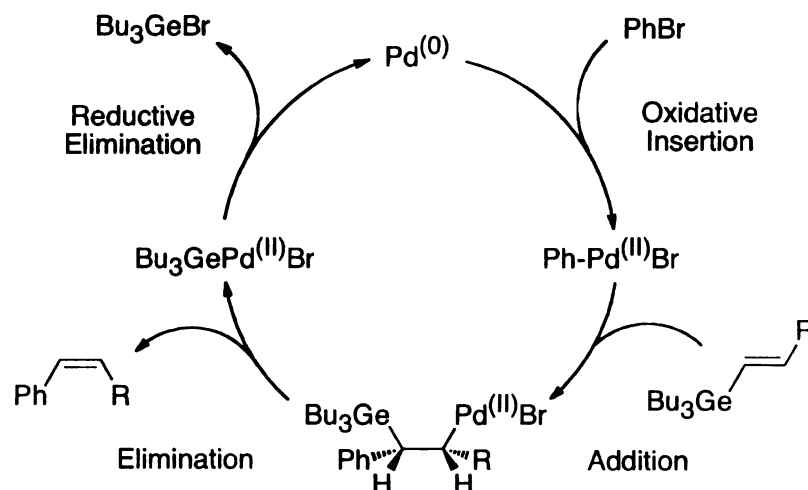
Since it was believed that germanium cross-couplings could proceed through a Stille-like mechanism, we first tested Stille conditions for the cross-coupling of **135a** with bromobenzene. The reaction proceeded in modest yield (only 28%), but with a surprising transformation of the olefin geometry; the *E* germane afforded the *Z* product.

Scheme 7.5. Germane Cross-Coupling with Inversion of Olefin Geometry³¹



This sort of change in geometry is not typical for traditional cross-coupling mechanisms. As such, we considered a Heck-type mechanism (Scheme 7.6). A syn β -germyl elimination would account for formation of the *Z* olefin. Such eliminations are not without mention in the literature. Palladium-germyl eliminations were used to explain the mechanism of Ikenaga and Kikukawa's aryldegermylation⁶⁴ and more recently in Faller's work⁶⁹ although they proceed through an E2 elimination pathway.

Scheme 7.6. Proposed Mechanism of Germanium Cross-Coupling



Further screening of Stille reaction conditions did not improve the initial results.³¹ Heck conditions were next considered based on those developed by Jeffrey.⁷⁹ Screening different quaternary ammonium salt additives, bases, and solvents (Table 7.2) identified Bu_4NBr and K_2CO_3 in a mixture of $\text{MeCN}/\text{H}_2\text{O}$ (9:1) as the most effective conditions (entry 1). The palladium catalyst loading was screened (entries 1 and 7-9) whereby 20 mol% struck the best balance between stoichiometry and yield (entry 8). Temperatures ranging from 60-70 °C proved best; lower temperatures did not effect coupling and higher temperatures afforded lower yields presumably due to catalyst decomposition.³¹

Table 7.2. Screening Heck Conditions

entry	mol% Pd	additive	base	solvent	% SM ^a	% Yield ^a (Z/E/int)
1	10	Bu ₄ NBr	K ₂ CO ₃	aq. MeCN ^c	53	47 (17/4/1)
2 ^b	10	Bu ₄ NHSO ₄	K ₂ CO ₃	aq. MeCN ^c	21	34
3	10	—	K ₂ CO ₃	aq. MeCN ^c	66	34 (21/1/5)
4	10	Bu ₄ NBr	NaHCO ₃	aq. MeCN ^c	57	43 (17/1/2)
5 ^b	10	Bu ₄ NBr	NaHCO ₃	DMF	80	6
6 ^b	10	Bu ₄ NBr	Ag ₂ CO ₃	aq. MeCN ^c	65	30
7	5	Bu ₄ NBr	K ₂ CO ₃	aq. MeCN ^c	54	46 (17/5/1)
8	20	Bu ₄ NBr	K ₂ CO ₃	aq. MeCN ^c	45	55 (10/3/1)
9 ^b	50	Bu ₄ NBr	K ₂ CO ₃	aq. MeCN ^c	63	37 (4/1/0)

^a Yields of product and unreacted starting material as well as Z/E/internal ratios were determined by ¹H NMR analysis of crude reactions with MeOH, mesitylene, or TMS-O-TMS as an internal standard.

^b Results from Jérôme Lavis' dissertation³¹

^c MeCN/H₂O (9:1)

We then ran a few coupling reactions under Stille and Heck conditions to determine if there is a general benefit to using Heck over Stille conditions (Table 7.3) across electrophiles. Although the Stille conditions were effective at times, Heck conditions proved superior.

Table 7.3. Comparing Stille vs. Heck Conditions

entry	Ar-X	% yield (Stille A) ^a	% yield (Stille B) ^b	% yield (Heck) ^c
1 ^d	PhI	30	25	47
2	PhBr	28 ^d	28 ^d	30
3	4-bromoacetophenone	15	31 ^d	61 ^d
4	1-bromo-4-nitrobenzene	10	0	48

^a Stille A: 20 mol % Pd₂dba₃, 80 mol % AsPh₃, **135a**, 2 equiv ArX, NMP, 70 °C, 48 h.

^b Stille B: Stille A conditions using Pd(OAc)₂ instead of Pd₂dba₃.

^c Heck: 20 mol % Pd(OAc)₂, 40 mol % PPh₃, **135a**, 2 equiv ArX, 1 equiv K₂CO₃, 1 equiv Bu₄NBr, MeCN/H₂O (9:1), 70 °C, 16 h.

^d Results from Jérôme Lavis' dissertation³¹

Convinced that Heck conditions provided the best results, we proceeded to outline the scope of the reaction over a variety of electrophiles. These results are presented in Table 7.4 and were performed by Jérôme Lavis.³¹ The reactions proceeded with moderate yields and favored formation of the Z product. Electron deficient aryl halides tended to afford higher yields and competitive formation of the E product, suggesting the

involvement of multiple mechanistic pathways. In all of these cases, the starting material was not fully consumed at the end of the reaction. Allowing the reaction to proceed for up to 24 hours did not appear to impact the yields to a large extent, presumably because the catalyst had decomposed; therefore all reactions were run for 16 h.

Table 7.4. Scope of Coupling with Various Aryl Halides at 0.05 M[†]

2 equiv Ar-X,
20 mol % Pd(OAc)₂, 40 mol % PPh₃,
1 equiv Bu₄NBr, 2.5 equiv K₂CO₃,
MeCN/H₂O (9:1), ~0.05 M, 70 °C, 16 h

entry	germane	halide	yield	Z/E ^a
1		Iodobenzene	136 : 47%	>20/1
2		Bromobenzene	136 : 26%	>20/1
3		4-Iodotoluene	137 : 47%	>20/1
4		4-Bromoanisole	138 : 27%	>20/1
5		4-Bromoacetophenone	139 : 61%	4.7/1
6		Methyl 4-bromobenzoate	140 : 68%	5/1
7		1-Bromo-4-nitrobenzene	141 : 56%	4.6/1
9		4-Bromoacetophenone	142 : 61%	>20/1
10		4-Bromoacetophenone	143 : 0%	-

^a Yields and Z/E ratios based on isolated material.

The results were not reproducible following an experimental indicating the reaction was run at a concentration of 0.2 M. These results are outlined in Table 7.5. Although the yields appeared to be in the same range and selectivity still favored formation of the Z product, the level of selectivity was much lower. It was finally assessed that the reactions

[†] Experiments performed by from Jérôme Lavis.³¹

performed by Lavis were actually run ~0.05M. It appears that the concentration is very important regarding isomeric outcome, and may provide insight into the mechanistic course. Thus the effect of concentration was explored next.

Table 7.5. Scope of Coupling with Various Aryl Halides at 0.2 M

entry	germane	halide	yield	Z/E/int ^a
1		Iodobenzene	136: 55%	10/3/1
2		Bromobenzene	136: 19%	1.4/1/0
3		4-Iodotoluene	137: 63%	2.1/1/0
4		4-Bromoanisole	138: 19%	2.95/1/0
5 ^b		1-Bromo-4-nitrobenzene	141: 48%	2.4/1/0
6 ^c		Iodobenzene	144: 12%	1/0/1.1

^a Yields and Z/E ratios based on isolated material.

^b Reaction run at 0.05 M

^c Reaction run at 0.06 M for 24 h

7.5. Mechanistic Insight

Concentration was found to affect the isomeric distribution of the products. When a dilute reaction mixture was utilized, the Z product was favored, while concentrated conditions led to decreased Z/E ratios.

However, the yields were relatively consistent regardless of concentration. These results are outlined in (Table 7.6). We believe the difference in isomeric distribution arises from competing Stille and Heck-like mechanistic pathways. For Heck-type reactions, the syn β -hydride elimination is proposed to be rate determining,⁸⁰ and should therefore be independent of concentration since it is an intramolecular transformation. However, the rate-determining transmetallation step of a Stille reaction should be affected by vinyltributylgermane concentration. Thus the data suggests the Stille pathway becomes kinetically competitive at higher molarities.

Table 7.6. Concentration Impact on Z/E Ratios

Entry	Molarity	% Yield	Z % Yield	E % Yield	Z/E
1 ³¹	~0.05	26	25	1	>20/1
2	0.1	29	27	2	13.5/1
3	0.168	26	21	5	4.2/1
4	0.2	23	17	6	2.8/1

^a Amount of solvent adjusted to obtain the indicated molarity.

It was unclear whether the concentration was affecting the isomeric distribution of products, or if it was a reflection on the amount of water

present since the solvent system employed was a 9:1 mixture of MeCN/H₂O. Jeffrey had discussed the impact of water on the reaction depending on the quaternary ammonium salt and base, along with whether a phosphine ligand was used.⁷⁹ We therefore ran a reaction in the absence of water to see if the isomeric ratio was affected. The standard conditions were used, although with anhydrous MeCN as solvent at 0.19 M. The K₂CO₃ was not solubilized, and perhaps this is why the reaction only afforded 28% yield. However, the Z/E ratio of products (3.9:1) was consistent with an analogous reaction run in MeCN/H₂O (9:1) that afforded 55% of Z/E (3.7:1).

Next, we reacted vinyltributylgermanes that were not fully substituted at the allylic position. Within the context of our putative Heck mechanism, two carbons possessing β -hydrogens flank the Pd-intermediate formed upon addition across the olefin of such substrates. In theory this would allow us to probe any competition between Pd–Ge and Pd–H eliminations. The results are shown in Table 7.7.

Table 7.7. Cross-coupling of Unhindered Vinyltributylgermanes

$ \begin{array}{c} \text{Bu}_3\text{Ge}-\text{CH}=\text{CH}-\text{R} \\ \mathbf{135} \end{array} \xrightarrow[\begin{array}{c} \text{1 equiv Bu}_4\text{NBr}, \\ \text{2.5 equiv K}_2\text{CO}_3, \\ \text{MeCN/H}_2\text{O (9:1)}, \\ \sim 0.05 \text{ M}, 70^\circ\text{C}, 16 \text{ h} \end{array}]{ \begin{array}{c} \text{2 equiv Halide}, \\ \text{20 mol \% Pd(OAc)}_2, \\ \text{40 mol \% PPh}_3, \end{array} } \begin{array}{c} \text{Ar}-\text{CH}=\text{CH}-\text{R} \\ (\text{Z}) \end{array} + \begin{array}{c} \text{Ar}-\text{CH}=\text{CH}-\text{R} \\ (\text{E}) \end{array} + \begin{array}{c} \text{Ar}-\text{C}(\text{CH}_3)=\text{CH}_2 \\ \text{int} \end{array} $				
entry	germane	halide	% yield	Z/E/int
1	135g	4-Bromoacetophenone	15	100% int
2 ^a	135e ^b	4-Bromoacetophenone	49	4/1/20
3 ^a	135d ^b	Iodobenzene	35	5/1/19
4 ^a	135d ^b	4-Bromoacetophenone	49	3/1/20
5	135h ^c	4-Bromoacetophenone	39 ^d	1.2/1/7.1
6 ^a	135h ^e	4-Bromoacetophenone	37 ^d	1.1/1/4.2

^a Results Jérôme Lavis' dissertation.³¹

^b Starting E/int ratio of 4/1

^c Starting E/int ratio of 10/1

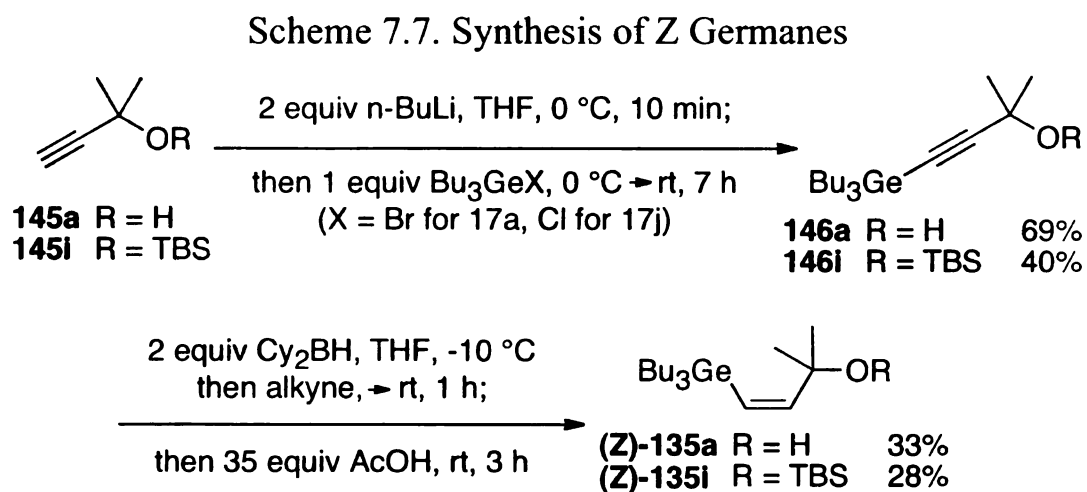
^d Determined by ¹H NMR analysis of the crude reaction using anisole as an internal standard.

^e Starting E/int ratio 4.3/1

Interestingly, (*E*)-**135g** gave exclusively the cine (internal) product, albeit in only 15% yield. Regioisomeric mixtures of **135e**, **125d**, and **135h** each afforded mixtures of E, Z, and cine products, where the cine products were formed in yields exceeding the amounts of starting internal germane. Notably, submitting the starting material to the reaction conditions without the aryl bromide did not change the E/internal ratio. All these experiments

suggest that (*E*)-vinyltributylgermanes unhindered at the allylic position give rise in significant part to the cine products. This conclusion, in combination with the low yield of the *Z* products and no indication of Pd-H elimination, indicates the involvement of non-Heck pathways.


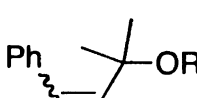
Lastly, we sought to examine the stereospecificity of the reaction. Since *E* germanes favor formation of the *Z* product, we asked whether a *Z* germane would afford the *E* product? The *Z* germane was prepared germylation of the terminal alkyne, hydroboration of the germylalkyne, and finally deborylation with acetic acid (Scheme 7.7).



(*Z*)-Germane **135a**, was then cross-coupled with PhI under our standard conditions at 0.2 M. TLC analysis indicated that the reaction did not proceed after 6 h although starting material was still present. The reaction was stopped and purified to afford 45% yield favoring the *E* isomer ((Table 7.8, entry 1). The reaction of (*E*)-**135a** afforded only 35% at 6 h in

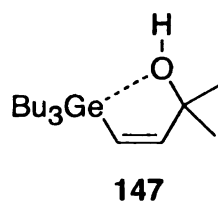
favor of the Z product (entry 2). The increased reactivity of the Z germane can be may be explained by the observation made by Faller that *O*-chelated germatranes are more reactive than *C*-chelated ones.⁶⁹ We suggest that our system is undergoing a similar activation in which electron donation of the oxygen increases the reactivity of the germanium (Figure 7.1).³¹ To this end, we synthesized the TBS ether (Z)-**1j** (Scheme 7.7) in order to shut down any chelation by the oxygen. When this substrate was subjected to our Heck conditions, only trace amounts of Z product were present by ¹H NMR analysis of the crude mixture after 6 and 24 h, supporting our hypothesis that oxygen activates the Stille pathway via germanium chelation. Furthermore, the level of stereoselectivity for entries 1 and 2 were much different. The Z germane favored the E product by 1.4/1 (E/Z) whereas the E germane favored the Z product 8.8/1 (Z/E). We believe the level of stereoselectivity is a reflection of the oxygen chelation. Since oxygen can activate the Ge-carbon bond, the Z germane is more activated towards Stille coupling thus affords a larger amount of the Z product.

Table 7.8. Effect of Germane Geometry on Coupling

		2 equiv PhI 20 mol % Pd(OAc) ₂ , 40 mol % PPh ₃ , 1 equiv Bu ₄ NBr, 2.5 equiv K ₂ CO ₃ , MeCN/H ₂ O (9:1), 0.2 M, 70 °C, 6 h			
135a R = H 135i R = TBS				59 R = H 144 R = TBS	
entry	germane	% total yield	Z % yield	E % yield	Z/E
1	(Z)- 135a	45 (59)	19	26	0.73/1
2 ^a	(E)- 135a	35 (59)	31	4	8.8/1
3	(Z)- 135i	traces (144)	traces	not detected	Z only

^a (E)-**135a** required 16 h to reach 47% yield

Figure 7.1. Activation of Ge-Carbon Bond by Oxygen Chelation



7.6. Conclusions

We have described a method by which tributylvinylgermanes are cross-coupled with aryl halides under Pd catalysis. A mixture of mechanistic pathways are possible whereby E germanes afford the E, Z, or cine substituted products. Concentration and oxygen chelation are among the factors that can influence preference for one pathway over the other.

Chapter 8. Future Work

Throughout the course of study, a number of interesting observations warrant further investigation. We found that using TFP as the Pd ligand effects autocatalytic behavior. Although we attempted preparation of a hydrido palladium iodide species, similar to what Hartwig showed⁴⁷ to exhibit autocatalysis in oxidative additions, we were unable to characterize the compound. Furthermore, it did not influence a change in the rate-determining step when employed instead of the Pd₂dba₃/TFP precatalyst system. Allowing the oxidative addition to proceed for several hours prior to addition of the stannane in an effort to prepare the autocatalytic species *in situ* led to no acceleration either. We have observed autocatalytic behavior as well with other phosphine ligands, including PPh₃ and P(*t*-Bu)₃. It is known that coordinative phosphine ligands can inhibit reaction rates since progress is dependent on ligand dissociations (See Section 1.2 and 4.3). This suggests that perhaps the induction period simply involves ligand dissociation to afford the solvent stabilized bisligated system TFP₂Pd(S). However, when iodobenzene is coupled with vinyltributyl tin, there is no induction period and the reaction follows first order behavior. The behavior of phosphine ligands appears to be substrate depended and should be further studied to understand

the influence of the vinylstannane substituents (e.g. oxygen). Coupling of either a carbon substituted stannane or silyl-protected stannane (Figure 8.1) would allow one to probe the oxygen influence. Identification of the autocatalytic species is also important, and should focus on preparation of the known L_2PdHBr species.

The role of additives also needs to be examined further. Preliminary results indicate that fluoride activates Stille reactions and to different levels for trimethyl and tributyl stannanes coupled with iodobenzene. When aryl bromides were tested, the trimethyl stannane was accelerated with autocatalytic behavior, while the tributyl stannane was accelerated but not with autocatalytic behavior. A systematic study should be performed to truly understand the role of fluoride in activation. Once these studies are performed, one may apply the information towards the development of an efficient next generation Stille reaction catalytic in tributyltin. With respect to copper additives, now that we have identified that the order of addition of CuI is important, it would be prudent to extend the systematic studies to include reactions with CuI and other Cu salts (e.g. CuTc, $CuCl_2$).

Figure 8.1. Stannanes with No Coordinative Oxygen



Again in an effort to advance the hydrostannation/Stille sequence, we must determine how to suppress unwanted tin containing by-products. It is in our favor that Me_4Sn is produced in Stille couplings while the corresponding Bu_4Sn is not. However, for both trialkyl tin reactions, a substantial amount of the trialkyl aryl tins are formed. Although these species are still reactive, they are far less reactive than the vinyl stannanes and therefore keep the tin from proceeding efficiently through the desired cycle. If we can suppress formation of the aryl tins, which are formed by an R for R transmetallation instead of an R for X transmetallation, higher tin turnovers will follow. If this is not possible, perhaps using CuI as a co-catalyst, which has been shown to facilitate aryl transfer, will allow us to achieve higher tin turnovers, albeit with continued side product formation.

As the initial focus of this dissertation has been to determine the relative rates of reaction per the nontransferable ligands on tin, it would be fascinating to exploit these differences in a useful application, e.g. one-pot or library synthesis. In Pattenden's synthesis of presumed amphidinolide A, he utilized a sequential Stille coupling sequence (Figure 8.2) where first the

vinyltin and vinyl iodide are coupled, followed by deprotection of the TES groups and Stille coupling of the remaining vinyl tin with the allylic acetate.⁸¹ If one were to access the unprotected stannane as seen in Figure 8.3 bearing both a trimethyl and tributyl stannane, a one-pot Stille coupling process might ensue. Of course, tailoring the conditions may provide a further bias to coupling of the proper ends.

Figure 8.2. Pattenden's Sequential Stille Coupling Partners

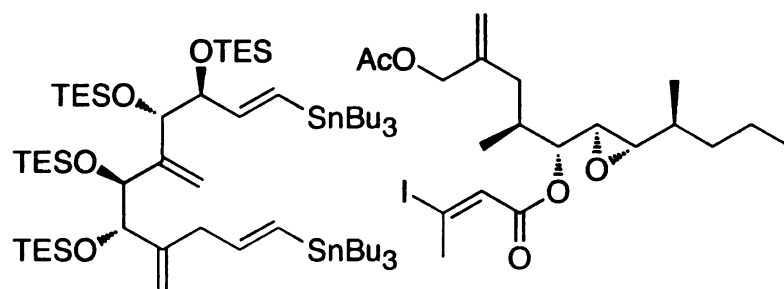
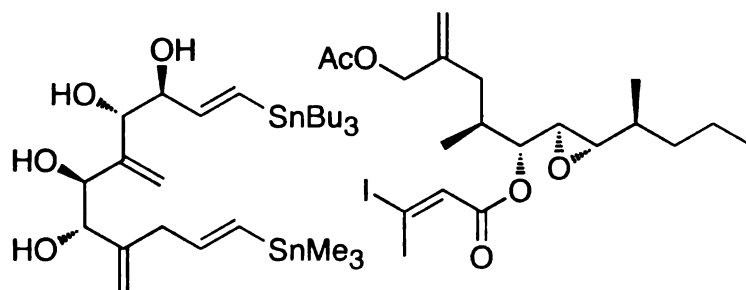


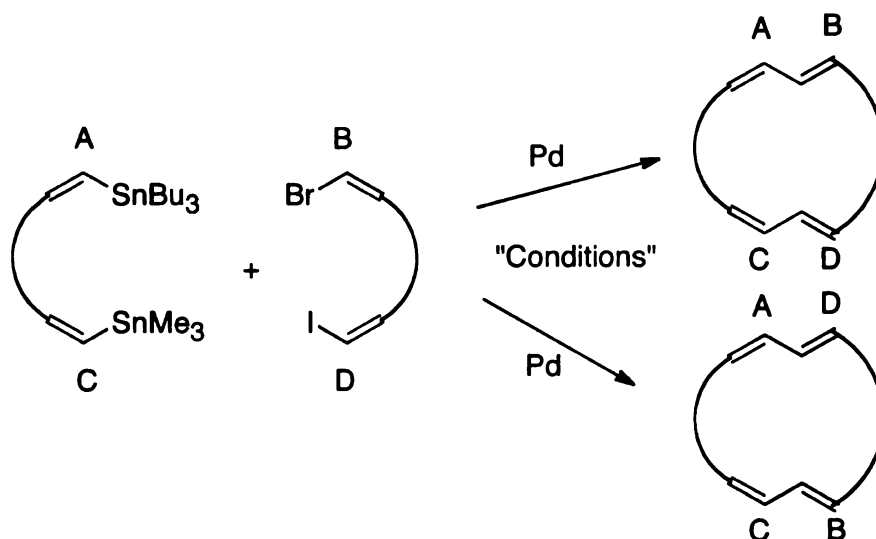
Figure 8.3. Proposed One-Pot Stille Coupling Partners



In this regard, one may also imagine using this type of method for library synthesis by controlling the head to tail coupling. As described earlier, solvent can play a role in coupling rates. Benzene was shown to inhibit trimethyl tin coupling because of competitive Pd coordination. We may be able to switch reactivity in favor of one stannane over another

simply based on a solvent change, providing access to multiple products from the same starting materials.

Figure 8.4. Head to Tail Controlled Couplings



Our rate studies provide further insight into the mechanistic details of the Stille reaction. They may be directly utilized in advancing Stille coupling procedures or may even be applied to other cross-coupling reactions where the carbon-metal bond has similar polarity.

Chapter 9. Experimental Details

9.1. Materials and Methods

Tetrahydrofuran was freshly distilled from sodium/benzophenone under nitrogen. Benzene was freshly distilled from calcium hydride under nitrogen. Benzene- d_6 was purchased from the Cambridge Isotope Labs and used without further purification. Anhydrous *N*-methyl-2-pyrrolidinone was purchased from Aldrich in a Sure/Seal™ bottle and used without further purification. Deionized water was used unless otherwise noted. Triphenylarsine was recrystallized in EtOH and 4-iodobenzotrifluoride was distilled and run through activated neutral alumina (Brockmann 1). Tri-2-furyl phosphine (TFP) was either purchased from Aldrich or prepared by the method of Zapata and Rondon.⁸² All other commercial reagents were used without purification unless otherwise noted. Flash chromatography was performed with silica gel 60 Å (230–400 mesh) purchased from Silicycle. Yields of cross-coupled products via organostannanes and organogermanes were determined by ^1H NMR of crude material versus mesitylene or hexamethyldisiloxane (NMR grade) as an internal standard. All other yields refer to chromatographically and spectroscopically pure compounds. Melting points were determined on a Thomas-Hoover Apparatus,

uncorrected. Infrared spectra were recorded on a Nicolet IR/42 spectrometer. ^1H , ^{13}C , ^{19}F , ^{31}P , and ^{119}Sn NMR spectra were recorded on a 500 MHz spectrometer (500 MHz for ^1H , 125 MHz for ^{13}C , 470 MHz for ^{19}F , 202 MHz for ^{31}P , and 186 MHz for ^{119}Sn) with chemical shifts reported relative to the residue peaks of solvent chloroform (δ 7.24 for ^1H and δ 77.0 for ^{13}C). High-resolution mass spectra (HRMS) were obtained on a Waters QTOF Ultima mass spectrometer at the Michigan State University Mass Spectrometry Facility by Luis Sanchez.

9.1.1. Standard Reaction Methods

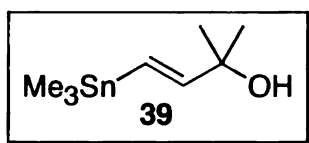
All reactions were carried out in oven-dried glassware, with magnetic stirring, and monitored by thin-layer chromatography with 0.25-mm precoated silica gel plates, unless otherwise noted. Visualization of reaction progress was achieved by UV lamp or phosphomolybdic acid stain.

9.1.2. Kinetic Methods

All reactions were carried out in 507-HP-7 Norell NMR tubes in a Varian Unity Plus-500 MHz NMR spectrometer tuned to the ^{119}Sn (186 MHz) or ^{19}F (470 MHz) nucleus. All glassware (NMR tubes and volumetric flasks) were carefully cleaned by soaking in aqua regia ($\text{HCl}:\text{HNO}_3$, 3:1),

then rinsing with base bath (KOH in *i*-PrOH/H₂O), and then rinsing with water and acetone. They were then dried on top of an oven to avoid compromising the integrity of the glass. Vials used to weigh out reagents for solution preparation were flame dried and cooled under nitrogen. All reactions were set up in air unless otherwise noted. T₁ measurements, temperature calibration, and arrayed kinetics experiments on the NMR were set up using the protocol described on the Max T. Rogers' NMR Facility webpage.⁸³ Heteronuclear (¹¹⁹Sn and ¹⁹F) parameters were set up by Dr. Daniel Holmes of the Max T. Rogers NMR Facility.

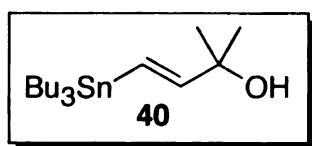
9.2. Preparation of Stannanes



Representative Hydrostannation Procedure:
Preparation of (E)-2-methyl-4-

(trimethylstannyl)but-3-en-2-ol (39) (Table 3.1, entry 1). PMHS (0.09 mL, 1.5 mmol) was added to a solution of 2-methyl-3-butyne-2-ol (0.1 mL, 1.0 mmol), Me₃SnCl (1.2 mL, 1 mmol; 1 M solution in THF), aqueous KF (176 mg, 3 mmol; 3 mL H₂O), (PPh₃)₂PdCl₂ (7 mg, 0.01 mmol), and TBAF (1 drop of a 1 M solution in THF; ca. 8 μL) in THF (5 mL). The biphasic reaction mixture was stirred at room temperature for 2 hours and a 0.5 M

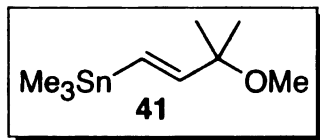
solution of NaOH (1 mL) was subsequently added and stirred for an additional 2 hours. The two phases were then separated and the aqueous layer was extracted with diethyl ether (x3). The combined organics were washed with brine, dried over MgSO₄, filtered, and concentrated. The crude material was purified by column chromatography [silica; 90:10 hexanes/EtOAc, 1% TEA] to afford (*E*)-3-methyl-1-trimethylstannyl-1-buten-2-ol (39) as a colorless oil in 47% yield. ¹H NMR (500 MHz, CDCl₃) δ 0.09 (s, 9 H), 1.26 (s, 6 H), 1.67 (s, 1 H), 6.00-6.20 (AB, *J*_{AB} = 19.0 Hz, 2 H); ¹³C NMR (125 MHz, CDCl₃) δ -9.7, 29.3, 72.2, 123.4, 155.0; ¹¹⁹Sn NMR (186 MHz, CDCl₃) δ -35.8. Spectroscopic data (¹H and ¹³C NMR) were consistent with prior literature reports.⁵⁷



Preparation of (*E*)-2-methyl-4-(tributylstannyl)but-3-en-2-ol (40) (Table 3.1, entry 2).

Applying the above conditions to 2-methyl-3-butyn-2-ol (0.1 mL, 1.0 mmol), with Bu₃SnCl (0.2 mL, 1 mmol) stirring at room temperature for 1 hour and after column chromatography [silica; 90:10 hexanes/EtOAc, 1% TEA] afforded (*E*)-3-methyl-1-tributylstannyl-1-buten-2-ol (**40**) as a colorless oil in 80% yield. IR (neat) 3357 (br, m) cm⁻¹; ¹H NMR (500 MHz,

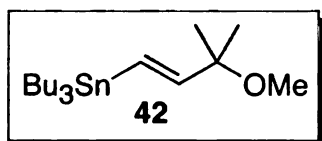
CDCl₃) δ 0.69-1.01 (m, 15 H), 1.21-1.34 (m, 12 H), 1.37-1.52 (m, 6 H), 1.52-1.55 (s, 1 H), 6.02-6.19 (AB, J_{AB} = 19.5 Hz, 2 H); ¹³C NMR (125 MHz, CDCl₃) δ 155.6, 122.4, 72.4, 29.4, 29.0, 27.2, 13.7, 9.4; ¹¹⁹Sn NMR (186 MHz, CDCl₃) δ -46.6. Spectroscopic data (¹H and ¹³C NMR) were consistent with prior literature reports.²⁹ This procedure was scaled up to 100 mmol to afford enough material for kinetic studies. The internal isomer was isolated when run on larger scale (*E*:int of 100:1) as indicated by the ¹H NMR of the crude material. Internal isomer: ¹H NMR (500 MHz, CDCl₃) δ 0.82-0.94 (m, 15 H), 1.21-1.36 (m, 12 H), 1.39-1.55 (m, 6 H), 5.12 (d, J = 1.5 Hz, 1 H), 5.7 (d, J = 1.5 Hz, 1 H); ¹³C NMR (125 MHz, CDCl₃) δ 8.8, 10.7, 13.7, 27.3, 29.1, 30.7, 120.9, 165.0; ¹¹⁹Sn NMR (186 MHz, CDCl₃) δ -51.2.



Preparation of (*E*)-(3-methoxy-3-methylbut-1-enyl)trimethylstannane (41) (Table 3.2, entry 1).

To a flame dried 200 mL round bottom flask fitted with a condenser, stir bar, rubber septa, and nitrogen inlet/outlet was added THF (40 mL) and (*E*)-2-methyl-4-(trimethylstannyl)but-3-en-2-ol (**39**) (2.5161 g, 10.1073 mmol). NaH suspension in mineral oil (60% by weight; 0.5012 g, 12.5525 mmol)

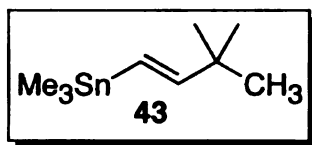
was washed with hexanes (x3) and then transferred to the reaction vessel with the assistance of THF. Hydrogen evolution was evidenced via the bubbler. MeI (0.95 mL, 15.26 mmol) was then added slowly via a syringe and the solution was submerged into a preheated oil bath at 75 °C and stirred for 2 hrs. The reaction was cooled to room temperature and quenched with H₂O (3 mL) slowly. The organics were separated and the aqueous layer was extracted with Et₂O (x3). The combined organics were washed with brine, dried with MgSO₄, filtered, and concentrated. The crude mixture was purified by column chromatography [silica; 90:10 hexanes/EtOAc] to afford **41** as a colorless oil in 89% yield. IR (neat) 1076 (C-O-C, vs) cm⁻¹; ¹H NMR (500 MHz, CDCl₃) δ 0.08 (s, 9 H), 1.19 (s, 6 H), 3.08 (s, 3 H), 5.74-6.20 (AB, *J*_{AB} = 19.5 Hz, 2 H); ¹³C NMR (125 MHz, CDCl₃) δ -9.7, 25.2, 50.3, 76.3, 127.4, 152.6; ¹¹⁹Sn NMR (186 MHz, CDCl₃) δ -35.5.



Preparation of (*E*)-(3-methoxy-3-methylbut-1-enyl)tributylstannane (42**) (Table 3.2, entry 2).**

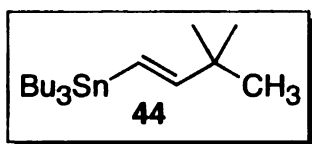
NaH (0.1213 g, 5.05 mmol) was washed with hexanes (x3) and then transferred with hexanes to a round bottom flask charged with (*E*)-2-methyl-4-(tributylstannyl)but-3-en-2-ol (**40**) (1.5 g, 4.0 mmol) and THF (~20 mL).

MeI (0.4 mL, 6.42 mmol) was then added slowly via a syringe. Hydrogen evolution was evidenced through the bubbler. The reaction was stirred over nitrogen at reflux until no hydrogen evolution persisted and full consumption of starting material checked by TLC. The reaction mixture was then quenched with very slow addition of water. The two phases were then separated and the aqueous layer was extracted with diethyl ether (x2). The combined organics were washed with brine, dried over MgSO₄, filtered, and concentrated. The crude material was purified by column chromatography [silica; 90:10 hexanes/EtOAc, 1% TEA] to afford **42** as a colorless oil in 97% yield. IR (neat) 1078 (C-O-C, s) cm⁻¹; ¹H NMR (500 MHz, CDCl₃) δ 0.76-0.94 (m, 15 H), 1.22 (s, 3 H), 1.23-1.33 (m, 6 H), 1.38-1.55 (m, 6 H), 3.12 (s, 3 H), 5.76-6.13 (AB, *J*_{AB} = 19.5 Hz, 2 H); ¹³C NMR (125 MHz, CDCl₃) δ 9.4, 13.7, 25.4, 27.2, 29.1, 50.4, 76.6, 126.7, 153.0; ¹¹⁹Sn NMR (186 MHz, CDCl₃) δ -47; HRMS (ESI) *m/z* 359.1764 [(M⁺-OMe) calcd. for C₁₇H₃₅Sn 359.1761]. Spectroscopic data (¹H and ¹³C NMR) were consistent with prior literature reports.⁸⁴



Preparation of (*E*)-(3,3-dimethylbut-1-enyl)trimethylstannane (43**) (Table 3.1, entry 5).**

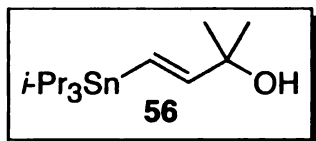
PMHS (0.9 mL, 15 mmol) was added to a solution of 3,3-dimethyl-1-butyne (1.2 mL, 9.7 mmol), Me₃SnCl (10 mL, 10 mmol; 1 M solution in THF), aqueous KF (1.73 g, 29.8 mmol; 30 mL H₂O), (PPh₃)₂PdCl₂ (71.4 mg, 0.102 mmol), and TBAF (1 drop of a 1 M solution in THF) in THF (50 mL). The biphasic reaction mixture was stirred at room temperature for 1 h and 20 min and a 1 M solution of NaOH (10 mL) was subsequently added and stirred for an additional 2 h. The two phases were then separated and the aqueous layer was extracted with diethyl ether (x2). The combined organics were washed with water then brine, dried over MgSO₄, filtered, and concentrated. The crude material was purified by column chromatography [silica; hexanes, 1% TEA] to afford (*E*)-(3,3-dimethylbut-1-enyl)trimethylstannane (**43**) as a colorless oil in 19% yield. ¹H NMR (500 MHz, CDCl₃) δ 0.08 (s, 9 H), 0.98 (s, 9 H), 5.78-6.0 (AB, *J*_{AB} = 19.0 Hz, 2 H); ¹¹⁹Sn NMR (186 MHz, CDCl₃) δ -36.4. Spectroscopic data (¹H) was consistent with prior literature reports.^{85,86}



Preparation of (*E*)-tributyl(3,3-dimethylbut-1-enyl)stannane (44**) (Table 3.1, entry 6).**

PMHS (0.9 mL, 15 mmol) was added to a solution of 3,3-dimethyl-1-butyne (1.23 mL, 9.99 mmol), Bu₃SnCl (2.7 mL, 10 mmol), aqueous KF (1.75 g, 30.1 mmol; 30 mL H₂O), (PPh₃)₂PdCl₂ (69.9 mg, 0.010 mmol), and TBAF (1 drop of a 1 M solution in THF) in THF (50 mL). The biphasic reaction mixture was stirred at room temperature for 2 h and 40 min and a 0.5 M solution of NaOH (10 mL) was subsequently added and stirred for an additional 1.5 h. The two phases were then separated and the aqueous layer was extracted with diethyl ether (x2). The combined organics were washed with water then brine, dried over MgSO₄, filtered, and concentrated. The crude material was purified by column chromatography [silica; hexanes, 1% TEA] to afford (*E*)-tributyl(3,3-dimethylbut-1-enyl)stannane (**44**) as a colorless oil in 28% yield. ¹H NMR (500 MHz, CDCl₃) δ 0.80-0.88 (m, 6 H), 0.87 (t, *J* = 7.3 Hz, 9 H) 0.98 (s, 9 H), 1.23-1.34 (m, 6 H), 1.43-1.52 (m, 6 H), 5.63-6.05 (AB, *J*_{AB} = 19.3 Hz, 2 H); ¹³C NMR (125 MHz, CDCl₃) δ 9.4, 13.7, 27.2, 29.1, 29.2, 35.9, 119.7, 160.0; ¹¹⁹Sn NMR (186 MHz, CDCl₃) δ -47.7; HRMS (ESI) *m/z* 317.1293 [(M⁺

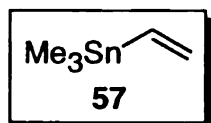
Bu) calcd. for C₁₄H₂₉Sn 317.1291]. Spectroscopic data (¹H and ¹³C NMR) were consistent with prior literature reports.^{87,88}



Preparation of (E)-2-methyl-4-(tri-isopropylstannyl)but-3-en-2-ol (56) (Table 3.1, entry 4).

PMHS (0.09 mL, 1.5 mmol) was added to a solution of 2-methyl-3-buten-2-ol (0.1 mL, 1.0 mmol), *i*Pr₃SnF (1.9937 g, 7.5 mmol), aqueous KF (0.4339 g, 1 mmol; 1 mL H₂O), (PPh₃)₂PdCl₂ (52.4 mg, 0.07 mmol), and TBAF (1 drop of a 1 M solution in THF) in THF (50 mL). The biphasic reaction mixture was stirred at room temperature for 2 hours and a 0.5 M solution of NaOH (1 mL) was subsequently added and stirred for an additional 2 hours. The two phases were then separated and the aqueous layer was extracted with diethyl ether (x3). The combined organics were washed with brine, dried over MgSO₄, filtered, and concentrated. The crude material was purified by column chromatography [silica; 90:10 hexanes/EtOAc, 1% TEA] to afford (E)-3-methyl-1-triisopropylstannyl-1-buten-2-ol (**56**) as a colorless oil in 94% yield. ¹H NMR (500 MHz, CDCl₃) δ 1.26-1.30 (d, *J* = 7.5 Hz, 18 H), 1.32 (s, 6 H), 1.42-1.57 (m, *J* = 7.5 Hz, 3 H), 1.60 (s, 1 H), 5.91-6.28

(AB, J_{AB} = 19.5 Hz, 2 H); ^{13}C NMR (125 MHz, CDCl_3) δ 14.5, 22.3, 29.8, 72.8, 120.6, 157.1; ^{119}Sn NMR (186 MHz, CDCl_3) δ 60.5; HRMS (ESI) m/z 317.1292 [$(\text{M}^+ - \text{OH})$ calcd. for $\text{C}_{14}\text{H}_{29}\text{Sn}$ 317.1291].

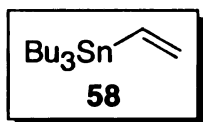


Preparation of trimethylvinylstannane (57) (Table 3.3, entry 1).

A flame-dried three-neck round bottom flask was fitted with an oven dried dewer-like condenser, oven dried addition funnel, and a magnetic stir bar. The system was purged with nitrogen. Vinylmagnesium bromide (100 mL of a 1M solution in THF, 100 mmol) was added to the flask via cannula. The condenser was filled with an acetone/dry ice mixture and maintained at -78°C for the entirety of the reaction. The reaction mixture was then heated to a gentle reflux at 66°C . Trimethyltin chloride (50 mL of a 1M solution in THF, 50 mmol) was added via cannula to the addition funnel. The trimethyltin chloride was added dropwise very slowly to maintain reflux (~ 1 drop/2 sec for 1h, 20 mL total) and then the rate of addition was increased to 2 drops/sec until all of the solution was added. At 5.5 h, there was no starting material present by TLC analysis (eluting solvent = hexanes/ethyl acetate 9:1). The reaction was then cooled to rt while still maintaining a -78°C condensor. A saturated solution of NH_4Cl (30 mL) was added to the

addition funnel. The solution was added dropwise (~ 1 drop/sec). After 10 mL were added, the solution became a solid. The remaining 20 mL were added as well as an additional 30 mL of H_2O which then formed a solution once again. This solution was stirred until the reaction soled down. The solution was transferred to a separatory funnel with the aid of 30 mL of pentane to wash. The organic layer was then washed with sat. NH_4Cl (40 mL). The aqueous layer was extracted with 40 mL of pentane twice. The organic layer wash washed again with sat. NH_4Cl 5 times. The organic layer was then washed with a 10% HCl solution 10 times followed by a wash with NaCl (40 mL) 2 times. The solution was filtered through a SiO_2 pad in a glass frit (diameter = 4 cm, height of pad = 3 cm) first by gravity for about half of the solution, and then with aspirator vacuum for the second half. The solution was then distilled with a Vigreux column and a short path distillation head. The first fraction to remove was pentane (bp 35-36 $^\circ\text{C}$) which distilled at an oil bath temp of 41 $^\circ\text{C}$ and a vapor temp of 35 $^\circ\text{C}$. The next fractions were of THF (bp 65-67 $^\circ\text{C}$) followed by mixtures of THF and trimethylvinylstannane **57** (bp 99-100 $^\circ\text{C}$). Trimethylvinylstannane is very volatile and much was lost sitting in the hood. The total amount of **57** obtained for further studies was $\sim 4\%$, 2 mmol. IR (as solution in THF) 945 (s), 770 (Sn-CH_3 rock,⁸⁹ vs) cm^{-1} ; ^1H NMR (500 MHz, CDCl_3) δ 0.12 (s, 9

H), 5.46-5.84 (1 H), 5.90-6.30 (1 H), 6.31-6.70 (1 H); ^{13}C NMR (125 MHz, CDCl_3) δ -9.9, 133.2, 140.0; ^{119}Sn NMR (186 MHz, CDCl_3) δ -40.0; HRMS (ESI) m/z 164.9728 [$(\text{M}^+ - \text{CH}_2 = \text{CH})$ calcd. for $\text{C}_3\text{H}_9\text{Sn}$ 164.9726]. Procedure from: *Org. Syn.* **1993**, 8, 97.



Preparation of tributylvinylstannane (58) (Table 3.3, entry 2).

A flame dried three-neck round bottom flask was fitted with an oven-dried condenser, oven dried addition funnel, and a magnetic stir bar. The system was purged with nitrogen. Vinylmagnesium bromide^{Note} (120 mL of a 1M solution in THF, 120 mmol) was added to the flask via cannula. The reaction mixture was then heated to a gentle reflux at 70 °C. Tributyltin chloride (14 mL, 51.6113 mmol) was added to the addition funnel then added dropwise very slowly to maintain reflux at the rate of 2 drops/sec until all of the solution was added. The reaction was refluxed overnight for 20 h. The reaction was cooled to rt, then quenched slowly with NH_4Cl via the addition funnel. The salts were filtered with a Büchner funnel and rinsed with Et_2O . The filtrate was transferred to a separatory funnel upon which 100 mL of water was added to dissolve the residual salts. The organics were then separated and the aqueous layer was extracted with Et_2O x 2 (75 mL). The

combined organics were washed with brine (75 mL), dried with MgSO_4 , filtered, and concentrated. The crude material was purified by vacuum distillation to afford a fraction at 2 mbar, oil bath temp = 126 °C, vapor temp = 94 °C. The oil temp was raised to 140 °C and another fraction was collected with a vapor temp of 102-110 °C. ^{119}Sn NMR indicated that both of the fractions were product with a very slight tin halide impurity for a total yield of 87%. Spectroscopic data matches commercially available material. For higher purity, the sample was dissolved in CH_2Cl_2 , vigorously shaken with aq. KF for 1 min, decanted, dried with MgSO_4 , filtered, and concentrated.

Note The vinylmagnesium bromide was not completely dissolved; therefore the bottle was gently warmed to dissolve as much as possible. Since it was not dissolved completely, the concentration was lower than 1 M therefore excess was used.

9.3. Determination of Kinetics Protocol and Control Experiments

9.3.1. Initial Stille Reaction of Interest to Determine the Standard Kinetics Procedure.

Coupling of 39 or 40 with iodobenzene (Scheme 3.3).

Pd_2dba_3 (0.0305 g, 0.0333 mmol) and AsPh_3 (0.0408 g, 0.1333 mmol) were weighed into a 20 mL vial. The mixture was then transferred to a 5 mL volumetric flask with the assistance of THF. The solution was then diluted to volume with THF. A stir bar was carefully added and the solution was tightly capped and stirred to homogeneity for 10 min. As the solution was stirring, (*E*)-2-methyl-4-(trimethylstannyl)but-3-en-2-ol (**39**) (0.2489 g, 1.0 mmol) was weighed directly into a 1 mL volumetric flask and diluted to volume with THF. Again, a stir bar was carefully added, the flask was capped, and the 1 M solution was stirred for 10 min. An NMR tube was charged with C_6D_6 (50 μL), the Pd/As solution (600 μL , containing 0.0037 g, 0.004 mmol Pd_2dba_3 and 0.0245g, 0.016 mmol AsPh_3), stannane solution (200 μL , 0.0498g, 0.2 mmol), and an additional amount of THF such that the final reaction concentration is 0.1857 M in stannane. The NMR tube was then capped and inserted into a 500 MHz NMR spectrometer. The NMR probe was set to 50 °C and once equilibrated, tuned to the ^{119}Sn nucleus (186 MHz). The sample was then locked and shimmed. The sample was ejected and iodobenzene (27 μL , 0.0490 g, 0.24 mmol) was added to the sample. Immediately thereafter the sample was injected, reshimmed, and an arrayed kinetics experiment was initiated to monitor the consumption of

stannane. Complete consumption of stannane was observed by 250 min. The data was analyzed as described in Section 2.4.

Each subsequent kinetic experiment will be run at the same concentration. Upon taking into account the volume of the electrophile (e.g. iodobenzene) employed, the amount of additional solvent will be tailored to achieve a concentration of 0.1857 M in Sn. The basis of this concentration is derived from using 50 μL of C_6D_6 , 200 μL of the 1 M stannane solution, 600 μL of the Pd/As solution, 27 μL of iodobenzene, and 200 μL of additional solvent to obtain a stannane concentration of 0.1857 M (0.2 mmol in 1077 μL total volume).

9.3.2. Determination of Zero-Order Electrophile Dependence (Figure 3.4).

A kinetics experiment was performed applying the standard kinetics procedure to (*E*)-2-methyl-4-(tributylstannyl)but-3-en-2-ol (**40**) (200 μL of a 1 M stannane solution in THF, 0.0750 g, 0.2 mmol), and iodobenzene (27 μL , 0.0490 g, 0.24 mmol). A second experiment utilizing a large excess of iodobenzene (0.0915g, 50 μL , 0.4485 mmol) and only 177 μL of additional THF was also performed. Comparison of the kinetic profiles indicates that

excess electrophile does not increase the rate of reaction, thus the reaction is zero-order in electrophile.

9.3.3. Determination of the Impact of Stannane Concentration on the Reaction Rate (Figure 3.5).

A kinetics experiment was performed applying the standard kinetics procedure to (*E*)-2-methyl-4-(trimethylstannyl)but-3-en-2-ol (**39**) (200 μ L of a 1 M stannane solution in THF, 0.0498 g, 0.2 mmol), and iodobenzene (27 μ L, 0.0490 g, 0.24 mmol). A second experiment utilizing half the amount of stannane (100 μ L of a 1 M stannane solution in THF, 0.0249g, 0.1 mmol) and 300 μ L of additional THF was also performed. Comparison of the kinetic profiles indicates that although the overall rate is slower when less stannane is used as indicated by comparing the slope of the tangent line at corresponding times, the rate constants obtained are the same, thus the reaction is first order in stannane.

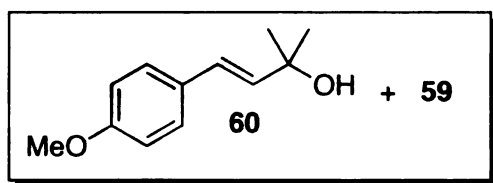
9.3.4. Determination of the Pd Dependence (Figure 3.6).

A series of kinetics experiments at different Pd concentrations were performed for couplings of both **39** and **40** with iodobenzene. Two different Pd solutions were prepared. Pd/As solution **A** is standard concentration solution as described in the standard kinetics procedure. Pd/As solution **B** is

prepared by the same method using Pd_2dba_3 (0.0610 g, 0.0666 mmol) and AsPh_3 (0.0816 g, 0.2666 mmol). The volume of the Pd/As solution and the amount of additional solvent were tailored to achieve a concentration on 0.1857 M in stannane. The following table outlines the amount of reagents added for each experiment to obtain the desired Pd loading at a Sn concentration of 0.1857 M.

Table 9.1. Reagent Amounts for Pd Dependence Study

	Volume of Reagents Added at Different Pd Loadings				
	2.7 mol%	4.0 mol%	5.3 mol%	6.7 mol%	8 mol %
Stannane 39 (1 M Solution)	200 μ L	200 μ L	200 μ L	200 μ L	200 μ L
PhI (Neat)	27 μ L	27 μ L	27 μ L	27 μ L	27 μ L
Pd/As Solution A	400 μ L	600 μ L	800 μ L		
Pd/As Solution B				500 μ L	600 μ L
Additional Solvent	400 μ L	200 μ L	none	300 μ L	200 μ L
Total Volume	1027 μ L	1027 μ L	1027 μ L	1027 μ L	1027 μ L
	Volume of Reagents Added at Different Pd Loadings				
	2.7 mol%	3.3 mol%	4.0 mol%	8 mol %	
Stannane 40 (1 M Solution)	200 μ L	200 μ L	200 μ L	200 μ L	
PhI (Neat)	27 μ L	27 μ L	27 μ L	27 μ L	
Pd Solution A	400 μ L	500 μ L	600 μ L		
Pd Solution B				600 μ L	
Additional Solvent	400 μ L	300 μ L	200 μ L	200 μ L	
Total Volume	1027 μ L	1027 μ L	1027 μ L	1027 μ L	



9.3.5. Indication of Phenyl Transfer

Upon Coupling of **40** with 4-Bromoanisole (Scheme 3.4).

Preparation of (*E*)-4-(4-methoxyphenyl)-2-methylbut-3-en-2-ol (**60**).

Pd_2dba_3 (0.0183 g, 0.02 mmol) and AsPh_3 (0.0247 g, 0.08 mmol) were added to 2 mL of THF and stirred at rt for 15 min. (*E*)-2-Methyl-4-(tributylstannyl)but-3-en-2-ol (**40**) (0.3770 g, 1.005 mmol) was weighed into a vial and transferred to the reaction mixture with the assistance of 3 mL of THF followed by the addition of 4-bromoanisole (150 μL , 1.006 mmol). The reaction was stirred at 55 $^\circ\text{C}$ for 10.5 h. The reaction was cooled to rt and quenched with H_2O (3 mL). The layers were separated and the aqueous layer was extracted with Et_2O (x3). The combined organics were then washed with brine, dried with MgSO_4 , filtered and concentrated. The crude material was purified by column chromatography [silica; 80:20 hexanes/ EtOAc] to afford (*E*)-4-(4-methoxyphenyl)-2-methylbut-3-en-2-ol (**60**) and (*E*)-2-methyl-4-phenylbut-3-en-2-ol (**59**).

9.3.6. Determination of Cross-Coupled vs. Phenyl Transfer Product Distribution

(Table 3.6, entry 1).

Pd_2dba_3 (0.0183 g, 0.02 mmol) and AsPh_3 (0.0245 g, 0.08 mmol) were stirred at room temperature in THF for 15 min. (*E*)-2-Methyl-4-(trimethylstannyl)but-3-en-2-ol (**39**) (0.2489 g, 1.0 mmol) and 4-bromoanisole (0.15 mL, 1.2 mmol) were added to the reaction mixture and stirred at 50 °C for 3 hours. The reaction mixture was concentrated and purified by column chromatography [silica; 80:20 hexanes/EtOAc] to afford (*E*)-4-(4-methoxyphenyl)-2-methylbut-3-en-2-ol **60** as a brownish-red oil in 17% yield and the phenyl exchange product, (*E*)-2-methyl-4-phenylbut-3-en-2-ol (**59**) as a brownish-yellow oil in 13% yield.

(Table 3.6, entry 2).

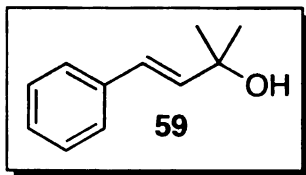
The identical reaction run in parallel using (*E*)-2-methyl-4-(tributylstannyl)but-3-en-2-ol (**40**) was performed and after column chromatography afforded (**60**) in 14% yield and (**59**) in 12% yield.

9.4. Kinetics Experiments for Chapter 3

To determine rate constants, kinetics experiments were performed applying the representative kinetics study procedure utilizing the given reagent and

solvent combinations. To determine yields and product distribution, separate bench-top reactions were run utilizing the kinetics procedure, except a 3.7 mL vial with Teflon lined cap and stir bar was used as the reaction vessel and the reaction was run in a preheated oil bath at 50-55 °C. Reactions run in THF and benzene were quenched by simply bringing the reaction to room temperature and removing the solvent in vacuo, Reactions run in NMP were quenched with sat. aq. NH₄Cl (1 mL), the organics separated, the aqueous layer extracted with Et₂O (~3 mL x 2), the combined organics washed with H₂O (2 mL) then brine (2 mL), dried with MgSO₄, filtered, and concentrated in vacuo. All yields were determined by adding a known amount of mesitylene or hexamethyldisiloxane (NMR grade) as an internal standard, and the yields were determined by ¹H NMR analysis.

9.4.1. Aryl Iodide Couplings in THF – Table 3.7



9.4.1.1. Preparation of (*E*)-2-methyl-4-phenylbut-3-en-2-ol (59).

The standard kinetics study procedure was applied to the following reagent and solvent combinations:

Coupling of 39 with iodobenzene (Table 3.7, entry 1).

(*E*)-2-Methyl-4-(trimethylstannyl)but-3-en-2-ol (**39**) (200 μ L of a 1 M solution in THF; 0.0498 g, 0.2 mmol) as the stannane, iodoobenzene (27 μ L, 0.0490 g, 0.24 mmol) as the electrophile, Pd₂dba₃/AsPh₃ solution in THF (600 μ L containing 0.004 mmol Pd₂dba₃ and 0.016 mmol AsPh₃), 50 μ L of C₆D₆, and 200 μ L of additional THF. The reaction was monitored for 620 min, 100% starting material consumption.

Bench-top reaction time: 16 h. Yields determined by ¹H NMR analysis of the crude reaction mixture using hexamethyldisiloxane as an internal standard: (*E*)-2-methyl-4-phenylbut-3-en-2-ol (**59**) (34%), (3*E*,5*E*)-2,7-dimethylocta-3,5-diene-2,7-diol (**102a**) (14% of stannane used to afford the homocoupled product), and an unidentified *E*-coupled product (8%). No unreacted starting material was observed.

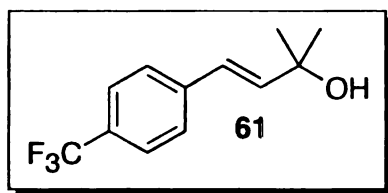
Coupling of 40 with iodobenzene (Table 3.7, entry 2).

(*E*)-2-Methyl-4-(tributylstannyl)but-3-en-2-ol (**40**) (200 μ L of a 1 M solution in THF; 0.0750 g, 0.2 mmol) as the stannane, iodoobenzene (27 μ L, 0.0490 g, 0.24 mmol) as the electrophile, Pd₂dba₃/AsPh₃ solution in THF (600 μ L containing 0.004 mmol Pd₂dba₃ and 0.016 mmol AsPh₃), 50 μ L of

C₆D₆, and 200 μ L of additional THF. The reaction was monitored for 870 min, ~98% starting material consumption.

Bench-top reaction time: 13 h 40 min. Yields determined by ¹H NMR analysis of the crude reaction mixture using hexamethyldisiloxane as an internal standard: (*E*)-2-methyl-4-phenylbut-3-en-2-ol (**59**) (51%) and (3*E*,5*E*)-2,7-dimethylocta-3,5-diene-2,7-diol (**102a**) (21% of stannane used to afford the homocoupled product). No unreacted starting material was observed.

Characterization: ¹H NMR (500 MHz, CDCl₃) δ 1.41 (s, 6 H). 1.60 (s, 1 H), 6.27-6.63 (AB, J_{AB} = 16.1 Hz, 2 H), 7.19-7.24 (m, 1 H), 7.27-7.33 (m, 2 H), 7.34-7.39 (m, 2 H); ¹³C NMR (125 MHz, CDCl₃) δ 29.9, 71.0, 126.3, 126.4, 127.4, 128.5, 136.9, 137.5. Spectroscopic data were consistent with prior literature reports.^{57,90-92}



9.4.1.2. Preparation of (*E*)-2-methyl-4-(4-(trifluoromethyl)-phenyl)but-3-en-2-ol (**61**).

The standard kinetics study procedure was applied to the following reagent and solvent combinations:

Coupling of 39 with 4-iodobenzotrifluoride (Table 3.7, entry 3).

(*E*)-2-Methyl-4-(trimethylstannyl)but-3-en-2-ol (**39**) (200 μ L of a 1 M solution in THF; 0.0498 g, 0.2 mmol) as the stannane, 4-iodobenzotrifluoride (35 μ L, 0.0653 g, 0.24 mmol) as the electrophile, Pd₂dba₃/AsPh₃ solution in THF (600 μ L containing 0.004 mmol Pd₂dba₃ and 0.016 mmol AsPh₃), 50 μ L of C₆D₆, and 192 μ L of additional THF. The reaction was monitored for 190 min, 100% starting material consumption.

Bench-top reaction time: 16 h. Yields determined by ¹H NMR analysis of the crude reaction mixture using hexamethyldisiloxane as an internal standard: (*E*)-2-methyl-4-(4-(trifluoromethyl)phenyl)but-3-en-2-ol (**61**) (87%), (*E*)-2-methyl-4-phenylbut-3-en-2-ol (**59**) (2%, phenyl transfer product from AsPh₃), and (3*E*,5*E*)-2,7-dimethylocta-3,5-diene-2,7-diol (**102a**) (11% of stannane used to afford the homocoupled product). No unreacted starting material was observed.

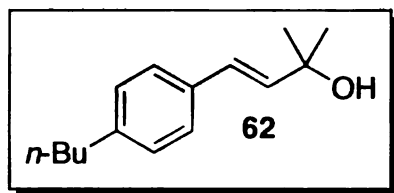
Coupling of 40 with 4-iodobenzotrifluoride (Table 3.7, entry 4).

(*E*)-2-Methyl-4-(tributylstannyl)but-3-en-2-ol (**40**) (200 μ L of a 1 M solution in THF; 0.0750 g, 0.2 mmol) as the stannane, 4-iodobenzotrifluoride (35 μ L, 0.0653 g, 0.24 mmol) as the electrophile, Pd₂dba₃/AsPh₃ solution in THF (600 μ L containing 0.004 mmol Pd₂dba₃

and 0.016 mmol AsPh₃), 50 μ L of C₆D₆, and 192 μ L of additional THF. The reaction was monitored for 700 min, 100% starting material consumption.

Bench-top reaction time: 13 h 40 min. Yields determined by ¹H NMR analysis of the crude reaction mixture using hexamethyldisiloxane as an internal standard: (*E*)-2-methyl-4-(4-(trifluoromethyl)phenyl)but-3-en-2-ol (**61**) (79%), (*E*)-2-methyl-4-phenylbut-3-en-2-ol (**59**) (1%, phenyl transfer product from AsPh₃), and (3*E*,5*E*)-2,7-dimethylocta-3,5-diene-2,7-diol (**102a**) (9% of stannane used to afford the homocoupled product). No unreacted starting material was observed.

Characterization: IR (neat) 3424 (br, vs) cm⁻¹; ¹H NMR (500 MHz, CDCl₃) δ 1.42 (s, 6 H), 1.64 (s, 1 H), 6.39-6.45 (AB, *J*_{AB} = 16.1 Hz, 1 H), 6.58-6.64 (AB, *J*_{AB} = 16.1 Hz, 1 H), 7.42-7.46 (AB, *J*_{AB} = 8.3 Hz, 2 H), 7.51-7.56 (d, *J* = 8.3 Hz, 2 H); ¹³C NMR (125 MHz, CDCl₃) δ 29.9, 71.1, 124.2 (CF₃, q, *J*_{CF} = 272.0 Hz), 125.2, 125.5 (CF₃, q, *J*_{CF} = 3.6 Hz), 126.6, 129.2 (q, *J*_{CF} = 32.2 Hz), 140.2, 140.5. HRMS (ESI) showed *m/z* > 600, which are likely more easily ionizable Pd impurities. Spectroscopic data were consistent with prior literature reports.^{90,93}



9.4.1.3. Preparation of (*E*)-4-(4-butylphenyl)-2-methylbut-3-en-2-ol (**62**).

The standard kinetics study procedure was applied to the following reagent and solvent combinations:

Coupling of **39** with 4-*n*-butyliodobenzene (Table 3.7, entry 5).

(*E*)-2-Methyl-4-(trimethylstannyl)but-3-en-2-ol (**39**) (200 μ L of a 1 M solution in THF; 0.0498 g, 0.2 mmol) as the stannane, 4-*n*-butyliodobenzene (43 μ L, 0.0624 g, 0.24 mmol) as the electrophile, Pd₂dba₃/AsPh₃ solution in THF (600 μ L containing 0.004 mmol Pd₂dba₃ and 0.016 mmol AsPh₃), 50 μ L of C₆D₆, and 184 μ L of additional THF. The reaction was monitored for 650 min, 100% starting material consumption.

Bench-top reaction time: 16 h. Yields determined by ¹H NMR analysis of the crude reaction mixture using hexamethyldisiloxane as an internal standard: (*E*)-4-(4-butylphenyl)-2-methylbut-3-en-2-ol (**62**) (30%), (*E*)-2-methyl-4-phenylbut-3-en-2-ol (**59**) (4%, phenyl transfer product from AsPh₃), (3*E*,5*E*)-2,7-dimethylocta-3,5-diene-2,7-diol (**102a**) (29% of stannane used to afford the homocoupled product), and an unidentified *E*-coupled product (9%). No unreacted stannane was observed.

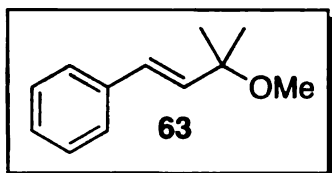
Coupling of 40 with 4-*n*-butyliodobenzene (Table 3.7, entry 6).

(*E*)-2-Methyl-4-(tributylstannyl)but-3-en-2-ol (**40**) (200 μ L of a 1 M solution in THF; 0.0750 g, 0.2 mmol) as the stannane, 4-*n*-butyliodobenzene (43 μ L, 0.0624 g, 0.24 mmol) as the electrophile, Pd₂dba₃/AsPh₃ solution in THF (600 μ L containing 0.004 mmol Pd₂dba₃ and 0.016 mmol AsPh₃), 50 μ L of C₆D₆, and 184 μ L of additional THF. The reaction was monitored for 710 min, ~85% starting material consumption.

Bench-top reaction time: 13 h 40 min. Yields determined by ¹H NMR analysis of the crude reaction mixture using hexamethyldisiloxane as an internal standard: (*E*)-4-(4-butylphenyl)-2-methylbut-3-en-2-ol (**62**) (36%), (*E*)-2-methyl-4-phenylbut-3-en-2-ol (**59**) (2%, phenyl transfer product from AsPh₃), and (3*E*,5*E*)-2,7-dimethylocta-3,5-diene-2,7-diol (**102a**) (23% of stannane used to afford the homocoupled product). No unreacted starting material was observed.

Characterization: ¹H NMR (500 MHz, CDCl₃) δ 0.90 (t, 3 H), 1.30-1.36 (m, 2 H), 1.40 (s, 6 H), 1.52-1.60 (m, 2 H), 2.57 (t, *J* = 7.7 Hz, 2 H), 6.27-6.23 (AB, *J*_{AB} = 16.1 Hz, 1 H), 6.51-6.57 (AB, *J*_{AB} = 16.1 Hz, 1 H), 7.09-7.13 (AB, *J*_{AB} = 7.8 Hz, 2 H), 7.26-7.30 (AB, *J*_{AB} = 8.8 Hz, 2 H); ¹³C NMR

(125 MHz, CDCl₃) δ 13.9, 22.3, 29.9, 33.6, 35.3, 71.0, 126.2, 126.3, 128.6, 134.3, 136.5, 142.3. Spectroscopic data were consistent with prior literature reports.^{56,94}



9.4.1.4. Preparation of (*E*)-(3-methoxy-3-methylbut-1-enyl)benzene (**63**).

The standard kinetics study procedure was applied to the following reagent and solvent combinations:

Coupling of **41** with iodobenzene (Table 3.7, entry 7).

(*E*)-(3-Methoxy-3-methylbut-1-enyl)trimethylstannane (**41**) (200 μ L of a 1 M solution in THF; 0.0526 g, 0.2 mmol) as the stannane, iodobenzene (27 μ L, 0.0490 g, 0.24 mmol) as the electrophile, Pd₂dba₃/AsPh₃ solution in THF (600 μ L containing 0.004 mmol Pd₂dba₃ and 0.016 mmol AsPh₃), 50 μ L of C₆D₆, and 200 μ L of additional THF. The reaction was monitored for 620 min, 100% starting material consumption.

Bench-top reaction time: 16 h 25 min. Yields determined by ¹H NMR analysis of the crude reaction mixture using hexamethyldisiloxane as an internal standard: (*E*)-(3-methoxy-3-methylbut-1-enyl)benzene (**63**) (60%) and (3*E*,5*E*)-2,7-dimethoxy-2,7-dimethylocta-3,5-diene (**102b**) (34% of

stannane used to afford the homocoupled product). No unreacted stannane was observed.

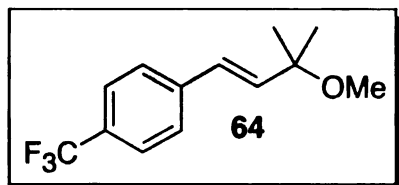
Coupling of 42 with iodobenzene (Table 3.7, entry 8).

(*E*)-(3-Methoxy-3-methylbut-1-enyl)tributylstannane (**42**) (200 μ L of a 1 M solution in THF; 0.0778 g, 0.2 mmol) as the stannane, iodobenzene (27 μ L, 0.0490 g, 0.24 mmol) as the electrophile, Pd₂dba₃/AsPh₃ solution in THF (600 μ L containing 0.004 mmol Pd₂dba₃ and 0.016 mmol AsPh₃), 50 μ L of C₆D₆, and 200 μ L of additional THF. The reaction was monitored for 680 min, 100% starting material consumption.

Bench-top reaction time: 16 h. Yields determined by ¹H NMR analysis of the crude reaction mixture using hexamethyldisiloxane as an internal standard: (*E*)-(3-methoxy-3-methylbut-1-enyl)benzene (**63**) (65%) and (3*E*,5*E*)-2,7-dimethoxy-2,7-dimethylocta-3,5-diene (**102b**) (29% of stannane used to afford the homocoupled product). No unreacted starting material was observed.

Characterization: IR (neat) 1075 (vs) cm⁻¹; ¹H NMR (500 MHz, CDCl₃) δ 1.36 (s, 6 H), 3.20 (s, 3 H), 6.15-6.51 (AB, J_{AB} = 16.1 Hz, 2 H), 7.20-7.24 (tt, J = 1.2, 7.3 Hz, 1 H), 7.28-7.33 (ddd, J = 7.6, 6.8, 2.0 Hz, 2 H), 7.35-7.40

(ddd, $J = 7.6, 1.2, 0.5$ Hz, 2 H); ^{13}C NMR (125 MHz, CDCl_3) δ 25.9, 50.5, 75.1, 126.4, 127.5, 128.6, 129.1, 135.2, 136.9; HRMS (ESI) m/z 177.1283 $[(\text{M}^+ + \text{H})]$ calcd. for $\text{C}_{12}\text{H}_{16}\text{OH}$ 177.1279].



9.4.1.5. Preparation of (*E*)-1-(3-methoxy-3-methylbut-1-enyl)-4-(trifluoromethyl)benzene (64).

The standard kinetics study procedure was applied to the following reagent and solvent combinations:

Coupling of 41 with 4-iodobenzotrifluoride (Table 3.7, entry 9).

(*E*)-(3-Methoxy-3-methylbut-1-enyl)trimethylstannane (**41**) (200 μL of a 1 M solution in THF; 0.0526 g, 0.2 mmol) as the stannane, 4-iodobenzotrifluoride (35 μL , 0.0653 g, 0.24 mmol) as the electrophile, $\text{Pd}_2\text{dba}_3/\text{AsPh}_3$ solution in THF (600 μL containing 0.004 mmol Pd_2dba_3 and 0.016 mmol AsPh_3), 50 μL of C_6D_6 , and 192 μL of additional THF. The reaction was monitored for 270 min, 100% starting material consumption.

Bench-top reaction time: 16 h 25 min. Yields determined by ^1H NMR analysis of the crude reaction mixture using hexamethyldisiloxane as an internal standard: (*E*)-1-(3-methoxy-3-methylbut-1-enyl)-4-

(trifluoromethyl)benzene (**64**) (87%), (*E*)-(3-methoxy-3-methylbut-1-enyl)benzene (**63**) (1%), (3*E*,5*E*)-2,7-dimethoxy-2,7-dimethylocta-3,5-diene (**102b**) (12% of stannane used to afford the homocoupled product). No unreacted stannane was observed.

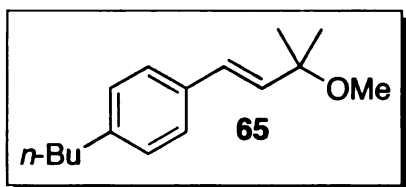
Coupling of 42 with 4-iodobenzotrifluoride (Table 3.7, entry 10).

(*E*)-(3-Methoxy-3-methylbut-1-enyl)tributylstannane (**42**) (200 μ L of a 1 M solution in THF; 0.0778 g, 0.2 mmol) as the stannane, 4-iodobenzotrifluoride (35 μ L, 0.0653 g, 0.24 mmol) as the electrophile, Pd₂dba₃/AsPh₃ solution in THF (600 μ L containing 0.004 mmol Pd₂dba₃ and 0.016 mmol AsPh₃), 50 μ L of C₆D₆, and 192 μ L of additional THF. The reaction was monitored for 480 min, 100% starting material consumption.

Bench-top reaction time: 11 h. Yields determined by ¹H NMR analysis of the crude reaction mixture using mesitylene as an internal standard: (*E*)-1-(3-methoxy-3-methylbut-1-enyl)-4-(trifluoromethyl)benzene (**64**) (82%), (*E*)-(3-methoxy-3-methylbut-1-enyl)benzene (**63**) (3-4%), and (3*E*,5*E*)-2,7-dimethoxy-2,7-dimethylocta-3,5-diene (**102b**) (12% of stannane used to afford the homocoupled product). No unreacted stannane was observed.

Characterization: IR (neat) 1325 (CF₃, s) cm⁻¹; ¹H NMR (500 MHz, CDCl₃) δ 1.37 (s, 6 H), 3.20 (s, 3 H), 6.19-6.49 (AB, *J*_{AB} = 16.4 Hz, 2 H),

7.43-7.48 (AB, $J_{AB} = 8.3$ Hz, 2 H), 7.52-7.57 (AB, $J_{AB} = 8.3$ Hz, 2 H); ^{13}C NMR (125 MHz, CDCl_3) δ 25.8, 50.6, 75.0, 124.2 (CF_3 , q, $J_{\text{CF}} = 271.6$ Hz), 125.5 (CF_3 , q, $J_{\text{CF}} = 3.7$ Hz), 126.5, 127.7, 129.3 (q, $J_{\text{CF}} = 32.2$ Hz), 138.1, 140.4.



9.4.1.6. Preparation of (*E*)-1-butyl-4-(3-methoxy-3-methylbut-1-enyl)benzene (65).

The standard kinetics study procedure was applied to the following reagent and solvent combinations:

Coupling of 41 with 4-*n*-butyliodobenzene (Table 3.7, entry 11).

(*E*)-(3-Methoxy-3-methylbut-1-enyl)trimethylstannane (41) (200 μL of a 1 M solution in THF; 0.0526 g, 0.2 mmol) as the stannane, 4-*n*-butyliodobenzene (43 μL , 0.0624 g, 0.24 mmol) as the electrophile, $\text{Pd}_2\text{dba}_3/\text{AsPh}_3$ solution in THF (600 μL containing 0.004 mmol Pd_2dba_3 and 0.016 mmol AsPh_3), 50 μL of C_6D_6 , and 184 μL of additional THF. The reaction was monitored for 600 min, 100% starting material consumption.

Bench-top reaction time: 16 h 25 min. Yields determined by ^1H NMR analysis of the crude reaction mixture using hexamethyldisiloxane as an internal standard: (*E*)-1-butyl-4-(3-methoxy-3-methylbut-1-enyl)benzene

(65) (45%), (*E*)-(3-methoxy-3-methylbut-1-enyl)benzene **(63)** (2%), (*3E,5E*)-2,7-dimethoxy-2,7-dimethylocta-3,5-diene **(102b)** (42% of stannane used to afford the homocoupled product). No unreacted stannane was observed.

Coupling of 42 with 4-*n*-butyliodobenzene (Table 3.7, entry 12).

(*E*)-(3-Methoxy-3-methylbut-1-enyl)tributylstannane **(42)** (200 μ L of a 1 M solution in THF; 0.0778 g, 0.2 mmol) as the stannane, 4-*n*-butyliodobenzene (43 μ L, 0.0624 g, 0.24 mmol) as the electrophile, Pd₂dba₃/AsPh₃ solution in THF (600 μ L containing 0.004 mmol Pd₂dba₃ and 0.016 mmol AsPh₃), 50 μ L of C₆D₆, and 184 μ L of additional THF. The reaction was monitored for 715 min, 100% starting material consumption.

Bench-top reaction time: 16 h. Yields determined by ¹H NMR analysis of the crude reaction mixture using hexamethyldisiloxane as an internal standard: (*E*)-1-butyl-4-(3-methoxy-3-methylbut-1-enyl)benzene **(65)** (70%), (*E*)-(3-methoxy-3-methylbut-1-enyl)benzene **(63)** (8%), and (*3E,5E*)-2,7-dimethoxy-2,7-dimethylocta-3,5-diene **(102b)** (22% of stannane used to afford the homocoupled product). No unreacted starting material was observed.

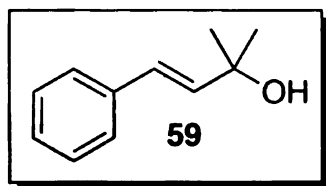
Characterization: IR (as mixture of **65** and **63**) 1205 (C-O-C, s), 741 (*para* substitution, vs) cm^{-1} ; ^1H NMR (500 MHz, CDCl_3) δ 0.90 (t, $J = 7.3$ Hz, 3 H), 1.29-1.34 (m, 2 H), 1.35 (s, 6 H), 1.52-1.61 (m, 2 H), 2.58 (t, $J = 7.8$ Hz, 2 H), 3.18 (s, 3 H), 6.10-6.16 (AB, $J_{\text{AB}} = 16.1$ Hz, 1 H), 6.42-6.47 (AB, $J_{\text{AB}} = 16.1$ Hz, 1 H), 7.10-7.14 (AB, $J_{\text{AB}} = 7.8$ Hz, 2 H), 7.27-7.31 (AB, $J_{\text{AB}} = 8.3$ Hz, 2 H); ^{13}C NMR (125 MHz, CDCl_3) δ 13.9, 22.3, 26.0, 33.6, 35.3, 50.5, 75.1, 126.3, 128.6, 129.0, 134.2, 134.3, 142.4; HRMS (ESI) m/z 201.1644 [$\text{M}^+ - \text{OMe}$] calcd. for $\text{C}_{15}\text{H}_{21}\text{O}$ 201.1643].

9.4.2. Control Experiment – Temperature Dependence

Determination of Temperature Dependence Figure 3.7 & Table 3.8.

The coupling of trimethyl and tributyl stannanes **39** and **40** coupled with iodobenzene as described above for Table 3.7 entries 1 and 2 were performed at 40, 50, and 55 °C.

9.4.3. Aryl Bromide Couplings in THF – Table 3.9



9.4.3.1. Preparation of (*E*)-2-methyl-4-phenylbut-3-en-2-ol (**59**).

The standard kinetics study procedure was applied to the following reagent and solvent combinations:

Coupling of 39 with bromobenzene (Table 3.9, entry 1).

(*E*)-2-Methyl-4-(trimethylstannyl)but-3-en-2-ol (**39**) (200 μ L of a 1 M solution in THF; 0.0498 g, 0.2 mmol) as the stannane, bromobenzene (25 μ L, 0.0337 g, 0.24 mmol) as the electrophile, Pd₂dba₃/AsPh₃ solution in THF (600 μ L containing 0.004 mmol Pd₂dba₃ and 0.016 mmol AsPh₃), 50 μ L of C₆D₆, and 202 μ L of additional THF. The reaction was monitored for 700 min, ~55% starting material consumption.

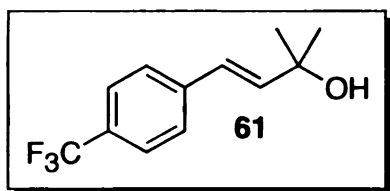
Bench-top reaction time: 13 h 15 min. Yields determined by ¹H NMR analysis of the crude reaction mixture using mesitylene as an internal standard: (*E*)-2-methyl-4-phenylbut-3-en-2-ol (**59**) (35%), (3*E*,5*E*)-2,7-dimethylocta-3,5-diene-2,7-diol (**102a**) (42% of stannane used to afford the homocoupled product), and unreacted stannane (10%).

Coupling of 40 with bromobenzene (Table 3.9, entry 2).

(*E*)-2-Methyl-4-(tributylstannyl)but-3-en-2-ol (**40**) (200 μ L of a 1 M solution in THF; 0.0750 g, 0.2 mmol) as the stannane, bromobenzene (25 μ L, 0.0337 g, 0.24 mmol) as the electrophile, Pd₂dba₃/AsPh₃ solution in THF (600 μ L containing 0.004 mmol Pd₂dba₃ and 0.016 mmol AsPh₃), 50

μL of C_6D_6 , and 202 μL of additional THF. The reaction was monitored for 870 min, $\sim 57\%$ starting material consumption.

Bench-top reaction time: 16 h. Yields determined by ^1H NMR analysis of the crude reaction mixture using hexamethyldisiloxane as an internal standard: (*E*)-2-methyl-4-phenylbut-3-en-2-ol (**59**) (33%), (3*E*,5*E*)-2,7-dimethylocta-3,5-diene-2,7-diol (**102a**) (23% of stannane used to afford the homocoupled product), and unreacted stannane (35%).



9.4.3.2. Preparation of (*E*)-2-methyl-4-(4-(trifluoromethyl)-phenyl)but-3-en-2-ol (**61**).

The standard kinetics study procedure was applied to the following reagent and solvent combinations:

Coupling of **39** with 4-bromobenzotrifluoride (Table 3.9, entry 3).

(*E*)-2-Methyl-4-(trimethylstannyl)but-3-en-2-ol (**39**) (200 μL of a 1 M solution in THF; 0.0498 g, 0.2 mmol) as the stannane, 4-bromobenzotrifluoride (33 μL , 0.0540 g, 0.24 mmol) as the electrophile, $\text{Pd}_2\text{dba}_3/\text{AsPh}_3$ solution in THF (600 μL containing 0.004 mmol Pd_2dba_3 and 0.016 mmol AsPh_3), 50 μL of C_6D_6 , and 194 μL of additional THF. The reaction was monitored for 650 min, 100% starting material consumption.

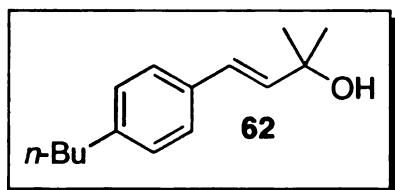
Bench-top reaction time: 13 h 15 min. Yields determined by ^1H NMR analysis of the crude reaction mixture using mesitylene as an internal standard: (*E*)-2-methyl-4-(4-(trifluoromethyl)phenyl)but-3-en-2-ol (**61**) (49%), (*E*)-2-methyl-4-phenylbut-3-en-2-ol (**59**) (11%, phenyl transfer product from AsPh_3), and (3*E*,5*E*)-2,7-dimethylocta-3,5-diene-2,7-diol (**102a**) (36% of stannane used to afford the homocoupled product). No unreacted starting material was observed.

Coupling of 40 with 4-bromobenzotrifluoride (Table 3.9, entry 4).

(*E*)-2-Methyl-4-(tributylstannyl)but-3-en-2-ol (**40**) (200 μL of a 1 M solution in THF; 0.0750 g, 0.2 mmol) as the stannane, 4-bromobenzotrifluoride (33 μL , 0.0540 g, 0.24 mmol) as the electrophile, $\text{Pd}_2\text{dba}_3/\text{AsPh}_3$ solution in THF (600 μL containing 0.004 mmol Pd_2dba_3 and 0.016 mmol AsPh_3), 50 μL of C_6D_6 , and 194 μL of additional THF. The reaction was monitored for 600 min, 100% starting material consumption.

Bench-top reaction time: 10 h. Yields determined by ^1H NMR analysis of the crude reaction mixture using mesitylene as an internal standard: (*E*)-2-methyl-4-(4-(trifluoromethyl)phenyl)but-3-en-2-ol (**61**) (82%), (*E*)-2-methyl-4-phenylbut-3-en-2-ol (**59**) (9%, phenyl transfer product from AsPh_3), and (3*E*,5*E*)-2,7-dimethylocta-3,5-diene-2,7-diol (**102a**) (9% of

stannane used to afford the homocoupled product). No unreacted starting material was observed.



9.4.3.3. Preparation of (*E*)-4-(4-butylphenyl)-2-methylbut-3-en-2-ol (**62**).

The standard kinetics study procedure was applied to the following reagent and solvent combinations:

Coupling of **39** with 4-*n*-butylbromobenzene (Table 3.9, entry 5).

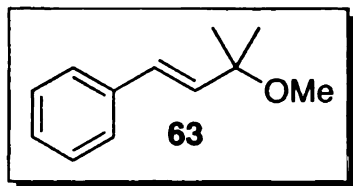
(*E*)-2-Methyl-4-(trimethylstannyl)but-3-en-2-ol (**39**) (200 μ L of a 1 M solution in THF; 0.0498 g, 0.2 mmol) as the stannane, 4-*n*-butylbromobenzene (42 μ L, 0.0511 g, 0.24 mmol) as the electrophile, Pd₂dba₃/AsPh₃ solution in THF (600 μ L containing 0.004 mmol Pd₂dba₃ and 0.016 mmol AsPh₃), 50 μ L of C₆D₆, and 185 μ L of additional THF. The reaction was monitored for 600 min, ~45% starting material consumption.

Bench-top reaction time: 16 h. Yields determined by ¹H NMR analysis of the crude reaction mixture using mesitylene as an internal standard: (*E*)-4-(4-butylphenyl)-2-methylbut-3-en-2-ol (**62**) (23%), (*E*)-2-methyl-4-phenylbut-3-en-2-ol (**59**) (11%, phenyl transfer product from AsPh₃), (3*E*,5*E*)-2,7-dimethylocta-3,5-diene-2,7-diol (**102a**) (39% of stannane used to afford the homocoupled product), and unreacted stannane (10%).

Coupling of 40 with 4-*n*-butylbromobenzene (Table 3.9, entry 6).

(*E*)-2-Methyl-4-(tributylstannyl)but-3-en-2-ol (**40**) (200 μ L of a 1 M solution in THF; 0.0750 g, 0.2 mmol) as the stannane, 4-*n*-butylbromobenzene (42 μ L, 0.0511 g, 0.24 mmol) as the electrophile, Pd₂dba₃/AsPh₃ solution in THF (600 μ L containing 0.004 mmol Pd₂dba₃ and 0.016 mmol AsPh₃), 50 μ L of C₆D₆, and 185 μ L of additional THF. The reaction was monitored for 690 min, ~55% starting material consumption.

Bench-top reaction time: 16 h. Yields determined by ¹H NMR analysis of the crude reaction mixture using mesitylene as an internal standard: (*E*)-4-(4-butylphenyl)-2-methylbut-3-en-2-ol (**62**) (23%), (*E*)-2-methyl-4-phenylbut-3-en-2-ol (**59**) (10%, phenyl transfer product from AsPh₃), (3*E*,5*E*)-2,7-dimethylocta-3,5-diene-2,7-diol (**102a**) (24% of stannane used to afford the homocoupled product), and unreacted stannane (38%).



9.4.3.4. Preparation of (*E*)-(3-methoxy-3-methylbut-1-enyl)benzene (**63**).

The standard kinetics study procedure was applied to the following reagent and solvent combinations:

Coupling of 41 with bromobenzene (Table 3.9, entry 7).

(*E*)-(3-Methoxy-3-methylbut-1-enyl)trimethylstannane (**41**) (200 μ L of a 1 M solution in THF; 0.0526 g, 0.2 mmol) as the stannane, bromobenzene (25 μ L, 0.0337 g, 0.24 mmol) as the electrophile, Pd₂dba₃/AsPh₃ solution in THF (600 μ L containing 0.004 mmol Pd₂dba₃ and 0.016 mmol AsPh₃), 50 μ L of C₆D₆, and 202 μ L of additional THF. The reaction was monitored for 760 min, ~70% starting material consumption.

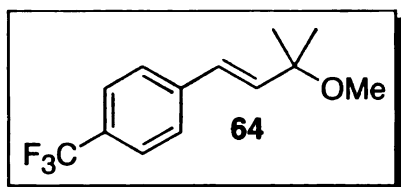
Bench-top reaction time: 16 h 25 min. Yields determined by ¹H NMR analysis of the crude reaction mixture using hexamethyldisiloxane as an internal standard: (*E*)-(3-methoxy-3-methylbut-1-enyl)benzene (**63**) (45%) and (3*E*,5*E*)-2,7-dimethoxy-2,7-dimethylocta-3,5-diene (**102b**) (55% of stannane used to afford the homocoupled product). No unreacted stannane was observed.

Coupling of 42 with bromobenzene (Table 3.9, entry 8).

(*E*)-(3-Methoxy-3-methylbut-1-enyl)tributylstannane (**42**) (200 μ L of a 1 M solution in THF; 0.0778 g, 0.2 mmol) as the stannane, bromobenzene (25 μ L, 0.0337 g, 0.24 mmol) as the electrophile, Pd₂dba₃/AsPh₃ solution in THF (600 μ L containing 0.004 mmol Pd₂dba₃ and 0.016 mmol AsPh₃), 50

μL of C_6D_6 , and 202 μL of additional THF. The reaction was monitored for 670 min, $\sim 73\%$ starting material consumption.

Bench-top reaction time: 16 h. Yields determined by ^1H NMR analysis of the crude reaction mixture using mesitylene as an internal standard: (*E*)-(3-methoxy-3-methylbut-1-enyl)benzene (**63**) (23%), (*3E,5E*)-2,7-dimethoxy-2,7-dimethylocta-3,5-diene (**102b**) (39% of stannane used to afford the homocoupled product), and unreacted stannane (10%).



9.4.3.5. Preparation of (*E*)-1-(3-methoxy-3-methylbut-1-enyl)-4-(trifluoromethyl)benzene (**64**).

The standard kinetics study procedure was applied to the following reagent and solvent combinations:

Coupling of 41 with 4-bromobenzotrifluoride (Table 3.9, entry 9).

(*E*)-(3-Methoxy-3-methylbut-1-enyl)trimethylstannane (**41**) (200 μL of a 1 M solution in THF; 0.0526 g, 0.2 mmol) as the stannane, 4-bromobenzotrifluoride (33 μL , 0.0540 g, 0.24 mmol) as the electrophile, $\text{Pd}_2\text{dba}_3/\text{AsPh}_3$ solution in THF (600 μL containing 0.004 mmol Pd_2dba_3 and 0.016 mmol AsPh_3), 50 μL of C_6D_6 , and 194 μL of additional THF. The reaction was monitored for 660 min, 100% starting material consumption.

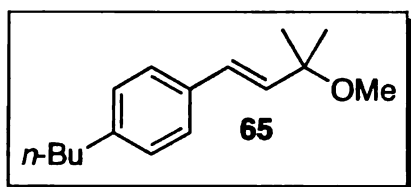
Bench-top reaction time: 16 h 25 min. Yields determined by ^1H NMR analysis of the crude reaction mixture using hexamethyldisiloxane as an internal standard: (*E*)-1-(3-methoxy-3-methylbut-1-enyl)-4-(trifluoromethyl)benzene (**64**) (44%), (*E*)-(3-methoxy-3-methylbut-1-enyl)benzene (**63**) (10%), (*3E,5E*)-2,7-dimethoxy-2,7-dimethylocta-3,5-diene (**102b**) (40% of stannane used to afford the homocoupled product). No unreacted stannane was observed.

Coupling of 42 with 4-bromobenzotrifluoride (Table 3.9, entry 10).

(*E*)-(3-Methoxy-3-methylbut-1-enyl)tributylstannane (**42**) (200 μL of a 1 M solution in THF; 0.0778 g, 0.2 mmol) as the stannane, 4-bromobenzotrifluoride (33 μL , 0.0540 g, 0.24 mmol) as the electrophile, $\text{Pd}_2\text{dba}_3/\text{AsPh}_3$ solution in THF (600 μL containing 0.004 mmol Pd_2dba_3 and 0.016 mmol AsPh_3), 50 μL of C_6D_6 , and 194 μL of additional THF. The reaction was monitored for 600 min, 100% starting material consumption.

Bench-top reaction time: 16 h. Yields determined by ^1H NMR analysis of the crude reaction mixture using mesitylene as an internal standard: (*E*)-1-(3-methoxy-3-methylbut-1-enyl)-4-(trifluoromethyl)benzene (**64**) (58%), (*E*)-(3-methoxy-3-methylbut-1-enyl)benzene (**63**) (1%), and (*3E,5E*)-2,7-

dimethoxy-2,7-dimethylocta-3,5-diene (**102b**) (29% of stannane used to afford the homocoupled product). No unreacted stannane was observed.



9.4.3.6. Preparation of (*E*)-1-butyl-4-(3-methoxy-3-methylbut-1-enyl)benzene (**65**).

The standard kinetics study procedure was applied to the following reagent and solvent combinations:

Coupling of **41** with 4-*n*-butylbromobenzene (Table 3.9, entry 11).

(*E*)-(3-Methoxy-3-methylbut-1-enyl)trimethylstannane (**41**) (200 μ L of a 1 M solution in THF; 0.0526 g, 0.2 mmol) as the stannane, 4-*n*-butylbromobenzene (42 μ L, 0.0511 g, 0.24 mmol) as the electrophile, Pd₂dba₃/AsPh₃ solution in THF (600 μ L containing 0.004 mmol Pd₂dba₃ and 0.016 mmol AsPh₃), 50 μ L of C₆D₆, and 185 μ L of additional THF. The reaction was monitored for 660 min, ~65% starting material consumption.

Bench-top reaction time: 16 h 25 min. Yields determined by ¹H NMR analysis of the crude reaction mixture using hexamethyldisiloxane as an internal standard: (*E*)-1-butyl-4-(3-methoxy-3-methylbut-1-enyl)benzene (**65**) (33%), (*E*)-(3-methoxy-3-methylbut-1-enyl)benzene (**63**) (10%), (3*E*,5*E*)-2,7-dimethoxy-2,7-dimethylocta-3,5-diene (**102b**) (56% of stannane

used to afford the homocoupled product). No unreacted stannane was observed.

Coupling of 42 with 4-*n*-butylbromobenzene (Table 3.9, entry 12).

(*E*)-(3-Methoxy-3-methylbut-1-enyl)tributylstannane (**42**) (200 μ L of a 1 M solution in THF; 0.0778 g, 0.2 mmol) as the stannane, 4-*n*-butylbromobenzene (42 μ L, 0.0511 g, 0.24 mmol) as the electrophile, Pd₂dba₃/AsPh₃ solution in THF (600 μ L containing 0.004 mmol Pd₂dba₃ and 0.016 mmol AsPh₃), 50 μ L of C₆D₆, and 185 μ L of additional THF. The reaction was monitored for 700 min, ~60% starting material consumption.

Bench-top reaction time: 16 h. Yields determined by ¹H NMR analysis of the crude reaction mixture using mesitylene as an internal standard: (*E*)-1-butyl-4-(3-methoxy-3-methylbut-1-enyl)benzene (**65**) and (*E*)-(3-methoxy-3-methylbut-1-enyl)benzene (**63**) (37%), (*3E,5E*)-2,7-dimethoxy-2,7-dimethylocta-3,5-diene (**102b**) (45% of stannane used to afford the homocoupled product), and unreacted stannane (18%).

9.4.4. Control Experiment – Electrophile Dependence

Determination of Electrophile Dependence for Aryl Bromide Couplings (Figure 3.8).

A series of kinetics reactions at different electrophile concentrations were carried out for couplings of both **39** and **40** with 4-bromobenzotrifluoride under the standard kinetic reaction conditions. The amounts of the reagents are described in the following table:

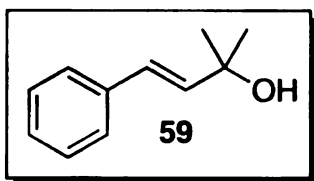
Table 9.2. Reagent Amounts for Aryl Bromide Dependence Study

	Volume of Reagents added at different Electrophile Concentrations			
	1.2 equiv	3.6 equiv	5.4 equiv	7.1 equiv
Stannane 39 or 40 (1 M solution)	200 μ L	200 μ L	200 μ L	200 μ L
Pd/As solution	600 μ L	600 μ L	600 μ L	600 μ L
4-bromobenzotrifluoride	34 μ L	100 μ L	150 μ L	200 μ L
Additional Solvent	400 μ L	127 μ L	77 μ L	27 μ L
Total Volume	1027 μ L	1027 μ L	1027 μ L	1027 μ L

9.5. Kinetics Experiments for Chapter 4

9.5.1. Aryl Iodide Couplings in NMP (Table 4.1).

The kinetics procedures are identical to those described for Table 3.7 entries 1-6 using NMP instead of THF for solution preparation and additional solvent. The following are the results from the bench-top reactions.



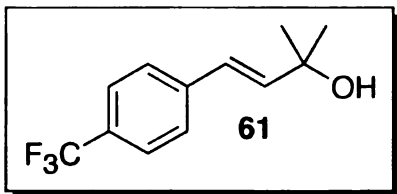
9.5.1.1. Preparation of (*E*)-2-methyl-4-phenylbut-3-en-2-ol (**59**) in NMP.

Coupling of **39** with iodobenzene (Table 4.1, entry 1).

Bench-top reaction time: 16 h. Yields determined by ^1H NMR analysis of the crude reaction mixture using hexamethyldisiloxane as an internal standard: (*E*)-2-methyl-4-phenylbut-3-en-2-ol (**59**) (81%) and (3*E*,5*E*)-2,7-dimethylocta-3,5-diene-2,7-diol (**102a**) (11% of stannane used to afford the homocoupled product). No unreacted starting material was observed.

Coupling of **40** with iodobenzene (Table 4.1, entry 2).

Bench-top reaction time: 16 h. Yields determined by ^1H NMR analysis of the crude reaction mixture using hexamethyldisiloxane as an internal standard: (*E*)-2-methyl-4-phenylbut-3-en-2-ol (**59**) (87%), and (3*E*,5*E*)-2,7-dimethylocta-3,5-diene-2,7-diol (**102a**) (13% of stannane used to afford the homocoupled product). No unreacted stannane was observed.



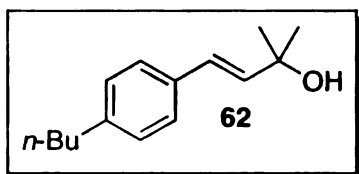
9.5.1.2. Preparation of (*E*)-2-methyl-4-(4-(trifluoromethyl)-phenyl)but-3-en-2-ol (**61**) in NMP.

Coupling of 39 with 4-iodobenzotrifluoride (Table 4.1, entry 3).

Bench-top reaction time: 16 h. Yields determined by ^1H NMR analysis of the crude reaction mixture using hexamethyldisiloxane as an internal standard: (*E*)-2-methyl-4-(4-(trifluoromethyl)phenyl)but-3-en-2-ol (**61**) (82%), (*E*)-2-methyl-4-phenylbut-3-en-2-ol (**59**) (trace amounts, phenyl transfer product from AsPh_3), and (3*E*,5*E*)-2,7-dimethylocta-3,5-diene-2,7-diol (**102a**) (4% of stannane used to afford the homocoupled product). No unreacted starting material was observed.

Coupling of 40 with 4-iodobenzotrifluoride (Table 4.1, entry 4).

Bench-top reaction time: 16 h. Yields determined by ^1H NMR analysis of the crude reaction mixture using hexamethyldisiloxane as an internal standard: (*E*)-2-methyl-4-(4-(trifluoromethyl)phenyl)but-3-en-2-ol (**61**) (90%), (*E*)-2-methyl-4-phenylbut-3-en-2-ol (**59**) (trace amounts, phenyl transfer product from AsPh_3), and (3*E*,5*E*)-2,7-dimethylocta-3,5-diene-2,7-diol (**102a**) (8% of stannane used to afford the homocoupled product). No unreacted starting material was observed.



9.5.1.3. Preparation of (*E*)-4-(4-butylphenyl)-2-methylbut-3-en-2-ol (**62**) in NMP.

Coupling of **39** with 4-*n*-butyliodobenzene (Table 4.1, entry 5).

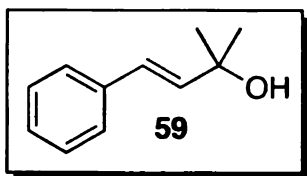
Bench-top reaction time: 16 h. Yields determined by ^1H NMR analysis of the crude reaction mixture using hexamethyldisiloxane as an internal standard: (*E*)-4-(4-butylphenyl)-2-methylbut-3-en-2-ol (**62**) (69%), (*E*)-2-methyl-4-phenylbut-3-en-2-ol (**59**) (trace amounts, phenyl transfer product from AsPh_3), and (3*E*,5*E*)-2,7-dimethylocta-3,5-diene-2,7-diol (**102a**) (11% of stannane used to afford the homocoupled product). No unreacted starting material was observed.

Coupling of **40** with 4-*n*-butyliodobenzene (Table 4.1, entry 6).

Bench-top reaction time: 16 h. Yields determined by ^1H NMR analysis of the crude reaction mixture using hexamethyldisiloxane as an internal standard: (*E*)-4-(4-butylphenyl)-2-methylbut-3-en-2-ol (**62**) (86%), (*E*)-2-methyl-4-phenylbut-3-en-2-ol (**59**) (4%, phenyl transfer product from AsPh_3), and (3*E*,5*E*)-2,7-dimethylocta-3,5-diene-2,7-diol (**102a**) (17% of stannane used to afford the homocoupled product). No unreacted stannane was observed.

9.5.2. Aryl Bromide Couplings in NMP (Table 4.2).

The kinetics procedures are identical to those described for Table 3.9 entries 1-6 using NMP instead of THF for solution preparation and additional solvent. The following are the results from the bench-top reactions.



9.5.2.1. Preparation of (*E*)-2-methyl-4-phenylbut-3-en-2-ol (**59**) in NMP.

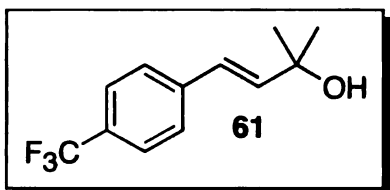
Coupling of **39** with bromobenzene (Table 4.2, entry 1).

Bench-top reaction time: 16 h at 55 °C. Yields determined by ^1H NMR analysis of the crude reaction mixture using hexamethyldisiloxane as an internal standard: (*E*)-2-methyl-4-phenylbut-3-en-2-ol (**59**) (60%) and (3*E*,5*E*)-2,7-dimethylocta-3,5-diene-2,7-diol (**102a**) (40% of stannane used to afford the homocoupled product). No unreacted starting material was observed.

Coupling of **40** with bromobenzene (Table 4.2, entry 2).

Bench-top reaction time: 16 h 55 min. Yields determined by ^1H NMR analysis of the crude reaction mixture using hexamethyldisiloxane as an internal standard: (*E*)-2-methyl-4-phenylbut-3-en-2-ol (**59**) (76%), (3*E*,5*E*)-

2,7-dimethylocta-3,5-diene-2,7-diol (**102a**) (23% of stannane used to afford the homocoupled product), and unreacted stannane (1%).



9.5.2.2. Preparation of (*E*)-2-methyl-4-(4-(trifluoromethyl)-phenyl)but-3-en-2-ol (61**) in NMP.**

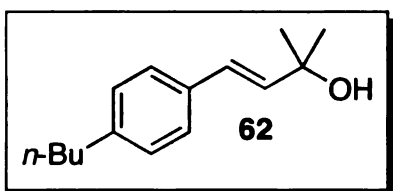
Coupling of 39 with 4-bromobenzotrifluoride (Table 4.2, entry 3).

Bench-top reaction time: 16 h at 55 °C. Yields determined by ¹H NMR analysis of the crude reaction mixture using hexamethyldisiloxane as an internal standard: (*E*)-2-methyl-4-(4-(trifluoromethyl)phenyl)but-3-en-2-ol (**61**) (69%), (*E*)-2-methyl-4-phenylbut-3-en-2-ol (**59**) (7%, phenyl transfer product from AsPh₃), and (3*E*,5*E*)-2,7-dimethylocta-3,5-diene-2,7-diol (**102a**) (24% of stannane used to afford the homocoupled product). No unreacted starting material was observed.

Coupling of 40 with 4-bromobenzotrifluoride (Table 4.2, entry 4).

Bench-top reaction time: 16 h 55 min. Yields determined by ¹H NMR analysis of the crude reaction mixture using hexamethyldisiloxane as an internal standard: (*E*)-2-methyl-4-(4-(trifluoromethyl)phenyl)but-3-en-2-ol (**61**) (88%), (*E*)-2-methyl-4-phenylbut-3-en-2-ol (**59**) (6%, phenyl transfer product from AsPh₃), and (3*E*,5*E*)-2,7-dimethylocta-3,5-diene-2,7-diol

(**102a**) (6% of stannane used to afford the homocoupled product). No unreacted starting material was observed.



9.5.2.3. Preparation of (*E*)-4-(4-butylphenyl)-2-methylbut-3-en-2-ol (**62**) in NMP.

Coupling of **39** with 4-*n*-butylbromobenzene (Table 4.2, entry 5).

Bench-top reaction time: 16 h at 55 °C. Yields determined by ¹H NMR analysis of the crude reaction mixture using hexamethyldisiloxane as an internal standard: (*E*)-4-(4-butylphenyl)-2-methylbut-3-en-2-ol (**62**) (44%), (*E*)-2-methyl-4-phenylbut-3-en-2-ol (**59**) (12%, phenyl transfer product from AsPh₃), and (3*E*,5*E*)-2,7-dimethylocta-3,5-diene-2,7-diol (**102a**) (44% of stannane used to afford the homocoupled product). No unreacted starting material was observed.

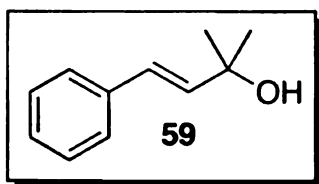
Coupling of **40** with 4-*n*-butylbromobenzene (Table 4.2, entry 6).

Bench-top reaction time: 16 h 55 min. Yields determined by ¹H NMR analysis of the crude reaction mixture using hexamethyldisiloxane as an internal standard: (*E*)-4-(4-butylphenyl)-2-methylbut-3-en-2-ol (**62**) (61%), (*E*)-2-methyl-4-phenylbut-3-en-2-ol (**59**) (12%, phenyl transfer product from AsPh₃), (3*E*,5*E*)-2,7-dimethylocta-3,5-diene-2,7-diol (**102a**) (21% of

stannane used to afford the homocoupled product), and unreacted stannane (1%).

9.5.3. Aryl Halide Couplings in Benzene (Table 4.3).

The kinetics procedures are identical to those described for Table 3.7 and Table 3.9 entries 1-6 using benzene instead of THF for solution preparation and additional solvent. The following are the results from the bench-top reactions.



9.5.3.1. Preparation of (*E*)-2-methyl-4-phenylbut-3-en-2-ol (**59**) in benzene.

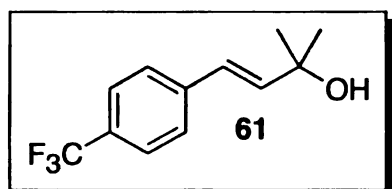
Coupling of **39** with iodobenzene (Table 4.3, entry 1).

Bench-top reaction time: 15 h. Yields determined by ^1H NMR analysis of the crude reaction mixture using mesitylene as an internal standard: (*E*)-2-methyl-4-phenylbut-3-en-2-ol (**59**) (27%) and (3*E*,5*E*)-2,7-dimethylocta-3,5-diene-2,7-diol (**102a**) (37% of stannane used to afford the homocoupled product). No unreacted starting material was observed.

Coupling of **40** with iodobenzene (Table 4.3, entry 2).

Bench-top reaction time: 15 h. Yields determined by ^1H NMR analysis of the crude reaction mixture using mesitylene as an internal standard: (*E*)-2-

methyl-4-phenylbut-3-en-2-ol (**59**) (53%) and (3*E*,5*E*)-2,7-dimethylocta-3,5-diene-2,7-diol (**102a**) (28% of stannane used to afford the homocoupled product). No unreacted starting material was observed.



9.5.3.2. Preparation of (*E*)-2-methyl-4-(4-(trifluoromethyl)-phenyl)but-3-en-2-ol (61**) in benzene.**

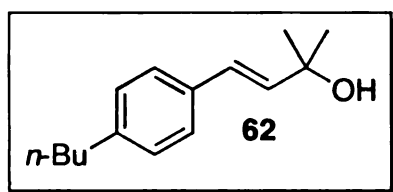
Coupling of 39 with 4-iodobenzotrifluoride (Table 4.3, entry 3).

Bench-top reaction time: 15 h. Yields determined by ^1H NMR analysis of the crude reaction mixture using mesitylene as an internal standard: (*E*)-2-methyl-4-(4-(trifluoromethyl)phenyl)but-3-en-2-ol (**61**) (83%), (*E*)-2-methyl-4-phenylbut-3-en-2-ol (**59**) (trace amounts, phenyl transfer product from AsPh_3), and (3*E*,5*E*)-2,7-dimethylocta-3,5-diene-2,7-diol (**102a**) (16% of stannane used to afford the homocoupled product). No unreacted starting material was observed.

Coupling of 40 with 4-iodobenzotrifluoride (Table 4.3, entry 4).

Bench-top reaction time: 15 h. Yields determined by ^1H NMR analysis of the crude reaction mixture using mesitylene as an internal standard: (*E*)-2-methyl-4-(4-(trifluoromethyl)phenyl)but-3-en-2-ol (**61**) (91%), (*E*)-2-methyl-4-phenylbut-3-en-2-ol (**59**) (2%, phenyl transfer product from

AsPh₃), and (3*E*,5*E*)-2,7-dimethylocta-3,5-diene-2,7-diol (**102a**) (7% of stannane used to afford the homocoupled product). No unreacted starting material was observed.



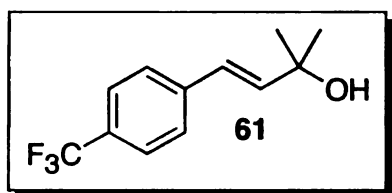
9.5.3.3. Preparation of (*E*)-4-(4-butylphenyl)-2-methylbut-3-en-2-ol (**62**) in benzene.

Coupling of **39** with 4-*n*-butyliodobenzene (Table 4.3, entry 5).

Bench-top reaction time: 15 h. Yields determined by ¹H NMR analysis of the crude reaction mixture using mesitylene as an internal standard: (*E*)-4-(4-butylphenyl)-2-methylbut-3-en-2-ol (**62**) (18%), (*E*)-2-methyl-4-phenylbut-3-en-2-ol (**59**) (trace amounts, phenyl transfer product from AsPh₃), (3*E*,5*E*)-2,7-dimethylocta-3,5-diene-2,7-diol (**102a**) (44% of stannane used to afford the homocoupled product), and unreacted stannane (20%).

Coupling of **40 with 4-*n*-butyliodobenzene (Table 4.3, entry 6).** Bench-top reaction time: 15 h. Yields determined by ¹H NMR analysis of the crude reaction mixture using mesitylene as an internal standard: (*E*)-4-(4-butylphenyl)-2-methylbut-3-en-2-ol (**62**) (45%), (*E*)-2-methyl-4-phenylbut-3-en-2-ol (**59**) (2%, phenyl transfer product from AsPh₃), and (3*E*,5*E*)-2,7-

dimethylocta-3,5-diene-2,7-diol (**102a**) (23% of stannane used to afford the homocoupled product). No unreacted starting material was observed.



9.5.3.4. Preparation of (*E*)-2-methyl-4-(4-(trifluoromethyl)-phenyl)but-3-en-2-ol (61**) in benzene.**

Coupling of 39 with 4-bromobenzotrifluoride (Table 4.3, entry 7).

Bench-top reaction time: 16 h. Yields determined by ^1H NMR analysis of the crude reaction mixture using hexamethyldisiloxane as an internal standard: (*E*)-2-methyl-4-(4-(trifluoromethyl)phenyl)but-3-en-2-ol (**61**) (17%), (*E*)-2-methyl-4-phenylbut-3-en-2-ol (**59**) (6%, phenyl transfer product from AsPh_3), and (3*E*,5*E*)-2,7-dimethylocta-3,5-diene-2,7-diol (**102a**) (40% of stannane used to afford the homocoupled product). No unreacted starting material was observed.

Coupling of 40 with 4-bromobenzotrifluoride (Table 4.3, entry 8).

Bench-top reaction time: 16 h. Yields determined by ^1H NMR analysis of the crude reaction mixture using hexamethyldisiloxane as an internal standard: (*E*)-2-methyl-4-(4-(trifluoromethyl)phenyl)but-3-en-2-ol (**61**) (30%), (*E*)-2-methyl-4-phenylbut-3-en-2-ol (**59**) (6%, phenyl transfer product from AsPh_3). (3*E*,5*E*)-2,7-dimethylocta-3,5-diene-2,7-diol (**102a**)

(30%, of stannane used to afford the homocoupled product), and unreacted stannane (19%).

9.5.4. Experiments Discussed Throughout the Text

9.5.4.1. Determination of Stannane Coordination in Benzene: Me vs. Bu Competition Experiment (Scheme 4.2 & Figure 4.5).

A standard kinetics experiment was setup using a 1:1 mixture of trimethyl and tributyl stannanes **1** and **2** to invoke a competition. Specifically, the following reagents were used: (*E*)-2-methyl-4-(trimethylstannyl)but-3-en-2-ol (**39**) (100 μ L of a 1 M solution in benzene; 0.0249 g, 0.1 mmol) and (*E*)-2-methyl-4-(tributylstannyl)but-3-en-2-ol (**40**) (100 μ L of a 1 M solution in benzene; 0.0375 g, 0.1 mmol) as the stannanes, iodoobenzene (27 μ L, 0.0490 g, 0.24 mmol) as the electrophile, Pd₂dba₃/AsPh₃ solution in benzene (600 μ L containing 0.004 mmol Pd₂dba₃ and 0.016 mmol AsPh₃), 50 μ L of C₆D₆, and 200 μ L of additional benzene.

9.5.4.2. Initial Stille Couplings Using a Pd/TFP Catalyst System (Figure 4.6).

A series of kinetics experiments were performed using TFP as the Pd ligand instead of AsPh₃. To prepare the Pd/TFP solution, Pd₂dba₃ (0.0305 g,

0.0333 mmol) and TFP (0.0309 g, 0.1333 mmol) were weighed into a 20 mL vial. The mixture was then transferred to a 5 mL volumetric flask with the assistance of THF. The solution was then diluted to volume with THF. A stir bar was carefully added and the solution was tightly capped and stirred to homogeneity for 10 min. The remainder of the procedure is as described in the standard kinetics procedure and was applied to couplings of stannanes **39**, **40**, and **56** (200 μ L of a 1 M solution in THF; 0.2 mmol) with iodobenzene (27 μ L, 0.0490 g, 0.24 mmol) by Pd_2dba_3 /TFP solution in THF (600 μ L containing 0.004 mmol Pd_2dba_3 and 0.016 mmol TFP), 50 μ L of C_6D_6 , and 200 μ L of additional THF.

9.5.4.3. Determining the Effect of Stille Products on the Autocatalytic Behavior of a Pd/TFP Catalyst System (Scheme 4.3).

The indicated Stille products were added to standard Stille reactions to determine the effect on the induction period. The amount of additional solvent was tailored to maintain the standard Sn concentration of 0.1857 M.

Effect of Bu_3SnI :

The standard kinetics procedure was applied to the following reagents: (*E*)-2-methyl-4-(tributylstannyl)but-3-en-2-ol (**40**) (160 μ L of a 1 M solution in

THF; 0.0600 g, 0.16 mmol) as the stannane, iodoobenzene (27 μ L, 0.0490 g, 0.24 mmol) as the electrophile, Bu₃SnI (12 μ L, 0.0167 g, 0.040 mmol) as the Stille product additive, Pd₂dba₃/TFP solution in THF (600 μ L containing 0.004 mmol Pd₂dba₃ and 0.016 mmol TFP), 50 μ L of C₆D₆, and 228 μ L of additional THF.

Effect of (*E*)-2-methyl-4-phenylbut-3-en-2-ol (59**):**

The standard kinetics procedure was applied to the following reagents: (*E*)-2-methyl-4-(tributylstannyl)but-3-en-2-ol (**40**) (80 μ L of a 1 M solution in THF; 0.0300 g, 0.08 mmol) as the stannane, iodoobenzene (13.5 μ L, 0.0245 g, 0.12 mmol) as the electrophile, (*E*)-2-methyl-4-phenylbut-3-en-2-ol (**59**) (40 μ L of a 0.5 M solution in THF; 0.0032 g, 0.02 mmol) as the Stille product additive, Pd₂dba₃/TFP solution in THF (300 μ L containing 0.002 mmol Pd₂dba₃ and 0.008 mmol TFP), 25 μ L of C₆D₆, and 80 μ L of additional THF.

Effect of Bu₃SnI and (*E*)-2-methyl-4-phenylbut-3-en-2-ol (59**):**

The above procedure was applied with both Bu₃SnI (6 μ L, 0.0083 g, 0.02 mmol) and (*E*)-2-methyl-4-phenylbut-3-en-2-ol (**59**) (40 μ L of a 0.5 M solution in THF; 0.0032 g, 0.02 mmol) as the Stille product additives.

9.5.4.4. Determination of the Effect of the Free Hydroxyl on Autocatalysis: Coupling of Methoxy Protected Stannane (42) under Pd/TFP (Figure 4.8).

The standard kinetics procedure was applied to the following reagents: (*E*)-(3-methoxy-3-methylbut-1-enyl)tributylstannane (**42**) (200 μ L of a 1 M solution in THF; 0.0778 g, 0.2 mmol) as the stannane, iodoobenzene (27 μ L, 0.0490 g, 0.24 mmol) as the electrophile, Pd₂dba₃/TFP solution in THF (600 μ L containing 0.004 mmol Pd₂dba₃ and 0.016 mmol TFP), 50 μ L of C₆D₆, and 200 μ L of additional THF.

9.5.4.5. Oxidative Addition of Pd₂dba₃/TFP to PhI in THF: In Search of the Autocatalytic Species (Figure 4.10).

The substrate solution preparation was prepared as described in the standard kinetics procedure. An NMR tube was charged with Pd/TFP solution in THF (600 μ L containing 0.004 mmol Pd₂dba₃ and 0.016 mmol TFP), iodobenzene (27 μ L, 0.0490 g, 0.24 mmol), 50 μ L of C₆D₆, and 200 μ L of additional THF. The reaction mixture was inserted in a preheated NMR at 50 °C and tuned to the ³¹P nucleus. The reaction was allowed to proceed for 2 h, during which a small signal appeared at -1.5 ppm. To probe whether this

peak is a catalytic species responsible for autocatalysis, (*E*)-2-methyl-4-(tributylstannyl)but-3-en-2-ol (**40**) (2000 μ L of a 1 M solution in THF; 0.0750 g, 0.2 mmol) was added to the sample. The NMR was then tuned to the ^{119}Sn nucleus and monitored for another 1.5 h. The new species did not affect the induction period, as the rate profile was the same as seen in Figure 4.6.

9.5.4.6. Coupling of Unsubstituted Stannanes Under a Pd/TFP Catalyst System (Section 4.3.1.4).

Coupling of 57 with iodobenzene:

The standard kinetics procedure was applied to the following reagents: trimethylvinylstannane (**57**) (200 μ L of a 1 M solution in THF; 0.0382 g, 0.2 mmol) as the stannane, iodoobenzene (27 μ L, 0.0490 g, 0.24 mmol) as the electrophile, Pd_2dba_3 /TFP solution in THF (600 μ L containing 0.004 mmol Pd_2dba_3 and 0.016 mmol TFP), 50 μ L of C_6D_6 , and 200 μ L of additional THF.

Coupling of 58 with iodobenzene:

The above conditions were applied to tributylvinylstannane (**58**) (200 μ L of a 1 M solution in THF; 0.0634 g, 0.2 mmol).

9.5.4.7. Coupling Under a Pd/P(*t*-Bu)₃ Catalyst System (Section 4.3.2).

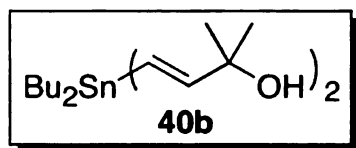
To a 3.7 mL vial fitted with a septa cap was added Pd₂dba₃ (0.0038 g, 0.0041 mmol), P(*t*-Bu)₃ (80 μL of a 2 M solution in pentane, 0.016 mmol), and THF (520 μL). The reaction was stirred at rt for 10 min. Mesitylene (200 μL of a 1 M solution in THF, 0.2 mmol), (*E*)-2-methyl-4-(trimethylstannyl)but-3-en-2-ol (**39**) (200 μL of a 1 M solution in THF; 0.0498 g, 0.2 mmol), and bromobenzene (25 μL, 0.24 mmol) were then added. The reaction was capped, inserted into a preheated oil bath at 50 °C, and allowed to stir over 7 h, during which aliquots were taken for GC analysis. The reaction was allowed to stir overnight and samples taken after 21 and 26 h. A GC calibration curve of the stannane vs. mesitylene was obtained and the consumption of stannane was calculated accordingly. The kinetic data indicates that an autocatalytic reaction proceeded.

9.5.4.8. Coupling Under a Pd/PPh₃ Catalyst System (Section 4.3.3).

To a 3.7 mL vial was added Pd₂dba₃ (0.0091 g, 0.0099 mmol), PPh₃ (0.0105 g, 0.04 mmol), and THF (500 μL). The reaction was stirred at rt for 15 min. (*E*)-(3-methoxy-3-methylbut-1-enyl)tributylstannane (**42**) (0.1950 g, 0.5010 mmol) was then transferred to the reaction vial with the assistance of 2 mL of THF after which 4-iodobenzotrifluoride (88 μL, 0.6 mmol) was added.

The reaction was capped, inserted into a preheated oil bath at 50 °C, and allowed to stir for 6 h. A sample was taken for GC/MS analysis that did not show any product formation. The reaction was allowed to react further overnight for a total of 13 h 20 min where trace amounts of product were formed. After 4 days, there was full consumption of the starting material and a large amount of product was formed. No internal standards were utilized to quantify the kinetics.

9.6. Experiments Related to Side Reactions of the Stille Reaction from Chapter 5

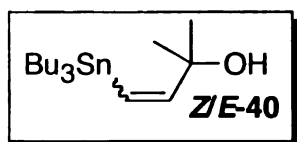


9.6.1. Preparation of (3*E*,3'*E*)-4,4'-(dibutylstannanediy)bis-(2-methylbut-3-en-2-ol)

(40b) (Section 5.3).

PMHS (0.45 mL, 15 mmol) was added to a solution of 2-methyl-3-butyn-2-ol (0.97 mL, 9.9 mmol), Bu₂SnCl₂ (1.5166 g, 4.99 mmol), aqueous KF (1.76 g, 30.3 mmol; 10 mL H₂O), (PPh₃)₂PdCl₂ (0.0357 g, 0.05 mmol), and TBAF (1 drop of a 1 M solution in THF) in THF (30 mL). The biphasic reaction mixture was stirred at room temperature for 17.5 hours and a 1 M solution of NaOH (10 mL) was subsequently added and stirred for an additional 2 hours. The two phases were then separated and the aqueous

layer was extracted with diethyl ether (x3). The combined organics were washed with brine, dried over MgSO_4 , filtered, and concentrated. The crude material was purified by column chromatography [silica; 90:10 hexanes/EtOAc, 1% TEA] to afford (3*E*,3'*E*)-4,4'-(dibutylstannanediy)bis(2-methylbut-3-en-2-ol) as a yellow oil in 3% yield along with a slight unidentified impurity and small amount of PMHS. ^1H NMR (500 MHz, CDCl_3) δ 0.87 (t, 4 H), 1.23 (t, 4 H), 1.33 (m, 6 H), 1.34 (s, 12 H), 1.6 (m, 4 H), 3.13 (s, 1 H), 5.95-6.22 (2 H), 6.28-6.80 (2 H); ^{13}C NMR (125 MHz, CDCl_3) δ 13.9, 21.5, 26.9, 28.3, 30.4, 75.9, 129.3, 150.7; ^{119}Sn NMR (186 MHz, CDCl_3) δ -5.0.



9.6.2. Preparation of (*E/Z*) 2-methyl-4-(tributylstannyl)but-3-en-2-ol (40) (Section 5.3).

To a flame dried 25 mL round bottom flask fitted with a condenser, stir bar, rubber septa, and nitrogen balloon was added THF (10 mL), 2-methyl-3-butyn-2-ol (0.20 mL, 2.05 mmol), Bu_3SnCl (0.65 mL, 2.41 mmol), KF (0.35 g, 6.02 mmol; in 6 mL H_2O), AIBN (0.0500 g, 0.3045 mmol), and PMHS (0.18 mL, 3.00 mmol). The reaction was submerged in a preheated 80 °C oil bath and stirred for 17 hrs. The reaction was then cooled to room

temperature and quenched with 6 mL of a 1 M solution of NaOH. The organics were then separated and the aqueous layer was extracted with Et₂O (x2). The combined organics were washed with brine, dried with MgSO₄, filtered, and concentrated. The crude mixture was purified by column chromatography [silica; 95:5 hexanes/EtOAc] to afford the title compound as an E/Z mixture with an undetermined yield.^{Note} ¹¹⁹Sn NMR (186 MHz, CDCl₃) δ Z isomer: -61.6, E isomer: -45.8.

^{Note} This compound was synthesized to compare ¹¹⁹Sn NMR spectra therefore yield determination and isolation of pure material were not performed.

9.6.3. Testing for Conditions to Produce the Unknown Tin Species (Table 5.1).

Stannane treated with Pd/AsPh₃ (entry 1).

Stannane and catalyst solutions were prepared as described in the standard kinetic procedure. An NMR tube was charged with (*E*)-2-methyl-4-(trimethylstannyl)but-3-en-2-ol (**39**) (200 μL of a 1 M solution in THF; 0.0498 g, 0.2 mmol), Pd₂dba₃/AsPh₃ solution in THF (600 μL containing 0.004 mmol Pd₂dba₃ and 0.016 mmol AsPh₃), and C₆D₆ (50 μL) for NMR

lock. The NMR tube was capped and placed in a preheated oil bath at 50 °C and periodically shaken over the course of 1 h 15 min. A ^{119}Sn NMR spectra was then taken where only the starting material was observed. The sample was heated again in an oil bath for an additional 2 h 45 min and another ^{119}Sn NMR taken. Still only starting stannane was present.

Stannane treated with Me_3SnI (entry 2).

Stannane and catalyst solutions were prepared as described in the standard kinetic procedure. An NMR tube was charged with (*E*)-2-methyl-4-(trimethylstannyl)but-3-en-2-ol (**39**) (200 μL of a 1 M solution in THF; 0.0498 g, 0.2 mmol), Me_3SnI (0.0603 g, 0.208 mmol) and THF (300 μL), and C_6D_6 (50 μL) for NMR lock. The NMR tube was capped and placed in a preheated oil bath at 50 °C and periodically shaken over the course of 1.5 h. A ^{119}Sn NMR was taken to reveal only the two starting tins. The reaction was allowed to heat overnight and another ^{119}Sn NMR taken. Still only the two tins were present.

Stannane treated with Pd/TFP then Bu_3SnI (entry 3).

Stannane and catalyst solutions were prepared as described in the standard kinetic procedure with TFP instead of AsPh_3 . An NMR tube was charged

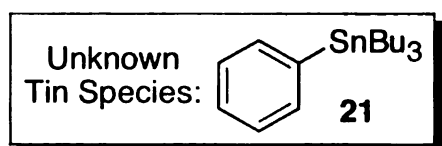
with (*E*)-2-methyl-4-(trimethylstannyl)but-3-en-2-ol (**39**) (200 μ L of a 1 M solution in THF; 0.0498 g, 0.2 mmol), Pd/TFP solution in THF (600 μ L containing 0.004 mmol Pd₂dba₃ and 0.016 mmol TFP), and (and C₆D₆ (50 μ L) for NMR lock. The sample was capped and placed in a preheated oil bath at 50 °C and periodically shaken over the course of 6 h. A ¹¹⁹Sn NMR was taken to reveal only the starting stannane. An unspecified amount of Bu₃SnI was then added and allowed to stir overnight. A ¹¹⁹Sn NMR was then taken to reveal only starting stannane.

Stannane treated with I₂ (entry 4).

Stannane and catalyst solutions were prepared as described in the standard kinetic procedure. An NMR tube was charged with (*E*)-2-methyl-4-(trimethylstannyl)but-3-en-2-ol (**39**) (200 μ L of a 1 M solution in THF; 0.0498 g, 0.2 mmol) and C₆D₆ (50 μ L) for NMR lock. I₂ (0.0319 g, 0.1257 mmol) was weighed into a vial and transferred to the NMR tube with the assistance of 500 μ L of THF. The sample was then placed in a preheated oil bath at 50 °C for 1 h. A ¹¹⁹Sn NMR was taken to reveal that the starting material converted to Me₃SnI. The reaction was allowed to heat overnight and another ¹¹⁹Sn NMR taken that indicated no further reaction.

Stannane treated with Pd(OAc)₂ (entry 5).

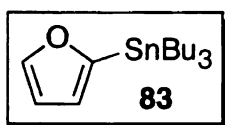
Stannane and catalyst solutions were prepared as described in the standard kinetic procedure. An NMR tube was charged with (*E*)-2-methyl-4-(trimethylstannyl)but-3-en-2-ol (**39**) (200 μ L of a 1 M solution in THF; 0.0498 g, 0.2 mmol), Pd(OAc)₂ (0.0049 g, 0.0073 mmol), THF (600 μ L), and C₆D₆ (50 μ L) for NMR lock. The sample was then placed in a preheated oil bath at 50 °C for 1 h 45 min. A ¹¹⁹Sn NMR was taken to reveal that the starting material converted to Me₄Sn.



9.6.4. Identification of the Unknown Tin Species as tributylphenylstannane (Section 5.3).

To a flame dried 25 mL round bottom flask was added Pd₂dba₃ (0.0488 g, 0.0533 mmol), AsPh₃ (0.0653 g, 0.2132 mmol), and THF (10 mL). The reaction was stirred at rt for 10 min until a green color persisted. (*E*)-2-Methyl-4-(tributylstannyl)but-3-en-2-ol (**40**) (1.0003 g, 2.6660 mmol) was then weighed and transferred to the reaction flask with the assistance of THF (4 mL) and stirred for 15 min to allow for a similar situation as when kinetic experiments are performed. Iodobenzene (360 μ L, 3.2169 mmol) was then

added and the reaction vessel capped with a plastic plug to prevent evaporation of the solvent. The reaction was submerged into a preheated oil bath at 49-51 °C and allowed to stir for 3 h 20 min after which it was removed from the heat and the reaction vessel was submerged into an ice bath to cold quench the reaction. A 1 mL aliquot was removed, concentrated, and a ^{119}Sn NMR in C_6D_6 was taken to see if the unknown tin signal was present. Once confirmed, the remainder of the reaction mixture was concentrated and column chromatography performed [silica; 90:10 hexanes/EtOAc, 1% TEA]. Of the 125 fractions collected, the unknown species was found in fractions 10-12 ($R_f = 0.93$). The sample was spiked with authentic Bu_3SnPh and the ^{119}Sn NMR revealed still only one signal. Spectroscopic data matches commercially available material.



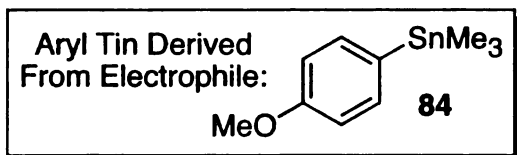
9.6.5. Determination of the Source for Aryl Exchange.

Preparation of 2-furyl-tributylstannane (83) (Scheme 5.3).^{95,96}

To a 250 mL round bottom flask was added THF (100 mL) and furan (8.5 mL, 118.78 mmol). An addition funnel was attached and capped with a rubber septa and N_2 inlet/outlet. The reaction was submerged into a cooling bath at -32 °C (acetone bath with chiller). *n*-BuLi (42 mL of a 1.6 M

solution in hexane, 67 mmol) was added dropwise via the addition funnel and the mixture became a milky yellow color and was stirred for 1 h 20 min. Bu_3SnCl was then added dropwise through the addition funnel at a rate of 2 drop/sec and the reaction became a clear yellow color and was stirred for 30 min at $-32\text{ }^\circ\text{C}$. The reaction was quenched with sat. aq. NH_4Cl (50 mL) and stirred for 15 min. H_2O (100 mL) was then added to dissolve the salts. The layers were separated; the aqueous layer was extracted with Et_2O (50 mL x 3); the combined organics washed with brine (75 mL), dried with Na_2SO_4 , filtered, and concentrated. The crude material was purified by vacuum distillation (0.4 Torr ; oil bath temp = $130\text{ }^\circ\text{C}$; vapor temp = $111\text{ }^\circ\text{C}$) to afford the title compound in 94% yield. ^1H NMR (500 MHz, CDCl_3) δ 0.89 (t, J = 7.3 Hz, 9 H), 1.08 (m, 6 H), 1.33 (m, J = 7.2, 7.3, 7.4 Hz, 6 H), 1.46-1.68 (m, 6 H), 6.41 (dd with 2nd order effects, J = 1.7, 3.1 Hz, 1 H), 6.55 (d with 2nd order effects, J = 3.1 Hz, 1 H), 7.72 (d with 2nd order effects, J = 1.7 Hz, 1 H); ^{13}C NMR (125 MHz, CDCl_3) δ 10.0 ($J_{119\text{Sn-C}}$ = 180.7, $J_{117\text{Sn-C}}$ = 172.4 Hz), 13.641, 27.2 ($J_{\text{Sn-C}}$ = 29.5 Hz), 28.9 ($J_{\text{Sn-C}}$ = 10.8, 10.4 Hz), 109.0, 121.1, 146.9, 160.6; ^{119}Sn NMR NMR (186 MHz, CDCl_3) δ -63.8.

Spectroscopic data (^1H and ^{13}C NMR) were consistent with prior literature reports.^{95,96}



9.6.6. Determination of the Source for Aryl Exchange.

Coupling with 4-bromoanisole to afford 4-tributylstannylanisole (Figure 5.2).

To a flame dried 10 mL round bottom flask was added Pd_2dba_3 (0.0174 g, 0.0190 mmol), AsPh_3 (0.0232 g, 0.0756 mmol), and THF (2.5 mL). The reaction was stirred at rt for 15 min until a green color persisted. (*E*)-2-Methyl-4-(trimethylstannyl)but-3-en-2-ol (**39**) (0.2354 g, 0.9456 mmol) was then weighed and transferred to the reaction flask with the assistance of THF (2.5 mL) followed by the addition of 4-bromoanisole (140 μL , 1.1183 mmol). The reaction was submerged in a preheated oil bath at 50 $^\circ\text{C}$ for 1 h 50 min. An aliquot was removed, concentrated, and a ^{119}Sn NMR in C_6D_6 was taken to see if the new tin signal was present. Once confirmed, the remainder of the reaction mixture quenched with sat. aq. NH_4Cl . The layers were separated; the aqueous layer was extracted with Et_2O (5 mL x 2); the

combined organics were washed with H₂O (10 mL), dried with MgSO₄, filtered, and concentrated. A ¹¹⁹Sn NMR was taken to observe the new signal, then the NMR sample was spiked with an authentic sample of 4-tributylstannylanisole to provide still one signal. The NMR sample was then spiked with an authentic sample of tributylphenylstannane to reveal two signals in close proximity.

9.6.7. Testing for Conditions to Produce the Unknown Tin Species from Bu₃SnI in the Presence of an Electrophile (Table 5.2).

Tributyltin iodide treated with iodobenzene (entry 1).

Bu₃SnI (30 μL, 0.1050 mmol), iodobenzene (12 μL, 0.1072 mmol), THF (500 μL), and C₆D₆ (50 μL) were mixed in an NMR tube and allowed to sit in an oil bath at 50 °C for 1.5 h. A ¹¹⁹Sn NMR was then taken to reveal only the starting stannane.

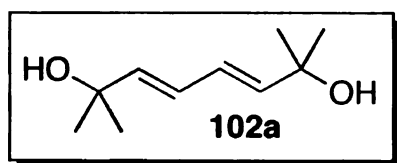
Tributyltin iodide treated with iodobenzene and Pd/AsPh₃ (entry 2).

Pd₂dba₃ (0.0018 g, 0.0020 mmol) and AsPh₃ (0.0029 g, 0.0095 mmol) were weighed into a 3.7 mL vial to which was added THF (500 μL). The vial was capped and stirred for 15 min at rt until a greenish color persisted. The

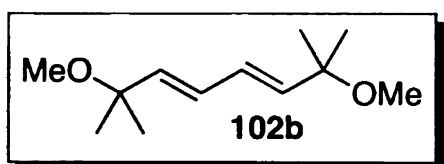
solution was then transferred to an NMR tube charged with Bu₃SnI (30 μL, 0.1050 mmol) and PhI (12 μL, 0.1072 mmol). The sample was allowed to sit in a 50 °C oil bath for 45 min. A ¹¹⁹Sn NMR was taken that revealed the Bu₃SnI signal at +77 ppm, and an unidentified signal at +50 ppm, but no tributylphenyltin signal.

9.6.8. Yields for Tables 5.3 and 5.4 can be found above for the corresponding kinetics experiments (See Section 9.4).

Characterization of homocoupled dienes:



Characterization of (3*E*,5*E*)-2,7-dimethylocta-3,5-diene-2,7-diol (102a). White solid [mp = 91-92 °; lit. mp = 107-108 °C].⁹⁷ IR (neat) 3264 (br, s), 3027 (s, w), 1154 (s, m), 988 (s, m) cm⁻¹; ¹H NMR (500 MHz, CDCl₃) δ 1.32 (m, 12 H), 1.39 (s, 2 H), 5.76-6.23 (AA'BB', *J*_{AB} = 14.8 Hz, 14.7 Hz); ¹³C NMR (125 MHz, CDCl₃) δ 29.7, 70.7, 126.2, 141.2; HRMS (ESI) *m/z* 153.1278 [(M⁺-OH) calcd. for C₁₀H₁₇O 153.1279].



Characterization of (3*E*,5*E*)-2,7-dimethoxy-2,7-dimethylocta-3,5-diene (102b). IR (neat) 1240 cm⁻¹; ¹H NMR (500 MHz, CDCl₃) δ 1.27 (s, 12 H), 3.14 (s, 6 H), 5.58-

6.20 (AA'BB', $J_{AB} = 15.1$ Hz, 4 H); ^{13}C NMR (125 MHz, CDCl_3) δ 25.8, 50.5, 74.9, 129.1, 138.8; HRMS (ESI) m/z 199.1698 [$(\text{M}^+ + \text{H})$ calcd. for $\text{C}_{12}\text{H}_{22}\text{O}_2\text{H}$ 199.1698]

9.7. Experiments Related to Additives for the Stille Reaction from Chapter 6

9.7.1. Determination of aq. KF/TBAF Effect on Stannane (Section 6.4.1).

To an NMR tube was added (*E*)-2-methyl-4-(trimethylstannyl)but-3-en-2-ol (**39**) (200 μL of a 1 M solution in THF; 0.0498 g, 0.2 mmol), KF (200 μL of a 3 M aqueous solution, 0.6 mmol) and TBAF (1 drop of a 1 M solution in THF; ca. 8 μL), and THF (200 μL) to bring the volume of the sample to an appropriate level for the NMR. A ^{119}Sn NMR was taken and showed only the starting material. No other tin signals were observed upon scanning from +400 to -200 ppm.

9.7.2. Representative Procedure for Kinetic Studies with Additives: Additive = Aqueous KF/TBAF or Water.

The standard kinetic procedure is followed with the use of additives:

Aqueous KF/TBAF Effect on the Coupling of 39 with Iodobenzene (Scheme 6.6 and Figure 6.1a).

Pd₂dba₃ (0.0305 g, 0.0333 mmol) and AsPh₃ (0.0408 g, 0.1333 mmol) were weighed into a 20 mL vial. The mixture was then transferred to a 5 mL volumetric flask with the assistance of THF. The solution was then diluted to volume with THF. A stir bar was carefully added and the solution was tightly capped and stirred to homogeneity for 10 min. As the solution was stirring, (*E*)-2-methyl-4-(trimethylstannyl)but-3-en-2-ol (**39**) (0.2489 g, 1.0 mmol) was weighed directly into a 1 mL volumetric flask and diluted to volume with THF. Again, a stir bar was carefully added, the flask was capped, and the 1 M solution was stirred for 10 min. A solution of aqueous KF (3 M) was prepared by weighing KF (0.1743 g, 3 mmol) into a 1 mL volumetric flask and diluted to volume with deionized water. A stir bar was carefully added and the solution was capped and stirred to homogeneity for 10 min. An NMR tube was charged with C₆D₆ (50 µL), the Pd/As solution (600 µL, containing 0.0037 g, 0.004 mmol Pd₂dba₃ and 0.0245g, 0.016 mmol AsPh₃), (*E*)-2-methyl-4-(trimethylstannyl)but-3-en-2-ol (**39**) (200 µL of a 1 M solution in THF; 0.0498g, 0.2 mmol), and an additional amount of THF such that the final reaction concentration is 0.1857 M in stannane. The

additives, aq. KF solution (200 μ L, 0.6 mmol) and 1 drop of TBAF (1 M solution in THF), were then added to the NMR tube. The NMR tube was then capped and inserted into a 500 MHz NMR spectrometer. The NMR probe was set to 50 $^{\circ}$ C and once equilibrated, tuned to the 119 Sn nucleus (186 MHz). The sample was then locked and shimmed. The sample was ejected and iodobenzene (27 μ L, 0.0490 g, 0.24 mmol) was added to the sample. Immediately thereafter the sample was injected, reshimmed, and an arrayed kinetics experiment was initiated to monitor the consumption of stannane.

9.7.2.1. Coupling of 40 with iodobenzene and aq. KF/TBAF (Scheme 6.6 and Figure 6.1b).

The representative kinetics procedure with additives was applied to (*E*)-2-methyl-4-(tributylstannyl)but-3-en-2-ol (**40**) (200 μ L of a 1 M solution in THF; 0.0750 g, 0.2 mmol), iodobenzene (27 μ L, 0.0490 g, 0.24 mmol), and aq. KF solution (200 μ L, 0.6 mmol) and 1 drop of TBAF (1 M solution in THF).

9.7.2.2. Water Effect on the Coupling of 39 with Iodobenzene (Section 6.5).

The representative kinetics procedure with additives was applied to (*E*)-2-methyl-4-(trimethylstannyl)but-3-en-2-ol (**39**) (200 μ L of a 1 M solution in THF; 0.0498 g, 0.2 mmol), iodobenzene (27 μ L, 0.0490 g, 0.24 mmol), and water (200 μ L, 11.1 mmol). Using dionized water from the faucet, HPLC grade water, or Milli-Q water provided the same kinetics.

9.7.2.3. Water Effect on the Coupling of 40 with Iodobenzene (Section 6.5).

The representative kinetics procedure with additives was applied to (*E*)-2-methyl-4-(tributylstannyl)but-3-en-2-ol (**40**) (200 μ L of a 1 M solution in THF; 0.0750 g, 0.2 mmol), iodobenzene (27 μ L, 0.0490 g, 0.24 mmol), and water (200 μ L, 11.1 mmol).

9.7.2.4. Water Dependence Study (Figure 6.3).

The conditions described above for water-activated reactions (Scheme 6.5) were performed over a range of equiv of water. For couplings of **1** with iodobenzene, 2.8, 5.5, 16.6, and 55.4 equiv of water was implemented. For couplings of **2** with iodobenzene, 1.4, 2.8, 4.2, and 55.4 equiv of water was implemented.

9.7.2.5. Additive Effect on Aryl Bromide Couplings (Section 6.6).

Additive = Fluoride:

The representative kinetics procedure with additives was applied to (*E*)-2-methyl-4-(tributylstannyl)but-3-en-2-ol (**40**) (200 μ L of a 1 M solution in THF; 0.0750 g, 0.2 mmol), bromobenzene (25 μ L, 0.0377 g, 0.24 mmol), and aq. KF solution (200 μ L, 0.6 mmol) and 1 drop of TBAF (1 M solution in THF).

Additive = Water:

The representative kinetics procedure with additives was applied to (*E*)-2-methyl-4-(tributylstannyl)but-3-en-2-ol (**40**) (200 μ L of a 1 M solution in THF; 0.0750 g, 0.2 mmol), bromobenzene (25 μ L, 0.0337 g, 0.24 mmol), 202 μ L of additional THF, and water (200 μ L, 11.1 mmol).

9.7.2.6. Effect of Water on an Unsubstituted Vinyl Stannane Coupled with Iodobenzene (Section 6.7).

The representative kinetics procedure with additives was applied to tributylvinylstannane (30 μ L, 0.0326 g, 0.1026 mmol), iodobenzene (27 μ L, 0.0490 g, 0.12 mmol), 170 μ L of additional THF, and water (100 μ L, 5.5508 mmol, 54.1 equiv).

9.7.3. Purification of CuI by the Method of Kauffman.⁵⁹

KI (65.00 g, 391.6 mmol) was added to 50 mL of H₂O in a 250 mL Erlenmeyer flask. The solution was swirled and water was added until all of the KI was dissolved. CuI (6.55 g, 34.39 mmol) was added to the solution and allowed to magnetically stir until all the CuI was dissolved, ~20 min. The brownish solution was decolorized with 1 g of decolorizing charcoal and shaken vigorously for 1 min then filtered to afford a clear solution. The solution was diluted with water to precipitate out the CuI. The muddy precipitate was filtered in a Büchner funnel, then covered with a kimwipe and stored in a vacuum dessicator overnight. The crispy wafer of CuI was transferred to an amber bottle and ground to a fine powder. The CuI was dried again under vacuum with light heating (30 °C) for 3 h. Light gray CuI (4.6032, 24.1701) in 70.3% yield was recovered.

9.7.4. Representative Procedure for Kinetic Studies with CuI. Coupling of 39 with iodobenzene in the presence of CuI under Pd/PPh₃ in THF (Table 6.4, entry 2).

Pd₂dba₃ (0.0305 g, 0.0333 mmol) and PPh₃ (0.0350 g, 0.1333 mmol) were weighed into a 20 mL vial. The mixture was then transferred to a 5 mL volumetric flask with the assistance of THF. The solution was then diluted to

volume with THF. A stir bar was carefully added and the solution was tightly capped and stirred to homogeneity for 10 min. As the solution was stirring, (*E*)-2-methyl-4-(trimethylstannyl)but-3-en-2-ol (**39**) (0.2489 g, 1.0 mmol) was weighed directly into a 1 mL volumetric flask and diluted to volume with THF. Again, a stir bar was carefully added, the flask was capped, and the 1 M solution was stirred for 10 min. An NMR tube was charged with C₆D₆ (50 μ L), the Pd/PPh₃ solution (600 μ L, containing 0.0037 g, 0.004 mmol Pd₂dba₃ and 0.0245g, 0.016 mmol PPh₃), (*E*)-2-methyl-4-(trimethylstannyl)but-3-en-2-ol (**39**) (200 μ L of a 1 M solution in THF; 0.0498g, 0.2 mmol), and 200 μ L of THF to achieve a final reaction concentration of 0.1857 M in stannane. The additive, CuI (0.0031 g, 0.0163 mmol, Cu:L 1:1), was then weighed into weigh paper and carefully transferred to the NMR tube. The NMR tube was then capped and inserted into a 500 MHz NMR spectrometer. The NMR probe was set to 50 °C and once equilibrated, tuned to the ¹¹⁹Sn nucleus (186 MHz). The sample was then locked and shimmed. The sample was ejected and iodobenzene (27 μ L, 0.0490 g, 0.24 mmol) was added to the sample. Immediately thereafter the sample was injected, reshimmed, and an arrayed kinetics experiment was initiated to monitor the consumption of stannane.

9.7.4.1. Coupling of 40 with iodobenzene in the presence of CuI under Pd/PPh₃ in THF (Table 6.4, entry 4).

The representative kinetics procedure in the presence of CuI was applied to (*E*)-2-methyl-4-(tributylstannyl)but-3-en-2-ol (**40**) (200 μ L of a 1 M solution in THF; 0.0750g, 0.2 mmol), iodobenzene (27 μ L, 0.0490 g, 0.12 mmol), Pd/PPh₃ solution (600 μ L, containing 0.0037 g, 0.004 mmol Pd₂dba₃ and 0.0245g, 0.016 mmol PPh₃), C₆D₆ (50 μ L), 200 μ L of additional THF, and CuI (0.0031 g, 0.0163 mmol, Cu:L 1:1).

9.7.4.2. Coupling of 39 with iodobenzene in the presence of CuI under Pd/AsPh₃ in NMP (Table 6.4, entry 6).

The representative kinetics procedure in the presence of CuI was applied to (*E*)-2-methyl-4-(trimethylstannyl)but-3-en-2-ol (**39**) (200 μ L of a 1 M solution in NMP; 0.0498 g, 0.2 mmol), iodobenzene (27 μ L, 0.0490 g, 0.12 mmol), Pd/AsPh₃ solution (600 μ L, containing 0.0037 g, 0.004 mmol Pd₂dba₃ and 0.0245g, 0.016 mmol AsPh₃), C₆D₆ (50 μ L), 200 μ L of additional NMP, and CuI (0.0031 g, 0.0163 mmol, Cu:L 1:1).

9.7.4.3. Coupling of 40 with iodobenzene in the presence of CuI under Pd/AsPh₃ in NMP (Table 6.4, entry 8).

The representative kinetics procedure in the presence of CuI was applied to (*E*)-2-methyl-4-(tributylstannyl)but-3-en-2-ol (**40**) (200 μ L of a 1 M solution in NMP; 0.0750 g, 0.2 mmol), iodobenzene (27 μ L, 0.0490 g, 0.12 mmol), Pd/AsPh₃ solution (600 μ L, containing 0.0037 g, 0.004 mmol Pd₂dba₃ and 0.0245g, 0.016 mmol AsPh₃), C₆D₆ (50 μ L), 200 μ L of additional NMP, and CuI (0.0031 g, 0.0163 mmol, Cu:L 1:1).

9.7.4.4. Coupling of tributylvinylstannane and iodobenzene in the presence and absence of CuI under Pd/AsPh₃ in NMP on the bench-top (Table 6.5).

Pd₂dba₃ (0.0018 g, 0.002 mmol), AsPh₃ (0.0025 g, 0.008 mmol), and NMP (470 μ L) were added to a 3.7 mL vial with Teflon lined cap and stirred for 1 h 15 min at rt. CuI (0.0015 g, 0.008 mmol) and tributylvinylstannane (30 μ L, 0.0326 g, 0.1026 mmol) were then added and 4 min later, iodobenzene (13.5 μ L, 0.1211 mmol) was added. The reaction was allowed to stir for exactly 5 min at rt and immediately cold quenched in an ice bath. A control reaction under the same conditions except without CuI was run in parallel. A ¹H

NMR of the crude CuI reaction showed more starting material than product, while the control reaction showed ~equal amounts. This indicates that the reaction without CuI was faster, as it had higher conversion, thus CuI slows down the reaction.

9.7.5. Overcoming the Inhibitory Effects of CuI with Water (Figure 6.8)

9.7.5.1. Determining the Amount of Water Necessary to Effect the Same Acceleration as Farina Observed with CuI (Figure 6.8, 2.8 equiv H₂O).

The representative procedure for kinetic studies with additives was applied to tributylvinylstannane (30 μ L, 0.0326 g, 0.1026 mmol), iodobenzene (13.5 μ L, 0.1211 mmol), Pd₂dba₃/AsPh₃ solution in NMP (300 μ L containing 0.002 mmol Pd₂dba₃ and 0.008 mmol AsPh₃), 25 μ L of C₆D₆, 170 μ L of additional NMP, and H₂O (5 μ L, 0.2775 mmol, 2.7754 equiv).

9.7.5.2. Determining the Amount of Water Necessary to Compensate for the Inhibitory Effect of CuI (Figure 6.8, 0.08 equiv CuI + 2.8 equiv H₂O).

The representative procedure for kinetic studies with additives was applied to tributylvinylstannane (30 μ L, 0.0326 g, 0.1026 mmol), iodobenzene (13.5 μ L, 0.1211 mmol), Pd₂dba₃/AsPh₃ solution in NMP (300 μ L containing

0.002 mmol Pd₂dba₃ and 0.008 mmol AsPh₃), 25 μL of C₆D₆, 170 μL of additional NMP, CuI (0.0015 g, 0.008 mmol), and H₂O (5 μL, 0.2775 mmol, 2.7754 equiv).

9.7.5.3. Determining the Amount of Water Necessary to Compensate for the Inhibitory Effect of CuI (Figure 6.8, 0.08 equiv CuI + 8.3 equiv H₂O).

The representative procedure for kinetic studies with additives was applied to tributylvinylstannane (30 μL, 0.0326 g, 0.1026 mmol), iodobenzene (13.5 μL, 0.1211 mmol), Pd₂dba₃/AsPh₃ solution in NMP (300 μL containing 0.002 mmol Pd₂dba₃ and 0.008 mmol AsPh₃), 25 μL of C₆D₆, 170 μL of additional NMP, CuI (0.0015 g, 0.008 mmol), and H₂O (15 μL, 0.2775 mmol, 8.3262 equiv).

9.7.6. Aryl Bromide Couplings In the Presence of CuI.

9.7.6.1. Coupling of 39 with Bromobenzene in a Pd/PPh₃ Catalyst System in THF (Section 6.8.2).

The representative procedure for kinetic studies with CuI was applied to (*E*)-2-methyl-4-(trimethylstannyl)but-3-en-2-ol (**39**) (200 μL of a 1 M solution in THF; 0.0750 g, 0.2 mmol), 4-bromobenzotrifluoride (34 μL, 0.0540 g,

0.24 mmol), Pd/PPh₃ solution (600 μL, containing 0.004 mmol Pd₂dba₃ and 0.016 mmol PPh₃), 50 μL of C₆D₆, 193 μL of additional THF, and CuI (0.0031 g, 0.0163 mmol, Cu:L 1:1).

9.7.6.2. Coupling of 40 with Bromobenzene in a Pd/AsPh₃ Catalyst System in NMP (Section 6.8.2).

The representative procedure for kinetic studies with CuI was applied to (*E*)-2-methyl-4-(tributylstannyl)but-3-en-2-ol (**40**) (100 μL of a 1 M solution in NMP; 0.0375 g, 0.1 mmol), 4-bromobenzotrifluoride (17 μL, 0.0270 g, 0.12 mmol), Pd/AsPh₃ solution (300 μL, containing 0.002 mmol Pd₂dba₃ and 0.008 mmol AsPh₃), 25 μL of C₆D₆, 96.5 μL of additional NMP, and CuI (0.0016 g, 0.0084 mmol, Cu:L 1.05:1).

9.7.6.3. Effect of CuI on an Aryl Bromide Coupling that is Already Proceeding (Table 6.6).

Set A:

Pd₂dba₃ (0.0305 g, 0.0333 mmol) and PPh₃ (0.0350 g, 0.1333 mmol) were weighed into a 20 mL vial. The mixture was then transferred to a 5 mL volumetric flask with the assistance of THF. The solution was then diluted to volume with THF. A stir bar was carefully added and the solution was

tightly capped and stirred to homogeneity for 10 min. THF (380 μ L), Pd/AsPh₃ solution (600 μ L, containing 0.004 mmol Pd₂dba₃ and 0.016 mmol AsPh₃), and tributylvinylstannane (60 μ L, 0.0651 g, 0.2053 mmol) were added to a 3.7 mL vial with septa lined cap. 4-bromotrifluorobenzene (34 μ L, 0.0540 g, 0.24 mmol) was then added and stirred at 50 °C for 10 min exactly. CuI (0.0031 g, 0.0163 mmol, Cu:L 1:1) was then added and stirred at 50 °C for another 50 min (1 h total). The reaction was then removed from the oil bath and concentrated. A control reaction under the same conditions except without CuI was run in parallel. A ¹H NMR of the crude CuI reaction showed a starting material to product ratio of 100:15 while the reaction without CuI showed a starting material to product ratio of 100:23. This indicates that adding CuI to the reaction after it begins shuts down and/or slows down the reaction to some extent.

Set B:

The reactions above were repeated except the CuI was added after 25 min and stirred for an additional 30 min (55 min total). A ¹H NMR of the crude CuI reaction showed a starting material to product ratio of 100:26 while the reaction without CuI showed a starting material to product ratio of 100:25. This indicates that when CuI is added after the reaction has proceeded for a

longer time, there is little impact on the reaction. Comparing the results from Set A and Set B indicate that the order of addition may be important.

9.7.7. Determining the Effect of the Order of Addition with CuI (Table 6.7).

Conditions A:

See the coupling of tributylvinylstannane and iodobenzene in the presence and absence of CuI under Pd/AsPh₃ in NMP on the Bench-top (Section 9.7.4.4).

Conditions B:

The following reagents were added to a 3.7 mL vial in the following order: iodobenzene (13.5 μ L, 0.1211 mmol), CuI (0.0016 g, 0.0084 mmol, Cu:L 1.05:1), and 170 μ L of additional NMP, Pd/AsPh₃ solution (300 μ L, containing 0.002 mmol Pd₂dba₃ and 0.008 mmol AsPh₃), and tributylvinylstannane (30 μ L, 0.0326 g, 0.1026 mmol). The reaction was stirred under N₂ at rt for exactly 5 min and immediately cold quenched in an ice bath. A control reaction under the same conditions except in air as well as one without CuI under N₂ were run in parallel. A ¹H NMR of the crude CuI reaction in both N₂ and air showed more product than starting material,

while the control reaction without CuI in N₂ showed more starting material than product. This indicates that the the order of addition is important but N₂ is not.

Conditions C:

The following reagents were added to a 3.7 mL vial in the following order: CuI (0.0016 g, 0.0084 mmol, Cu:L 1.05:1), and 170 μ L of additional NMP, tributylvinylstannane (30 μ L, 0.0326 g, 0.1026 mmol), Pd/AsPh₃ solution (300 μ L, containing 0.002 mmol Pd₂dba₃ and 0.008 mmol AsPh₃), and iodobenzene (13.5 μ L, 0.1211 mmol). The reaction was stirred in air at rt for exactly 5 min and immediately cold quenched in an ice bath. A control reaction under Conditions **B** was run in parallel. A ¹H NMR of the crude CuI reaction under Conditions **C** showed there was more starting material than product while for Conditions **B** there was more product than starting material.

9.7.7.1. CuI Effect on Me/Bu Ratio Under Conditions B (Table 6.9).

Coupling of 39 with iodobenzene (Entry 3).

The representative procedure for kinetic studies with CuI following the order in Conditions **B** was applied to the following reagents. iodobenzene (13.5

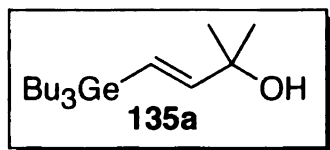
μL , 0.1211 mmol), CuI (0.0016 g, 0.0084 mmol, Cu:L 1.05:1), and 100 μL of additional NMP, Pd/AsPh₃ solution (300 μL , containing 0.002 mmol Pd₂dba₃ and 0.008 mmol AsPh₃), and (*E*)-2-methyl-4-(trimethylstannyl)but-3-en-2-ol (**39**) (100 μL of a 1 M solution in THF; 0.0375 g, 0.1 mmol).

Coupling of 40 with iodobenzene (Entry 4).

The representative procedure for kinetic studies with CuI following the order in Conditions B was applied to the following reagents. iodobenzene (13.5 μL , 0.1211 mmol), CuI (0.0016 g, 0.0084 mmol, Cu:L 1.05:1), and 100 μL of additional NMP, Pd/AsPh₃ solution (300 μL , containing 0.002 mmol Pd₂dba₃ and 0.008 mmol AsPh₃), and (*E*)-2-methyl-4-(tributylstannyl)but-3-en-2-ol (**40**) (100 μL of a 1 M solution in THF; 0.0248 g, 0.1 mmol).

9.8. Experimentals for Tributylgermane Couplings From Chapter 7

9.8.1. Preparation of Vinyl Germanes

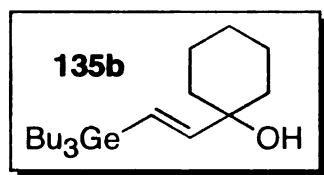


Representative Procedure for the Hydrogermylation of Alkynes. Preparation of (*E*)-

2-methyl-4-(tributylgermyl)but-3-en-2-ol (135a) (Table 7.1, entry 1).

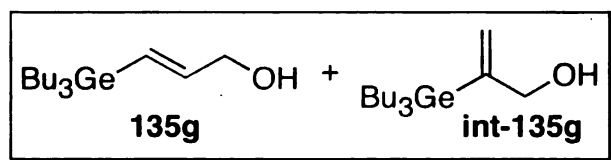
To a flame dried 25 mL round bottom flask fitted with a stir bar was flushed with nitrogen, fitted with a septa, and placed in a nitrogen glove-bag. Inside

the glove bag, $\text{Pd}(\text{PPh}_3)_4$ (0.0725 g, 0.0627 mmol) was added. Outside of the glovebag the reaction was fitted with a N_2 balloon, then THF (10 mL), 2-methyl-3-butyn-2-ol (0.19 mL, 1.9447 mmol), and Bu_3GeH (0.6 mL, 2.3242 mmol) were added via syringe. The yellow reaction mixture was allowed to stir at room temperature for 20.5 hrs. The reaction can be stopped once the solution turns from yellow to dark brown or orange. The dark brown reaction was then quenched with 4 mL of 1 M NaOH and stirred in open air for 30 min. The organics were then separated and the aqueous layer was extracted with Et_2O (5 mL x 2). The combined organics were washed with water then brine, dried with MgSO_4 , filtered, and concentrated. The crude mixture was purified by column chromatography [silica; 90:10 hexanes/ EtOAc] to afford the title compound in 96% yield. ^1H NMR (500 MHz, CDCl_3) δ 0.67-0.82 (m, 6 H), 0.82-0.96 (m, 9 H), 1.20-1.40 (m, 18 H), 1.28 (s, 6 H), 1.44 (s, 1 H), 5.73-6.17 (AB, $J_{\text{AB}} = 18.8$ Hz, 2 H); ^{13}C NMR (125 MHz, CDCl_3) δ 12.8, 13.8, 26.4, 27.3, 29.5, 72.1, 122.9, 152.4; HRMS (ESI) m/z 313.1954 [($\text{M}^+ - \text{OH}$) calcd. for $\text{C}_{17}\text{H}_{35}\text{Ge}$ 313.1951]. Spectroscopic data (^1H and ^{13}C NMR) were consistent with prior reports.³¹ For IR data, see Jérôme Lavis' dissertation.³¹



Preparation of (E)-1-(2-(tributylgermyl)vinyl)cyclohexanol (135b) (Table 7.1, entry 2).

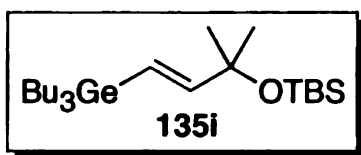
Applying the representative hydrogermylation conditions with 1-ethynyl-1-cyclohexanol (0.1242 g, 1.0 mmol) after 8 h and column chromatography [silica; 90:10 hexanes/EtOAc] afforded the title compound in 89% yield. ^1H NMR (500 MHz, CDCl_3) δ 0.75 (t, $J = 8.4$, 6 H), 0.86 (t, $J = 7.08$, 9 H), 1.22-1.38 (m, 12 H), 1.43-1.56 (m, 6 H), 1.58-1.68 (m, 2 H), 5.8-6.1 (AB, $J_{\text{AB}} = 18.8$ Hz, 2 H); ^{13}C NMR (125 MHz, CDCl_3) δ 12.8, 13.8, 22.2, 25.6, 26.4, 27.4, 37.7, 72.6, 123.7, 152.4. Spectroscopic data (^1H and ^{13}C NMR) were consistent with prior reports,³¹ and rectify the incorrect coupling constant and proton count. For IR and HRMS data, see Jérôme Lavis' dissertation.³¹



Preparation of (E)-3-(tributylgermyl)prop-2-en-1-ol (135g) (Table 7.1, entry 7).

Applying the representative hydrogermylation conditions with propargyl alcohol (0.12 mL, 2.0614 mmol) after 21.5 h afforded an mixture of isomers

(crude *E*:int = 1.7:1 determined by ^1H NMR). After column chromatography [silica; 95:5 hexanes/EtOAc] several fractions of various isomeric ratios were obtained as well as fractions with 100% pure *E* and up to 98% pure internal (64:1 int:*E*) for a total combined yield of 91%. *E* isomer: ^1H NMR (500 MHz, CDCl_3) δ 0.72-0.81 (m, 6 H), 0.82-0.93 (m, 9 H), 1.24-1.36 (m, 12 H), 4.16 (s, 2 H), 5.95-6.13 (AB, $J_{\text{AB}} = 18.6$ Hz, 2 H); ^{13}C NMR (125 MHz, CDCl_3) δ 12.8, 13.8, 26.5, 27.3, 65.8, 128.5, 143.8. internal isomer: ^1H NMR (500 MHz, CDCl_3) δ 0.81 (t with 2nd order effects, $J = 8.3$ Hz, 6 H), 0.87 (t with 2nd order effects, $J = 7.08$ Hz, 9 H), 1.25-1.37 (m, 12 H), 4.22 (s, 2 H), 5.21-5.26 (m, 1 H), 5.76-5.81 (m, 1 H); Spectroscopic data (^1H and ^{13}C NMR) were consistent with prior reports,³¹ and rectify the incorrect coupling constant and proton count. For ^{13}C data of the internal isomer, and IR and HRMS data of both *E* and internal isomer, see Jérôme Lavis' dissertation.³¹

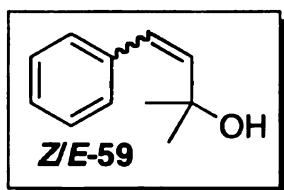


Preparation of (*E*)-*tert*-butyldimethyl(2-methyl-4-(tributylgermyl)but-3-en-2-yloxy)silane (135i)

(Table 7.1, entry 9).

Applying the representative hydrogermylation conditions with *tert*-butyldimethyl(2-methylbut-3-yn-2-yloxy)silane (0.3962 g, 1.9972 mmol) overnight and column chromatography [silica; 90:10 hexanes/EtOAc] afforded the title compound in 91% yield.

9.8.2. Screening Heck Conditions (Table 7.2)



Preparation of an *E/Z* Int Mixture of 59.

All reactions were run in a 3.7 mL vial with a Teflon lined cap to avoid solvent evaporation. Small-scale reactions run in a round bottom flask with a condenser proved problematic.

9.8.2.1. Representative Procedure for Catalyst Loading Screen: 10 mol% (Entry 1).

A TBABr/ K₂CO₃/germane/PhI solution was prepared as follows: To a 2 mL volumetric flask was added Bu₄NBr (0.1291 g, 0.4005 mmol), K₂CO₃ (0.1387, 1.0035 mmol), and 1.5 mL of MeCN/H₂O (9:1). A magnet was carefully added to the flask then capped and stirred for 30 min. (*E*)-2-Methyl-4-(tributylgermyl)but-3-en-2-ol (**135a**) (0.1314 g, 0.3993) was then

weighed into a pipette and transferred to the volumetric flask with a small amount of solvent. The magnet was removed and rinsed into the flask with a small amount of solvent up to the 2 mL mark. The magnet was then replaced and the solution was stirred to homogeneity. The reaction was set up as follows: The solution (500 μ L; containing 0.1 mmol Bu_4NBr , 0.25 mmol K_2CO_3 , 0.1 mmol germane, and 0.2 mmol PhI), and PPh_3 (0.0053 g, 0.0202 mmol) were added to a 3.7 mL vial then capped and stirred at rt for 15 min. $\text{Pd}(\text{OAc})_2$ (0.0023 g, 0.0103 mmol) was then the reaction was stirred at 70 $^\circ\text{C}$ for 16 h. The reaction was cooled to rt then quenched with sat. aq. NH_4Cl (1 mL). The layers were separated and the aqueous layer was extracted with Et_2O (x2). The combined organics were washed with brine, dried with MgSO_4 , filtered, and concentrated. Yield as determined by ^1H NMR with mesitylene as an internal standard: unreacted starting germane (53%) and a mixture of cross-coupled isomers ($Z/E/\text{int} = 17/4/1$) were formed in 47% yield.

Pd loading of 5 mol% (Entry 7).

The representative conditions were applied to a 5 mol% catalyst system of PPh_3 (0.0025 g, 0.0095 mmol) and $\text{Pd}(\text{OAc})_2$ (0.0012 g, 0.0053 mmol).

Yield as determined by ^1H NMR with mesitylene as an internal standard: unreacted starting germane (54%) and a mixture of cross-coupled isomers ($Z/E/\text{int} = 17/5/1$) were formed in 46% yield.

Pd loading of 20 mol% (Entry 8).

The representative conditions were applied to a 20 mol% catalyst system of PPh_3 (0.0105 g, 0.0400 mmol) and $\text{Pd}(\text{OAc})_2$ (0.0046 g, 0.0205 mmol).

Yield as determined by ^1H NMR with mesitylene as an internal standard: unreacted starting germane (45%) and a mixture of cross-coupled isomers ($Z/E/\text{int} = 10/3/1$) were formed in 55% yield.

9.8.2.2. Reaction with No Bu_4NBr (Entry 3).

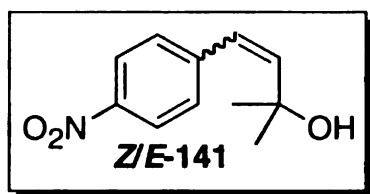
K_2CO_3 (0.0346 g, 0.2503 mmol) and 0.5 mL of $\text{MeCN}/\text{H}_2\text{O}$ (9:1) were added to a 3.7 mL vial and stirred for 15 min at rt. (*E*)-2-Methyl-4-(tributylgermyl)but-3-en-2-ol (**135a**) (0.0330 g, 0.1003 mmol) was weighed into a pipette and transferred to the reaction vial with the assistance of 1.5 mL of solvent. PPh_3 (0.0053 g, 0.0202 mmol) and PhI (22.5 μL , 0.2011 mmol) were then added and stirred for 15 min at rt. $\text{Pd}(\text{OAc})_2$ (0.0023 g, 0.0103 mmol) was then added and the reaction was capped and stirred at 60-65 $^\circ\text{C}$ for 16 h. The reaction was quenched as described above. Yield as

determined by ^1H NMR with hexamethyldisiloxane as an internal standard: unreacted starting germane (66%) and a mixture of cross-coupled isomers ($Z/E/\text{int} = 21/1/5$) were formed in 34% yield.

9.8.2.3. Reaction with NaHCO_3 Instead of K_2CO_3 (Entry 4).

Bu_4NBr (0.0321 g, 0.0996 mmol) was added to a reaction vial. The remainder of the procedure follows the above conditions substituting NaHCO_3 (0.0212 g, 0.2524 mmol) for K_2CO_3 . Yield as determined by ^1H NMR with hexamethyldisiloxane as an internal standard: unreacted starting germane (57%) and a mixture of cross-coupled isomers ($Z/E/\text{int} = 17/1/2$) were formed in 43% yield.

9.8.3. Comparison of Stille vs. Heck Conditions (Table 7.3)



Representative Stille A conditions for coupling with 4-bromonitrobenzene (Table 7.3, entry 4):

Pd_2dba_3 (0.0183 g, 0.0200 mmol), AsPh_3 (0.0245 g, 0.0800 mmol), and NMP (2 mL) were added to a vial with a Teflon lined cap. The reaction was stirred at rt for 15 min then (*E*)-2-methyl-4-(tributylgermyl)but-3-en-2-ol (**135a**) (0.0320 g, 0.0972 mmol) (weighed into a pipette and transferred with 3 mL NMP) and 4-bromonitrobenzene (0.0405 g, 0.2005 mmol) were added.

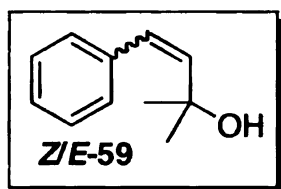
The reaction was capped and stirred at 70 °C for 24 h. Reaction concentration is ~0.02 M, e.g. 0.1 mmol Ge in 5 mL NMP. The reaction was then cooled to rt and quenched with sat. aq. NH₄Cl (10 mL). The layers were separated and the aqueous layer was extracted with Et₂O (5 mL x2). The combined organics were then washed with H₂O then brine, dried with MgSO₄, filtered, and concentrated. Yield as determined by ¹H NMR with hexamethyldisiloxane as an internal standard: unreacted starting germane (51%) and a mixture of cross-coupled isomers (*Z/E* = 10/1) were formed in 10% yield.

Representative Stille B conditions for coupling with 4-bromonitrobenzene (Table 7.3, entry 4).

Stille A conditions except Pd(OAc)₂ used instead of Pd₂dba₃ were applied to Pd(OAc)₂ (0.0045 g, 0.0199 mmol), AsPh₃ (0.0245 g, 0.0800 mmol), (*E*)-2-methyl-4-(tributylgermyl)but-3-en-2-ol (**135a**) (0.0320 g, 0.0972 mmol), and 4-bromonitrobenzene (0.0404 g, 0.2000 mmol). Reaction concentration is ~0.02 M, e.g. 0.1 mmol Ge in 5 mL NMP. GC/MS and ¹H NMR of the crude reaction indicated no reaction took place. Otherwise, reaction quenching follows the Stille A procedure.

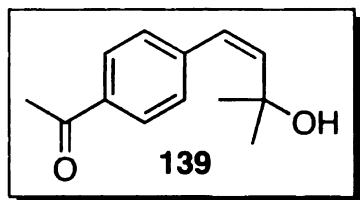
Representative Heck conditions for for coupling with 4-bromonitrobenzene (Table 7.3, entry 4).

Bu₄NBr (0.0197 g, 0.0611 mmol), K₂CO₃ (0.0207 g, 0.1497 mmol) and 0.8 mL of MeCN/H₂O (9:1) were added to a vial and stirred for 15 min at rt. (*E*)-2-Methyl-4-(tributylgermyl)but-3-en-2-ol (**135a**) (0.0187 g, 0.0568 mmol) was weighed into a pipette and transferred to the reaction vial with the assistance of 0.4 mL of solvent. PPh₃ (0.0066 g, 0.0252 mmol) and 4-bromonitrobenzene (0.0241 g, 0.1195 mmol) were then added and stirred for 15 min at rt. Pd(OAc)₂ (0.0030 g, 0.0134 mmol) was then added and the reaction was capped and stirred at 70 °C for 16 h 20 min. Reaction concentration is ~0.05 M; 0.06 mmol Ge in 1.2 mL NMP. The reaction was then cooled to rt and quenched with sat. aq. NH₄Cl (0.5 mL). The layers were separated and the aqueous layer was extracted with Et₂O (4 mL x2). The combined organics were then washed with H₂O then brine, dried with MgSO₄, filtered, and concentrated. The crude material was purified by column chromatography [silica; 90:10 hexanes/EtOAc] to afford a mixture of cross-coupled isomers (*Z/E* = 2.4/1) in 48% yield.



9.8.3.1. Coupling with bromobenzene under Heck Conditions (Table 7.3, entry 2 – Heck).

The representative Heck conditions were applied to (*E*)-2-methyl-4-(tributylgermyl)but-3-en-2-ol (**135a**) (0.0329 g, 0.1 mmol) and bromobenzene (21 μ L, 0.1944 mmol). Yield as determined by ^1H NMR with hexamethyldisiloxane as an internal standard: unreacted starting germane (48%) and a mixture of cross-coupled isomers ($Z/E = 26/1$) were formed in 30% yield.

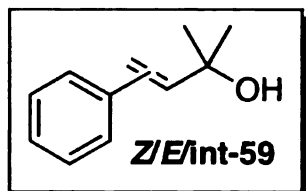


9.8.3.2. Coupling with 4-bromoacetophenone under Stille A Conditions (Table 7.3, entry 3 – Stille A).

The representative Stille A conditions were applied to (*E*)-2-methyl-4-(tributylgermyl)but-3-en-2-ol (**135a**) (0.0329 g, 0.1 mmol) and 4-bromoacetophenone (0.0399 g, 0.2005 mmol). Yield as determined by ^1H NMR with mesitylene as an internal standard: unreacted starting germane (69%) and a mixture of cross-coupled isomers ($Z/E = 1.88/1$) were formed in 24% yield. The crude material was purified by column chromatography [silica; 80:20 hexanes/EtOAc] to afford only the *Z* isomer in 15% yield and recovered starting material (**135a**) in 48% yield.

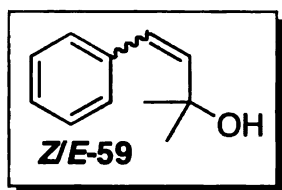
9.8.4. Aryl Halide Scope for Couplings Under Heck Conditions at 0.2

M* (Table 7.5) * unless otherwise noted



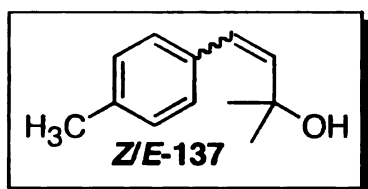
9.8.4.1. Preparation of 2-methyl-4-phenylbut-3-en-2-ol: Coupling of 135a with iodobenzene (Table 7.5, entry 1).

Experimental details described in Section 9.8.2 for Table 7.2, entry 8.



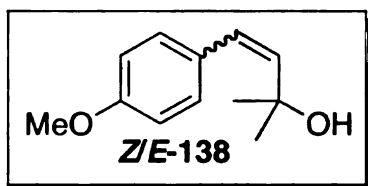
9.8.4.2. Preparation of 2-methyl-4-phenylbut-3-en-2-ol: Coupling of 135a with bromobenzene (Table 7.5, entry 2).

The representative Heck conditions were applied to (*E*)-2-methyl-4-(tributylgermyl)but-3-en-2-ol (**135a**) (0.0330 g, 0.1003 mmol) and bromobenzene (25 μ L, 0.1994 mmol) in 0.5 mL of MeCN/H₂O (9:1). Yield as determined by ¹H NMR with mesitylene as an internal standard: unreacted starting germane (41%) and a mixture of cross-coupled isomers (*Z/E* = 1.4/1) were formed in 19% yield.



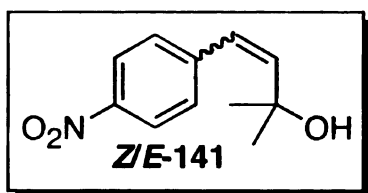
9.8.4.3. Preparation of 2-methyl-4-*p*-tolylbut-3-en-2-ol: Coupling of 135a with 4-iodotoluene (Table 7.5, entry 3).

The representative Heck conditions were applied to (*E*)-2-methyl-4-(tributylgermyl)but-3-en-2-ol (**135a**) (0.0324 g, 0.0984 mmol) and 4-iodotoluene (0.0436 g, 0.2 mmol) in 0.5 mL of MeCN/H₂O (9:1). Yield as determined by ¹H NMR with mesitylene as an internal standard: unreacted starting germane (37%) and a mixture of cross-coupled isomers (*Z/E* = 2.1/1) were formed in 63% yield.



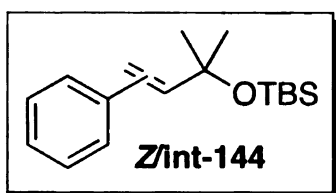
9.8.4.4. Preparation of 4-(4-methoxyphenyl)-2-methylbut-3-en-2-ol: Coupling of 135a with 4-bromoanisole (Table 7.5, entry 4).

The representative Heck conditions were applied to (*E*)-2-methyl-4-(tributylgermyl)but-3-en-2-ol (**135a**) (0.0332 g, 0.1009 mmol) and 4-bromoanisole (25 μL, 0.1997 mmol) in 0.5 mL of MeCN/H₂O (9:1). Yield as determined by ¹H NMR with mesitylene as an internal standard: unreacted starting germane (54%) and a mixture of cross-coupled isomers (*Z/E* = 2.95/1) were formed in 19% yield.



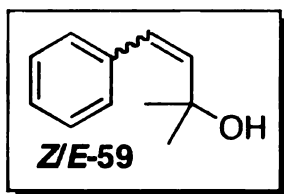
9.8.4.5. Preparation of (*E*)-2-methyl-4-(4-nitrophenyl)but-3-en-2-ol: Coupling of 135a with 4-bromonitrobenzene (Table 7.5, entry 5).

Experimental details described in Section 9.8.2 for Table 7.2, entry 8. The reaction was run at 0.05 M.



9.8.4.6. Preparation of *tert*-butyldimethyl(2-methyl-4-phenylbut-3-en-2-yloxy)silane: Coupling of 135i with iodobenzene (Table 7.5, entry 6).

The representative Heck conditions were applied to (*E*)-*tert*-butyldimethyl(2-methyl-4-(tributylgermyl)but-3-en-2-yloxy)silane (0.0316 g, 0.0712 mmol) and iodobenzene (17 μ L, 0.1519 mmol) in 1.3 mL of MeCN/H₂O (9:1). The reaction was run at 0.05 M. Yield as determined by ¹H NMR with 1,3,5-trimethoxybenzene as an internal standard: unreacted starting germane and a mixture of cross-coupled isomers (*Z*/int = 1/1.1) were formed in 10% yield.



9.8.4.7. Impact of Concentration on the *Z/E* Ratios (Table 7.6).

Preparation of *Z/E*-59 at 0.1 M (Entry 2).

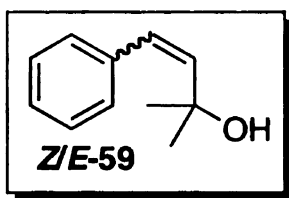
The representative Heck conditions were applied to (*E*)-2-methyl-4-(tributylgermyl)but-3-en-2-ol (**135a**) (0.0330 g, 0.1003 mmol) and bromobenzene (21 μ L, 0.1994 mmol) in 1.0 mL of MeCN/H₂O (9:1). Yield as determined by ¹H NMR with mesitylene as an internal standard: unreacted starting germane (66%) and a mixture of cross-coupled isomers (*Z/E* = 11.6/1) were formed in 29% yield.

Preparation of *Z/E*-59 at 0.168 M (Entry 3).

The representative Heck conditions were applied to (*E*)-2-methyl-4-(tributylgermyl)but-3-en-2-ol (**135a**) (0.0331 g, 0.1006 mmol) and bromobenzene (21 μ L, 0.1994 mmol) in 0.6 mL of MeCN/H₂O (9:1). Yield as determined by ¹H NMR with mesitylene as an internal standard: unreacted starting germane (62%) and a mixture of cross-coupled isomers (*Z/E* = 4.2/1) were formed in 26% yield.

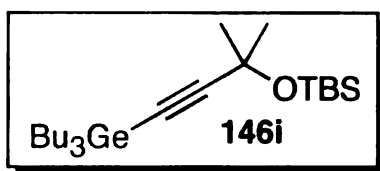
Preparation of *Z/E*-59 at 0.2 M (Entry 4).

The representative Heck conditions were applied to (*E*)-2-methyl-4-(tributylgermyl)but-3-en-2-ol (**135a**) (0.0327 g, 0.09936 mmol) and bromobenzene (21 μ L, 0.1994 mmol) in 0.5 mL of MeCN/H₂O (9:1). Yield as determined by ¹H NMR with mesitylene as an internal standard: unreacted starting germane (61%) and a mixture of cross-coupled isomers (*Z/E* = 2.8/1) were formed in 23% yield.



9.8.4.8. Preparation of *Z/E*-59: Coupling of **135a** with iodobenzene under anhydrous conditions (Section 7.5).

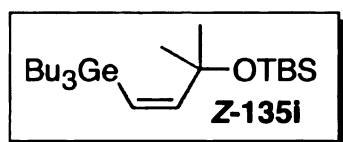
The representative Heck conditions were applied to (*E*)-2-methyl-4-(tributylgermyl)but-3-en-2-ol (**135a**) (0.0168 g, 0.0511 mmol) and iodobenzene (12 μ L, 0.1072 mmol) in 270 μ L of anhydrous MeCN instead of a MeCN/H₂O mixture. Yield as determined by ¹H NMR with mesitylene as an internal standard: unreacted starting germane (49%) and a mixture of cross-coupled isomers (*Z/E* = 3.9/1) were formed in 28% yield.



9.8.4.9. Preparation of *tert*-butyldimethyl(2-methyl-4-(tributylgermyl)but-3-yn-2-yloxy)silane (146i) (Scheme 7.7).

To a flame dried 100 mL 3-neck round bottom flask fitted with a 10 mL addition funnel, stir bar, rubber septa, and nitrogen balloon was added 10 mL of THF, and *tert*-butyldimethyl(2-methylbut-3-yn-2-yloxy)silane (0.9934 g, 5.0076 mmol). The reaction was cooled to 0 °C and a solution *n*-butyllithium (1.6 M in hexanes, 6.5 mL, 10.4 mmol) was added dropwise over 10 min via the addition funnel and allowed to stir for an additional 10 min at 0 °C. Bu₃GeCl (1.3982 g, 5.0047 mmol) was then added and the solution was allowed to warm to room temperature and stirred for 31 hrs. The reaction was quenched with saturated NH₄Cl (5 mL) and stirred for 30 min. The organics were separated; the aqueous layer was extracted with Et₂O (x2). The combined organics were washed with water (30 mL), and then brine (30 mL), dried with MgSO₄, filtered, and concentrated. The crude reaction mixture was purified by column chromatography [silica; hexanes] to afford the title compound as a clear oil in 40% yield. ¹H NMR (500 MHz, CDCl₃) δ 0.16 (s, 6 H), 0.78 (m, 24 H), 1.28-1.46 (m, 18 H); ¹³C NMR (125

MHz, CDCl₃) δ -3.0, 13.8, 14.0, 25.8, 26.1, 27.4, 33.3, 66.6, 70.6, 84.5, 111.8.



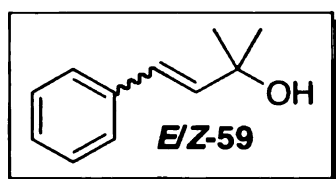
9.8.4.10. Preparation of (*Z*)-*tert*-butyldimethyl(2-methyl-4-(tributylgermyl)but-3-en-2-yloxy)silane

(*Z*-135i) (Scheme 7.7)

To a flame dried 25 mL round bottom flask fitted with a stir bar, rubber septa, and a nitrogen inlet/outlet was added THF (3 mL) and a solution of BH₃•DMS (2 M solution in THF, 2 mL, 4 mmol). The solution was cooled to 0 °C and cyclohexene was added (0.61 mL, 6.0 mmol). The solution was stirred for 1 hr maintaining the temperature between 0-5 °C, during which a white precipitate forms. The solution was then cooled to -8 °C using a saturated NH₄Cl ice bath and *tert*-butyldimethyl(2-methyl-4-(tributylgermyl)but-3-en-2-yloxy)silane (0.8702 g, 1.9717 mmol) was added dropwise. After the addition, the reaction was warmed to 10 °C and stirred for 1.25 hrs maintaining a temperature between 8-12 °C. The solution was then allowed to warm to room temperature after which acetic acid (3 mL) was added very slowly and allowed to stir for 21 hrs. Et₂O (3 mL) and H₂O (2 mL) were added to the reaction as the solvent evaporated overnight. The organics were then separated, the aqueous layer extracted with Et₂O (20 mL

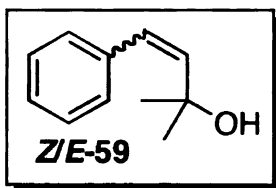
x2), the combined organics washed with water (20 mL) and then brine (20 mL), dried with MgSO₄, filtered, and concentrated. The crude mixture was purified by column chromatography [silica; 2 cm diameter, 13 cm height; hexanes] to afford the title compound as a clear oil in 52% yield. ¹H NMR (500 MHz, CDCl₃) δ 0.05 (s, 6 H), 0.74-0.98 (m, 24 H), 1.18-1.44 (m, 18 H), 5.26-6.70 (AB, *J*_{AB} = 14.9 Hz, 15.0 Hz, 2 H); ¹³C NMR (125 MHz, CDCl₃) δ -2.1, 13.7, 15.1, 18.0, 25.8, 26.5, 27.5, 30.4, 75.0, 123.6, 156.7.

9.8.5. Impact of Germane Geometry on Product Geometry (Table 7.8).



9.8.5.1. Preparation of *E/Z*-59 (Entry 1) from *Z*-135a.

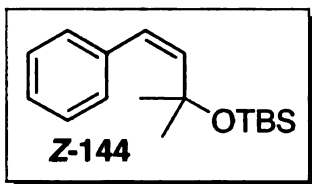
The representative Heck conditions were applied to (*Z*)-2-methyl-4-(tributylgermyl)but-3-en-2-ol (**135a**) (0.0193 g, 0.0586 mmol) and iodobenzene (13 μL, 0.1162 mmol) at ~0.6 M in Ge for 6 h. Yield as determined by ¹H NMR with mseitylene as an internal standard: unreacted starting germane (8%) and a mixture of cross-coupled isomers (*E/Z* = 1.4/1) were formed in 45% yield.



9.8.5.2. Preparation of *E/Z*-59 (Entry 2) from *E*-135a.

The representative Heck conditions were applied to (*E*)-2-methyl-4-(tributylgermyl)but-3-en-2-ol (135a)

(0.0326 g, 0.0991 mmol) and iodobenzene (22.5 μ L, 0.2011 mmol) at ~0.6 M in Ge for 6 h. Yield as determined by ^1H NMR with mseitylene as an internal standard: unreacted starting germane (52%) and a mixture of cross-coupled isomers ($Z/E = 8.8/1$) were formed in 35% yield.



9.8.5.3. Preparation of *E/Z*-144 (Entry 3) from *Z*-135i.

The representative Heck conditions were applied to (*Z*)-*tert* butyldimethyl(2-methyl-4-(tributylgermyl)but-3-en-2-yloxy)-silane (0.0334 g, 0.0753 mmol) and iodobenzene (17 μ L, 0.1519 mmol) for 6 h. Only trace amounts of *Z*-product were observed by ^1H NMR of the crude material. A parallel reaction was also run for 24 h providing only trace amounts of product as indicated by ^1H NMR of the crude material.

REFERENCES

- (1) Stille, J. K. *Angew. Chem. Int. Ed. Engl.* **1986**, 25, 508–524.
- (2) Espinet, P.; Echavarren, A. M. *Angew. Chem. Int. Ed.* **2004**, 43, 4704–4734.
- (3) Miyaura, N.; Suzuki, A. *Chem. Rev.* **1995**, 95, 2457–2483.
- (4) Negishi, E. I. *Acc. Chem. Res.* **1982**, 15, 340–348.
- (5) Trost, B. M.; Ball, Z. T. *Synthesis* **2005**, 853–887.
- (6) Crabtree, R. H. *The Organometallic Chemistry of the Transition Metals*; Third ed.; John Wiley & Sons: New York, 2001.
- (7) Langford, C. H. *Ligand Substitution Processes*; W.A. Benjamin: New York, 1965.
- (8) Nova, A.; Ujaque, G.; Maseras, F.; Lledos, A.; Espinet, P. *J. Am. Chem. Soc.* **2006**, 128, 14571–14578.
- (9) Amatore, C.; Bucaille, A.; Fuxa, A.; Jutand, A.; Meyer, G.; Ntepe, A. N. *Chem.—Eur. J.* **2001**, 7, 2134–2142.
- (10) Stille, J. K.; Lau, K. S. Y. *Acc. Chem. Res.* **1977**, 10, 434–442.
- (11) Fitton, P.; Rick, E. A. *J. Organomet. Chem.* **1971**, 28, 287–291.
- (12) Semmelhack, M. F.; Ryono, L. *Tetrahedron Lett.* **1973**, 2967–2970.
- (13) Vicente, J.; Arcas, A.; Bautista, D.; Jones, P. G. *Organometallics* **1997**, 16, 2127–2138.
- (14) Labadie, J. W.; Stille, J. K. *J. Am. Chem. Soc.* **1983**, 105, 6129–6137.
- (15) Scott, W. J.; Stille, J. K. *J. Am. Chem. Soc.* **1986**, 108, 3033–3040.

- (16) Casado, A. L.; Espinet, P.; Gallego, A. M. *J. Am. Chem. Soc.* **2000**, *122*, 11771–11782.
- (17) Ye, J. H.; Bhatt, R. K.; Falck, J. R. *J. Am. Chem. Soc.* **1994**, *116*, 1–5.
- (18) Casado, A. L.; Espinet, P. *J. Am. Chem. Soc.* **1998**, *120*, 8978–8985.
- (19) Casado, A. L.; Espinet, P.; Gallego, A. M.; Martinez-Ilarduya, J. M. *Chem. Commun.* **2001**, 339–340.
- (20) Perez-Temprano, M. H.; Nova, A.; Casares, J. A.; Espinet, P. *J. Am. Chem. Soc.* **2008**, *130*, 10518–10520.
- (21) Alvarez, R.; Faza, O. N.; Lopez, C. S.; de Lera, A. R. *Org. Lett.* **2006**, *8*, 35–38.
- (22) Farina, V.; Kapadia, S.; Krishnan, B.; Wang, C. J.; Liebeskind, L. S. *J. Org. Chem.* **1994**, *59*, 5905–5911.
- (23) Liebeskind, L. S.; Fengl, R. W. *J. Org. Chem.* **1990**, *55*, 5359–5364.
- (24) Farina, V.; Krishnamurthy, V.; Scott, W. J. *The Stille Reaction*; Wiley: New York, 1997; Vol. 50.
- (25) Farina, V.; Krishnan, B. *J. Am. Chem. Soc.* **1991**, *113*, 9585–9595.
- (26) Littke, A. F.; Schwarz, L.; Fu, G. C. *J. Am. Chem. Soc.* **2002**, *124*, 6343–6348.
- (27) Farina, V.; Krishnan, B.; Marshall, D. R.; Roth, G. P. *J. Org. Chem.* **1993**, *58*, 5434–5444.
- (28) *OriginPro 7.5*; OriginLab Corporation: Northampton, MA, 2004.
- (29) Zhang, H. X.; Guibe, F.; Balavoine, G. *J. Org. Chem.* **1990**, *55*, 1857–1867.
- (30) Vedejs, E.; Haight, A. R.; Moss, W. O. *J. Am. Chem. Soc.* **1992**, *114*, 6556–6558.

- (31) Lavis, J. M. Improving the Stille reaction from rate enhancement to germanium. Doctor of Philosophy Dissertation, Michigan State University, East Lansing, 2004.
- (32) Trebbe, R.; Schager, F.; Goddard, R.; Porschke, K. R. *Organometallics* **2000**, *19*, 521–526.
- (33) Maleczka, R. E., Jr.; Gallagher, W. P. *Org. Lett.* **2001**, *3*, 4173–4176.
- (34) Seyferth, D.; Stone, F. G. A. *J. Am. Chem. Soc.* **1957**, *79*, 515–517.
- (35) Scott, W. J.; Crisp, G. T.; Stille, J. K. *Org. Synth.* **1990**, *68*, 116–129.
- (36) Davies, A. G. *Organotin Chemistry*; Second ed.; Wiley-VCH Verlag GmbH & Co. KGaA: Weinheim, 2004.
- (37) Segelstein, B. E.; Butler, T. W.; Chenard, B. L. *J. Org. Chem.* **1995**, *60*, 12–13.
- (38) Kong, K. C.; Cheng, C. H. *J. Am. Chem. Soc.* **1991**, *113*, 6313–6315.
- (39) Goodson, F. E.; Wallow, T. I.; Novak, B. M. *J. Am. Chem. Soc.* **1997**, *119*, 12441–12453.
- (40) Grushin, V. V. *Organometallics* **2000**, *19*, 1888–1900.
- (41) Kwong, F. Y.; Lai, C. W.; Yu, M.; Chan, K. S. *Tetrahedron* **2004**, *60*, 5635–5645.
- (42) Kwong, F. Y.; Lai, C. W.; Chan, K. S. *J. Am. Chem. Soc.* **2001**, *123*, 8864–8865.
- (43) McKean, D. R.; Parrinello, G.; Renaldo, A. F.; Stille, J. K. *J. Org. Chem.* **1987**, *52*, 422–424.
- (44) de Vries, A. H. M.; Mulders, J. M. C. A.; Mommers, J. H. M.; Henderickx, H. J. W.; de Vries, J. G. *Org. Lett.* **2003**, *5*, 3285–3288.
- (45) Amatore, C.; Jutand, A. *J. Organomet. Chem.* **1999**, *576*, 254–278.

- (46) Littke, A. F.; Fu, G. C. *Angew. Chem. Int. Ed.* **1999**, *38*, 2411–2413.
- (47) Barrios-Landeros, F.; Carrow, B. P.; Hartwig, J. F. *J. Am. Chem. Soc.* **2008**, *130*, 5842–5843.
- (48) Clark, H. C.; Goel, A. B.; Goel, S. *Inorg. Chem.* **1979**, *18*, 2803–2808.
- (49) Portnyagin, I. A.; Lunin, V. V.; Nechaev, M. S. *J. Organomet. Chem.* **2008**, *693*, 3847–3850.
- (50) Hitchcock, S. A.; Mayhugh, D. R.; Gregory, G. S. *Tetrahedron Lett.* **1995**, *36*, 9085–9088.
- (51) Labadie, S. S.; Teng, E. *J. Org. Chem.* **1994**, *59*, 4250–4254.
- (52) Milstein, D.; Stille, J. K. *J. Am. Chem. Soc.* **1979**, *101*, 4981–4991.
- (53) Vanasselt, R.; Elsevier, C. J. *Organometallics* **1994**, *13*, 1972–1980.
- (54) Flemming, J. P.; Pilon, M. C.; Borbulevitch, O. Y.; Antipin, M. Y.; Grushin, V. V. *Inorg. Chim. Acta* **1998**, *280*, 87–98.
- (55) Jutand, A.; Negri, S. *Organometallics* **2003**, *22*, 4229–4237.
- (56) Gallagher, W. P.; Terstiege, I.; Maleczka, R. E., Jr. *J. Am. Chem. Soc.* **2001**, *123*, 3194–3204.
- (57) Gallagher, W. P.; Maleczka, R. E., Jr. *J. Org. Chem.* **2005**, *70*, 841–846.
- (58) Herve, A.; Rodriguez, A. L.; Fouquet, E. *J. Org. Chem.* **2005**, *70*, 1953–1956.
- (59) Kauffman, G. B.; Fang, L. Y.; Viswanathan, N.; Townsend, G. *Inorg. Synth.* **1983**, 101–1103.
- (60) Hiyama, T. *J. Organomet. Chem.* **2002**, *653*, 58–61.

- (61) Sano, H.; Miyazaki, Y.; Okawara, M.; Ueno, Y. *Synthesis* **1986**, 776–777.
- (62) Ueno, Y.; Sano, H.; Okawara, M. *Tetrahedron Lett.* **1980**, 21, 1767–1770.
- (63) Oda, H.; Morizawa, Y.; Oshima, K.; Nozaki, H. *Tetrahedron Lett.* **1984**, 25, 3221–3224.
- (64) Ikenaga, K.; Matsumoto, S.; Kikukawa, K.; Matsuda, T. *Chem. Lett.* **1990**, 185–188.
- (65) Kosugi, M.; Tanji, T.; Tanaka, Y.; Yoshida, A.; Fugami, K.; Kameyama, K.; Migita, T. *J. Organomet. Chem.* **1996**, 508, 255–257.
- (66) Nakamura, T.; Kinoshita, H.; Shinokubo, H.; Oshima, K. *Org. Lett.* **2002**, 4, 3165–3167.
- (67) Yorimitsu, H.; Oshima, K. *Inorg. Chem. Commun.* **2005**, 8, 131–142.
- (68) Itami, K.; Mitsudo, K.; Yoshida, J.-i. *J. Org. Chem.* **1999**, 64, 8709–8714.
- (69) Faller, J. W.; Kultyshev, R. G. *Organometallics* **2002**, 21, 5911–5918.
- (70) Faller, J. W.; Kultyshev, R. G.; Parr, J. *Tetrahedron Lett.* **2003**, 44, 451–453.
- (71) Wnuk, S. F.; Garcia, P. I.; Wang, Z. Z. *Org. Lett.* **2004**, 6, 2047–2049.
- (72) Wang, Z. H.; Wnuk, S. F. *J. Org. Chem.* **2005**, 70, 3281–3284.
- (73) Wang, Z. Z.; Gonzalez, A.; Wnuk, S. F. *Tetrahedron Lett.* **2005**, 46, 5313–5316.
- (74) Endo, M.; Fugami, K.; Enokido, T.; Sano, H.; Kosugi, M. *Adv. Synth. Catal.* **2007**, 349, 1025–1027.

- (75) Spivey, A. C.; Gripton, C. J. G.; Hannah, J. P.; Tseng, C. C.; de Fraine, P.; Parr, N. J.; Scicinski, J. J. *Appl. Organomet. Chem.* **2007**, *21*, 572–589.
- (76) Marciniec, B.; Lawicka, H.; Majchrzak, M.; Kubicki, M.; Kownacki, I. *Chem.—Eur. J.* **2006**, *12*, 244–250.
- (77) Marciniec, B.; Lawicka, H.; Dudziec, B. *J. Organomet. Chem.* **2008**, *693*, 235–240.
- (78) Enokido, T.; Fugami, K.; Endo, M.; Kameyama, M.; Kosugi, M. *Adv. Synth. Catal.* **2004**, *346*, 1685–1688.
- (79) Jeffery, T. *Tetrahedron* **1996**, *52*, 10113–10130.
- (80) Shmidt, A. F.; Smirnov, V. V. *Kinet. Catal.* **2001**, *42*, 800–804.
- (81) Lam, H. W. P., G. *Angew. Chem. Int. Ed.* **2002**, *41*, 508–511.
- (82) Zapata, A. J.; Rondon, A. C. *Org. Prep. Proced. Int.* **1995**, *27*, 567–568.
- (83) Holmes, D. MSU Varian NMR Guide. [http://www2.chemistry.msu.edu/facilities/nmr/how do i.html](http://www2.chemistry.msu.edu/facilities/nmr/how%20do%20i.html) (2009).
- (84) Porco, J. A.; Su, S.; Lei, X. G.; Bardhan, S.; Rychnovsky, S. D. *Angew. Chem. Int. Ed.* **2006**, *45*, 5790–5792.
- (85) Cliff, M. D.; Pyne, S. G. *Tetrahedron Lett.* **1995**, *36*, 763–766.
- (86) Mitchell, T. N.; Reimann, W.; Nettelbeck, C. *Organometallics* **2002**, *4*, 1044–1048.
- (87) Baldur, S.; Peter, P.; J^rrg, M.; Karsten, R.; Kathrin, M.; Stephan, R. h.; Armin de, M. *Chem.—Eur. J.* **2005**, *11*, 308–320.
- (88) Hodgson, D. M.; Boulton, L. T.; Maw, G. N. *Tetrahedron* **1995**, *51*, 3713–3724.
- (89) Clark, H. C.; O'Brien, R. J. *Inorg. Chem.* **1963**, *2*, 740–744.

- (90) Prakash, G. K. S.; Krishnamurthy, V. V.; Olah, G. A.; Farnum, D. G. *J. Am. Chem. Soc.* **1985**, *107*, 3928–3935.
- (91) Marko, I. E.; Leung, C. W. *J. Am. Chem. Soc.* **1994**, *116*, 371–372.
- (92) Satoh, T.; Kaneko, Y.; Yamakawa, K. *Bull. Chem. Soc. Jpn.* **1986**, *59*, 2463–2470.
- (93) Berthiol, F.; Doucet, H.; Santelli, M. *Appl. Organomet. Chem.* **2006**, *20*, 855–868.
- (94) Maleczka, R. E., Jr.; Gallagher, W. P.; Terstiege, I. *J. Am. Chem. Soc.* **2000**, *122*, 384–385.
- (95) Pinhey, J. T.; Roche, E. G. *J. Chem. Soc.-Perkin Trans. 1* **1988**, 2415–2421.
- (96) Liebeskind, L. S.; Wang, J. *Tetrahedron* **1993**, *49*, 5461–5470.
- (97) Bates, E. B.; Jones, E. R. H.; Whiting, M. C. *J. Chem. Soc.* **1954**, 1854–1860.

MICHIGAN STATE UNIVERSITY LIBRARIES



3 1293 03063 4772